Modification de la surface de la cellulose par les organosilanes

Olivier Paquet

UNIVERSITÉ DE GRENOBLE

THÈSE

Pour obtenir le grade de

DOCTEUR DE L'UNIVERSITÉ DE GRENOBLE

Spécialité : **Matériaux, Mécanique, Génie Civil, Électrochimie**

Arrêté ministériel : 7 août 2006

Présentée par

Olivier PAQUET

Thèse dirigée par **Naceur M. BELGACEM** et **Evelyne MAURET**
codirigée par **Elisa ZENO**

préparée au sein du **Laboratoire de Génie des Procédés Papetiers**
dans **l'École Doctorale Ingénierie – Matériaux Mécanique Energétique Environnement Procédés Production**

Modification de la surface de la cellulose par les organosilanes

Thèse soutenue publiquement le 06 juin 2012,
devant le jury composé de :

M. Didier LEONARD
Professeur, ISA / Polytech Lyon, Université de Lyon 1, Président
M. Antonio PIZZI
Professeur, ENSTIB, Université de Nancy, Rapporteur
Mme Maria Emília CABRAL AMARAL
Professeur, Université de Beira Interior, Rapporteur
Mme Evelyne MAURET
Professeur, Grenoble INP-Pagora, Co-encadrante
Mme Elisa ZENO
Ingénieur, Centre Technique du Papier, Co-directrice de thèse
M. Naceur M. BELGACEM
Professeur, Grenoble INP-Pagora, Directeur de thèse

Remerciements

Cette thèse, c'est avant tout l'histoire d'un partenariat entre plusieurs acteurs, universitaires et industriels, qui se sont réunis autour d'objectifs communs dans le cadre d'une convention CIFRE. Sans cette volonté commune du Laboratoire de Génie des Procédés Papetiers, du Centre Technique du Papier, de Dow Corning et de l'Association Nationale de la Recherche et de la Technologie, ce projet n'aurait jamais pu voir le jour. Pour cela, je tiens à exprimer ma sincère gratitude envers tous ceux qui ont œuvrés à l'existence de cette thèse, et aux responsables de ces instituts qui m'ont accordé leur confiance.

Plus particulièrement, je tiens à remercier mes encadrants pour toute l'énergie qu'ils ont dépensés pour que ce projet se réalise, pour leurs conseils précieux et pour m'avoir poussé à toujours aller de l'avant.

Merci à Naceur Belgacem pour avoir accepté de prendre la direction de cette thèse, pour sa patience et pour l'ensemble des connaissances qu'il m'a transmis. Sans oublier son engagement pour assurer la continuité de ce projet dans les moments les plus difficiles.

Aussi, je remercie très chaleureusement Elisa Zeno. C'est elle qui est à l'initiative de ce projet et qui a su réunir et convaincre les différents partenaires. Je n'avais pas pour vocation de faire une thèse, mais grâce à sa confiance et son amitié, je me suis lancé dans ce projet et j'ai pu en tirer de riches enseignements et le goût d'un travail de qualité.

Un grand merci aussi à Évelyne Mauret, pour son apport sur ce travail. Ce n'était pas facile de rejoindre cette thèse en cours de route, mais elle a su le faire avec tact. Je la remercie pour avoir apporté ses connaissances et avoir toujours gardé sa porte ouverte pour moi.

Enfin, j'ai tiens à exprimer toute ma gratitude envers François de Buyl pour son enthousiasme à la création de ce projet et pour sa confiance et sa disponibilité. Sans lui, nous n'aurions pas eu l'occasion de combiner le pouvoir du silicium à celui de la cellulose !

Je souhaite exprimer toute ma gratitude aux membres du jury qui ont accepté d'évaluer ce travail et m'ont fait part de leurs remarques avec une grande gentillesse. Merci à Didier Léonard d'avoir accepté la présidence de ce jury et pour ses remarques toujours constructives. En plus de porter à merveille la casquette de président de jury, M. Léonard a aussi apporté une grande contribution à ce travail grâce à ses connaissances en ToF-SIMS et à la patience infinie dont il a fait preuve face à mes mille et une questions. Merci aussi à Mme Maria Emília Cabral Amaral et à M. Antonio Pizzi pour avoir accepté d'être rapporteurs de ce travail et pour leur attitude chaleureuse.

Si ce travail comporte autant de technique analytiques et touche autant de domaines, c'est grâce à la contribution de nombreuses personnes.

Au LGP2, je tiens à remercier vivement Marie-Christine Brochier-Salon pour son immense contribution à ce travail. Toutes les données de RMN présentées dans cette thèse ont été acquises par Marie-Christine et leur interprétation a pu être faite grâce aux connaissances qu'elle m'a transmis. Je remercie aussi Raphaël Passas et Bertine Khelifi pour m'avoir laissé accéder de manière autonome au

MEB et pour m'avoir formé sur cet appareil. Merci aussi aux membres de l'équipe Transfo pour m'avoir accueilli et soutenu tout au long de cette thèse.

Au CTP, je remercie Bruno Carré et tous les membres de l'UST7 de m'avoir accueilli dans leur équipe, ainsi que tous les membres de l'UST5 et du FCBA pour m'avoir accueilli dans leurs laboratoires. Ma contribution au projet *Tissue+* m'a aussi donné l'occasion de travailler avec des personnes qui m'ont beaucoup appris, je remercie donc Jean Ruiz ainsi que Sandra Tapin-Lingua et Michaël Lecourt pour leur présence et leurs conseils précieux. Les meilleurs techniciens du monde sont au CTP sans aucun doute possible, pour m'avoir supporté dans leurs labos et m'avoir aidé dans une multitude de petits détails, je remercie vivement Dallal, Fred, Geneviève, Marie, Adrien, Arthur, Claude, Jean, Mathieu, Patrick, Pascal, Pierre, Tiphaine et je m'excuse auprès des oubliés !

Il n'y a pas de recherche sans un peu d'administratif. Heureusement, j'ai toujours eu des interlocuteurs extraordinaires pour m'aider. Un grand merci à Augustine Alessio, Malou Caillat, Sylvie Combaz, Annie Coupat, Anne-Marie Piedimont, Joan Thomas, Florise Uomobono et tous les autres !

La thèse est une expérience éprouvante, heureusement la petite communauté des thésards et post-docs est toujours là pour vous épauler et vous avancer une dosette de café ! Je remercie tous ceux que j'ai rencontrés au CTP et au LGP2. Ils sont trop nombreux pour que je les cite tous, mais le cœur y est. En outre, j'ai eu la chance extraordinaire de toujours avoir des collègues de bureau au top. Si je suis toujours allé au bureau B125 avec le sourire, c'est bien grâce à mes amis Eder, Olivier, Robin, Satoru et à notre princesse : Elsa Kimpatsu ! Merci aussi à Céline, ma stagiaire d'élite !

Merci à ma famille pour son soutien tout au long de ce travail. En particulier, je remercie Yvette et Charles pour leur support inconditionnel durant toutes mes études. Merci à ma sœur, Isabelle, et à mon frère, François, pour leur présence et pour avoir fait de moi un oncle comblé ! Morgane, Baptiste, Clément, Evan, Saïan : c'est quand je suis avec vous que je sais ce qui est vraiment important dans la vie. Merci aussi à la meilleure des marraines, Sylvie, et à tous ceux qui me chouchoutent !

Les amis, je parle de vous à la fin, mais dans mon cœur vous êtes tout en haut de la liste. Merci à mes amis de toujours, Christophe, Sébastien, Pierre-Marie. Malgré les années et la distance, vous êtes toujours là, je ne saurais jamais assez vous remercier !

Et puis vous tous amis Grenoblois, après une journée de rédaction, quoi de mieux que de sortir avec vous pour reprendre des forces ?? Merci à Thomas le meilleur colocataire du monde ; Raph & Bino les complices de Pablo ; Cindy, Céline et Tibo ; et puis les escrimeurs aussi ; et puis tous les autres aussi !

Et enfin, s'il ne devait y avoir qu'une personne à remercier, ce serait bien toi. Celle qui est dans mes pensées chaque jour et me donne la force de continuer. Celle qui me complète depuis le tout début de cette thèse. Mon autre moitié. Merci Raluca.

Résumé étendu en Français

Table des matières

Introduction générale ..... **vii**

Partie 1 - Étude des alkoxysilanes en milieux aqueux. ..... **ix**

I. Les alkoxysilanes et leur réactions ix

II. Étude expérimentale du comportement des alkoxysilanes dans l'eau xi

Conclusions xv

Partie 2 - Adsorption des silanes sur des surfaces modèles. ..... **xvi**

I. Chimie de surface de la cellulose et surfaces modèles xvi

II. Partie expérimentale xvii

Conclusions xxii

Partie 3 - Interactions silane-cellulose. ..... **xxiii**

I. Modification de la cellulose par les silanes : littérature. xxiii

II. Partie expérimentale xxiv

Conclusions xxx

Partie 4 - Impact de la modification par les organosilanes sur les propriétés du papier. ..... **xxxi**

I. Fabrication du papier, douceur et propriétés mécaniques xxxi

II. Partie expérimentale xxxii

Conclusions xxxv

Conclusions générales ..... **xxxvi**

Perspectives ..... **xxxvii**

Références bibliographiques ..... **xxxvii**

Introduction générale

Dans un contexte de développement durable de toutes les activités humaines, l'intérêt des producteurs et des consommateurs converge vers la fabrication de produits à base de ressources naturelles renouvelables, en utilisant des procédés propres et sans solvants. Cette tendance ouvre la voie à des nouvelles perspectives et à des nouveaux défis pour la cellulose. Notamment, la fonctionnalisation de sa surface par greffage chimique permet de moduler les propriétés des fibres de cellulose et d'accroître leur intérêt pour les applications les plus diverses. Dans ce cadre, le greffage par les organosilanes est une voie très prometteuse, au vu de la grande diversité de composés disponibles et des fonctions chimiques que ces composés pourraient apporter en surface de fibres naturelles. Cependant, il est primordial, pour qu'un tel procédé de greffage ait une valeur industrielle, qu'il soit compatible avec les conditions utilisées en milieu papetier. En particulier, il est essentiel que ce procédé se déroule en milieu purement aqueux, en évitant tout solvant organique.

Cette thèse traite de l'étude de la modification de surface de la cellulose par les organosilanes, en milieu aqueux. Le but de ce travail est de répondre à plusieurs questions fondamentales, et d'évaluer la portée des techniques développées dans le cadre d'une application industrielle. Plus particulièrement, les principaux objectifs de cette thèse sont : (i) de confirmer la faisabilité de la modification de la cellulose par les organosilanes en milieux aqueux ; (ii) d'étudier le comportement de plusieurs organosilanes en solution et de déterminer quels sont les principaux facteurs influençant ces comportements ; (iii) d'approfondir les connaissances actuelles concernant la nature des interactions entre silanes et cellulose, y compris les cinétiques de réactions ; et (iv) d'évaluer l'intérêt des organosilanes dans un cas pratique de problématique industrielle liée à l'industrie papetière.

Pour répondre aux problématiques énoncées ci-dessus, le programme suivi au cours de la thèse s'articule en quatre parties, que l'on retrouve dans le manuscrit, dont chaque partie débute par une description de l'état de l'art suivie par les principaux résultats obtenus.

Le *premier chapitre* de cette thèse porte sur *l'étude des alkoxysilanes en milieu aqueux*. Celle-ci a été réalisée principalement par spectroscopie par résonance magnétique nucléaire du silicium. En effet, seule cette technique permet d'assurer le suivi simultané des différentes espèces contenant du silicium présentes dans le milieu, ainsi que la détermination de leurs cinétiques de formation et de disparition. La partie expérimentale débute par une étude préliminaire visant à comparer les réactions d'un aminosilane dans un mélange éthanol/eau, à celles ayant lieu dans l'eau. Puis, les caractérisations des réactions de divers silanes portant différents groupes fonctionnels sont présentées, et l'impact de la concentration en silane, du pH de la solution et de la température sur ces réactions sont discutés. Enfin, le rôle de la structure du silane est décrit.

La *deuxième partie* de cette thèse décrit les cinétiques *d'adsorption de trois silanes sur des surfaces modèles de cellulose*. Dans une première section, le lecteur peut trouver des données générales concernant la chimie de surface des fibres de cellulose, le développement des surfaces de cellulose modèle, ainsi que sur les phénomènes d'adsorption. La partie expérimentale décrit les données obtenues au moyen d'une microbalance à quartz. La discussion se concentre d'abord sur les données obtenues pour l'adsorption des composés choisis sur des surfaces modèles de cellulose, en fonction de différents paramètres cités précédemment. En outre, des données obtenues sur des surfaces modèles de silice sont présentées et permettent l'élargissement de la discussion.

Le *troisième chapitre* de cet ouvrage est dédié à la caractérisation de *l'interaction silane-cellulose*. Il commence par une revue bibliographique sur les interactions atomiques, ainsi qu'une description de l'état de l'art concernant le greffage de la cellulose, en particulier avec les silanes. Les données obtenues par spectrométrie EDX après diverses extractions sont discutés dans une étude préliminaire. Les données les plus

importantes comprennent des spectres de ^{29}Si-RMN des solides, ainsi que des résultats d'XPS et de ToF-SIMS et permettent une meilleure description de l'interface silane-cellulose.

La *quatrième e*t dernière *partie* de cette thèse présente les résultats d'une *étude appliquée pour l'industrie des pâtes et papier*. Ce chapitre présente le processus de fabrication du papier, et le contexte dans lequel ce travail a été effectué. Les résultats présentés incluent les propriétés morphologiques de deux types de fibres, avant et après modification avec un silane modèle. Les propriétés physiques et la douceur de deux types de formettes (formettes de rétention et de douceur) obtenues à partir de ces fibres vierges ou modifiés sont discutées, et l'impact de l'ajout de silane sur la formation de la feuille est passé en revue.

Enfin, quelques *remarques générales* concluent le travail présenté dans ce rapport et permettent l'élaboration de *perspectives* liées au sujet de l'étude.

Le travail présenté dans ce mémoire de thèse comprend plusieurs *aspects novateurs*, tels que le greffage *des organosilanes en milieu purement aqueux, le développement des nouvelles méthodes* pour étudier *l'adsorption des organosilanes sur la cellulose (*l'étude directe de l'adsorption de silanes sur des surfaces modèles de cellulose native par microbalance à quartz) et comprendre *les interactions entre les silanes et la cellulose* (ToF-SIMS combiné avec l'utilisation de monoalkoxysilanes).

En conclusion, cette étude a permis de montrer la faisabilité du greffage sur les fibres cellulosiques des organosilanes en milieu purement aqueux et d'établir sa dépendance du comportement des silanes dans l'eau. Ce dernier a été étudié de manière très approfondie, en mettant en évidence sa relation avec des paramètres du milieu tel que le pH, la température et la concentration du silane. Ces mêmes paramètres, ainsi que la structure du silane, jouent un rôle crucial dans l'adsorption des silanes sur la cellulose, en permettant ainsi d'optimiser la modification de sa surface. Malheureusement, la nature exacte des liaisons silane-cellulose n'a pas pu être établie de manière définitive, bien qu'une approche innovante et prometteuse ait été mise au point. Des études supplémentaires, avec cette approche, pourraient permettre d'obtenir une réponse.

Partie 1 - Étude des alkoxysilanes en milieux aqueux.

I. Les alkoxysilanes et leur réactions

Les organosilanes ont été largement étudiés depuis les années 1940 [1-3] et ont contribués de manière importante au développement des matériaux composites. Ces agents de greffages s'articulent autour d'un atome central de silicium tétravalent et ont la particularité de pouvoir porter à la fois des groupements organiques et inorganiques. Plus particulièrement, les alkoxysilanes portent des groupements alkoxy pouvant être hydrolysés [4-6] en présence d'eau ou d'humidité, donnant ainsi des fonctions silanols (Si-OH). De tels silanols peuvent condenser [7] avec d'autres groupes hydroxyles (métalliques, organiques, …), permettant le greffage du silane et l'apport de nouvelles fonctions sur le substrat. Les réactions des organosilanes dans l'eau sont récapitulées dans la partie suivante :

a) Hydrolyse

La réaction d'hydrolyse (Figure 1) est influencé par divers paramètres tels que le pH, la concentration ou encore la température [8-10]. Dans le cas de polyalkoxysilanes, cette réaction peut donner naissance à diverses espèces partiellement ou totalement hydrolysées. Afin de les distinguer, nous appliquons la notation de Glaser et Wilkes [11] adaptées par Brochier-Salon [12-17] représentée en Figure 2.

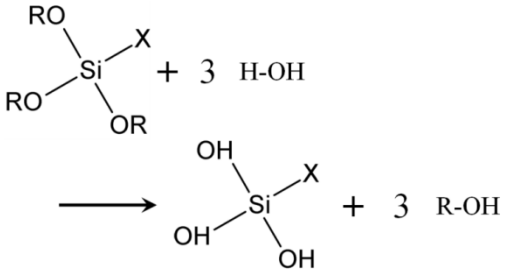

Figure 1 : Hydrolyse d'un trialkoxysilane (OR = groupement alkoxy ; X = groupement fonctionnel).

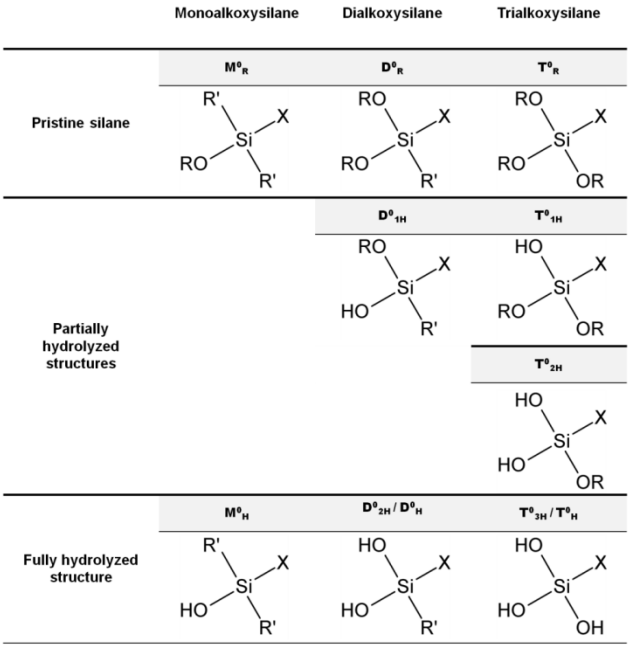

Figure 2 : Notation de Glaser et Wilkes pour les silanes non condensés

La réversibilité de cette réaction a été démontrée par divers chercheurs, dont Osterholtz et Pohl [18], Alam et al. [19] ou Prabakar et al. [20], qui ont aussi établi que la cinétique de la réaction inverse est environ 100 fois inférieure à celle de l'hydrolyse.

b) Condensation

La réaction de condensation d'un organosilane peut prendre deux formes. Dans le cas de la condensation avec un silanol issu d'une autre molécule de silane, on parlera d'homo-condensation. Tandis que dans le cas de la réaction avec un substrat, on parlera simplement de condensation. La première réaction (Figure 3) donne naissance à des liaisons siloxanes (Si-O-Si) [21], [22], et les molécules formées prennent le nom de

polysiloxanes. Les différentes structures pouvant être rencontrées en solution [11], [19] et leur nomenclature adaptée de Glaser et Wilkes sont présentées en Figure 4.

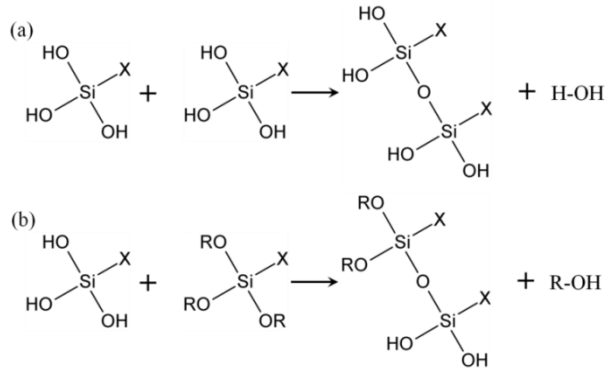

Bien que certains auteurs l'aient décrit dans des conditions très spécifiques [18], la réaction inverse de l'homo-condensation des silanes est généralement considérée comme inexistante.

Figure 3: Condensation de (a) deux silane triols, (b) un silane triol et un trialkoxysilane.

Les structures totalement condensés, M^1, D^2 et T^3, n'ont plus de groupements hydroxyles disponibles et ne sont donc pas adaptés pour la modification chimique de substrats. En revanche, les structures partiellement condensées, tel que D^1, T^1 et T^2, contiennent encore des groupes hydroxyles et sont par conséquent potentiellement réactives. Cela nous pousse à développer un outil pour évaluer la réactivité à un moment donné d'une solution de silane en fonction de sa composition. Dans ce contexte, nous avons considéré le concept général nommé *Active Si-OH function*, développé par Beari et al. [21], et proposons trois nouvelles expressions.

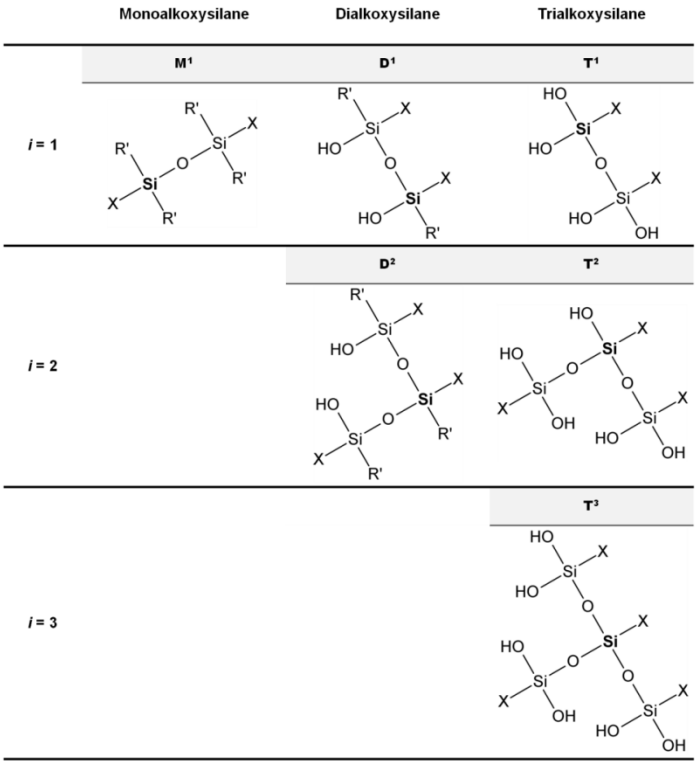

Ces expressions, qui seront nommés SR (Silanol Reactivity parameter), correspondent aux trois familles d'alkoxysilanes pris en compte dans ce travail, à savoir: les mono-, di- et tri-alkoxysilanes, et sont donnés dans les équations 1 à 3 respectivement.

Figure 4: Notation adaptée de Glaser et Wilkes pour les silanes condensés.

$$SR = \%M^0{}_H$$

Equation 1.

$$SR = \frac{\left(2 * \%D^0{}_H\right) + \left(1 * \%D^1\right)}{2}$$

Equation 2.

$$SR = \frac{\left(3 * \%T^0{}_H\right) + \left(2 * \%T^1\right) + \left(1 * \%T^2\right)}{3}$$

Equation 3.

Il est à noter qu'outre les structures décrites ci-dessus, l'existence de structures cycliques à été décrite dans la littérature [6], [7], et permet de mieux comprendre la stabilité de certains silanes (aminosilanes, ou diméthyl-silanes).

Afin de produire des solutions aqueuses de silane réactives, il est essentiel de maitriser les paramètres réactionnels [23]. Pour mieux connaitre l'état d'une solution à un moment donné, de nombreux outils analytiques ont été proposés.

Cependant, seule la RMN du silicium permet de déterminer *in-situ* la composition d'une solution et les cinétiques de formation et de disparitions des différents composés présents [12], [14], [24-26].

c) Cas particuliers

Les aminosilanes montrent des caractéristiques rares dans la famille des alkoxysilane, en raison de la présence d'au moins un groupe amine dans leur groupement fonctionnel. En particulier, ces composés sont totalement solubles dans l'eau. En outre, à leur pH naturel, qui est en général proche de 11, les solutions d'aminosilanes ont des cinétiques de réaction très rapides, grâce à l'auto-catalyse basique apportée par la fonction amine. L'ajout d'acide acétique au milieu réactionnel pour atteindre un pH proche de 4, avant l'insertion du silane, permet de stabiliser les espèces hydrolysées en limitant la condensation [1].

II. Étude expérimentale du comportement des alkoxysilanes dans l'eau

Le travail expérimental présenté dans ce chapitre consiste en l'analyse en spectroscopie RMN ^{29}Si des composés suivant : trimethylmethoxysilane (TMMS), dimethyldimethoxysilane (DMDMS), methyltrimethoxysilane (MTMS), methylvinyldiethoxysilane (MVDES), methylvinyldimethoxysilane (MVDMS), 3-aminopropyldimethylethoxysilane (APDMES), et 3-(2-amino-ethylamino)-propyltrimethoxysilane (DAMS). Les données principales concernant ces composés sont résumées en Tableau 1. Quand nécessaire, le pH des solutions a été fixé à 4 par ajout d'acide acétique. Des analyses ont été réalisées à 25°C et à 45°C, à différentes concentrations.

Des spectromètres Varian UNITY 400 et MERCURY 400 NMR ont été utilisés, avec une sonde BB de 10mm opérée à 79.455 MHz. Les déplacements sont indiqués par rapport à la référence apportée par un tube coaxial (référence externe) de TMS. La largeur spectrale est de 12KHz, et le temps de relaxation appliqué de 100s, avec un découplage de proton appliqué uniquement lors de l'acquisition de manière à éviter un effet nOe négatif. Le nombre de scans a été augmenté avec le temps de réaction. L'attribution des déplacements chimiques a été confirmée par des mesures indépendantes.

Name	Structure	Molecular formula	Molar weight (g/mol)	Density at 25°C (g/cm3)	Boiling point (°C)	Purity (%)	CAS Number	Distributor	Commercial Reference
Trimethylmethoxy-silane (TMMS)		$C_4H_{12}OSi$	104,22	0,756	57	>97	[1825-61-2]	abcr GmbH & Co. KG - Karlsruhe - Germany	AB 111500
Dimethyldimethoxy-silane (DMDMS)	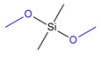	$C_4H_{12}O_2Si$	120,22	0,865	82	> 98 %	[1112-39-6]	Dow Corning, S.A. - Seneffe - Belgium	Z-6194
Methyltrimethoxy-silane (MTMS)	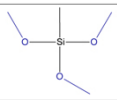	$C_4H_{12}O_3Si$	136,22	0,948	102	> 60 %	[1185-55-3]	Dow Corning, S.A. - Seneffe - Belgium	Z-6070
Methylvinyldimethoxy-silane (MVDMS)	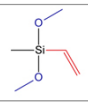	$C_5H_{12}O2Si$	132,22	0,881	104	> 95 %	[16753-62-1]	Dow Corning, S.A. - Seneffe - Belgium	Z-2349
Methylvinyldiethoxy-silane (MVDES)	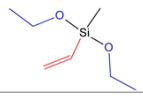	$C_7H_{16}O_2Si$	160,29	0,858	133	> 95 %	[5507-44-8]	Gelest, Inc. - Morrisville, PA - USA	SIV 9085.0
(3-Amino)-propyl-dimethylethoxysilane (APDMES)	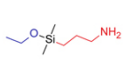	$C_7H_{19}NOSi$	161,32	0,857	78	> 95 %	[18306-79-1]	Gelest, Inc. - Morrisville, PA - USA	SIA 0603.0
3-(2-amino-ethylamino)propyl-trimethoxysilane (DAMS)	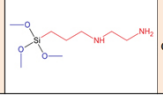	$C_8H_{22}N_2O_3Si$	222,36	1,02	264	> 98 %	[1760-24-3]	Dow Corning, S.A. - Seneffe - Belgium	Z-6094

Tableau 1: Données sur les silanes étudiés

a) Impact de la composition du solvant sur les réactions du DAMS

Souvent, la littérature décrit l'utilisation de solution à 1 ou 2% en masse de silane, en milieu eau/alcool [1-4]. Nous avons décidé d'évaluer le comportement d'un silane en solution aqueuse (le DAMS) et de le comparer à des données précédemment publiées [12] pour ce composé en milieu alcool/eau 80/20 en masse. L'impact du pH a été évalué dans les deux cas, et toutes les réactions ont été suivies par spectroscopie RMN ^{29}Si pour une période de 48 heures.

Les spectres obtenus en milieu alcool/eau sont présentés en Figure 5, et les cinétiques de formation ou de disparition des diverses espèces en solution sont données en Figure 6. Les mêmes types de données ont été obtenus en milieux purement aqueux. Il convient de noter que pour les deux expériences menées en milieu purement aqueux, la disparition complète des structures non-condensées n'a pas été observée sur la gamme de temps de l'étude : 48 heures. Il apparaît ici que dans le cas d'un silane aminé, l'utilisation de milieux aqueux conduit à un meilleur contrôle des réactions de condensation et donne un mélange réactif dans lequel l'équilibre entre les différentes structures en solution est atteint. En particulier, les structures T^0_H restent disponibles pour le greffage sur de longues périodes de temps.

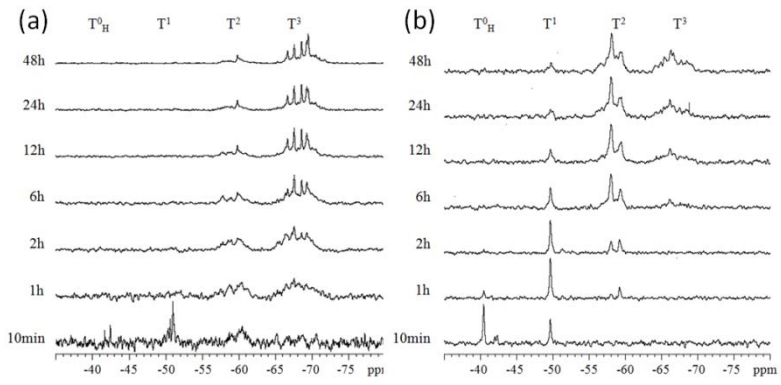

Figure 5: Spectres de RMN ^{29}Si – DAMS 10% en solution alcool/eau. (a) pH non modifié; (b) pH=4.

Bien que l'analyse montre des traces d'homo-condensation qui donnent naissances à des espèces insolubles dans le milieu et qui migrent dans le tube d'analyse, devenant invisibles pour le spectromètre, on constate clairement un intérêt fort des solutions aqueuses.

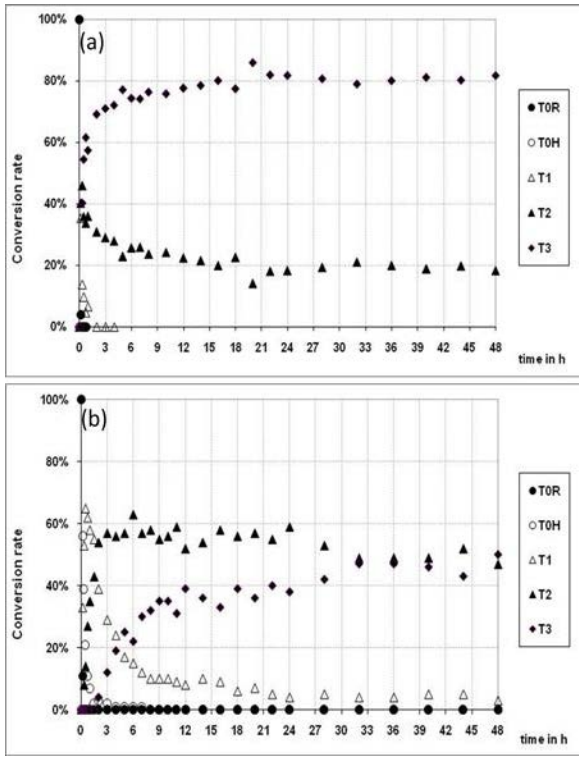

Figure 6: Cinétiques d'hydrolyse et d'homo-condensation correspondant aux données de la Figure 5.

Le paramètre SR, tracé pour les quatre réactions décrites dans cette section est présenté dans la Figure 7, qui montre deux tendances différentes:

(i) Le pH du milieu semble être le paramètre prépondérant au cours des deux premières heures de la réaction, dans tous les milieux. En effet, pour les deux expériences menées en conditions acides, SR atteint un maximum de près de 80% contre moins de 40% pour les réactions à pH non modifié. Cependant, une diminution moins rapide de SR dans le temps est observée pour la réaction en milieu aqueux à pH acide, par rapport à son homologue en milieu alcool/eau.

(ii) Sur des périodes plus longues, le paramètre SR est maintenu à un niveau satisfaisant en solutions aqueuses pures, par rapport aux solutions mixtes. Cela indique que les réactions de condensation sont limitées dans ce milieu, donnant ainsi lieu à un mélange plus réactif.

Ces résultats sont particulièrement intéressants pour la modification des fibres naturelles dans des conditions compatibles avec le processus de l'industrie papetière. Ainsi, sur la base de ces résultats, il a été décidé de procéder à des expériences sur d'autres silanes, dans des conditions purement aqueuses seulement.

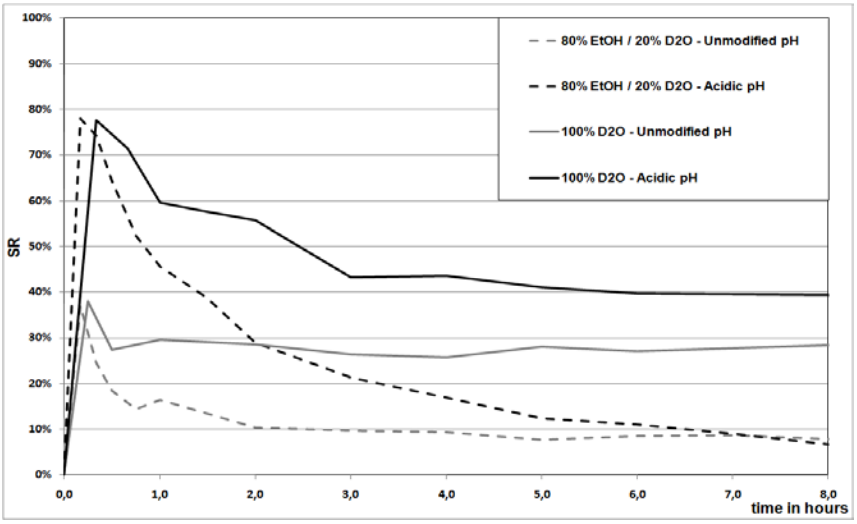

Figure 7: Paramètre SR pour le DAMS à 10% en milieu aqueux et en milieu alcool/eau.

b) Caractérisation de silanes en milieux aqueux.

Sur la base des données décrites ci-dessus, de nombreuses expériences ont été réalisées, dont les conditions sont résumées en Tableau 2. Le choix de ces différentes conditions à été fait pour pouvoir mieux comprendre le rôle de différents paramètres de réaction sur les cinétiques d'hydrolyse et de condensation de ces composés. En particulier, ce travail à porté sur les effets liés à la température de réaction, au pH de la solution, et à la concentration en silane. Pour chaque famille de composé, des observations expérimentales ont été présentées, permettant d'apporter un regard critique sur les données présentées, notamment lorsque des problèmes liés à la formation d'espèces insolubles ont été rencontrées.

		TMMS	DMDMS	MTMS	MVDES	MVDMS	APDMES	DAMS
pH = 4	Room temperature		200 mM 400 mM	400 mM		300 mM 400 mM	400 mM	10% w/w
	45°C		400 mM	400 mM	400 mM	400 mM	400 mM	
Unmodified pH	Room temperature	100mM	300 mM 400 mM	300 mM 400 mM		300 mM	400 mM	10% w/w
	45°C		400 mM	400 mM	400 mM	400 mM	400 mM	

Tableau 2: Liste des conditions expérimentales

Concernant les alkylsilanes, il est observé qu'un pH acide accélère considérablement la cinétique d'hydrolyse, ce qui est particulièrement appréciable pour ces composés ayant une faible solubilité et des cinétiques d'hydrolyse lentes. Pour le DMDMS, une diminution de pH à amené à la détection de structures cycliques, et à accéléré la formation d'une seconde phase liquide associée à la formation de structures condensées insolubles. Pour le MTMS, un pH plus bas n'a pas affecté considérablement la cinétique de condensation à température ambiante et a semblé ralentir considérablement la formation de structures insolubles à 45°C. Le pH de la solution doit être considéré au cas par cas selon l'usage prévu.

Pour les vinylalkoxysilanes, comme pour les alkylalkoxysilanes le passage à un pH acide augmente fortement les réactions d'hydrolyse à température ambiante. Les conclusions sont similaires.

Enfin, pour les aminoalkoxysilanes, la vitesse d'hydrolyse étant catalysée dans les deux pH utilisés, une réactivité très élevée est obtenue dans tous les cas. Cependant, un pH acide permet d'empêcher la formation de structures insolubles ou, du moins, de réduire leur cinétique de formation, probablement *via* la protonation des groupements amine. Ainsi, pour cette famille de composés, l'utilisation de solutions acides est recommandée.

Comme on peut s'y attendre, l'impact de la température consiste principalement en une accélération des réactions ayant lieu dans la solution. Cela peut être utile dans le cas d'un silane ayant une faible cinétique d'hydrolyse, cependant dans la majeure partie des cas étudiés ici, l'impact sur la cinétique de condensation est un désavantage majeur. En effet, le passage d'une température de 25°C à 45°C favorise largement la formation d'espèces condensées, ou d'espèces insolubles.

Enfin, en ce qui concerne l'impact de la concentration, là encore les effets observés sont ceux attendus. Bien que la cinétique d'hydrolyse semble peu affectée dans la gamme de concentration étudiée, on observe sur le long terme une hausse de la cinétique d'homo-condensation avec la concentration.

c) Effet de la structure du silane

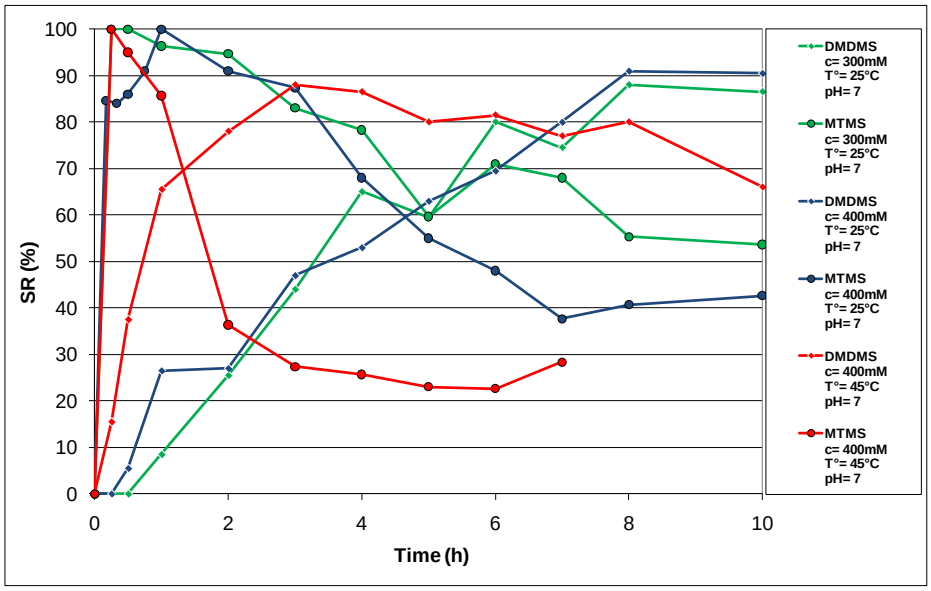

En croisant les données obtenues pour les différentes molécules étudiées, il est possible d'observer quelques tendances concernant l'effet de leur structure sur le comportement en milieu aqueux.

Figure 8: Comparaison de SR entre DMDMS et MTMS pour différentes conditions à pH neutre.

En comparant les données recueillies pour le TMMS, le DMDMS, et le MTMS, on peut étudier l'effet du nombre de substitutions par des groupements méthoxy sur le silicium (comparaison montrée pour différentes conditions à pH non modifié en Figure 8). L'augmentation du nombre de groupements hydrolysables a une grande influence sur la solubilité du silane dans l'eau. Aussi, elle favorise la cinétique d'hydrolyse, ce qui est en accord avec les données de la littérature. En outre, ce changement de la structure affecte de manière significative les réactions d'homo-condensation du silane, mais les tendances observées pour ce point dépendent d'autres paramètres réactionnels dont le pH. Il convient de noter que nous ne disposons pas de données permettant de juger d'une substitution par des groupements éthoxy.

La comparaison entre le DMDMS et le MVDMS montre que l'apport d'une fonction vinylique permet d'améliorer la solubilité du composé dans l'eau tout en maintenant des cinétiques de réaction assez lentes.

Enfin, le changement de nature des groupements alkoxy observé entre le MVDMS et le MVDES modifie les comportements observés à 25°C. En particulier, à température ambiante, le méthoxysilane est soluble dans l'eau, tandis que l'éthoxysilane ne l'est pas. A 45°C, les cinétiques observées sont relativement similaires.

Conclusions

L'étude présentée dans ce chapitre montre sans ambiguïté que tous les composés testés, à l'exception du TMMS, peuvent réagir pour former des solutions hautement réactives avec des SR pouvant atteindre 75% à 100%. Ainsi, l'impact de plusieurs paramètres a pu être établi, tels que: le temps de pré-hydrolyse nécessaire avant l'addition des fibres lorsque c'est nécessaire, le contrôle des paramètres de la réaction, la durée de la réactivité de la solution, etc. Les données les plus utiles obtenues à partir de cette étude sont résumées dans le Tableau 3. Ces données permettant l'optimisation des réactions de greffage de la cellulose par les organosilanes servent de base à la suite de ce travail de thèse.

Silane	*pH*	*Concentration (mM)*	*Temperature (°C)*	*Highest SR (%)*	*Time at highest SR (hours)*	*Estimated duration of period with high reactivity*
TMMS	Solubility not sufficient for NMR analysis					
DMDMS	**4**	**200mM**	**RT**	95	0	~ 1 hour
		400mM	**RT**	85	0	~ 1 hour
		400mM	**45ºC**	75	0	~ 30 minutes
	7	**300mM**	**RT**	90	8	a few days
		400mM	**RT**	90	8	a few days
		400mM	**45ºC**	90	3	~ 10 hours
MTMS	**4**	**400mM**	**RT**	100	0	~ 2 hours
		400mM	**45ºC**	85	0	~ 6 hours
	7	**300mM**	**RT**	100	0	~ 6 hours
		400mM	**RT**	100	0	~ 6 hours
		400mM	**45ºC**	100	0	~ 2 hours
MVDES	**4**	**400mM**	**45ºC**	85	0	~ 30 minutes
	7	**400mM**	**45ºC**	100	0	a few hours
MVDMS	**4**	**300mM**	**RT**	100	0	~ 4 hours
		400mM	**RT**	85	0	~ 2 hours
		400mM	**45ºC**	80	0	~ 30 minutes
	7	**300mM**	**RT**	90	4	~ 6 hours
		400mM	**45ºC**	**Phase separation too fast to allow NMR acquisition before signal loss**		
APDMES	**4**	**400mM**	**RT**	100	0	days
		400mM	**45ºC**	100	0	days
	11,5	**400mM**	**RT**	100	0	a few hours
		400mM	**45ºC**	100	0	~ 1 hour

Tableau 3: Bilan des données RMN

Partie 2 - Adsorption des silanes sur des surfaces modèles.

I. Chimie de surface de la cellulose et surfaces modèles

a) La cellulose

La cellulose est un polymère naturel produit par les plantes et les arbres. Ce polymère très abondant a fait l'objet de nombreuses études et sa structure est bien connue [27], [28]. La macromolécule de cellulose est composée d'unités de β-D-(1-4)-glucopyranose formant un polysaccharide linéaire tel que présenté dans la Figure 9. Chaque unité de glucopyranose porte trois groupements hydroxyles considérés comme autant de groupes réactifs. Cependant la cellulose est un matériau relativement inerte du fait qu'il est généralement très cristallin et que des interactions physiques fortes existent entre les chaînes de polysaccharides [29].

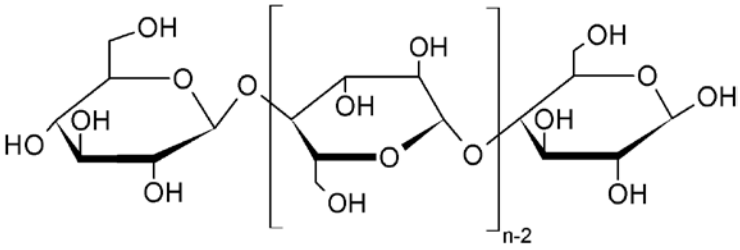

Figure 9: Structure de la cellulose

La cellulose native est composée de fragments cristallins et de zones amorphes. Ces premiers sont peu sensibles à la modification chimique, tandis que la partie amorphe est plus réactive [30]. En outre, il est connu que les molécules de faibles tailles peuvent pénétrer la surface des fibres de cellulose et réagir au sein de la paroi, en particulier si le solvant utilisé lors de la réaction favorise le gonflement de la cellulose. Dans le cas de modification par des petits organosilanes, il est attendu qu'une certaine pénétration du substrat ait lieu.

Afin de modéliser l'adsorption de composés sur la cellulose, de nombreux chercheurs ont travaillés à l'élaboration de surfaces modèles de cellulose [31], [32]. L'élaboration de films ultra-minces par spin-coating de cellulose dissoute [33], [34], puis de cellulose nanofibrillée [35-37] à permis d'obtenir des surfaces planes de cellulose native particulièrement intéressantes bien que présentant une forte cristallinité.

b) Les phénomènes d'adsorption et leur caractérisation

L'adsorption de composés sur une surface résulte d'interactions entre les atomes composant la surface et ceux à l'intérieur du matériau. Ces forces anisotropes génèrent un phénomène d'attraction local destiné à diminuer l'énergie libre du système via une réaction exothermique d'adsorption. Parmi les mécanismes d'adsorption, on distingue : (i) la physisorption mettant en jeu des forces de Van der Walls ; (ii) la chimisorption impliquant des interactions fortes; et (iii) les interactions électrostatiques liant des entités chargées via des liaisons ioniques.

Différents modèles théoriques basés sur des hypothèses bien définies ont été proposées depuis le début du XXème siècle pour décrire les phénomènes d'adsorption [38], [39], dont les isothermes de Freundlich et de Langmuir, ou encore la théorie BET ou la théorie DLVO. Les silanes ayant la capacité de réagir entre eux par homo-condensation, ils n'obéissent à aucun de ces modèles, bien que leur comportement d'adsorption sur une surface donnée puisse s'en approcher.

Les interactions ayant lieu à la surface de la cellulose avec différents composés ont été largement étudiées [40-43]. De même, l'adsorption d'organosilanes sur divers substrat a été décrite dans la littérature [44-47]. Il ressort de ces études que selon le solvant utilisé, la structure du silane et les conditions de dépôt, de

nombreux types d'adsorption peuvent être observés. Concernant l'adsorption de silane sur la cellulose, bien que plusieurs études aient été publiées à ce jour, aucune ne décrit l'observation *in-situ* de cinétiques d'adsorption sur des surfaces modèles.

c) La microbalance à quartz avec mesure de la dissipation (QCM-D)

Pour observer des cinétiques d'adsorption en milieu aqueux *in-situ*, il existe un appareil à haute sensibilité : la microbalance à quartz (QCM : Figure 10). Son fonctionnement se base sur l'effet piézo-électrique et permet de relier la fréquence de résonnance d'un capteur en quartz (Figure 11) à la masse de composé qui se dépose dessus. En outre, l'étude de la dissipation de l'énergie dans ce système permet de caractériser l'épaisseur et la rigidité de la couche déposée à la surface. L'utilisation de cette méthode est basée sur l'équation de Sauerbrey et surtout la relation de Sauerbrey qui est donnée en Equation 1.

$$\Delta m = \frac{C\,\Delta f}{n}$$

Equation 1: Relation de Sauerbrey [48]

Avec:

Δm = masse adsorbée ($g.cm^{-2}$)

Δf = variation de fréquence (Hz)

C = sensibilité du résonateur ($g.cm^{-2}.Hz^{-1}$)

n = numéro de l'harmonique

Figure 10: QCM-D (source http://www.q-sense.com)

Figure 11: AT-cut quartz (source http://www.q-sense.com)

Notre étude bibliographique montre qu'à ce jour, l'observation *in-situ* de la modification de surfaces de celluloses par les organosilanes en milieux aqueux n'a pas été rapportée. Nous avons donc décidés d'entreprendre la caractérisation de ces phénomènes au travers d'une étude par QCM.

II. Partie expérimentale

Notre étude expérimentale est basée sur l'utilisation de trois silanes, l'APDMES, le DAMS et le VDMES. Des expériences ont été menées au pH naturel de la solution de silane (soit 5,8 pour le VDMES, et 11,5 pour les aminosilanes), ainsi qu'à pH=4 pour chaque composé. Des tests ont été réalisés à 25°C et à 45°C. Les surfaces modèles utilisées sont disponibles commercialement et ont été préparées par spin-coating avec de la cellulose native nano-fibrillaire. Ils présentent une épaisseur de cellulose de 6nm environ et une très faible rugosité.

Toutes les comparaisons rapportées sont effectuées en se basant sur les valeurs obtenues pour une même harmonique (la 7ème). Dans un premier temps, la répétabilité des mesures obtenues par QCM a été testée, comme montré en Figure 12. Il apparait que toutes nos mesures peuvent avoir une erreur de +/- 10%. La Figure 13 montre un exemple typique des données acquises par QCM et de leur traitement. La courbe bleue montre la diminution de la fréquence due à l'adsorption du silane sur le quartz. On voit que l'adsorption commence dès que la solution de silane entre en contact avec le quartz et qu'une première phase très rapide (environ 600s ici) est observée, avant qu'une adsorption plus lente se mette en place. La courbe rouge montre la dissipation mesurée dans le système, qui est ici très faible. Cela indique que l'adsorption se fait sous la forme d'une couche très fine, rigide et peu hydratée, ce qui est normal pour des composés de faible taille.

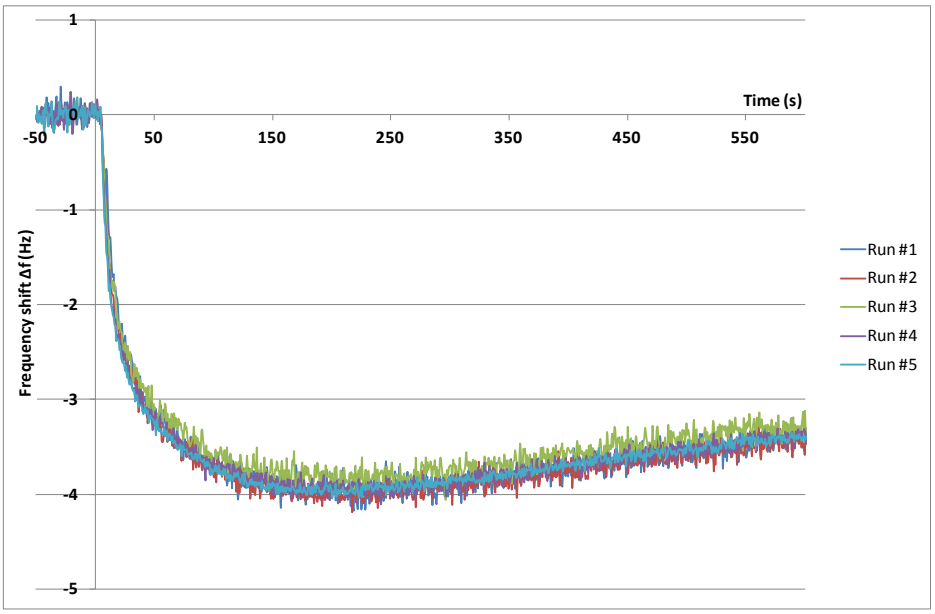

Enfin, la courbe noire correspond à la modélisation de Sauerbrey appliquée à la courbe bleue. En fin d'expérience, on voit une cassure sur la courbe, qui correspond au rinçage avec une solution d'eau pure. Cela montre qu'une partie de la couche adsorbée l'est par des interactions très faibles, tandis qu'une autre partie reste accrochée en l'absence de rinçage à l'éthanol.

Figure 12: Test de reproductibilité.

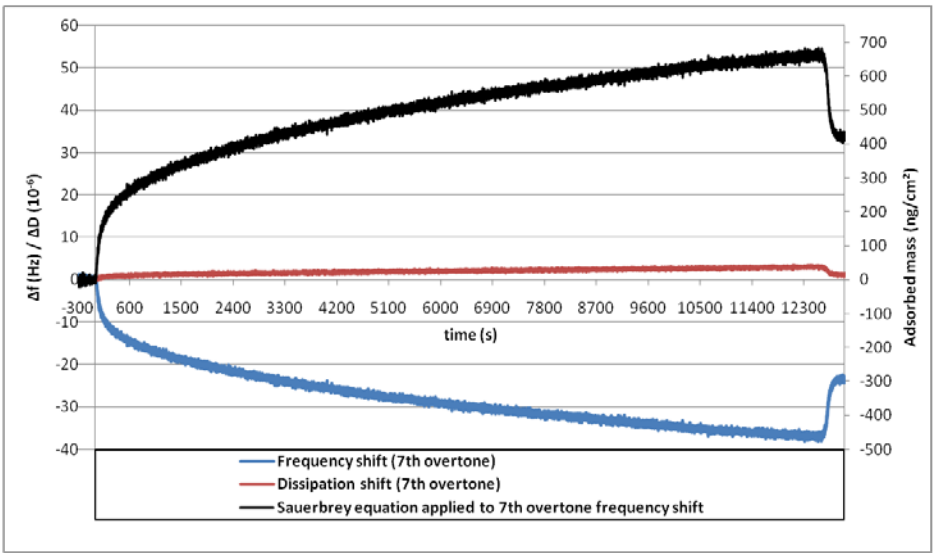

Les données présentées ici sont représentatives de toutes les données obtenues avec nos différents silanes sur des surfaces modèles de cellulose. On note, selon les conditions expérimentales, des variations quant au niveau d'adsorption atteint à un temps donné, ou encore concernant la cinétique d'adsorption, mais la forme générale reste la même.

Figure 13: Solution à 0.2% en APDMES sur un quartz de cellulose, a pH=11.5 et 45°C

a) Adsorption de l'APDMES

Les données obtenues avec l'APDMES, présentées en Tableau 4, indiquent la masse de silane adsorbés (en ng par centimètre carré de la sonde) à t_i, qui correspond à la fin de l'adsorption initiale, et à t = 30 min. Le montant équivalent de silane (nmol/cm ²), calculé à partir de la masse adsorbée et la masse molaire du composé hydrolysé (133,26 g/mol), est également donné dans ce tableau. En outre, pour chaque masse

adsorbée, une autre valeur est introduite, nommée le "montant équivalent retenu". Cette valeur correspond à la masse de silane qui est retenu sur la surface d'un type de pâte de cellulose, d'une surface spécifique de 3 m² / g, selon les paramètres de notre modélisation (fibres parfaitement cylindriques, non poreuses, couvrant toute la surface).

Temperature (°C)	*pH*	*Silane concentration (%)*	*Adsorbed mass at t_1 (ng/cm²)*	*Silane amount at t_1 (nmol/cm²)*	*Equivalent amount retained at t_1 (mg/$g_{cellulose}$)*	*Slope after initial adsorption*	*Adsorbed mass at t=30mn (ng/cm²)*	*Silane amount at t=30mn (nmol/cm²)*	*Equivalent amount retained at t=30mn (mg/$g_{cellulose}$)*
25°C	4	0,1	25	0,188	0,239	0,0166	61	0,458	0,583
		0,2	28	0,210	0,267	0,0103	46	0,345	0,439
		0,4	66	0,495	0,630	0,0575	165	1,238	1,576
	11,5	0,1	145	1,088	1,385	0,0508	245	1,839	2,340
		0,2	302	2,266	2,884	0,0576	384	2,882	3,667
		0,4	205	1,538	1,958	0,0482	273	2,049	2,607
45°C	4	0,1	7	0,053	0,067	0,0236	52	0,390	0,497
		0,2	30	0,225	0,286	0,0127	55	0,413	0,525
		0,4	50	0,375	0,477	0,0596	170	1,276	1,623
	11,5	0,1	105	0,788	1,003	0,0444	188	1,411	1,795
		0,2	230	1,726	2,196	0,0856	365	2,739	3,485
		0,4	160	1,201	1,528	0,0475	228	1,711	2,177

Tableau 4: Résultats pour l'APDMES

En outre, ce tableau indique les pentes observées sur nos courbes expérimentales après la période initiale d'adsorption, qui sont représentatives de la cinétique d'adsorption au cours de cette plage de temps de l'expérience. Comme prévu, ces valeurs sont inférieures dans des conditions de faible pH.

Nos valeurs expérimentales ont été confrontées à une approche théorique basée sur la zone de projection de notre composé sur la surface. A partie de cette valeur, nous avons évalué la quantité de silane nécessaire pour former une mono-couche sur notre surface modèle de cellulose et l'avons comparé à nos données. Pour l'APDMES, on obtient une valeur de 1,724 mg de silane par gramme de cellulose.

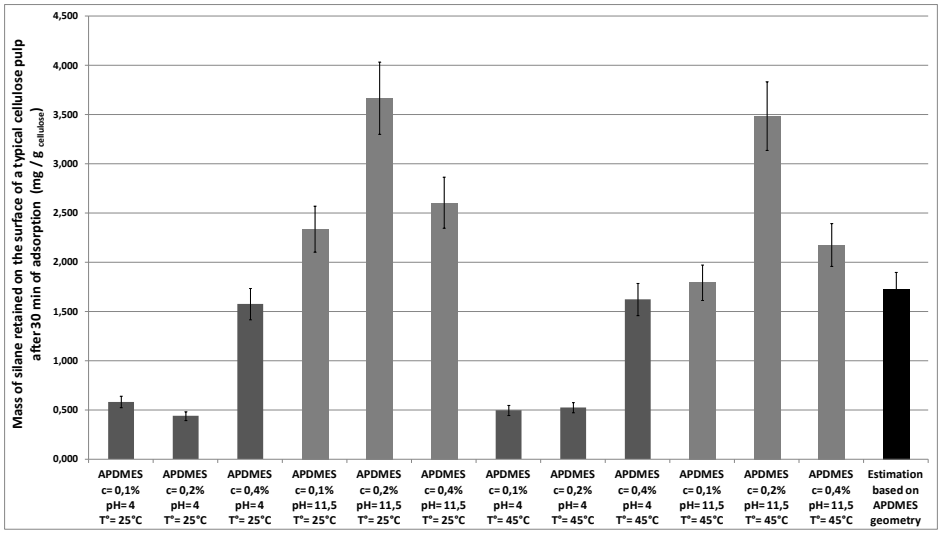

Figure 14: Estimation de la quantité d'APDMES adsorbée après 30mn.

Les valeurs d'adsorption obtenues à partir de nos données expérimentales et de notre modèle basé sur la géométrie sont comparées en Figure 14. Il apparait que l''adsorption mesurée à pH = 4 pour des concentrations de 0,1 et 0,2% est similaire. En conditions acides, seules les expériences à 0,4% de silane permettent d'atteindre l'équivalent d'une monocouche après 30mn. Pour toutes les expériences menées dans des conditions alcalines, le niveau d'adsorption atteint après 30mn est équivalent ou supérieur à la masse considérée comme nécessaire à la réalisation d'une monocouche de silane. Cependant, il doit être rappelé que l'adsorption se poursuit sur de longues durées, pouvant mener à l'adsorption de plus grandes quantités de silane.

b) Adsorption du DAMS

Pour le DAMS, une étude similaire à été menée, en se limitant à des concentrations de 0,2 et 0,4%. L'impact de la plus forte tendance à l'homo-condensation du DAMS transparait sur les pentes observées.

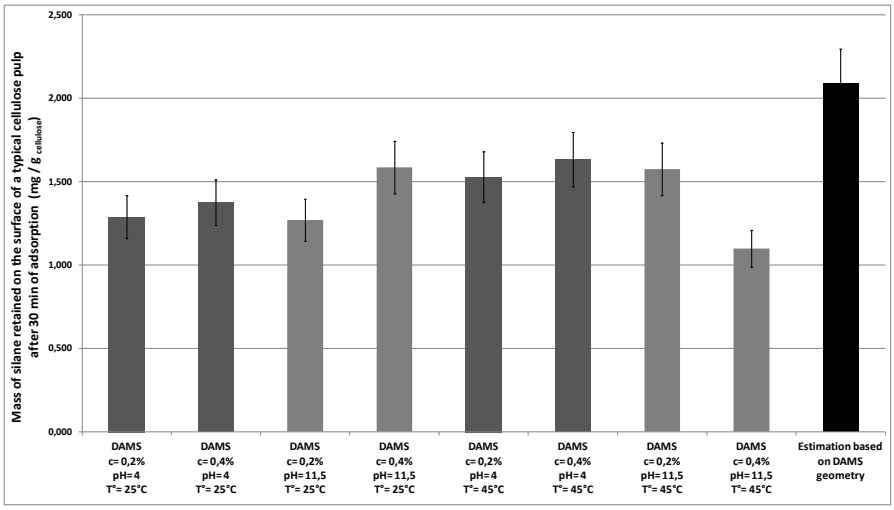

Pour ce composé, la masse molaire du composé hydrolysé est de 180,28 g/mol, et la quantité nécessaire à la formation d'une mono-couche complète d'après notre modèle géométrique est de 2,089 mg de silane par gramme de cellulose.

Figure 15: Estimation de la quantité de DAMS adsorbée après 30mn.

Les quantitées de silane adosrbées après 30mn de contact entre la solution et le substrat sont comparées à la valeur issue de notre modèle théorique en Figure 15. Il apparait que dans toutes les conditions testées, les masses adsorbées sont inférieures à ce qui serait nécessaire pour former une mono-couche. En outre, comparé à l'APDMES, il semble que la masse adsorbée soit moins sensible aux paramètres expérimentaux. Ces résultats montrent clairement que la nature du silane (mono- ou tri-alkoxy) influence non seulement les réactions en solution, mais aussi la capacité à s'adsorber sur un substrat cellulosique.

c) Adsorption du VDMES

Pour le VDMES, il n'a pas été possible d'observer d'adsorption pour des solutions ayant une concentration inférieure à 0,4%. Nous soupçonnons que les durées de pré-hydrolyses utilisées pour ce composé n'aient pas été suffisantes car à pH non modifié, il y a un décalage entre le début de l'expérience, et le moment où la mesure montre le début de l'adsorption qui n'est pas observée ailleurs.

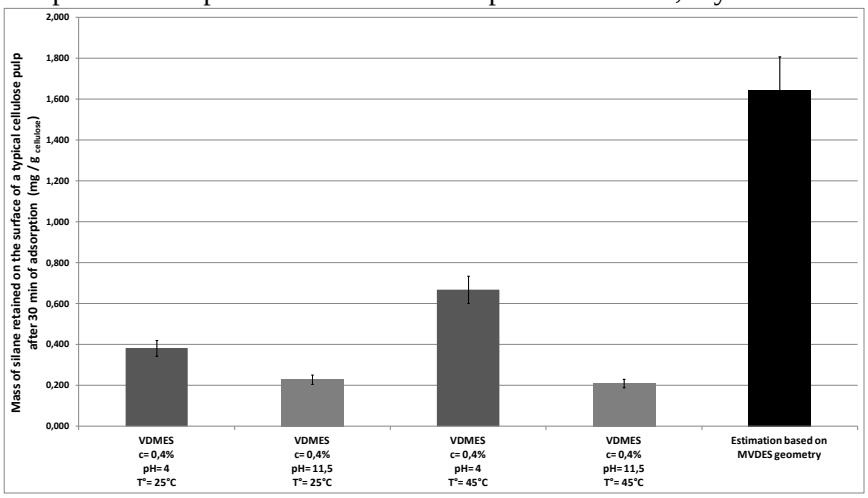

Pour ce silane hydrolysé, la masse molaire est de 102,21 g/mol, et la quantité estimée nécessaire à la formation d'une mono-couche est de 1.642 mg par gramme de cellulose. Cette valeur est comparée aux valeurs expérimentales d'adsorption après 30mn en Figure 16.

Figure 16: Estimation de la quantité de VDMES adsorbée après 30mn.

Il apparait que pour le VDMES, les quantitées de silane adsorbées à un moment donné sont bien plus faibles que celles obtenues avec des aminosilanes, et ce quelles que soient les conditions de pH et température utilisées. Cela confirme que la fonction amine portée par l'APDMES joue un rôle important sur les cinétiques d'adsorption observées pour ce composé. Néanmoins, les résultats présentés ici confirment

qu'il est possible d'adsorber un organosilane ayant une faible réactivité sur des surfaces de celluloses à partir de solutions purement aqueuses.

d) Adsorption sur des surfaces de silice

Afin de comprendre l'influence de la nature du substrat sur les valeurs mesurées, des tests ont été menés sur des surfaces de silice dans des conditions similaires à celles utilisées pour les surfaces de cellulose. Nous nous sommes limités à l'évaluation de l'adsorption de solutions d'APDMES et de DAMS en conditions acides à température ambiante. A pH non modifié, la fonction alcaline des organosilanes utilisés donnait lieu à une attaque du quartz, provoquant ainsi une perturbation de la mesure.

L'allure des courbes d'adsorption obtenues sur silice diffère peu de celle obtenue sur des surfaces de cellulose, en dehors du fait qu'ici il n'y a pas de continuation de l'adsorption après la fin de la première période. En effet, on arrive à un plateau après seulement quelques minutes de contact pour toutes les conditions utilisées.

La quantité mesurée de silane adsorbé après 30 minutes sur des surfaces de silices est comparée à celles mesurées sur des surfaces modèles de cellulose en Figure 17. Les valeurs données tiennent compte des écarts entre les surfaces spécifiques des deux matériaux. La première observation est que, pour toutes les expériences, les valeurs obtenues sur les deux substrats ont un ordre de grandeur similaire. Toutefois, les quantités adsorbées sur de la silice sont systématiquement plus élevés que celles adsorbés sur de la cellulose en conditions identiques. Deux explications peuvent être proposées pour cette observation. Tout d'abord, il est possible que la surface spécifique retenu pour les capteurs de cellulose ait été surestimée, affectant ainsi négativement l'évaluation de la quantité de silane retenu sur ce substrat. Ou bien, les silanes ayant une affinité plus forte envers les hydroxyles de silice qui ont un caractère plus acide que ceux de la cellulose [23], cela pourrait avoir une incidence sur l'adsorption. Les différences observées sont plus importantes pour le DAMS que pour l'APDMES.

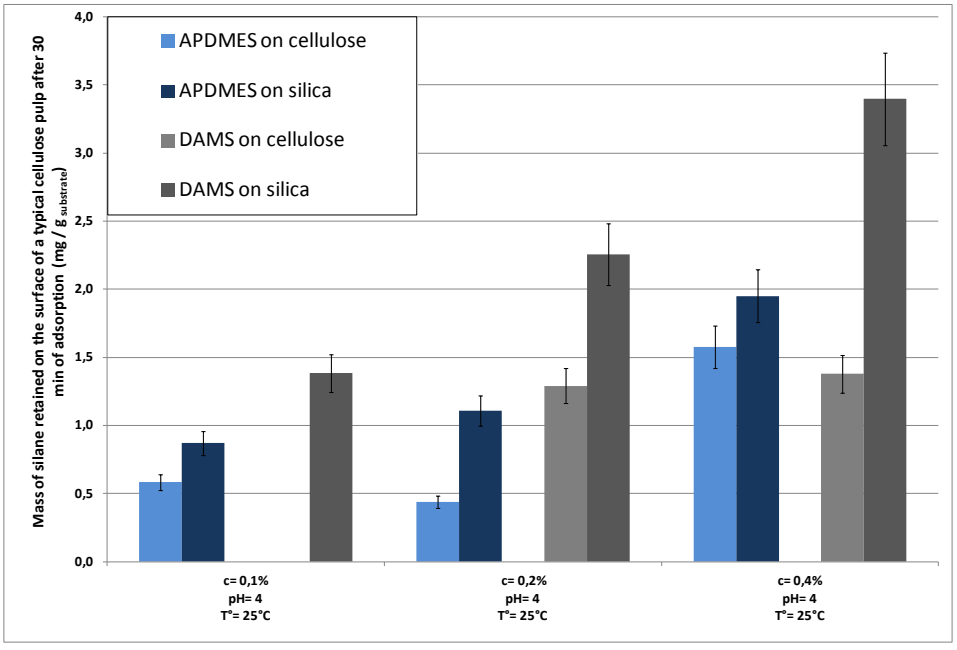

Figure 17: Comparaison entre les adsorptions sur cellulose ou silice.

Par ailleurs, il apparait que pour les capteurs de silice, la quantité de silane retenue augmente nettement avec la concentration de la solution, pour les deux silanes. Contrairement à ce qui est observé pour les APDMES, où une augmentation de 0,4% peut réduire l'adsorption sous certaines conditions.

Enfin, la différence la plus significative entre les deux surfaces pourrait être le fait que sur la cellulose, la quantité adsorbée continue d'augmenter, un phénomène qui n'a pas été détecté sur les substrats de silice. Pour expliquer cela, nous proposons de prendre la structure de la cellulose en compte. Effet, alors que la silice est une matière cristalline, la cellulose est un polymère organique. Même si les fibrilles utilisées pour la préparation des capteurs ne sont pas poreuses, elles peuvent gonfler ou absorber de l'eau. Par conséquent, nous proposons que cette différence de comportement soit due à l'absorption d'une quantité d'eau, ou de silane qui pénétrant dans la structure de la couche de cellulose progressivement au fil du temps.

Conclusions

En conclusion, il apparait que le travail de recherche original présenté dans cette partie est particulièrement enrichissant dans le cadre de notre étude. En effet, l'approche utilisée a permis la détermination de la cinétique de l'adsorption de trois silanes différents sur des surfaces modèles de cellulose, et a permis de mesurer quantitativement les teneurs en silanes retenues dans différentes conditions, au cours du temps. Il a été clairement démontré que les silanes hydrolysés s'adsorbent sur des fibres de cellulose, en seulement quelques minutes de temps de contact. En outre, ce résultat a été étendu à des surfaces de silice modèle, ce qui a permis de discuter l'influence de la structure de la cellulose sur les mesures effectuées. Aussi, l'effet de différents paramètres, à savoir la concentration, la température et le pH, a été discutée. Il a été montré par ailleurs que les molécules étudiées se comportent différemment en fonction de leur groupement fonctionnel et du nombre de leurs groupes hydrolysables. Enfin, les valeurs expérimentales obtenues à partir de notre analyse ont été comparés avec un modèle théorique simple, construit dans le but d'établir la quantité de molécules nécessaires pour fournir une couverture complète de la surface.

Partie 3 - Interactions silane-cellulose.

I. Modification de la cellulose par les silanes : littérature.

La caractérisation de l'adsorption de silanes sur des surfaces de cellulose, à partir de solutions aqueuses, a été décrite dans la partie précédente. Une fois le silane adsorbé, la question qui surgit concerne le type de liaison qui s'établi avec la cellulose et notamment s'il s'agit d'une liaison covalente (condensation entre OH du silanol et OH de la cellulose). Afin de mieux comprendre les phénomènes en jeu, cette partie présente les résultats de différentes techniques analytiques scrutant la matière à des échelles différentes.

a) Modification de la cellulose

La modification chimique des fibres de cellulose par diverses méthodes a été largement décrite dans la littérature [49], [50]. Dans la plupart des cas, la modification vise à modifier les propriétés de surface des fibres pour les rendre compatible avec l'application [51]. Dans un tel contexte, diverses techniques ont été décrites, tel que le greffage d'anhydride réactifs ou d'isocyanate [52], [53], le greffage d'acide succinique ou maléique [54], ou encore l'estérification de fibres de cellulose avec des chlorures d'acides gras [55].

La modification des produits cellulosiques par les organosilanes a été tentée par différentes équipes, en général dans des milieux réactionnels à base de solvants organiques. En outre, il y a plusieurs années, notre groupe a lancé une activité de recherche basée sur le greffage des fibres de cellulose [12-17], [23], [56-58]. La plupart des études ont été réalisées dans le but de valoriser les fibres de cellulose comme matériaux de renforcement dans des matrices organiques. Cependant, les mécanismes de réaction pouvant différer de ceux survenant lors du greffage de matériaux inorganique, nos travaux antérieurs ont montré que la réaction entre la cellulose et les alkoxysilanes ne peut avoir lieu que si les étapes suivantes sont respectés, à savoir: (i) l'agent de greffage est préalablement hydrolysé, (ii) le silanol résultant de cette hydrolyse est adsorbé à la surface de la cellulose, (iii) le complexe cellulose/silane formé est isolé de la phase liquide, (iv) la phase solide obtenue est séchée et traitée thermiquement, et (v) la cellulose modifiée obtenue est extraite au Soxhlet afin d'éliminer les molécules adsorbées physiquement non-réagies, avant d'être utilisée et / ou caractérisée

Dans ces études, les conditions optimales pour la réaction des agents de couplage avec la cellulose ont été établies. Il a été montré que, dans tous les cas, la présence de l'agent de greffage a été détecté à la fin de la réaction et après l'élimination des molécules non-réagies. Toutefois, seuls des trialkoxysilanes ont été étudiés, et l'utilisation de réactifs trifonctionnels ne permet pas de déterminer avec certitude si une liaison covalente avec la cellulose (Si-O-cellulose) est formée. En effet, les trialkoxysilanes pouvant subir des réactions d'homo-condensation et former des réseaux tridimensionnels insolubles, il est possible que des macromolécules siliconées non extractibles se forment autour des fibres sans pour autant que ces structures soient liée chimiquement au substrat. En outre, la plupart des travaux présentés portent sur des modifications effectuées dans un mélange d'éthanol et d'eau, hors il est possible que les réactions effectuées dans les médias purement aqueux puissent produire des structures différentes, notamment en raison de la différence de polarité entre ces solvants.

Ainsi, il apparait qu'un manque de connaissances existe concernant les interactions entre la cellulose et les silanes. Bien que de nombreuses données supportent l'idée généralement acceptée que la liaison covalente est possible entre les groupements hydroxyles de la cellulose et les silanol, il est nécessaire d'acquérir davantage de données sur ce sujet. Pour cela, il semble essentiel d'utiliser des molécules qui ne peuvent pas former de réseaux tridimensionnels, ainsi que des moyens d'analyse adaptés.

b) Techniques de caractérisation

La plupart des techniques utilisées pour la caractérisation de surface sont basées sur des sondes, utilisées pour irradier la surface, ce qui provoque l'émission de signaux spécifiques de la composition de la surface. Diverses sondes telles que des photons, électrons ou ions sont utilisées, avec chacune ses avantages et ses inconvénients. Par conséquent, il est souvent nécessaire d'utiliser plus d'une technique, afin d'acquérir une compréhension complète de la surface.

Plusieurs techniques sont disponibles pour déterminer les propriétés de la surface d'un matériau. Certaines d'entre elles concernent des aspects topographiques et optiques, ou encore donnent des informations de manière indirecte tel que l'angle de contact, tandis que d'autres donnent des informations sur la composition chimique. Dans cette dernière famille, il y a des analyses directes donnant un aperçu très précis sur la structure chimique de la surface, avec une profondeur d'analyse spécifique à chaque technique. Deux techniques sont particulièrement adaptées à l'étude de la modification chimique d'une surface : l'XPS et le ToF-SIMS. L'XPS a une profondeur d'analyse inférieure à 10 nm et fourni des spectres en faibles ou hautes résolutions. Dans le premier cas, on obtient une détermination de la composition élémentaire de la surface, tandis qu'en haute résolution, la déconvolution des pics correspondant à chaque atome permet de déterminer l'état électronique des éléments analysés. En comparaison, le ToF-SIMS permet une analyse bien plus fine de la surface, avec une profondeur d'analyse correspondant à la première couche moléculaire (environ 1nm). Cette technique est basée sur un bombardement de la surface par un faisceau d'ions pulsé, qui éjecte des ions secondaires spécifiques de l'échantillon. Cette technique bénéficie d'une excellente résolution en masse et donc est très sensible. Des exemples d'utilisation de cette technique pour l'analyse de la modification de substrats par les organosilanes sont décrits dans la littérature [59-62].

II. Partie expérimentale

Trois organosilanes ont été étudiés dans cette partie : le méthylvinyldiethoxysilane (MVDES), le 3-aminopropyldimethylethoxysilane (APDMES) et le 3-(2-amino-ethylamino)-propyltrimethoxysilane (DAMS). Ces composés ont été utilisés pour la modification de fibres de résineux blanchies et traitées selon le procédé Kraft. Après la modification en phase hétérogène, des formettes ayant un grammage proche de 110 g/m² ont été préparées et analysées. Dans certains cas, un traitement thermique de 1h à 110°C et/ou une extraction solvant ont précédé l'analyse.

Suite aux premiers résultats de nos analyses, le protocole de formation des échantillons à été modifié afin de diminuer le risque de contamination de la surface des échantillons durant la production. Différentes analyses ont été mise en œuvre, tel que : SEM-EDX, XPS, RMN solide, ou ToF-SIMS. En outre, une première série d'expériences portant sur l'évaluation de deux différentes méthodes d'extraction solvant et de divers solvants organique a été réalisée à l'aide du SEM-EDX. Cette étape a permis la sélection d'un protocole adapté pour enlever les molécules de silanes non greffées à l'aide d'un appareil d'extraction sous pression à haute température en combinaison avec de l'acétone.

a) Caractérisation de l'interface silane-cellulose

Pour chaque silane, différent échantillons ont été préparés et comparés avec des échantillons n'ayant subi aucun traitement. Dans chaque cas, (i) un échantillon modifié et n'ayant subi aucun autre traitement, (ii) un échantillon modifié puis ayant subi un traitement thermique, (iii) un échantillon modifié puis ayant subi une extraction solvant et enfin (iv) un échantillon modifié, traité thermiquement puis extrait, ont été préparés.

Une première analyse en SEM-EDX (voir Figure 18) a démontré la présence de silicium (élément signature du silane) sur les échantillons modifiés par l'APDMES. Il apparait aussi dans cette analyse (de manière qualitative) que le traitement thermique diminue légèrement la quantité de silane détectée, tandis

que l'extraction solvant enlève presque toute la matière apportée lors de la modification des fibres. Enfin, un traitement thermique réalisé avant l'extraction permet de maintenir une quantité de silane relativement importante.

Pour les échantillons traités avec le VDMES, il n'y a pas de silicium détecté, mais cela peut être dû à la faible sensibilité de la technique puisqu'il a été montré dans la seconde partie de ce travail que ce composé s'adsorbe sur la cellulose en faibles quantités. Enfin, les échantillons traités par le DAMS montrent une importante quantité de silane qui n'est pas ou peu affectée par les différents traitements, contrairement à l'APDMES.

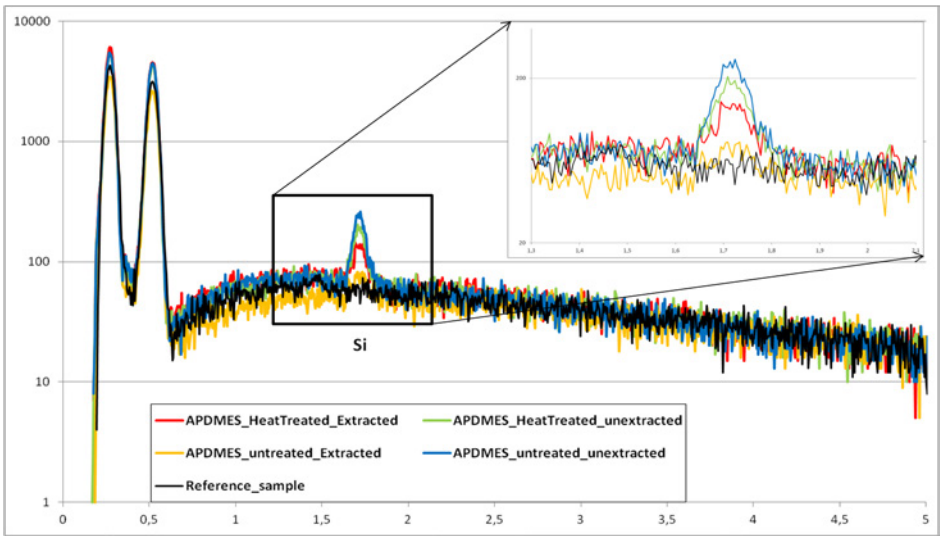

Figure 18: Spectre SEM-EDX pour les échantillons modifies à l'APDMES.

Pour chaque molécule, une partie d'échantillon ayant subit un traitement thermique suivi d'une extraction solvant a été broyée puis analysée par RMN solide du silicium. Dans le cas de l'APDMES (voir Figure 19), deux pics apparaissent sur le spectre obtenu après 48h d'analyse. L'un correspond au dimère formé par l'homo-condensation du silane, tandis que l'autre correspond soit à un monomère (mais ceci est peu probable au vu des résultats sur la rapidité de l'hydrolyse), soit à un silane greffé sur la cellulose. L'extraction subie par l'échantillon étant supposée enlever toutes les molécules non greffées, y compris les dimères, l'existence de deux pics est inattendue. Pour expliquer cela, il est possible de considérer le fait que la structure poreuse de la cellulose a pu permettre la rétention de molécules non-greffées malgré l'efficacité du lavage. Pour s'affranchir de cet effet de porosité, il est nécessaire de faire appel à des techniques d'extrême surface.

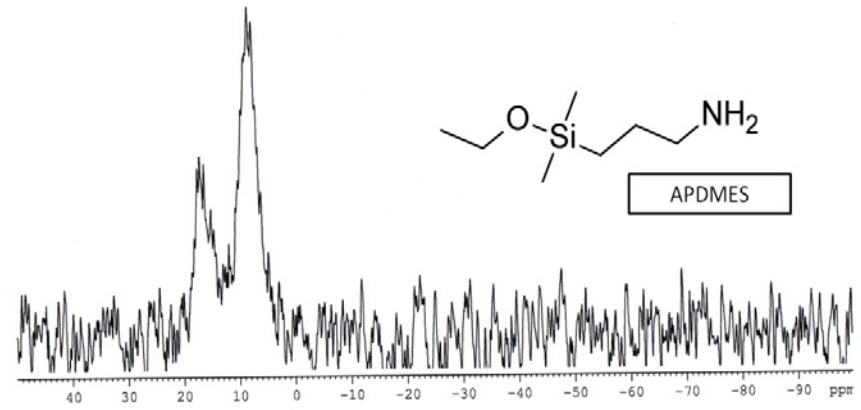

Figure 19: Spectre RMN solide ^{29}Si CP/MAS pour des fibres modifies avec l'APDMES.

Pour les fibres modifiées avec le VDMES, malgré une durée d'analyse portée à 72h, aucun signal de silicium n'a été obtenu. Cela n'est pas inattendu, la RMN solide étant une technique de masse et ayant donc une faible sensibilité. Quant aux fibres modifiées par le DAMS, l'analyse en RMN solide montre l'existence d'au moins deux environnements différents pour le silicium, l'un correspondant à des molécules de silane totalement condensées, et l'autre à des molécules ayant au moins un hydroxyle libre ou greffé sur la cellulose.

b) Caractérisation chimique de la surface

i. XPS

Afin de mieux comprendre la nature des interactions entre les silanes et la cellulose, les séries d'échantillons produites avec chaque silane selon le protocole amélioré ont été analysées par XPS. Cette technique s'est montrée particulièrement adaptée pour observer les modifications de la surface en termes de composition atomique. En l'occurrence, les principaux changements se produisant lors de la modification sont associés à la présence d'atomes non présents dans la cellulose non modifiée. À savoir : le silicium pour les trois agents de couplage et l'azote pour les deux aminosilanes (DAMS et APDMES). Les spectres en basse résolution de chaque échantillon ont pu être enregistrés. Comme prévu, pour les feuilles de papier non modifiées, les spectres montrent la présence de deux atomes principaux, dont les pics correspondants situés à 285 et 531 eV sont attribués aux atomes de carbone et d'oxygène respectivement. Les échantillons modifiés, cependant, montrent l'apparition de trois signaux supplémentaires, à savoir: (i) un nouveau pic à près de 398 eV, correspondant à l'azote pour les échantillons traités au DAMS et à l'APDMES, et (ii) deux autres bandes supplémentaires à 102 et 150 eV, correspondant aux atomes de silicium (Si_{2s} et Si_{2p} respectivement) et qui ont été observés pour les trois séries d'échantillons. Le spectre d'un échantillon traité à l'APDMES est présenté en Figure 20.

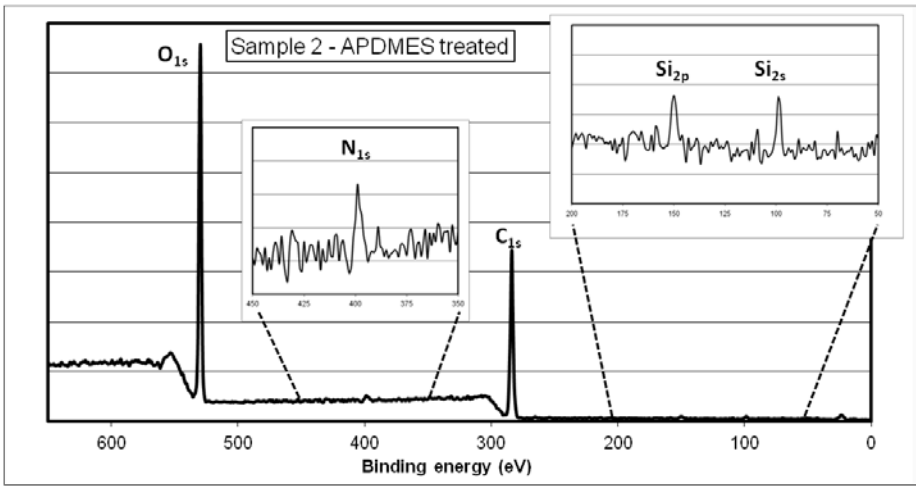

Figure 20: XPS spectrum of APDMES treated fibers.

Sample number	Treatment			Atom composition (in %)				Atomic ratio	
	Silane	Heat	Extraction	C	O	N	Si	O/C	N/Si
1	None	yes	yes	60,6	39,4	0,0	0,0	0,65	-
2	APDMES	no	no	59,8	38,0	1,3	0,9	0,64	1,56
3		yes	no	60,4	37,6	1,2	0,8	0,62	1,41
4		no	yes	59,6	39,7	0,5	0,2	0,67	2,70
5		yes	yes	60,5	38,2	0,8	0,6	0,63	1,33
6	VDMES	no	no	61,2	38,0	-	0,3	0,62	-
7		yes	yes	59,3	39,9	-	0,2	0,67	-
8	DAMS	no	no	66,1	32,3	1,2	0,4	0,49	2,79
9		yes	yes	61,7	35,7	1,5	1,1	0,58	1,29

Tableau 5 : Composition atomique des surfaces obtenue par XPS.

Les données présentées dans le Tableau 5 montrent la composition atomique des échantillons de cellulose modifiés ayant subi, ou non, différents traitements, ainsi que la composition d'un échantillon de référence. Il apparait que les éléments signatures de la modification apparaissent sur tous les échantillons traités, y compris sur ceux modifiés par le VDMES, alors que les analyses en SEM-EDX et RMN solide de ces échantillons ne montraient pas de trace de la modification. Cependant, les quantités détectes de ce silane sont

particulièrement faibles et présentent des écarts-types importants, ce qui suggère une déposition irrégulière sur la surface. Il apparait aussi que, bien qu'après traitement thermique la quantité de silane retenu sur la cellulose soit bien plus importante, même en son absence une faible quantité de silane reste après extraction.

Le ratio O/C n'est pas particulièrement affecté par la modification par l'APDMES, ce qui peut être expliqué par la faible taille des molécules déposées. Pour la modification par le DAMS, une légère modification du ratio apparait, ce qui se justifie par le plus grand nombre de CH_2 porté par cette molécule. Pour les ratios N/Si, des irrégularités par rapport aux valeurs théoriques sont observées pour certains échantillons, qui sont dues aux faibles valeurs mesurées et aux écarts-types de nos mesures sur ces échantillons.

Grâce à l'XPS, il a été possible de faire une première estimation de la quantité de silane retenue après la modification pour trois silanes différents, ainsi que de l'impact de certains traitements sur cette quantité. Malheureusement, du fait des forts écarts-types observés lors de nos analyses, il n'a pas été possible d'exploiter les spectres du carbone en haute résolution, qui auraient pu donner une indication sur une éventuelle modification de l'environnement de certains carbones de la cellulose, due au greffage des silanes. Les faibles quantités détectées se justifient par le fait que, dans l'hypothèse où la modification à lieu essentiellement à la surface de la fibre, la profondeur d'analyse de l'XPS (qui est proche de 10nm) est trop grande pour faire une analyse fine de la composition de l'extrême surface. De fait, nous avons fait appel à une technique encore plus sensible : le ToF-SIMS.

ii. ToF-SIMS

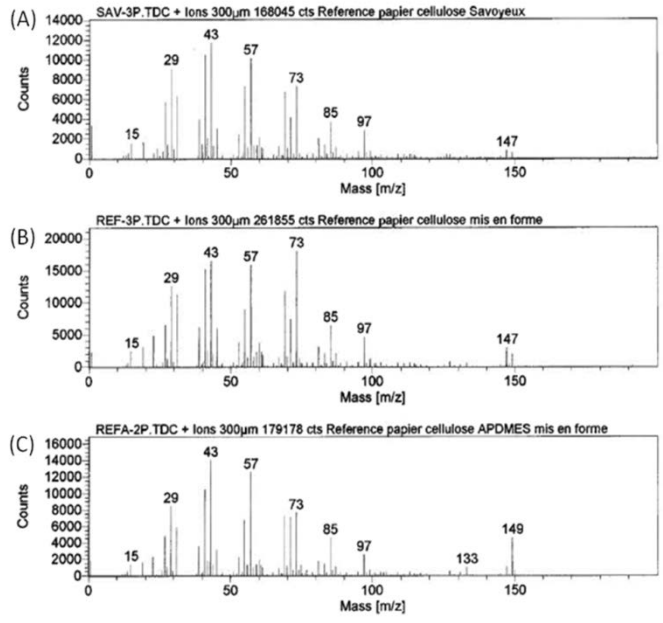

Figure 21: Spectres ToF-SIMS en mode positif (m/z=0 à 200) de (A) "Savoyeux"; (B) feuille de fibres non modifiées; (C) feuille de fibres modifiées APDMES.

L'étude réalisée à l'aide du ToF-SISM a été divisée en deux parties. Tout d'abord, une première série de tests a visé à déterminer si le protocole initialement utilisé pour la production de formettes de papier donnait lieu à des contaminations de surface ou non. Ensuite, une seconde étude ayant pour but d'analyser les modifications de la composition chimique de la surface des échantillons résultant de la modification par les silanes.

Lors de cette première partie, il est apparu (Figure 21) que les spectres obtenus pour des fibres non modifiées ou des fibres modifiées étaient parfaitement similaires à celui obtenu pour une feuille de "Savoyeux", qui est un support de papier utilisé pendant la formation des formettes.

Bien que la plupart des pics apparaissant sur ces spectres correspondent à la cellulose [63], tel qu'à : m/z(+) = 57 ($C_4H_9^+$), 115 ($C_8H_3O^+$), 127 ($C_6H_7O_3^+$), 135 ($C_6H_{15}O_3^+$), ou encore m/z(-) = 45 ($C_2H_5O^-$), 59 ($C_2H_3O_2^-$), 71 ($C_3H_3O_2^-$), 87 ($C_3H_3O_3^-$), 101 ($C_4H_5O_3^-$) et 113 ($C_5H_5O_3^-$), d'autres pics ont été identifiés. En particulier, les pics apparaissant à m/z(+) = 73 ($C_3H_9Si^+$), 133 ($C_3H_9Si_2O_2^+$) et 147 ($C_5H_{15}Si_2O^+$) appartiennent aux polydimethylsiloxanes (PDMS) et celui à m/z(+) = 149 ($C_8H_5O_3^+$) correspond aux phtalates. Ces deux contaminants communs pouvant provenir du processus de fabrication du Savoyeux, qui est un substrat commercial, il a donc été décidé de modifier le protocole de formation des feuilles afin de

s'affranchir de l'utilisation de ce substrat. Des expériences complémentaires ont montré que le spectre de fibres de cellulose non modifiées produit par ce nouveau protocole ne contenait plus les pics associés à ces contaminants, confirmant ainsi l'origine des contaminations observées précédemment.

La seconde partie de cette étude en ToF-SIMS a permis de comparer les spectres d'échantillons silanés ayant subi différents traitements, entre eux et avec celui de la cellulose non modifiée. Concernant les résultats obtenus avec l'APDMES, un exemple de spectres obtenus pour la cellulose non modifiée comparée avec le spectre de fibres modifiées ayant subi un traitement thermique puis une extraction solvant est présenté en Figure 22.

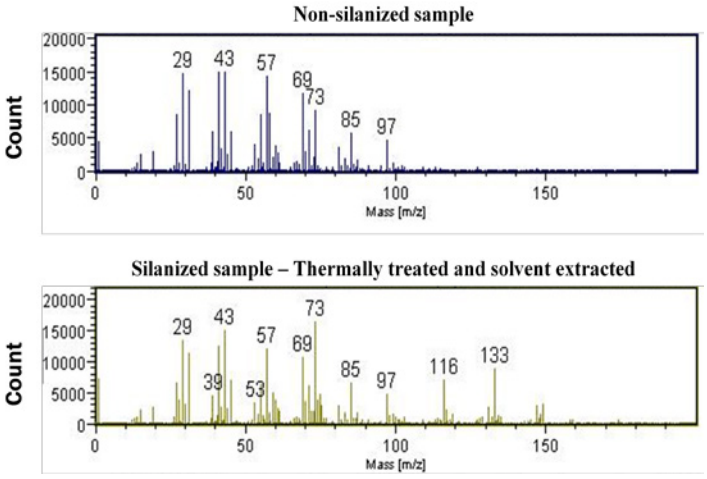

Figure 22: Comparaison des spectres ToF-SIMS en mode positif (m/z=0 à 200) d'une feuille de fibres non traitées et d'une feuille de fibres traitée avec l'APDMES et ayant subi un traitement thermique puis un lavage.

Pour ce silane, l'APDMES, chaque spectre montre les pics caractéristiques de la cellulose énumérés ci-dessus. Par ailleurs, les spectres montrent aussi la présence de fragments correspondant aux ions élémentaires spécifiques au silane, tel que m/z(+) = 28 (Si^+), en plus des ions élémentaires communs à la cellulose à m/z(-) = 12 (C^-) et 16 (O^-). Ces pics ne présentent pas de larges variations selon les traitements effectués. Cependant, d'autres pics élémentaires du silane à m/z(-) = 26 et 28, correspondant respectivement à CN^- and Si^- montrent de telles variations.

En se basant sur la littérature [64], le ratio entre l'intensité relative des pics correspondant à OH^- et CH^- à été comparé au ratio O/C obtenu en XPS, comme montré en Figure 23. Il apparait que le ratio O/C ne change pas de manière significative en XPS comme indiqué auparavant, tandis que des différences significatives sont mesurées pour le ratio OH^-/CH^-. Cette différence entre les deux techniques s'explique aisément par la plus grande sensibilité du ToF-SIMS qui met en valeur les changements de composition de l'extrême surface. Les variations observées en ToF-SIMS montrent une diminution de ce ratio, sauf pour l'échantillon ayant subi une extraction solvant sans traitement thermique au préalable. Cela est conforme aux tendances attendues au vu de la structure du silane greffé.

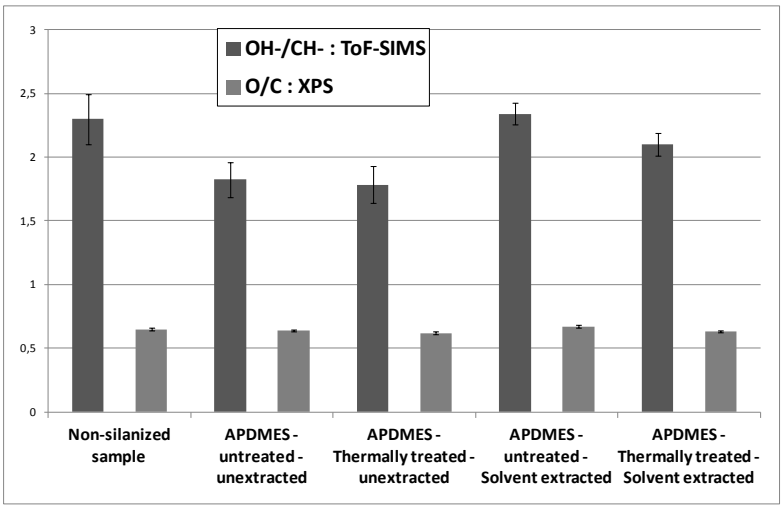

Figure 23: Comparison between the O/C ratio obtained by XPS, and the OH^-/CH^- ratio obtained by ToF-SIMS.

En ce qui concerne les fragments aux m/z plus importants, les pics significatifs se situent principalement en mode positif. En particulier, des fragments apparaissent à m/z(+) = 30, 73, 116, 133 and 190. Les structures proposées pour ces fragments sont données en Tableau 6. Les deux pics les plus importants

pouvant faire office de signature de la modification sont ceux présents à m/z(+) = 116 et à m/z(+) = 133. Le premier fragment peut avoir pour origine différentes structures : soit une molécule de silane hydrolysé, soit une molécule greffée sur le substrat, ou encore un dimère. Cette absence de distinction pose un problème puisque ce pic seul ne permet de démontrer l'existence d'une liaison chimique entre le silane et la cellulose. Concernant le pic à m/z(+) = 133, il ne peut survenir que dans le cas de la formation d'un dimère.

m/z(+) / Name	Formula	Structure
Hydrolyzed APDMES	$HO\text{-}Si(CH_3)_2\text{-}(CH_2)_3\text{-}NH_2^+$	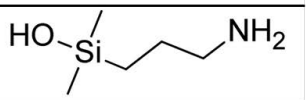
30	$CH_2\text{-}NH_2^+$	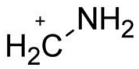
73	$SiC_3H_9^+$	
116	$-Si(CH_3)_2\text{-}(CH_2)_3\text{-}NH_2^+$	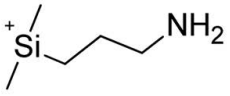
133	$(CH_3)_2Si\text{-}O\text{-}Si(CH_3)_2^+ + H$	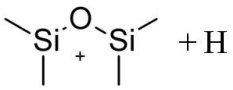
190	$-Si(CH_3)_2\text{-}(CH_2)_3\text{-}NH_2^+ + SiOC_2H_6$	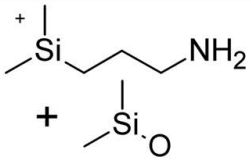

En comparant l'évolution de l'intensité relative de ces deux pics en fonctions des traitements auxquels les échantillons ont été soumis, il est possible de discuter l'effet de ces traitements. Le ratio entre les intensités relatives de ces deux pics est montré en Figure 24. Il apparait de cette comparaison que l'importance du pic à m/z(+) = 133 augmente lorsqu'un traitement thermique est réalisé, tandis qu'elle diminue lorsqu'une extraction solvant est faite.

Tableau 6 : Propositions de structures pour les pics caractéristiques de la modification par l'APDMES.

D'après ces données, il est évident que le traitement thermique, qui a pour but de favoriser le couplage entre la cellulose et le silane, a aussi pour effet de favoriser la formation de dimères. Bien que le protocole d'extraction utilisé permette d'enlever une grande part de ces dimères, l'analyse en ToF-SIMS montre qu'une part non négligeable de ces structures reste présente, y compris à l'extrême surface, après extraction. Il est intéressant dans le cas rencontré ici où deux fragments spécifiques sont identifiés et où l'un d'entre eux peut avoir différentes origines, de se tourner vers la littérature.

En effet, Dong *et al.* [65] ont démontré que lorsqu'une molécule siliconée portant une extrémité aminopropyl comme l'APDMES est fragmentée sous l'effet du bombardement des ions primaires dans le ToF-SIMS, des fragments signatures de la molécule sont détectés à m/z (+) = 116 car le mécanisme de fragmentation intervient préférentiellement au niveau de la liaison Si-O. En revanche, lorsqu'un dimère (cas d'une molécule liée par liaison siloxane) se fragmente, la répartition de la charge électronique au niveau du Silicium étant différente, la fragmentation va s'opérer préférentiellement sur la liaison Si-C, même si une certaine partie des molécules va encore se rompre au niveau de la liaison Si-O. Cela indique que le pic observé à m/z (+) = 116 à principalement pour origine des molécules non-greffées ou greffées et très peu de dimères. Le fait que ce pic représente une intensité relative important après les différents traitements auxquels les échantillons ont été soumis est une preuve indirecte qu'une partie du silane adsorbé réagit de manière forte avec la cellulose et ne forme pas de dimère. En outre, le fait que l'on observe une augmentation du ratio m/z (+) =116/133 après l'extraction solvant montre que le dimère est plus sensible au lavage que la structure donnant naissance au fragment détecté à m/z(+) = 116.

Si l'on considère que l'extraction à l'acétone opérée sur certains échantillons permet d'enlever les molécules adsorbées et non greffées chimiquement, alors on obtient une preuve indirecte de l'existence

d’une liaison chimique entre l’APDMES et la cellulose. Cependant, d’autres expériences doivent êtres réalisées pour lever les indéterminations dues à la présence de dimères et à la possibilité d’interactions ioniques entre les groupements amines de l’APDMES et les groupes carboxyliques de la cellulose pouvant exister dans les conditions utilisées pour nos réactions de greffage.

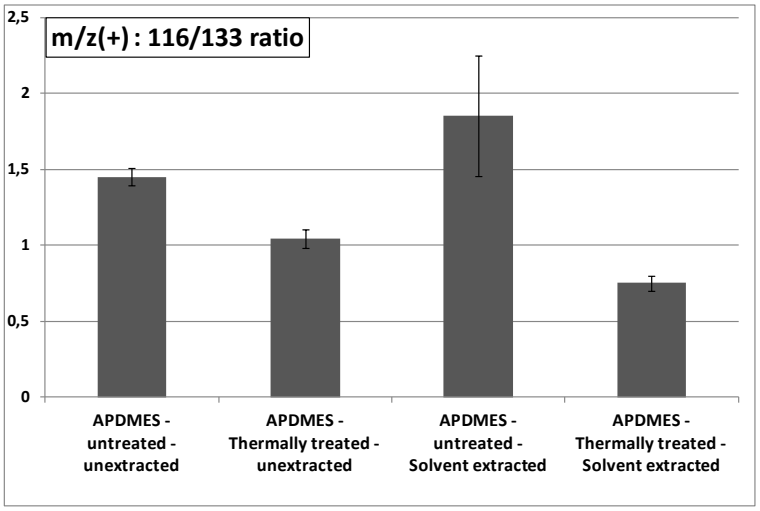

Pour les réactions faites avec le VDMES et le DAMS, les résultats sont plus mitigés. Dans les deux cas, des traces de contamination par l’APDMES ont été relevés sur les spectres. Cette contamination ne permet pas de donner de conclusions sur la présence de VDMES sur les échantillons modifiés. Pour le DAMS, bien que d’autres fragments caractéristiques aient pu être proposés, il est difficile de conclure en raison de ces contaminations.

Figure 24: Variation du ratio m/z(+) = 116/133 ratio pour les échantillons traités à l’APDMES

Conclusions

Dans cette partie, trois organosilanes, à savoir l’APDMES, le VDMES et le DAMS, ont été réagis avec des fibres de cellulose en suspensions aqueuses, puis les fibres modifiées ont été utilisées pour préparer des échantillons sous la forme de feuilles de papier. Il a d’abord été montré que les molécules non-greffées peuvent être éliminées par une extraction à l’acétone. Ensuite, les échantillons de papier modifiés ont été caractérisés par SEM-EDX, RMN solide, XPS et ToF-SIMS. Le ToF-SIMS a permis d'identifier précisément les fragments moléculaires supérieurs issus de la surface. Cette technique a été si sensible qu'elle a aussi permis d’identifier des contaminations de surface dues soit à une contamination par contact, soit à des phénomènes d'évaporation-adsorption de silanes. L’XPS et le ToF-SIMS ont montré indirectement qu'une interaction forte, très probablement de type greffage chimique, avait effectivement eu lieu entre la cellulose et au moins deux des agents de couplage. Les phénomènes de contamination observés ne permettent pas de conclure sur le greffage du VDMES.

Partie 4 - Impact de la modification par les organosilanes sur les propriétés du papier.

I. Fabrication du papier, douceur et propriétés mécaniques

Afin de tester l'impact de la modification de fibres cellulosiques par les organosilanes en suspensions aqueuses sur les propriétés de papiers obtenus à partir de ces fibres, nous avons appliqués les connaissances acquises dans les parties précédentes pour répondre à une problématique de l'industrie papetière.

La fabrication du papier est particulièrement complexe du fait de l'utilisation de nombreux additifs chimiques ainsi que de nombreux précédés mécaniques [66]. Les différentes étapes de la fabrication du papier vont de l'obtention de fibres ligno-cellulosiques à partir de ressources naturelles forestières, jusqu'à la mise en forme et la finition de la feuille. Ces différentes étapes présentées en Figure 25 doivent être contrôlées de manière à donner au papier ses propriétés finales. Cependant, certaines de ces étapes qui sont nécessaires à l'obtention de propriétés voulues peuvent parfois avoir un impact négatif sur d'autres propriétés. C'est le cas de l'étape de raffinage, qui est une opération mécanique durant laquelle les fibres sont soumises à des forces de compression et de cisaillement qui les fait gonfler, les coupe, et favorise la fibrillation. Cette étape essentielle à l'obtention de bonnes propriétés mécaniques a cependant pour inconvénient de diminuer le potentiel de douceur des fibres, un paramètre important pour les utilisateurs finaux de tissu. En effet, les papiers obtenus à partir de fibres fortement raffinés sont peu doux. A l'inverse, des fibres peu raffinées auront un bon potentiel de douceur, mais ne seront pas adaptées pour la production de papier résistant, ou pour des méthodes de production à cadence rapide, ce qui impacte négativement les profits des papetiers sur des applications telles que les tissus où la douceur est une propriété essentielle.

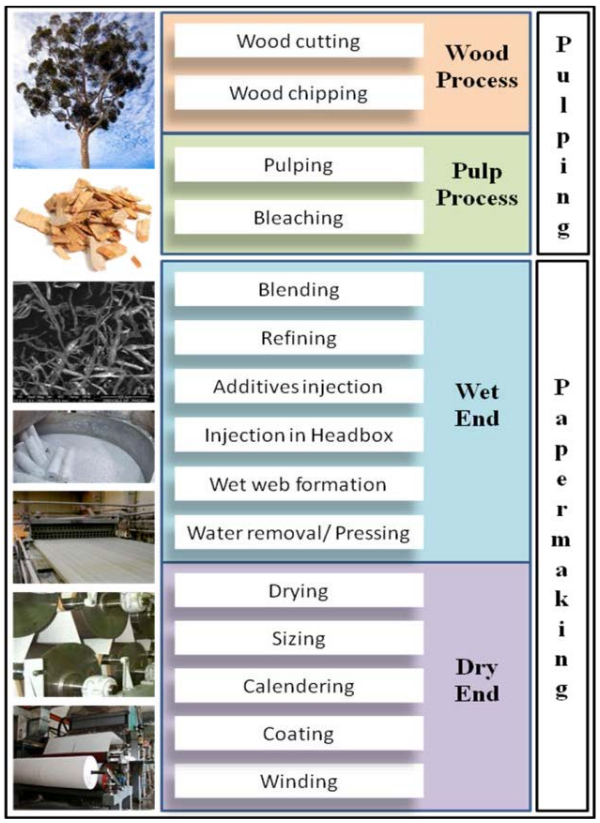

Figure 25 : Fabrication du papier

En ce qui concerne la propriété de douceur, elle est particulièrement difficile à décrire et à caractériser. C'est une propriété composite qui est le résultat de nombreuses qualité du matériau étudié, et qui dans le cas du papier à principalement deux composantes : la douceur de surface et la douceur de masse [67], [68]. Cette propriété est d'autant plus difficile à définir que sa perception varie selon les cultures et les pays. Bien que de nombreuses tentatives visant à mettre aux points des moyens de caractérisation de la douceur aient été réalisées [69], [70], à ce jour l'utilisation de panels de tests, mettant en œuvre des individus qualifiés pour comparer et évaluer des échantillons entre eux et par rapport à des références, reste la méthode la plus reconnue [68].

Pour les propriétés mécaniques, divers tests existent visant à évaluer la résistance du matériau papier à diverses contraintes. Les plus courants permettent d'évaluer des propriétés telles que la longueur de rupture

qui représente la résistance d'un papier à la traction longitudinale, ou encore l'indice d'éclatement ou de déchirement.

L'étude présentée ici prend place dans ce contexte. Elle vise à déterminer si la modification de la cellulose par les organosilanes représente une solution possible pour palier à l'antagonisme entre propriétés mécanique et douceur. Cette étude a été menée dans le cadre d'un projet de recherche industriel, "*Tissue+*" mené au Centre Technique du Papier et composé de plusieurs volets, dont celui traité ici, portant sur la fonctionnalisation de la cellulose

II. Partie expérimentale

L'étude présentée dans cette partie a été focalisée sur l'utilisation d'un seul silane, le 3-(2-amino-ethylamino)-propyltrimethoxysilane (DAMS). Trois types de fibres ont été analysés, deux résineux et un *Eucalyptus*. Le premier résineux correspondant aux fibres utilisées dans la partie précédente, son utilisation à été limitée à une étude préliminaire. Pour les autres fibres de résineux et d'*Eucalyptus*, plus utilisées dans la pratique industrielle pour l'application visée, les fibres ont été utilisées telles quelle, ou a deux intensités de raffinage différents. Toutes les fibres, aux différents niveaux de raffinage, ont été utilisées avec ou sans traitements par le silane pour faire des formettes qui ont été évaluées en terme de douceur et de propriétés mécaniques. Deux types de formettes ont été produits, des formettes de douceur ayant un grammage de l'ordre de 20g/m² et des formettes de rétention ayant un grammage proche de 110g/m². Dans tous les cas, les propriétés morphologiques des fibres ont été analysées avant et après traitement par le silane et il apparait qu'elles n'ont été significativement modifiées dans aucun cas.

Concernant les fibres de résineux utilisés dans la partie précédente de ce travail, le traitement au DAMS a permis des gains significatifs de propriétés mécaniques sans que la douceur soit affectée, comme montré dans le Tableau 7. En particulier, on observe une amélioration de 20% de la longueur de rupture pour les formettes de rétention et jusqu'à 40% pour les formettes douceur. Les indices d'éclatement et de déchirement mesurés uniquement sur les formettes de rétentions semblent aussi bénéficier de l'ajout du silane dans la préparation de la feuille, mais les écarts-types assez importants observés ne permettent pas de clairement statuer sur ce point.

***RsxTh* (32°SR)**			***Physical tests***							***Panel tests***
			Basis weight (g/m²)	**Thickness (µm)**	**Bulk (cm^3/g)**	**Breaking length (m)**	**Elongation (%)**	**Burst index: I_E (kPa/(m².g))**	**Tear index: I_D (mN/(m².g))**	**Softness (mean)**
Softness Handsheets	*Blank*	*x*	**23**	**136**	**5,87**	**1327**	**6,34**	-	-	**No distinctive difference between the blank and modified samples**
		σ(x)	0,7	5	0,25	69	1,15			
		σ%(x)	3,0	3,7	4,3	5,2	18,1			
	Silanized	*x*	**21**	**118**	**5,49**	**1879**	**6,68**	-	-	
		σ(x)	0,7	3	0,36	123	0,76			
		σ%(x)	3,3	2,2	6,6	6,6	11,4			
Retention Handsheets	*Blank*	*x*	**110**	**309**	**2,74**	**2129**	**1,74**	**1,87**	**3,72**	-
		σ(x)	1,3	20	0,17	263	0,42	0,28	0,42	
		σ%(x)	1,2	6,5	6,2	12,4	24,1	15,0	11,3	
	Silanized	*x*	**118**	**359**	**2,99**	**2576**	**2,43**	**2,03**	**4,01**	-
		σ(x)	2,4	14	0,10	280	0,39	0,17	0,62	
		σ%(x)	2,0	4,0	3,2	10,9	16,0	8,4	15,5	

Tableau 7: Propriétés mécaniques de la pâte de résineux 1, avant et après traitement par le DAMS

En se basant sur les bons résultats obtenus sur cette pâte de résineux, une autre pâte de résineux a été étudiée, à trois conditions de raffinages différentes. Avec cette pâte, il n'a pas été possible de produire des formettes douceur, et ce quel que soit le niveau du raffinage, après l'addition du silane. Par conséquent, aucune évaluation de douceur n'a pu être effectuée. La raison de cela est que l'addition du silane a augmenté la floculation, alors que la pâte vierge avait déjà tendance à floculer. Malgré ce phénomène de floculation, il

a été possible de produire des formettes de rétention avec des fibres non raffinées et des fibres raffinées à une intensité de 1,0 Ws / m. Toutefois, la pâte raffinée à 1,2 Ws/m n'a pas pu être utilisé ici non plus pour les mêmes raisons. Les résultats présentés dans le Tableau 8 montrent l'évolution des propriétés mécaniques suite au greffage des fibres par le DAMS. Des améliorations des propriétés sont observées, malgré les écarts-types assez importants. Plus précisément, la longueur de rupture augmente de 25% environ, l'indice d'éclatement de 38% environ, et l'indice de déchirement de 21% environ

Retention Handsheets			***Physical tests***						
			Basis weight (g/m^2)	**Thickness (µm)**	**Bulk (cm^3/g)**	**Breaking length (m)**	**Elongation (%)**	**Burst index: I_E ($kPa/(m^2.g)$)**	**Tear index: I_D ($mN/(m^2.g)$)**
RsxT+ Unrefined (13,5°SR)	*Blank*	*x*	**108**	**402**	**3,74**	**1032**	**1,18**	**0,9**	**2,02**
		σ(x)	2,2	5	0,08	145	0,18	0,12	0,19
		σ%(x)	2,0	1,3	2,1	14,1	15,3	13,3	9,4
	Silanized	*x*	**109**	**405**	**3,73**	**1304**	**1,4**	**1,27**	**2,4**
		σ(x)	2,7	15	0,1	153	0,19	0,11	0,31
		σ%(x)	2,5	3,8	2,7	11,7	13,6	8,7	12,9
RsxT+ 1,0 Ws/m (17°SR)	*Blank*	*x*	**108**	**384**	**3,6**	**1268**	**1,32**	**1,12**	**2,18**
		σ(x)	3,1	19	0,17	180	0,21	0,15	0,25
		σ%(x)	2,9	4,9	4,7	14,2	15,9	13,4	11,5
	Silanized	*x*	**113**	**403**	**3,57**	**1577**	**1,58**	**1,52**	**2,68**
		σ(x)	2,3	15	0,18	129	0,22	0,13	0,39
		σ%(x)	2,0	3,8	5,0	8,2	13,9	8,6	14,6
RsxT+ 1,2 Ws/m (23°SR)	*Blank*	*x*	**Flocculation**						
		σ(x)							
		σ%(x)							
	Silanized	*x*							
		σ(x)							
		σ%(x)							

Tableau 8: Propriétés mécaniques de la pâte de résineux 2, avant et après traitement par le DAMS

En ce qui concerne la pâte d'Eucalyptus, il a été possible de produire les deux types de formettes. Dans un premier temps, pour les formettes douceur, on peut noter que le traitement avec le DAMS a affecté la résistance à l'état humide des formettes, les rendant plus fragiles lorsque l'opérateur devait les enlever de la toile avant le séchage. Pour cette raison, il n'a pas été possible d'obtenir de telles formettes pour la condition de raffinage la plus intense. Deux explications sont proposées: (i) à un niveau supérieur de raffinage, et donc sur une pâte ayant une plus grande zone spécifique, une plus grande quantité de silane adsorbe, et l'action du silane favorise la floculation, conduisant à la formation de points de rupture du matelas fibreux humide, (ii) l'action du silane favorise la rétention d'eau et la quantité d'eau plus importante présente dans le matelas fibreux après sa formation ne permet pas de produire suffisamment de résistance à l'état humide pour permettre le retrait de la formette de la toile.

Softness Handsheets			***Physical tests***					***Panel tests***
			Basis weight (g/m^2)	**Thickness (µm)**	**Bulk (cm^3/g)**	**Breaking length (m)**	**Elongation (%)**	**Softness (mean)**
EucaT+ Unrefined (16°SR)	*Blank*	*x*	**22**	**110**	**5,05**	**895**	**2,04**	**3,8**
		σ(x)	0,6	4	0,3	85	0,23	
		σ%(x)	2,5	4,0	5,9	9,5	11,3	
	Silanized	*x*	**22**	**105**	**4,73**	**875**	**1,95**	**3,8**
		σ(x)	0,7	6	0,31	72	0,3	
		σ%(x)	3,0	5,2	6,6	8,2	15,4	
EucaT+ 0,2 Ws/m (20°SR)	*Blank*	*x*	**21**	**95**	**4,53**	**2031**	**4,12**	**1**
		σ(x)	0,1	3	0,15	109	0,36	
		σ%(x)	0,3	3,3	3,3	5,4	8,7	
	Silanized	*x*	**22**	**93**	**4,29**	**1936**	**3,7**	**0,5**
		σ(x)	0,2	3	0,15	162	0,45	
		σ%(x)	0,9	3,7	3,5	8,4	12,2	
EucaT+ 1,0 Ws/m (29°SR)	*Blank*	*x*	**22**	**96**	**4,44**	**1453**	**2,88**	**-**
		σ(x)	0,4	4	0,1	87	0,29	
		σ%(x)	2,0	4,2	2,3	6,0	10,1	
	Silanized	*x*	Impossible to withdraw wet sheets from wire					**-**
		σ(x)						
		σ%(x)						

Tableau 9: Propriétés mécaniques de la pâte d'*Eucalyptus*, avant et après traitement par le DAMS (formettes douceur)

Contrairement à ce qui a été observé sur les pâtes de résineux, la longueur de rupture n'est pas affectée par le traitement, de même que les autres propriétés mécaniques. Par ailleurs, comme le montrent les résultats des panels de tests, la douceur des papiers produits à partir de ces pâtes reste constante après la modification, comme indiqué dans le Tableau 9.

Pour les formettes de rétention, il a été possible de produire des échantillons à partir des trois conditions de raffinage. Pour ces formettes, les résultats présentés dans le Tableau 10 montrent que là aussi le traitement par le DAMS n'a pas affecté significativement les propriétés mécaniques ou la douceur des feuilles.

Retention Handsheets			***Physical tests***						
			Basis weight (g/m^2)	**Thickness (µm)**	**Bulk (cm^3/g)**	**Breaking length (m)**	**Elongation (%)**	**Burst index: I_E ($kPa/(m^2.g)$)**	**Tear index: I_D ($mN/(m^2.g)$)**
EucaT+ Unrefined (16°SR)	*Blank*	*x*	**110**	**366**	**3,33**	**955**	**1,28**	**0,5**	**1,58**
		σ(x)	1,1	18	0,17	90	0,24	0,05	0,21
		σ%(x)	1,0	4,9	5,1	9,4	18,8	10,0	13,3
	Silanized	*x*	**111**	**369**	**3,32**	**963**	**1,14**	**0,45**	**1,59**
		σ(x)	0,9	15	0,11	76	0,17	0,07	0,23
		σ%(x)	0,8	4,1	3,3	7,9	14,9	15,6	14,5
EucaT+ 0,2 Ws/m (20°SR)	*Blank*	*x*	**102**	**317**	**3,11**	**1702**	**1,13**	**0,74**	**2,92**
		σ(x)	0,8	17	0,15	174	0,18	0,1	0,33
		σ%(x)	0,8	5,4	4,8	10,2	15,9	13,5	11,3
	Silanized	*x*	**100**	**323**	**3,22**	**1681**	**1,83**	**0,94**	**3**
		σ(x)	0,7	11	0,11	189	0,35	0,08	0,41
		σ%(x)	0,7	3,4	3,4	11,2	19,1	8,5	13,7
EucaT+ 1,0 Ws/m (29°SR)	*Blank*	*x*	**110**	**362**	**3,24**	**1297**	**1,01**	**0,5**	**1,92**
		σ(x)	0,7	16	0,1	125	0,11	0,07	0,17
		σ%(x)	0,7	4,4	3,1	9,6	10,9	14,0	8,9
	Silanized	*x*	**113**	**348**	**3,11**	**1338**	**1,09**	**0,57**	**2,03**
		σ(x)	1,0	12	0,11	82	0,11	0,05	0,24
		σ%(x)	0,8	3,5	3,5	6,1	10,1	8,8	11,8

Tableau 10: Propriétés mécaniques de la pâte d'*Eucalyptus*, avant et après traitement par le DAMS (formettes de rétention)

Afin de comprendre pourquoi le traitement de fibres d'*Eucalyptus* par le DAMS ne donne pas les mêmes bénéfices que ceux obtenus lors du traitement de fibres de résineux, diverses expériences ont été réalisées.

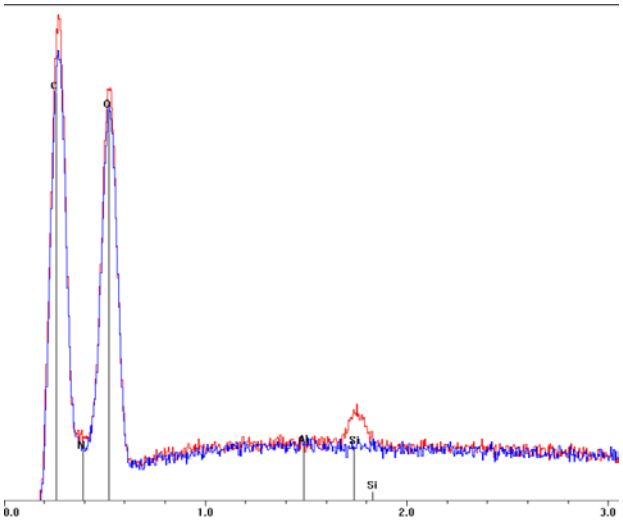

Figure 26: Spectres SEM-EDX de fibres d'*Eucalyptus* non modifiées, et modifiées par le DAMS

Tout d'abord, afin de vérifier que la modification avait bien eu lieu, des échantillons non modifies et modifiés ont été analysés en SEM-EDX. Ce test a montré la présence de silane en quantité qualitativement plus grande que pour les fibres de résineux. L'efficacité du protocole de modification étant avérée, il a été décidé de vérifier l'influence de la composition morphologique des fibres.

En effet, les analyses morphologiques ayant montré que les fibres d'*Eucalyptus* contenaient une plus grande proportion d'éléments fins, des tests ont été réalisé sur des pâtes nettoyées de leurs éléments fins. Les mesures ont montré que le taux d'éléments fins ne permet pas d'expliquer les différences observées entre les différents types de pâtes.

Enfin, avec le but de déterminer si la différence de chimie de surface entre les types de fibres pouvait justifier l'absence d'effets du traitement, des tests ont été réalisés sur une autre pâte d'*Eucalyptus*. De fait, la pâte utilisée jusque là a été soumise à un blanchiment à l'ozone lors de sa production, ce qui est connu pour causer une oxydation des fibres et augmenter leur charge négative. Cela peut affecter la nature des interactions silane-fibres dans les conditions utilisées dans ce travail, le silane sélectionné étant cationisé en conditions acides. Afin de vérifier cette hypothèse, des échantillons ont été préparés à partir d'une autre pâte d'eucalyptus, non traitée à l'ozone. Les tests réalisés sur les échantillons faits avec cette nouvelle pâte ont montré de légères améliorations de la longueur de rupture après le traitement par le DAMS, avec une augmentation allant jusqu'à 13%. Malgré les grands écarts-types associés à ces données, des améliorations légères en termes d'indice de rupture et de déchirure sont observées. En outre, il a été confirmé que la douceur n'est pas modifiée par le traitement, avec une pâte de feuillu. A partir de ces résultats, il apparaît que la chimie des fibres pourrait être impliquée dans le phénomène décrit ci-dessus, mais il est tout aussi évident que les effets positifs du traitement silane sur cette pâte sont très limités, en comparaison de ce qui a été observé sur des pâtes de résineux.

Afin de proposer un modèle pour expliquer le mode d'action du silane sur les fibres de résineux et l'apparente inefficacité sur les fibres d'*Eucalyptus*, nous avons utilisés les diverses observations exposées ci-dessus et pris en compte les différences connues entre ces fibres en termes de morphologie et de chimie. Dans les conditions utilisées pour les modifications réalisées dans ce travail, une assez grande quantité de silane est adsorbé à la surface des fibres. En outre, la variation du pH se produisant à l'étape de dilution, avant la formation de la feuille, est susceptible de favoriser l'auto-condensation de l'aminosilane utilisé ici. Cet aminosilane présente un caractère hydrophile élevée qui pourrait favoriser la rétention des molécules d'eau. Dans l'ensemble, il est possible que le traitement appliqué sur les fibres donne naissance à une interphase riche en hydroxyles à la surface des fibres. Cette interphase serait alors très hydratée et favoriserais la rétention d'eau pendant le séchage, agissant ainsi comme un additif de résistance à sec. Un tel réseau formerait une couche favorable à la zone de contact entre les fibres et agirait de la même manière que par exemple les xylanes [71]. La formation d'une telle structure sous forme de gel à l'échelle locale de la surface pourrait apporter des améliorations significatives dans le cas des fibres dont la composition est pauvre en xylane, comme des fibres de résineux. Toutefois, dans le cas de matériaux déjà riches en xylanes, tels que les fibres d'eucalyptus, cet effet serait déjà apporté par la fraction de composés présente à la surface et donc on n'observerait pas d'améliorations des propriétés physiques suite à l'ajout du silane. Bien entendu, le mécanisme proposé doit être considéré comme hypothétique et devrait faire l'objet d'une étude plus approfondie.

Conclusions

Les travaux décrits dans cette partie et réalisés dans le cadre d'un projet avec des partenaires industriels portent sur l'évaluation de l'utilisation des organosilanes dans les applications de fabrication de papier. Les effets de l'ajout d'un aminosilane dans différentes pâtes ont été étudiés, et les données obtenues ont été discutés. Cette discussion a conduit à la proposition d'un mécanisme pour les interactions entre le silane sélectionné et les fibres. La méthode présentée s'est révélée efficace pour modifier certaines pâtes, mais pas pour les fibres d'*Eucalyptus*. Malheureusement, ce type de fibre est largement utilisé dans les applications liées à la douceur, ainsi l'intérêt de la modification de la cellulose par le DAMS pour ces applications est faible. En outre, des quantités de silane beaucoup plus importantes que ce qui ce fait d'habitude ont été utilisées dans cette étude. Aussi, la formation de la feuille dans une machine à formette de laboratoire est loin d'être similaire à celle ayant lieu dans une machine à papier industrielle. En conséquence, il serait très difficile de prévoir les améliorations apportées par le traitement proposé ici sur une production à échelle industrielle. Seuls des essais pilotes peuvent permettre la transposition de nos résultats en conditions industrielles réelles.

Conclusions générales

Dans le contexte de la valorisation des ressources bio-renouvelables, ce travail de thèse a été consacrée à la modification des fibres cellulosiques par les organosilanes. Plus particulièrement, avec l'objectif de pouvoir intégrer le processus de fabrication du papier, nous avons concentré notre recherche sur la réalisation de telles modifications en milieux purement aqueux. Très peu de littérature étant disponibles sur ce sujet lorsque le projet a été initié, nous avons orientés nos travaux selon deux axes principaux : la caractérisation des réactions des silanes dans des milieux aqueux et la compréhension des interactions entre ces molécules et les substrats fibreux. Pour terminer, nous avons aussi fait une étude préliminaire pour appliquer une telle approche dans un cas concret de problématique industrielle liée à la fabrication du papier (amélioration de la douceur des papiers tissus).

La caractérisation *in-situ* des réactions de différents alkoxysilanes en milieux aqueux dans différentes conditions de concentration, pH et température, a été effectuée en utilisant la spectroscopie RMN du silicium. Il a été démontré que l'utilisation des médias purement aqueux peut fournir des solutions avec une réactivité ou une durée de conservation améliorée en comparaison avec le milieu de réaction classique éthanol / eau. Ce résultat est d'une importance cruciale et pas réellement attendu. Le pH a été confirmé comme étant le paramètre le plus important pour le contrôle des cinétiques de réactions. Par ailleurs, même s'il est apparu que, sous certaines conditions, des structures insolubles ont été formées, pour tous les composés étudiés nous avons trouvé des conditions permettant la préparation de solutions avec des réactivités allant de 75 à 100%.

Dans la deuxième partie de ce travail, nous avons fourni une description détaillée de l'interaction silane-cellulose en milieu aqueux. L'adsorption des composés choisis sur des surfaces modèles de cellulose a été observée *in-situ*, en utilisant une technique innovante, la microbalance à quartz. Cette technique a permis de décrire la cinétique d'adsorption de trois silanes différents sur la cellulose et l'évaluation de la quantité de silane retenue sur la surface au cours du temps. L'impact de la concentration, la température et le pH, sur la cinétique d'adsorption a également été évalué et discuté.

Ensuite, l'interface formée après formation de la feuille entre les silanes et la cellulose a été étudiée en combinant plusieurs techniques analytiques : le SEM-EDX, la RMN solide, l'XPS, et le ToF-SIMS. Les données obtenues confirment que les organosilanes hydrolysés sont capables de former des liaisons fortes, presque certainement de nature chimique, avec la cellulose. Le traitement thermique des échantillons modifiés a permis d'augmenter la quantité de silane à la surface de la cellulose, mais dans les conditions étudiées ne semblait pas nécessaire pour la création de ces liens forts.

Enfin, l'utilisation des organosilanes dans les applications de fabrication de papier a été évaluée. Un aminosilane a été utilisé dans le but de répondre à l'antagonisme entre le développement des propriétés de résistance et la douceur du papier. Le procédé de modification de cellulose développée dans ce travail s'est révélé adapté pour répondre à cette problématique sur certaines pâtes, mais n'a pas apporté d'améliorations dans le cas des fibres d'*Eucalyptus*. Comme ce type de fibre est largement utilisé dans les applications pour lesquelles la douceur est un point essentiel, l'intérêt de la modification de la cellulose par ce silane est apparu comme relativement faible. Un mécanisme permettant de décrire les interactions entre le silane sélectionné et les fibres a été proposé.

En conclusion, ce travail a permis plusieurs avancées. Tout d'abord, une meilleure compréhension de la modification de la cellulose par organosilanes dans des milieux aqueux a été atteinte et une base des données

de RMN ^{29}Si sur les réactions des silanes dans l'eau pure a été acquise. Ensuite, une méthode pour l'étude directe de l'adsorption des silanes sur de la cellulose native a été développée, ainsi qu'une approche originale pour déterminer la nature de l'interaction silane-cellulose, ce qui a conduit à une caractérisation des structures présentes à l'interface cellulose-silane plus approfondie que ce qui avait été précédemment reporté dans la littérature. Des essais préliminaires d'application ont aussi permis de mettre en évidence le potentiel de cette stratégie de modification, ainsi que certains aspects qu'il faudrait approfondir (sensibilité au type de pâte).

Perspectives

Les perspectives de ce travail se situent sur deux niveaux, un lié à la compréhension des phénomènes et l'autre à l'application de la stratégie de modification en vue de produits/procédés industriels.

Pour le premier axe, l'utilisation de la méthodologie et de l'approche développé au cours de cette thèse pourrait permettre d'étendre la connaissance du comportement d'autres organosilanes, y compris ceux en phase de développement. De plus, les données présentées dans ce rapport fournissent une meilleure compréhension de l'interaction entre les silanes et la cellulose, ce qui pourrait constituer un point de départ pour des travaux futurs sur la modification d'autres polysaccharides naturels par les organosilanes. Plus précisément, la modification d'autres bio-produits renouvelables, tels que l'amidon ou les hémicelluloses, pourrait être envisagée. De telles modifications étant effectuées en solution, il serait possible d'augmenter sensiblement la quantité de silane retenue et ainsi de créer de nouveaux matériaux bio-fonctionnels à base de ces composés.

Pour ce qui est de l'application, dans le secteur papetier, l'impact d'autres structure que celles utilisées dans l'étude sur les propriétés finales du réseau fibreux pourrait être évalué, en vue d'améliorer les propriétés du papier et son procédé de fabrication du papier. D'autant plus que la sélection de silanes utilisée dans notre travail a été limitée par rapport à l'ensemble des structures disponibles dans le commerce. Par exemple certaines molécules disponibles sur le marché ont été exclues à cause de leur une faible solubilité dans l'eau. Toutefois il peut être envisagé d'utiliser des techniques de mise en émulsion pour adsorber ces agents sur la surface des fibres, où ils pourraient réagir et moduler les propriétés souhaitées.

Références bibliographiques

[1] E. P. Plueddemann, *Silane coupling agents*. Springer, 1991.

[2] K. L. Mittal, *Silanes and other coupling agents*. VSP, 2000.

[3] K. L. Mittal et A. Pizzi, *Adhesion promotion techniques*. CRC Press, 1999.

[4] C. J. Brinker et G. W. Scherer, « Hydrolysis and condensation II - Silicates », in *Sol-gel science: the physics and chemistry of sol-gel processing*, 5^{e} éd., Gulf Professional Publishing, 1990, p. 97-234.

[5] A. Parker, « A technical review on organosilanes and adhesion ».

[6] S. Savard, L.-P. Blanchard, J. Léonard, et R. E. Prud'homme, « Hydrolysis and condensation of silanes in aqueous solutions », *Polymer Composites*, vol. 5, n°. 4, p. 242-249, 1984.

[7] J. Weis et N. Auner, *Organosilicon chemistry V*. Wiley-VCH, 2003.

[8] S. E. Rankin et A. V. McCormick, « Hydrolysis pseudoequilibrium: challenges and opportunities to sol-gel silicate kinetics », *Chemical Engineering Science*, vol. 55, n°. 11, p. 1955-1967, 2000.

[9] H. Jiang, Z. Zheng, Z. Li, et X. Wang, « Effects of temperature and solvent on the hydrolysis of alkoxysilane under alkaline conditions », *Industrial & Engineering Chemistry Research*, vol. 45, n°. 25, p. 8617-8622, 2006.

[10] H. Schmidt, H. Scholze, et A. Kaiser, « Principles of hydrolysis and condensation reaction of alkoxysilanes », *Journal of Non-Crystalline Solids*, vol. 63, n°. 1-2, p. 1-11, 1984.

[11] R. H. Glaser et G. L. Wilkes, « Structure property behavior of polydimethylsiloxane and poly(tetramethylene oxide) modified TEOS based sol-gel materials », *Polymer Bulletin*, vol. 19, n°. 1, p. 51-57, 1988.

[12] M. C. Brochier-Salon, M. Bardet, et M. N. Belgacem, « Solvolysis–hydrolysis of N-bearing alkoxysilanes: Reactions studied with 29Si NMR », *Silicon Chemistry*, vol. 3, n°. 6, p. 335-350, 2008.

[13] M. C. Brochier-Salon, G. Gerbaud, M. Abdelmouleh, C. Bruzzese, S. Boufi, et M. N. Belgacem, « Studies of interactions between silane coupling agents and cellulose fibers with liquid and solid-state NMR », *Magnetic Resonance in Chemistry*, vol. 45, n°. 6, p. 473-483, 2007.

[14] M. C. Brochier-Salon, P.-A. Bayle, M. Abdelmouleh, S. Boufi, et M. N. Belgacem, « Kinetics of hydrolysis and self condensation reactions of silanes by NMR spectroscopy », *Colloids and Surfaces A: Physicochemical and Engineering Aspects*, vol. 312, n°. 2-3, p. 83-91, 2008.

[15] M. C. Brochier-Salon, M. Abdelmouleh, S. Boufi, M. N. Belgacem, et A. Gandini, « Silane adsorption onto cellulose fibers: Hydrolysis and condensation reactions », *Journal of Colloid and Interface Science*, vol. 289, n°. 1, p. 249-261, 2005.

[16] R. Bel-Hassen, S. Boufi, M. C. Brochier-Salon, M. Abdelmouleh, et M. N. Belgacem, « Adsorption of silane onto cellulose fibers. II. The effect of pH on silane hydrolysis, condensation, and adsorption behavior », *Journal of Applied Polymer Science*, vol. 108, n°. 3, p. 1958-1968, 2008.

[17] M.-C. Brochier Salon et M. N. Belgacem, « Competition between hydrolysis and condensation reactions of trialkoxysilanes, as a function of the amount of water and the nature of the organic group », *Colloids and Surfaces A: Physicochemical and Engineering Aspects*, vol. 366, n°. 1-3, p. 147-154, 2010.

[18] F. D. Osterholtz et E. R. Pohl, « Kinetics of the hydrolysis and condensation of organofunctional alkoxysilanes: a review », *Journal of Adhesion Science and Technology*, vol. 6, p. 127-149, 1992.

[19] T. M. Alam, R. A. Assink, et D. A. Loy, « Hydrolysis and esterification in organically modified alkoxysilanes: A 29Si NMR investigation of Methyltrimethoxysilane », *Chemistry of Materials*, vol. 8, n°. 9, p. 2366-2374, 1996.

[20] S. Prabakar et R. A. Assink, « Hydrolysis and condensation kinetics of two component organically modified silica sols », *Journal of Non-Crystalline Solids*, vol. 211, n°. 1-2, p. 39-48, 1997.

[21] F. Beari et al., « Organofunctional alkoxysilanes in dilute aqueous solution: new accounts on the dynamic structural mutability », *Journal of Organometallic Chemistry*, vol. 625, n°. 2, p. 208-216, 2001.

[22] H. Schmidt, H. Scholze, et A. Kaiser, « Principles of hydrolysis and condensation reaction of alkoxysilanes », *Journal of Non-Crystalline Solids*, vol. 63, n°. 1-2, p. 1-11, 1984.

[23] M. Castellano, A. Gandini, P. Fabbri, et M. N. Belgacem, « Modification of cellulose fibres with organosilanes: Under what conditions does coupling occur? », *Journal of Colloid and Interface Science*, vol. 273, n°. 2, p. 505-511, 2004.

[24] H. Jiang, Z. Zheng, J. Xiong, et X. Wang, « Studies on dialkoxysilane hydrolysis kinetics under alkaline conditions », *Journal of Non-Crystalline Solids*, vol. 353, n°. 44-46, p. 4178-4185, 2007.

[25] F. de Buyl et A. Kretschmer, « Understanding hydrolysis and condensation kinetics of γ-Glycidoxypropyltrimethoxysilane », *The Journal of Adhesion*, vol. 84, n°. 2, p. 125, 2008.

[26] M.-C. Brochier Salon et M. N. Belgacem, « Hydrolysis-Condensation Kinetics of Different Silane Coupling Agents », *Phosphorus, Sulfur, and Silicon and the Related Elements*, vol. 186, n°. 2, p. 240-254, 2011.

[27] J. T. Marsh, *An introduction to the chemistry of cellulose*. Read Books, 2008.

[28] J. F. Kennedy, G. O. Phillips, et P. A. Williams, *Cellulose: structural and functional aspects*. Ellis Horwood, 1989.

[29] L. Wågberg et G. Annergren, « Physicochemical characterization of papermaking fibres », in *Fundamentals of Papermaking Materials*, Pira international., UK: Baker, C.F., 1997, p. 1-82.

[30] J. A. Trejo-O'Reilly, « Synthèse d'agents de couplage, réactions de greffage en surfacede fibres cellulosiques et propriétés d'interface fibres-matrices dans des matériauxcomposites à base de polystyrène », Institut Nationale Polytechnique de Grenoble, 1997.

[31] S. Gunnars, L. Wågberg, et M. A. Cohen Stuart, « Model films of cellulose: I. Method development and initial results », *Cellulose*, vol. 9, n°. 3, p. 239-249, 2002.

[32] S. Fält, L. Wågberg, E.-L. Vesterlind, et P. T. Larsson, « Model films of cellulose II – Improved preparation method and characterization of the cellulose film », *Cellulose*, vol. 11, n°. 2, p. 151-162, 2004.

[33] E. Kontturi, P. C. Thüne, et J. W. Niemantsverdriet, « Novel method for preparing cellulose model surfaces by spin coating », *Polymer*, vol. 44, n°. 13, p. 3621-3625, 2003.

[34] E. Kontturi, P. C. Thüne, et J. W. (Hans) Niemantsverdriet, « Cellulose model surfaces simplified preparation by spin coating and characterization by X-ray photoelectron spectroscopy, infrared spectroscopy, and atomic force microscopy », *Langmuir*, vol. 19, n°. 14, p. 5735-5741, 2003.

[35] C. Aulin et al., « Nanoscale cellulose films with different crystallinities and mesostructures - Their surface properties and interaction with water », *Langmuir*, vol. 25, n°. 13, p. 7675-7685, 2009.

[36] C. Aulin, E. Johansson, L. Wågberg, et T. Lindström, « Self-Organized Films from Cellulose I Nanofibrils Using the Layer-by-Layer Technique », *Biomacromolecules*, vol. 11, n°. 4, p. 872-882, 2010.

[37] C. D. Edgar et D. G. Gray, « Smooth model cellulose I surfaces from nanocrystal suspensions », *Cellulose*, vol. 10, n°. 4, p. 299-306, 2003.

[38] K. Y. Foo et B. H. Hameed, « Insights into the modeling of adsorption isotherm systems », *Chemical Engineering Journal*, vol. 156, n°. 1, p. 2-10, 2010.

[39] J. N. Israelachvili, *Intermolecular and Surface Forces, 3rd Ed.*, Academic Press. 2010.

[40] E. Poptoshev, A. Carambassis, M. Österberg, P. M. Claesson, et M. W. Rutland, « Comparison of model surfaces for cellulose interactions: elevated pH », in *Surface and Colloid Science*, Springer Berlin Heidelberg., vol. 116, Berlin, Heidelberg: Valdemaras Razumas, Björn Lindman and Tommy Nylander, 2001, p. 79-83.

[41] M. Österberg, L.-E. Enarsson, et L. Wågberg, « Interactions at cellulose model surfaces », in *Encyclopedia of Surface and Colloid Science, Second Edition*, Taylor & Francis, 2007, p. 1-19.

[42] M. Österberg, « On the interactions in cellulose systems : surface forces and adsorption », dissertation, KTH, 2000.

[43] M. Holmberg, J. Berg, S. Stemme, L. Ödberg, J. Rasmusson, et P. Claesson, « Surface force studies of Langmuir–Blodgett cellulose films », *Journal of Colloid and Interface Science*, vol. 186, n°. 2, p. 369-381, 1997.

[44] D. Kowalczyk, S. Slomkowski, M. M. Chehimi, et M. Delamar, « Adsorption of aminopropyltriethoxy silane on quartz: an XPS and contact angle measurements study », *International Journal of Adhesion and Adhesives*, vol. 16, n°. 4, p. 227-232, 1996.

[45] S. Ek et al., « Atomic layer deposition of a high-density Aminopropylsiloxane network on silica through sequential reactions of γ-Aminopropyltrialkoxysilanes and water », *Langmuir*, vol. 19, n°. 25, p. 10601-10609, 2003.

[46] M.-L. Abel, R. Joannic, M. Fayos, E. Lafontaine, S. J. Shaw, et J. F. Watts, « Effect of solvent nature on the interaction of -glycidoxy propyl trimethoxy silane on oxidised aluminium surface: A study by solution chemistry and surface analysis », *International Journal of Adhesion and Adhesives*, vol. 26, n°. 1-2, p. 16-27, 2006.

[47] A. Kornherr et al., « Molecular dynamics simulations of the adsorption of industrial relevant silane molecules at a zinc oxide surface », *The Journal of Chemical Physics*, vol. 119, n°. 18, p. 9719, 2003.

[48] F. Höök, « Development of a novel QCM technique for protein adsorption studies », Doctoral thesis, Chalmers University of Technology, 2004.

[49] M. N. Belgacem et A. Gandini, « Surface modification of cellulose fibres », *Polímeros*, vol. 15, p. 114-121, 2005.

[50] D. Klemm, *Comprehensive cellulose chemistry: Functionalization of cellulose*. Wiley-VCH, 1998.

[51] J. George, M. S. Sreekala, et S. Thomas, « A review on interface modification and characterization of natural fiber reinforced plastic composites », *Polymer Engineering & Science*, vol. 41, n°. 9, p. 1471-1485, 2001.

[52] J. A. Trejo-O'Reilly, J.-Y. Cavaille, et A. Gandini, « The surface chemical modification of cellulosic fibres in view of their use in composite materials », *Cellulose*, vol. 4, n°. 4, p. 305-320, déc. 1997.

[53] O. Paquet, M. Krouit, J. Bras, W. Thielemans, et M. N. Belgacem, « Surface modification of cellulose by PCL grafts », *Acta Materialia*, vol. 58, n°. 3, p. 792-801, févr. 2010.

[54] P. Stenstad, M. Andresen, B. Tanem, et P. Stenius, « Chemical surface modifications of microfibrillated cellulose », *Cellulose*, vol. 15, n°. 1, p. 35-45, févr. 2008.

[55] C. S. R. Freire, A. J. D. Silvestre, C. Pascoal Neto, A. Gandini, P. Fardim, et B. Holmbom, « Surface characterization by XPS, contact angle measurements and ToF-SIMS of cellulose fibers partially esterified with fatty acids », *Journal of Colloid and Interface Science*, vol. 301, n°. 1, p. 205-209, 2006.

[56] M. N. Belgacem et A. Gandini, « The surface modification of cellulose fibres for use as reinforcing elements in composite materials », *Composite Interfaces*, vol. 12, n°. 1, p. 41-75, 2005.

[57] M. Abdelmouleh, S. Boufi, M. N. Belgacem, A. P. Duarte, A. B. Salah, et A. Gandini, « Modification of cellulosic fibres with functionalised silanes: Development of surface properties », *International Journal of Adhesion and Adhesives*, vol. 24, n°. 1, p. 43-54, 2004.

[58] M. Abdelmouleh, S. Boufi, A. ben Salah, M. N. Belgacem, et A. Gandini, « Interaction of silane coupling agents with cellulose », *Langmuir*, vol. 18, n°. 8, p. 3203-3208, 2002.

[59] D. Wang, F. R. Jones, et P. Denison, « A ToF-SIMS study of the incorporation of aluminium into the silane coating on e-glass fibres », *Catalysis Today*, vol. 12, n°. 4, p. 375-383, 1992.

[60] D. Wang et F. R. Jones, « ToF-SIMS and XPS study of the interaction of aminosilanised E-glass fibres with epoxy resins. Part I: Diglycidyl ether of bisphenol S », *Composites Science and Technology*, vol. 50, n°. 2, p. 215-228, 1994.

[61] D. Wang, F. R. Jones, et P. Denison, « ToF-SIMS and XPS study of the interaction of hydrolysed -aminopropyltriethoxysilane with E-glass surfaces », *Journal of Adhesion Science and Technology*, vol. 6, n°. 1, p. 79-98, 1992.

[62] D. Wang et F. R. Jones, « ToF-SIMS and XPS studies of the interaction of silanes and matrix resins with glass surfaces », *Surface and Interface Analysis*, vol. 20, n°. 5, p. 457-467, 1993.

[63] A. M. Belu, M. C. Davies, J. M. Newton, et N. Patel, « ToF-SIMS characterization and imaging of controlled-release drug delivery systems », *Anal. Chem.*, vol. 72, n°. 22, p. 5625-5638, 2000.

[64] A. Chilkoti, B. D. Ratner, et D. Briggs, « Static secondary-ion mass spectrometric investigation of the surface structure of organic plasma-deposited films prepared from stable-isotope-labeled precursors. 1. Carbonyl precursors », *Anal. Chem.*, vol. 63, n°. 15, p. 1612-1620, 1991.

[65] X. Dong, A. Proctor, et D. M. Hercules, « Characterization of Poly(dimethylsiloxane)s by Time-of-Flight Secondary Ion Mass Spectrometry », *Macromolecules*, vol. 30, n°. 1, p. 63-70, 1997.

[66] R. Will, U. Fink, et Y. Ishikawa, *Speciality Paper Chemicals*, SRI Consulting. 2006.

[67] M. B. Lyne, A. Whiteman, et D. C. Donderi, « Multidimensional scaling of tissue quality », *Pulp & paper Canada*, vol. 85, n°. 10, p. 43-50, 1984.

[68] J. Liu et J. Hsieh, « Characterization of facial tissue softness », *TAPPI Journal*, vol. 3, n°. 4, p. 3-8, avr. 2004.

[69] H. Hollmark et R. S. Ampulski, « Measurement of tissue paper softness: A literature review », *Nordic Pulp and Paper Research Journal*, vol. 19, n°. 3, p. 345-353, 2004.

[70] M. K. Ramasubramanian, « Physical and mechanical properties of towel and tissue », in *Handbook of Physical Testing of Paper*, 2e éd., vol. 1, New York: CRC Press, 2002, p. 690-696.

[71] T. Lindström, L. Wagberg, et T. Larsson, « On the nature in joint strength of paper - A review of dry and wet strength resins used in paper manufacturing », in *Advances in paper science and technology*, Cambridge, U.K., 2005, vol. 1, p. 457-562.

General table of contents

General Introduction - 1 -

Chapter 1 – Alkoxysilanes in aqueous media - 5 -

Table of contents - 7 -

List of figures - 8 -

List of tables - 10 -

List of equations - 10 -

I. Alkoxysilanes solutions: literature review - 11 -

I.A Alkoxysilanes coupling agents - 12 -

I.B Alkoxysilanes reactions in presence of moisture - 13 -

I.B.1 Hydrolysis - 13 -

I.B.2 Alkoxysilane/solvent interactions - 16 -

I.B.3 Condensation - 16 -

I.B.4 The importance of controlling hydrolysis and condensation reactions - 20 -

I.C Characterization of alkoxysilane solutions - 21 -

I.D Parameters influencing alkoxysilanes reactions in solution - 23 -

I.D.1 Influence of alkoxysilane structure - 23 -

I.D.2 Influence of pH - 24 -

I.D.3 Influence of temperature - 25 -

I.D.4 Influence of concentration - 25 -

I.D.5 Influence of solvent composition - 26 -

I.D.6 Catalysis - 26 -

I.D.7 The special case of aminosilanes - 27 -

I.E Conclusions - 28 -

List of references - 29 -

II. Materials and Methods - 37 -

II.A Materials - 37 -

II.B Methods - 38 -

II.B.1 NMR Kinetics set-up - 38 -

II.B.2 ^{29}Si NMR study - 38 -

III. Results and Discussion - 40 -

III.A Impact of solvent composition on DAMS reactions - 40 -

III.B Characterization of other silanes in aqueous medium - 46 -

III.B.1 Alkylalkoxysilanes - 48 -

III.B.2 Vinylalkoxysilanes - 51 -

III.B.3 Aminoalkoxysilanes - 53-

III.C Impact of pH - 55 -
III.C.1 Alkylalkoxysilanes - 55 -
III.C.2 Vinylalkoxysilanes - 57 -
III.C.3 Aminoalkoxysilanes - 59 -
III.D Effect of temperature - 60 -
III.D.1 Alkylalkoxysilanes - 60 -
III.D.2 Vinylalkoxysilanes - 61 -
III.D.3 Aminoalkoxysilanes - 62 -
III.E Effect of concentration - 63 -
III.E.1 Alkylalkoxysilanes - 63 -
III.E.2 Vinylalkoxysilanes - 65 -
III.E.3 Aminoalkoxysilanes - 65 -
III.F Effect of silane structure - 66 -
III.F.1 TMMS-DMDMS-MTMS - 66 -
III.F.2 DMDMS-MVDMS - 68 -
III.F.3 MVDES-MVDMS - 69 -
IV. Conclusions and perspectives - 71 -
List of references - 73 -

Chapter 2 – Silane adsorption on model surfaces - 75 -
Table of contents - 77 -
List of figures - 78 -
List of tables - 80 -
List of equations - 80 -
I. Study of silanes adsorption onto cellulosic substrates - 81 -
I.A Cellulose - 81 -
I.A.1 Structure, surface chemistry and reactivity of cellulose - 81 -
I.A.2 Model cellulosic surfaces - 83 -
I.B Adsorption phenomena - 84 -
I.B.1 Definition - 84 -
I.B.2 Nature of the interactions involved in adsorption onto cellulose - 86 -
I.B.3 Analytical means for adsorption evaluation - 87 -
I.C Silanes adsorption - 87 -
I.C.1 Silanes adsorption onto inorganic substrates - 87 -
I.C.2 Silanes adsorption onto cellulose - 89 -
I.D Quartz Crystal Microbalance (QCM) - 90 -
I.D.1 Description - 90 -
I.D.2 Literature review on QCM use for cellulose characterization - 94 -
List of references - 96 -

II. Materials and Methods - 101 -
II.A Materials - 101 -
II.B Methods - 101 -
II.B.1 Quartz Crystal Microbalance set-up - 101 -
II.B.2 QCM study - 103 -
II.B.3 Data treatment - 103 -
III. Results and Discussion - 105 -
III.A Silane adsorption onto cellulose sensors - 105 -
III.A.1 Assessment of method reliability - 105 -
III.A.2 Adsorption of APDMES on cellulose model surfaces - 106 -
III.A.3 Adsorption of DAMS on cellulose model surfaces - 115 -
III.A.4 Adsorption of VDMES on cellulose model surfaces - 120 -
III.A.5 Influence of the silane structure on the adsorption onto cellulose - 122 -
III.B Silane adsorption onto silica sensors - 124 -
IV. Conclusions and perspectives - 127 -
List of references - 128 -

Chapter 3 – Silane adsorption on model surfaces - 131 -
Table of contents - 133 -
List of figures - 134 -
List of tables - 135 -
I. Literature review - 136 -
I.A Cellulose fibers chemical modifications - 136 -
I.B Cellulose fibers modifications by organosilanes - 137 -
I.C Surface modifications characterization - 138 -
I.C.1 Attenuated Total Reflection Fourier Transform Infrared spectroscopy - 139 -
I.C.2 Energy Dispersive X-ray spectroscopy - 139 -
I.C.3 X-ray Photoelectron Spectroscopy - 140 -
I.C.4 Time-of-Flight Secondary Ions Mass Spectrometry - 140 -
I.C.5 Relevant studies on silane grafting characterization - 141 -
List of references - 142 -
II. Materials and Methods - 145 -
II.A Materials - 145 -
II.A.1 Chemicals - 145 -
II.A.2 Cellulose fibers - 145 –

II.B Methods - 146 -
II.B.1 Pulp modification - 146 -
II.B.2 Handsheet formation - 146 -
II.B.3 Solvent extractions - 147 -
II.B.4 SEM-EDX - 147 -
II.B.5 XPS - 148 -
II.B.6 ToF-SIMS - 148 -
II.B.7 Solid-NMR - 148 -
III. Results and Discussion - 149 -
III.A Development of a suitable extraction method - 149 -
III.B Multi-scale characterization of the silane-cellulose interface - 152 -
III.B.1 SEM-EDX - 152 -
III.B.2 Solid NMR - 155 -
III.B.3 XPS - 157 -
III.C ToF-SIMS study - 160 -
III.C.1 Determination of surface contamination - 161 -
III.C.2 Surface characterization of APDMES treated fibers - 164 -
III.C.3 Surface characterization of VDMES treated fibers - 173 -
III.C.4 Surface characterization of DAMS treated fibers - 175 -
IV. Conclusions and perspectives - 178 -
List of references - 179 -

Chapter 4 – Evaluation of paper modification by organosilanes - 181 -
Table of contents - 183 -
List of figures - 184 -
List of tables - 184 -
I. Paper technology - 185 -
I.A The papermaking process - 185 -
I.B Paper properties - 188 -
I.C Softness - 189 -
I.C.1 Tissues' softness definition - 189 -
I.C.2 Softness in papermaking - 189 -
I.C.3 Softness evaluation - 192 -
I.D Tissue+ - 193 -
I.D.1 Chronology - 193 -
I.D.2 Motivations and objectives of Tissue+ - 193 -
I.D.3 Tissue+ work packages - 194 -
I.D.4 Tissue+ WP2: Cellulose surface modification - 195 -
I.E Patents on the topic - 196 -

List of references - 198 -
II. Materials and Methods - 201 -
II.A Materials - 201 -
II.A.1 Silane - 201 -
II.A.2 Fibers - 201–
II.B Methods - 202 -
II.B.1 Pulp modification - 202 -
II.B.2 Sheet formation - 202 -
II.B.3 Softness measurement - 203 -
II.B.4 Other physical Properties measurement - 203 -
II.B.5 Morphological analyses - 204 -
II.B.6 SEM-EDX - 204 -
III. Results and Discussion - 205 -
III.A Preliminary study - 205 -
III.B Tissue+ Softwood pulp - 207 -
III.C Tissue+ Eucalyptus pulp - 209 -
III.C.1 Softness handsheets - 209 -
III.C.2 Retention handsheets - 211 -
III.D Extended study on Eucalyptus pulps - 212 -
III.D.1 Assessment of the silane modification - 212 -
III.D.2 Role of fine elements - 213 -
III.D.3 Impact of pulp bleaching - 213 -
III.D.4 Effect of aspect ratio and flocculation - 214 -
III.E Discussion - 216 -
IV. Conclusions and perspectives - 219 -
List of references - 220 -

General conclusions and perspectives - 223 -

Annexes - 227 -
Annex 1 - 227 -
Annex 2 - 235 -

List of abbreviations - 237 -

General introduction

During the previous years, an increasing demand for solvent-free and/or water-based processes, coming from both consumers and industry, has been driving the research devoted to sustainable development in both fundamental and applied sciences. In this context, the exploitation of bio-renewable vegetal resources arising from the biomass is considered a leading idea. In particular, the possibility of multiplying uses for cellulose fibers follows the same growing interest.

Cellulose fibers are historically known as an essential component in paper manufacturing, and are also thoroughly investigated for other applications such as composite materials. In the papermaking industry, where profits are generally low due to an increase in the cost of energy and the competition from emerging countries, companies are seeking for new opportunities involving materials with high-added value solutions. Under these circumstances, the modification of cellulose fibers with carefully chosen grafting agents can give birth to new functional materials from renewable resources and help papermakers to distinguish themselves from the concurrence. Also, the creation of new markets for cellulose fibers can be envisaged. Moreover, modifying the fiber surface and/or grafting specific functions onto it can open the way to enhance different quality of fibers from various sources. It is worth to note that such a modification should leave unaltered the bulk properties of the fibers in order to get the highest benefices to the industry.

Organosilanes have been used as coupling agent for several years and recently their use for the surface modification of cellulosic fibers has gained an important interest. Such grafting agents present the advantages of being available in a wide range of structure and functionality. They can be used to tailor the functionality of a surface according the needs of the envisaged application. Furthermore, previous studies have shown that the silanol moieties, borne from the silane alkoxy moieties hydrolysis in presence of water or moisture, are able to react with the polar surface of cellulose. However, these reactions were often carried out in the presence of a solvent (ethanol/water for instance). It is thus essential to verify that such reactions can be carried out in purely aqueous solutions, compatible with the papermaking process. Even though organosilanes compounds have been widely studied over the past decades, including for the modification of cellulose substrates, the nature of the interaction between the coupling agent and the cellulose has never been clearly elucidated. Despite strong evidences of the formation of covalent bonds obtained in solvent media, uncertainties arose from the capacity of most silanes molecules to interact with

each other and form siloxane bonds, which yields tridimensional polysiloxane networks irremovable by solvent extraction.

A first study realized in the frame of a master thesis has shown the feasibility of cellulose modification by organosilanes in aqueous media. In this work, initial tests were carried out, aiming at modifying cellulose fibers with purely aqueous silane solutions. The presence of the grafting agent after modification and subsequent extraction was verified through the detection of silicon atoms at the surface of the fibers. However at the end of this project, much work was left.

Based on these elements, it was decided to perform more research on the topic of cellulose modification by organosilanes in purely aqueous media with very specific goals. The first objective of this work was to study the behaviors of different organosilane in purely aqueous media (hydrolysis and self-condensation kinetics), in order to establish the best conditions of use for these compounds. Then, based on this knowledge, the second objective aimed at providing a better understanding of the silane-cellulose interaction. This part included both characterizing the kinetics of the reactions involved in this heterogeneous media, and providing clear-cut evidences supporting or infirming previous findings on the topic. Finally, the third goal was to evaluate the impact of the silane modification of cellulose in the frame of an industrial problematic.

In order to report the work done to fulfill these objectives, we have decided to structure this dissertation in four main parts, with each of them starting with a bibliographic review and containing a section introducing the materials and methods used.

The first chapter of this thesis focuses on the study of alkoxysilanes in aqueous media. It is initiated by a general introduction on alkoxysilanes, and includes an extensive literature survey about their reactions in solution. Then, the experimental section starts with the description of the materials and methods used. The results described in this chapter were mostly acquired by the use of ^{29}Si nuclear magnetic resonance spectroscopy. Indeed, only this technique allows to follow-up individually and simultaneously the various silicon-containing species present in the medium and their kinetics of formation or consumption. A preliminary study is presented, which aimed at comparing the reactions of an aminosilane either in a traditional ethanol/water mixture, or in water. Then, the characterizations of the reactions of various alkoxysilanes bearing different functional moieties are presented, and the impact of the silane concentration, the solution pH, and the temperature on these reactions are discussed. Finally, the role of the silane structure is discussed.

The second part of this dissertation describes the kinetics of adsorption of three selected silane grafting agents onto cellulose. In a first section, the reader can find general data regarding the surface chemistry of cellulose fibers, and the development of model cellulose surfaces. Common models for chemicals adsorption onto surfaces are also discussed, and the literature about silanes adsorption on different substrates is reviewed, before focusing on the literature relevant to this

topic. In a second section, the materials and methods relevant to this part of the work are introduced, and the experimental data obtained by mean of a quartz crystal microbalance with dissipation monitoring are discussed. The discussion firstly focuses on the data obtained for the adsorption of chosen silanes on cellulose model surfaces, under various concentrations, pH values, and temperatures. Then, some data obtained on silica model surfaces are presented and allow enlarging the discussion.

The third chapter of this work is dedicated to the characterization of the silane-cellulose interaction. It starts with a bibliographic review on the nature of chemical and physical interactions. Then, studies relevant to the interactions specific to cellulosic substrates and those associated to silane grafting agents on various substrates are introduced. Finally the interactions arising between silanes and cellulosic substrates are reviewed. The experimental section of this chapter starts with the description of the materials and methods, and includes results obtained by various analytical means. Data obtained by SEM-EDX spectroscopy after various solvent extractions are discussed as a preliminary study. The most important data include ^{29}Si solid-NMR spectra, as well as results from XPS and ToF-SIMS experiments. These data allow a better description of the silane-cellulose interface.

The last part of this dissertation presents the results of an applied research for the pulp and paper industry using the modification process developed in this work. The chapter introduces the papermaking process to the reader, and the context in which this work has been carried out. The experimental section introduces the materials and methods needed for this part of the work and more specifically several tests to test adapted to paper sheets analysis. The results presented include the morphological properties of two types of fibers, before and after modification with a selected compound. The physical and softness properties of two types of laboratory handsheets (retention and softness handsheets) obtained from these pristine or modified fibers are discussed, and the impact of the silane addition on the formation of the sheet is reviewed.

Finally, general concluding remarks on the work presented in this report are given, and perspectives for future works are proposed.

The work presented in this thesis dissertation includes several innovative aspects. First, to the best of our knowledge, the approach consisting of the grafting of organosilanes in a purely aqueous medium for papermaking applications was not described previously. Also, this work reports an extensive characterization of the reactions of various organosilanes in water, thus providing an important set of new data to the scientific community. In addition, the study of the adsorption of organosilanes on model native cellulose surfaces, monitored *in-situ* by quartz crystal microbalance, was not reported up-to-date. Finally, this work introduces an innovative experimental technique of characterization (ToF-SIMS) based on the use of monoalkoxysilanes to discuss the interactions between silanes and cellulose.

Chapter 1 – Alkoxysilanes in aqueous media

Table of contents

List of figures - 8 -

List of tables - 10 -

List of equations - 10 -

I. Alkoxysilanes solutions: literature review - 11 -

I.A Alkoxysilanes coupling agents - 12 -

I.B Alkoxysilanes reactions in presence of moisture - 13 -

I.C Characterization of alkoxysilane solutions - 21 -

I.D Parameters influencing alkoxysilanes reactions in solution - 23 -

I.E Conclusions - 28 -

List of references - 29 -

II. Materials and Methods - 37 -

II.A Materials - 37 -

II.B Methods - 38 -

III. Results and Discussion - 40 -

III.A Impact of solvent composition on DAMS reactions - 40 -

III.B Characterization of other silanes in aqueous medium - 46 -

III.C Impact of pH - 55 -

III.D Effect of temperature - 60 -

III.E Effect of concentration - 63 -

III.F Effect of silane structure - 66 -

IV. General conclusions and perspectives - 71 -

List of references - 73 -

List of figures

Figure I–1: Number of occurrences of the concept "Silane" in articles and reviews, and patents, published between 1940 and 2010 - 11 -

Figure I–2: General structure of an alkoxysilane - 12 -

Figure I–3: Hydrolysis reaction of a trialkoxysilane - 13 -

Figure I–4: The nomenclature for pristine and hydrolyzed alkoxysilanes according to Glaser and Wilkes [32] - 14 -

Figure I–5: Base-catalyzed silane hydrolysis - 15 -

Figure I–6: Acid-catalyzed silane hydrolysis - 15 -

Figure I–7: Alcoholysis of a trimethoxysilane in ethanolic solvent - 16 -

Figure I–8: Condensation reactions of (a) two silane triols, (b) a silane triol and a trialkoxysilane - 17 -

Figure I–9: Adapted Glaser and Wilkes notation for condensed alkoxysilane structures - 17 -

Figure I–10: Structures for 3- and 4-membered rings obtained from Dimethyldiethoxysilane cyclization, as proposed by Zhang [51]. - 19 -

Figure I–11: γ-aminopropylsilanetriol internal hydrogen bonded six-member ring, based on [85]. - 28 -

Figure III–1: ^{29}Si NMR spectra over time for a 10% DAMS alcoholic solution at 25°C, under (a) unmodified pH, (b) acidic pH - 41 -

Figure III–2: Hydrolysis and self-condensation kinetics of 10% w/w DAMS in mixed ethanol/water solutions (80/20 w/w) at 25°C, as deduced from the ^{29}Si NMR spectra presented in Figure III–1, i.e. under (a) unmodified pH; (b) acidic conditions - 41 -

Figure III–3: ^{29}Si NMR spectra over time for a 10% DAMS purely aqueous solution at 25°C, under (a) unmodified pH, (b) acidic pH - 43 -

Figure III–4: Hydrolysis and self-condensation kinetics of a 10% w/w DAMS in pure water at 25°C, as deduced from the ^{29}Si NMR spectra presented in Figure III–3, i.e. under: (a) unmodified pH and (b) acidic conditions. - 43 -

Figure III–5: Active Silanol Reactivity (SR) parameter, as a function of time over 8 hours, for different reaction conditions - 45 -

Figure III–6: Silane selection - 47 -

Figure III–7: Structures of TMMS, DMDMS, and MTMS. - 48 -

Figure III–8: SR Parameter as a function of time for reactions of DMDMS - 50 -

Figure III–9: SR Parameter over time for reactions of MTMS - 50 -

Figure III–10: Structures of MVDMS, and MVDES. - 51 -

Figure III–11: SR Parameter over time for reactions of MVDES - 52 -

Figure III–12: SR Parameter over time for reactions of MVDMS - 52 -

Figure III–13: Structure of APDMES. - 53 -

Figure III–14: SR Parameter over time for reactions of APDMES - 54 -

Figure III–15: SR curves for DMDMS - 56 -

Figure III–16: SR curves for MTMS - 56 -

Figure III–17: SR curves for MVDES - 58 -

Figure III–18: SR curves for MVDMS - 58 -

Figure III–19: SR curves for APDMES - 60 -

Figure III–20: SR curves for MVDMS - 62 -

Figure III–21: SR curves for DMDMS - 64 -

Figure III–22: SR curves for MTMS - 64 -

Figure III–23: SR curves for MVDMS - 65 -

Figure III–24: Structures of TMMS, DMDMS, and MTMS. - 66 -

Figure III–25: SR curves for structural comparison between DMDMS and MTMS. All reactions in neutral pH conditions - 67 -

Figure III–26: SR curves for structural comparison between DMDMS and MTMS. All reactions in acidic pH conditions - 67 -

Figure III–27: Structures of DMDMS and MVDMS. - 68 -

Figure III–28: SR curves for structural comparison between DMDMS and MVDMS - 69 -

Figure III–29: Structures of MVDMS, and MVDES. - 70 -

Figure III–30: SR curves for structural comparison between MVDMS and MVDES - 70 -

List of tables

Table II–1: List of the silanes studied by NMR spectroscopy and their properties - 37 -

Table II–2: Chemical shifts of the various structures in solutions for monoalkoxysilanes, in ppm - 39 -

Table II–3: Chemical shifts of the various structures in solutions for dialkoxysilanes, in ppm - 39 -

Table II–4: Chemical shifts of the various structures in solutions for trialkoxysilanes, in ppm - 39 -

Table III–1: NMR experiment list - 41 -

Table III–2: DMDMS experiments - 49 -

Table III–3: MTMS experiments - 49 -

Table III–4: MVDES experiments - 51 -

Table III–5: MVDMS experiments - 53 -

Table III–6: APDMES experiments - 53 -

Table IV–1: NMR data summary - 72 -

List of equations

Equation I–1: SR parameter for a monoalkoxysilane - 18 -

Equation I–2: SR parameter for a dialkoxysilane - 18 -

Equation I–3: SR parameter for a trialkoxysilane - 18 -

I. Alkoxysilanes solutions: literature review

Historically, organo-functional silanes as coupling agents were discovered in the 1940s, as a consequence of the development of fibre glass-reinforced composites [1], [2]. Since then, many new applications have emerged for this family, such as the treatment of fillers [3], the reinforcement of joints [4], the adhesion promotion [5-10], the modification of surface energy [7], [11], [12], or the creation of barrier properties [13-16]. Moreover, these compounds have been applied in the formulation of many complex products, such as those of inks, coatings, or sealants [17]. Finally, alkoxysilanes are perfectly suited for the sol-gel process [18-25].

The growing interest in silanes can be observed through the increasing amount of scientific publications and patents containing the concept "silane". In order to monitor the interest in the field of silanes over time, a search was performed using the statistics tools of the data search engine *SciFinder*, provided by Chemical Abstract Service, a division of the American Chemical Society. The search through the database references was made with the keyword "silane", and refined to show only journal articles and reviews, or patents, published during the period ranging from 1940 to 2010. Then, the duplicates were removed from the selection before the results were sorted out by year of publication and analyzed.

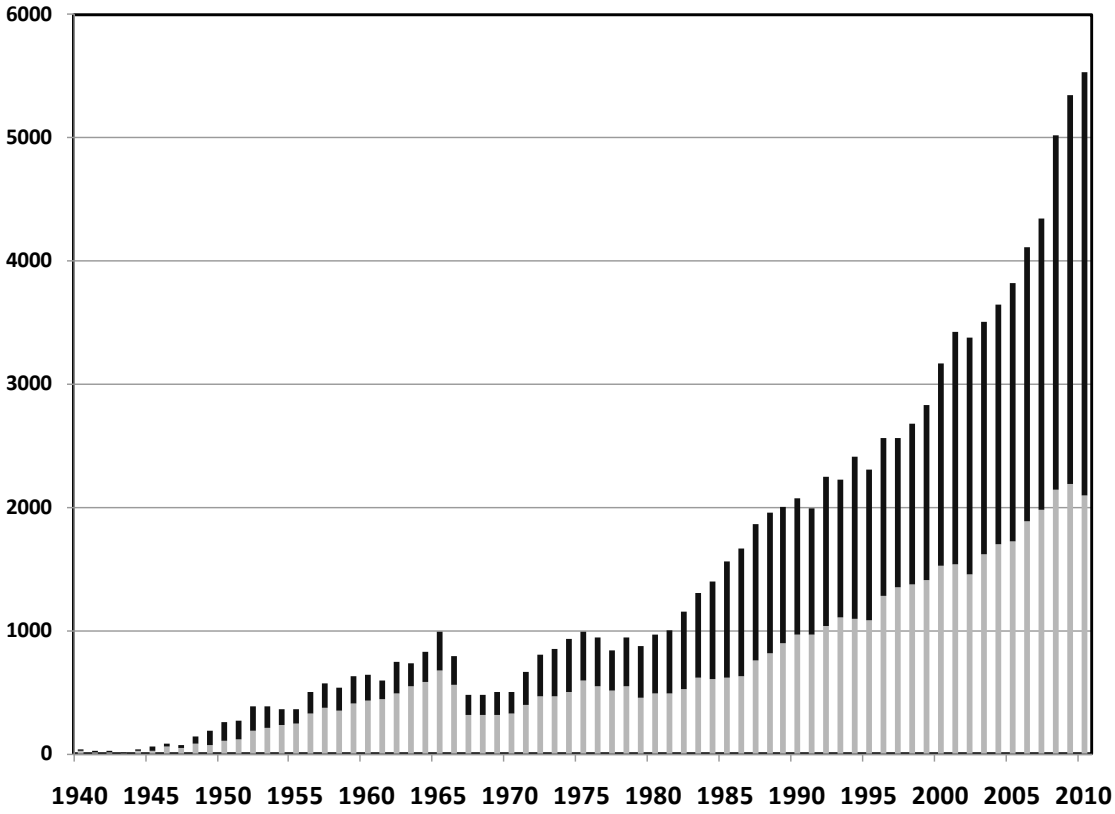

Figure I–1: Number of occurrences of the concept "Silane" in articles and reviews (grey), and patents (black), published between 1940 and 2010 (source: *SciFinder*)

Figure I–1 shows the variation of the occurrence of the word “silane” in published papers and reviews, and in patents published every year. One can clearly see the high number of publications issued over time, more than 2000 each year since 2007. Moreover, the steep increase of the number of patents since the beginning of the century shows that this interest comes not only from the academic world, but also from the industry.

Silanes are commonly applied in the form of solutions (mostly water/alcoholic), therefore it can be useful to briefly describe the general features of silane solutions. With this purpose in mind, some fundamentals regarding the structure of silane coupling agents will be described in a first part. Then, a description of the various reactions taking place in solution will be depicted, thus providing a good insight of the challenges one have to face when working with silane solutions. Also, in a third part, the analytical tools available for the characterization of such reactions will be briefly described, before we review in a fourth part the parameters influencing these reactions and their effect on the silane solution reactivity.

I.A Alkoxysilanes coupling agents

Alkoxysilanes molecules are monomeric chemical compounds organized around a central tetravalent silicon atom. The moieties attached to the silicon core can be either of organic or inorganic nature. Such silanes having at least one silicon-carbon bond are called *organosilanes* but may otherwise be known as *silane coupling agents*, or *adhesion promoters*. A typical structure for silane coupling agents is presented in Figure I–2 where OR refers to hydrolysable alkoxy groups such as methoxy, ethoxy or acetoxy, and X is an organic moiety, such as amino, epoxy or acryloxy.

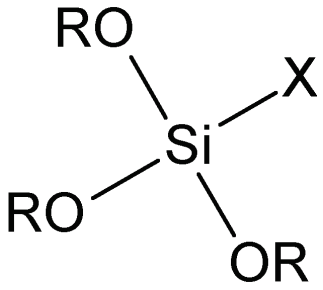

Figure I–2: General structure of an alkoxysilane

Even though many of the commercial alkoxysilane possess three alkoxy groups (as illustrated by Figure I–2) the number of these hydrolysable groups can also be 1, 2 or 4. Hence, in addition to trialkoxysilanes, it is possible to find mono-, di- and tetra-alkoxysilanes, respectively. For more details regarding the structural features and the synthesis of such compounds, the reader is invited to consult general textbooks on the subject [1], [2], [8], [26]. Tetraalkoxysilanes bearing no functional

group, they will not be considered in the frame of this work, and hence their reactions will not be discussed in the present literature review.

I.B Alkoxysilanes reactions in presence of moisture

In order to understand the high interest for alkoxysilanes, it is necessary to look at their chemistry. A very interesting feature of alkoxysilanes is the capacity of alkoxy groups to easily hydrolyze in presence of moisture or water in a wide variety of organic solvents, giving birth to silanol groups [5], [26], [27]. The hydroxyl moieties formed during this process can in turn undergo a condensation reaction with other hydroxyl functions, either born by other silanes in the solution, or present at the surface of a substrate. Besides, silanols are able to condense on metal-hydroxyls, hereby allowing the coupling capacity of silanes with materials bearing such groups [8].

I.B.1 Hydrolysis

In the presence of water (even if only moisture traces), the Si-OR bonds of alkoxysilanes can readily undergo hydrolysis, as shown in Figure I–3.

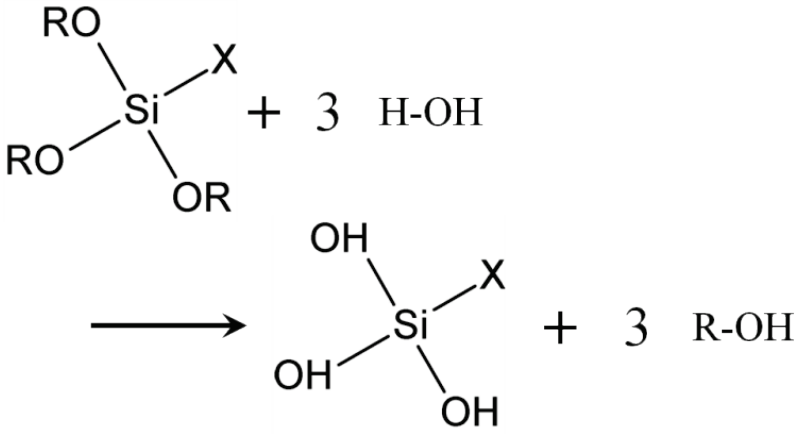

Figure I–3 : Hydrolysis reaction of a trialkoxysilane

During the hydrolysis reaction, for each alkoxy group consumed, a molecule of alcohol is released as a by-product. Of course, the nature of the alcohol molecule released depends on the nature of the hydrolyzed alkoxy group. As an example, methoxy groups will release methanol whereas ethoxy will produce ethanol. Various parameters are involved in the control of the kinetics of hydrolysis reactions [22], [28], [29], among which the pH, the concentration of the solution, the temperature of reaction, etc. The impact of these parameters will be further described in section I.D below.

Dialkoxysilanes and trialkoxysilanes have respectively two and three hydrolysable groups able to react with water. Hence, depending on the kinetic rates of hydrolysis, it is possible to observe the presence of both partially and totally hydrolyzed compounds. Moreover, it was shown that the hydrolysis of polyalkoxysilanes is a step-wise mechanism with separate kinetic rates for each step [30], [31], as discussed below. Having such a feature in mind, it is therefore easy to understand that the reaction species present in the hydrolyzing media are numerous. Thus, it is convenient to adopt a nomenclature to distinguish these different molecular structures, which can coexist in the reaction medium. For this purpose, in the frame of this work, we will use the convention proposed by Glaser and Wilkes [32] to differentiate the various structures that have been investigated. Indeed, in line with the commonly used nomenclature, silanes are noted M, D, T, Q depending on the number of Si-O- bridges attached to the silicon studied, these notations corresponding respectively to 1, 2, 3, or 4 Si-O- bridges. However, Glaser and Wilkes introduced a slightly different notation, adding an indice *i* to the previous notation, *i* referring to the number of –Si-O-Si bonds formed by the silicon atom of interest. Nevertheless, despite the fact that this nomenclature allows distinguishing the different structures, as a function of their level of condensation, both hydrolyzed and unhydrolyzed monomeric forms have an index equal to zero. Thus, a subscript R was added for pristine silanes, and a subscript H for hydrolyzed molecules, as introduced by Brochier-Salon [33-38].

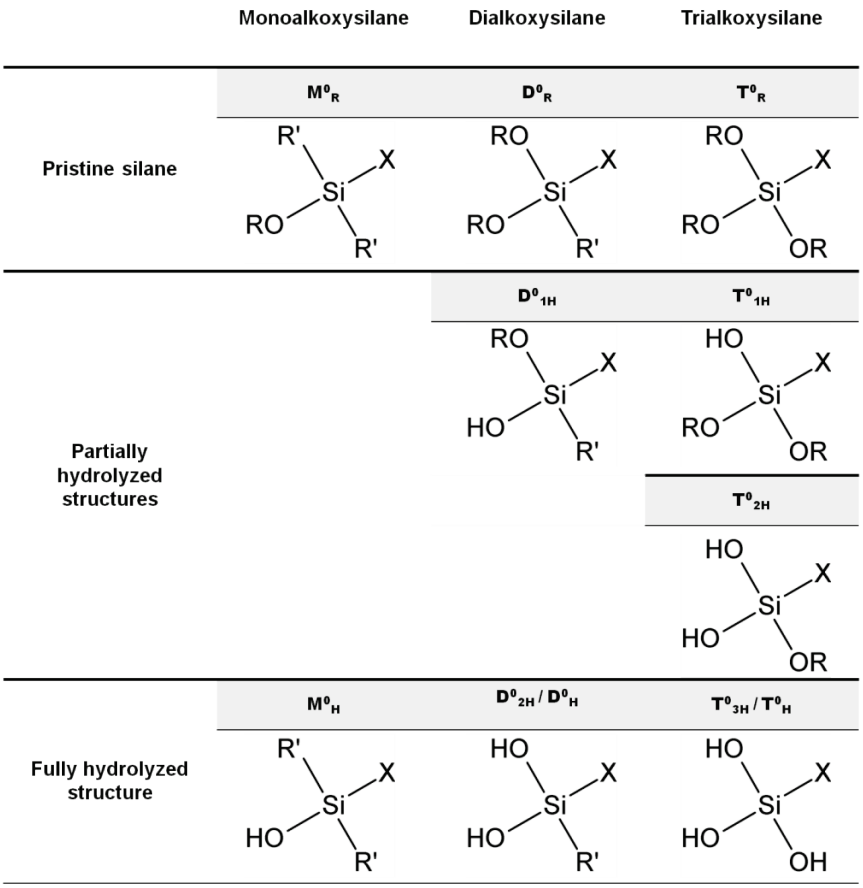

Figure I–4: The nomenclature for pristine and hydrolyzed alkoxysilanes according to Glaser and Wilkes [32]

The schematic structures and nomenclature of all the monomeric forms of monoalkoxy-, dimethoxy- and trimethoxy- silanes are presented in Figure I–4. In this figure, -X represents the functional group, -OR the alkoxy function and R' is generally a short alkyl chain.

The kinetic studies of the hydrolysis of polyalkoxysilanes reactions have shown that each hydrolysis step is faster than the previous one [39]. The mechanism of reaction involved in the hydrolysis of alkoxysilanes has been investigated, and two mechanisms have been proposed to account for the difference observed between base- and acid-catalyzed reactions. On one hand, the base-catalyzed hydrolysis of alkoxysilane has been proposed to proceed through a nucleophilic substitution mechanism ($S_N2@Si$), by the attack of hydroxyl anion on the silicon atom, with the formation of a penta-coordinated intermediate [28], [40], [41], as depicted in Figure I–5. Whereas on the other hand, in acid-catalyzed media, the hydrolysis of the same silane is thought to proceed through a rapid protonation of the leaving alkoxy group, followed by the attack of water through a nucleophilic substitution type mechanism [41-43], as sketched in Figure I–6.

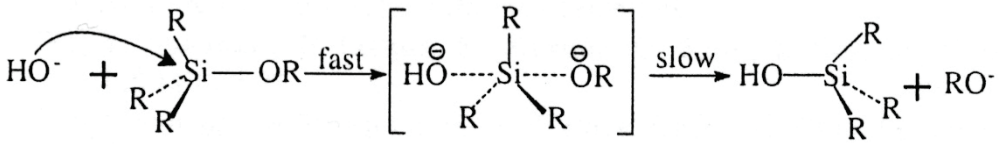

Figure I–5: Base-catalyzed silane hydrolysis, with OR an alkoxy moiety, and R a stable moiety (source:[28])

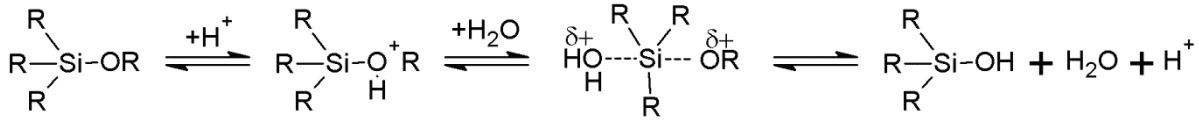

Figure I–6: Acid-catalyzed silane hydrolysis, with OR an alkoxy moiety, and R a stable moiety (adapted from [42], [43])

Investigations on the reversibility of alkoxysilanes hydrolysis were carried out, and showed that the existence of the reverse reaction could occur. Such evidences are detailed in the excellent literature review on the kinetics of hydrolysis and condensation of organofunctional alkoxysilanes by Osterholtz and Pohl [41]. More recently, Alam and coworkers [44] investigated the hydrolysis and esterification reactions of methyltrimethoxysilane in methanol under acid-catalyzed conditions using ^{29}Si NMR spectroscopy. By preparing hydrolyzed solutions in a *non pseudo-equilibrium* state, the authors demonstrated the reversibility of hydrolysis reactions in a short time scale. Furthermore, by measuring the extent of reaction of silane solutions at high water concentrations, the ratio between hydrolysis and the esterification rate constants was measured, and found to be approximately 100, under the conditions of scrutiny. These results are in good agreement with those obtained by Prabakar and coworkers [45] who tested a different protocol. Here, the authors

demonstrated by ^{29}Si NMR spectroscopy, that the reverse hydrolysis rate is significant in conditions where the amount of water is limited.

I.B.2 Alkoxysilane/solvent interactions

The solvolysis reactions in alkoxysilanes solutions mainly concern the hydrolysis and the alcoholysis reactions, since in most cases the reaction of such molecules was studied in a mixture of ethanol/water (80/20 v/v). And thus, the reactions carried out in more exotic media will not be covered in this dissertation. The hydrolysis of silanes has been widely investigated in literature in a wide variety of conditions. However, much less investigations were carried out on alcoholysis reactions. This phenomenon occurs when the alcohol solvent molecules are different in nature than the alkoxy moieties (e.g. methanol and ethoxy). More specifically, an exchange reaction can occur at the Si-O bond of the hydrolysable groups, with the solvent [33], [46]. As an example, methoxysilane moieties reacting in ethanol can be changed to ethoxy moieties, and methanol molecules will be released in the medium, as described in Figure I–7.

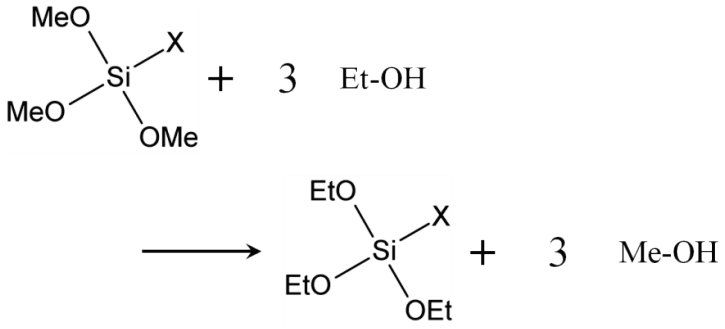

Figure I–7: Alcoholysis of a trimethoxysilane in ethanolic solvent

I.B.3 Condensation

As mentioned previously, the hydroxyl moieties resulting from the hydrolysis are metastable units which undergo condensation to thermodynamically more stable groups through Si-O-Si *siloxane* bonds [29], [47]. This reaction involving the elimination of water molecules is often referred to as *homo-*, or *self-condensation*, and must be distinguished from the condensation reaction occurring between silanes and solid substrates. This latter reaction will be described in the third chapter of this work. When the self-condensation phenomenon leads to the formation of bigger molecular structures, the ensuing oligomers or polymers are named *polysiloxanes*.

Self-condensation reactions can occur either between two silanols, or between a silanol and a silane molecule. As shown in Figure I–8 when silanols react together, the reaction releases water whereas when a silanol reacts with a silane alkoxy group a molecule of alcohol is produced.

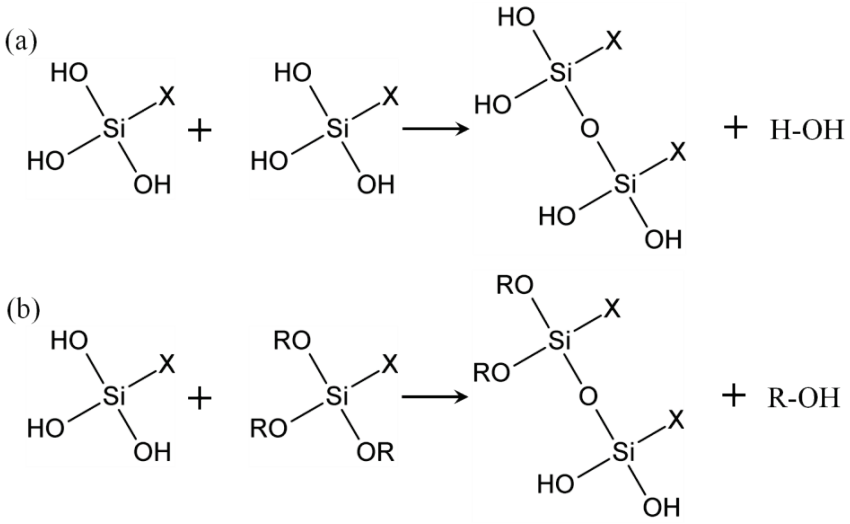

Figure I–8: Condensation reactions of (a) two silane triols, (b) a silane triol and a trialkoxysilane

For hydrolyzed polyalkoxysilanes, the self-condensation reactions may lead to the formation of a wide variety of structures, ranging from the dimer to three dimensional networks. It is possible to describe each block of these assembly using the nomenclature adapted from Glaser and Wilkes, as described in section I.B.1 [32], [44].

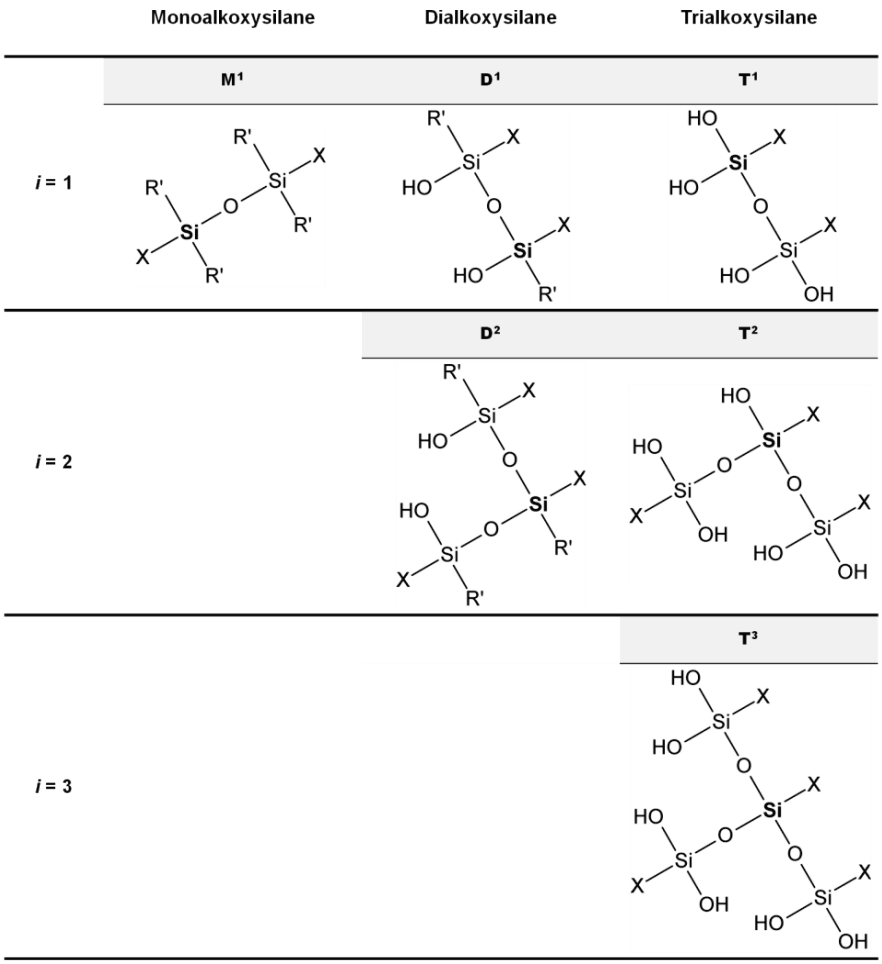

Figure I–9: Adapted Glaser and Wilkes notation for condensed alkoxysilane structures

According to this classification, molecules whose silicon atom is bounded by a single siloxane link have an index *i* equal to 1. Therefore, such molecules will be part of a dimer, or will be localised at the end of a polysiloxane linear chain. On another hand, silane units having an index equal to 2 can be either a part of a cyclic structure, or an internal block of a linear chain. Finally, for totally condensed trialkoxysilanes, with *i* having a value of 3, the corresponding block is a connecting point of a three-dimensional network. The various conformations described here and their notations are summarized in Figure I–9, where the silicon atoms described by these notations are emphasised by bold characters.

This nomenclature does not allow describing condensed molecules formed from partly hydrolyzed silanols. However, the role of such intermediates was shown to be important only under specific conditions, where the hydrolysis reaction is the limiting phenomenon [48]. Thus, these structures are rarely detected when the reaction is carried out under usual conditions.

The totally condensed structures, M^1, D^2 and T^3, have no more hydroxyl moieties available; hence they are not suitable anymore for the chemical modification with OH-rich substrates. Whereas in partly condensed systems, such as D^1, T^1 and T^2, the formed intermediates still contain hydroxyl groups and they are consequently potentially reactive with such surfaces. This observation has been the most relevant driving forces pushing us to develop a tool to evaluate the reactivity of any solution at a given time, as a function of its composition. In this context, we considered the general concept named *Active Si-OH function*, developed by Beari and coworkers [47], and dealing with trialkoxysilanes coupling agents, in order to propose three new expressions. These expressions, which will be named *SR* (Silanol Reactivity Parameter), correspond to the three families of alkoxysilanes considered in this work, namely: mono-, di- and tri-alkoxysilanes, and are given in Equations I-1 to I-3 respectively:

$$\mathrm{SR} = \%M^{0}{}_{\mathrm{H}}$$

Equation I-1: SR parameter for a monoalkoxysilane

$$\mathrm{SR} = \frac{\left(2 * \%D^{0}{}_{\mathrm{H}}\right) + \left(1 * \%D^{1}\right)}{2}$$

Equation I-2: SR parameter for a dialkoxysilane

$$\mathrm{SR} = \frac{\left(3 * \%T^{0}{}_{\mathrm{H}}\right) + \left(2 * \%T^{1}\right) + \left(1 * \%T^{2}\right)}{3}$$

Equation I-3: SR parameter for a trialkoxysilane

Neither the unhydrolyzed nor the totally condensed species appear in the equations introduced for all three families, since they bear no hydroxyl moieties that could be used for grafting. Importantly, this model is based on two main approximations: (i) The first one concerns the very fast kinetic of hydrolysis frequently observed in applicative solution, it is assumed here that the hydrolysis is complete for all molecules and that there are no partially hydrolyzed silanols in solution. (ii) The second approximation is related to the fact that these expressions do not take into account the steric hindrance effect associated with silanol groups which can belong to a rather different chemical environment (substituents, elecro-negativity, etc.). As an example, in highly condensed tri-dimensional molecule made of mixed T^2 and T^3, some remaining hydroxyls (those of the T^2 structures) may be squeezed in the tri-dimensional network and hence be hardly accessible for the adsorption and the grafting. Therefore, it can be assumed that the reactivity of the solutions evaluated by SR is systematically over-estimated. However, despite its imperfections, this model provides a fast comparison tool between solutions in different conditions.

A specific case of silane condensation is the formation of cyclic compounds instead of linear chains. The existence of such structures has been reported in many studies [8], [27], [30], [49-55]. In particular, Rankin and co-workers [20] reported that for methylethoxysilanes, the formation of 4-membered silicon rings was observed for both T and D structures, whereas the formation of 3-membered silicon rings were formed at appreciable rates only for D structures. The stability for such 3-membered rings was reported to be better for diethylethoxysilanes condensation when compared to dimethylethoxysilane. However, the observations of both 3-membered and 4-membered rings were confirmed by Zhang [50] for a solution of dimethyldiethoxysilane. The proposed structures for such cyclic compounds are presented in Figure I–10.

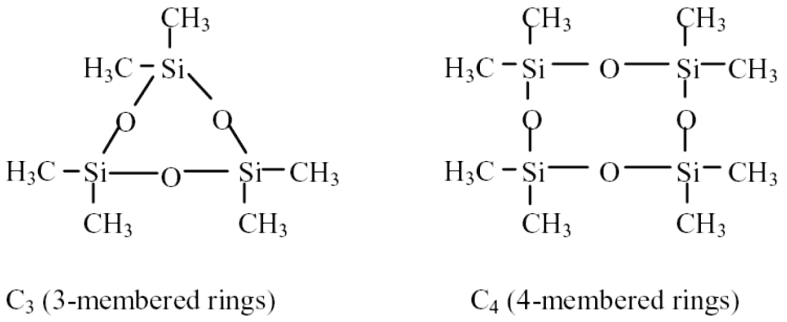

Figure I–10: Structures for 3- and 4-membered rings obtained from Dimethyldiethoxysilane cyclization, as proposed by Zhang [50].

In opposition to hydrolysis, the mechanism through which self-condensation reaction occurs is much less understood, most likely due to its more complex nature involving several reactions and steps occurring at similar orders of time [56]. Chojnowski and coworkers [49], [57] proposed that

the origin of condensation reactions in base media can be related to the destabilization of neighboring Si-O bonds by the deprotonation of silanols.

The reversibility of self-condensation reactions has been discussed in literature and is more controversial than that of reverse hydrolysis. Osterholtz and Pohl proposed reverse condensation reactions as an explanation to the slower rate of condensation observed in presence of alcohol under certain conditions [41]. In another study, Prabakar and Assink concluded that condensation reactions were irreversible in the mixtures of silanes on which they based their works [45]. Finally, Rankin and co-workers [20] proposed a model describing the hydrolysis and condensation of methylethoxysilane with varied number of alkoxy groups. In this work, they established a sensitivity parameter evaluating the hydrolysis and condensation reactions, and excluded (arbitrarily) from their modelling the possibility of Si-O-Si breakage. In another study, they pointed out the fact that under acidic conditions, the M^2 dimer, hexamethyldisiloxane, is well known to hydrolyze readily [30]. Most likely, it seems that self-condensation, for a specific molecular configurations, is a reversible reaction; however the rate of the reverse reaction is very low in most conditions. Furthermore, the pH and the environment of the siloxane group under attack might play a very important role. As an example, siloxane bonds in a totally condensed environment are unlikely to be removed, whereas on end chain units with silanol groups, the electron withdrawing effect of the neighbouring silanols on the silicon may destabilize the siloxane link.

I.B.4 The importance of controlling hydrolysis and condensation reactions

In order to verify if alkoxy groups react directly with hydroxyl functions of cellulose surfaces, Castellano and coworkers [58] have carried out a set of experiments in rigorously anhydrous conditions. The result of their investigations established unambiguously that siloxane moieties do not react with the hydroxyl groups of cellulose even at high temperature and in relatively polar media. Further investigations proved that the addition of moisture to these systems enabled the condensation to take place. Since anhydrous reaction of alkoxysilanes on more electrophilic hydroxyl moieties were previously described, the authors suggested that the poor acidic character of the alcoholic functions borne by cellulose may be the origin of such a phenomenon. Also, the central role of hydrolysis is particularly emphasized in Parker's review on organosilanes and adhesion were the author defends the idea that the use of silanes in many applications was deemed as a failure due to a lack of control on the hydrolysis of the adhesion promoter [5].

The silane modification of cellulose has been further investigated by Brochier-Salon and co-workers [34] who established that the control of hydrolysis is necessary but not sufficient. Indeed, it was shown that self-condensation reactions should be reduced as much as possible and the formation of totally condensed units should be strongly limited in order to enhance cellulose grafting by organosilanes in alcoholic solutions [35].

Such results were confirmed for the use of silane solution on different substrates. It was suggested that optimum metal joint enhancement was provided with a good durability by solutions in which virtually complete hydrolysis of alkoxy groups has occurred with minimal silanol condensation [4], [27]. Also, adhesion promotion by the use of aqueous solutions of γ-glycidoxypropylsilane was investigated by Bertelsen and Boerio [59] who demonstrated that the lower results from wedge tests was directly correlated to the increasing concentrations of condensed structures in the solution over time. Similarly, in the sol-gel process, it has been shown that the final properties of gels are dependent on the early hydrolysis and condensation steps in forming the sol-gel [60]. Therefore, a good knowledge of the silanol concentration and of the degree of oligomerization is of decisive importance for the practical use of these solutions [47]. So, it is extremely important to be able to characterize the reaction rates of these consecutive and competitive reactions, under the processing condition used for chemical grafting of any OH-rich solid substrate.

I.C Characterization of alkoxysilane solutions

As early as the 1950s, many researchers understood the need to investigate and model the reaction rates of alkoxysilanes [51], [61-63], using various analytical means. Thus, Fourier Transform Infrared spectroscopy (FTIR) has been extensively used, due to the easy availability of the equipment and the very good time resolution of the method. Many authors have proposed FTIR peak attributions for silane solutions, and have ascertained the kinetics of hydrolysis and condensation by this tool [40], [41], [50], [56], [64], [65]. However, one of the limitations of the method is the possibility of overlapping of some peaks. As an example, Jiang and co-workers [28], [40] studied the reaction of dimethyldimethoxysilane with water in dioxane. In this work, FTIR was proven to be a good tool, however the authors noted that the peaks corresponding to Si-O-Si adsorption, which shall be used to set-up the rate of condensation reactions, are located between 1100 cm^{-1} and 1000 cm^{-1}, and therefore may be overlapped by C-O or Si-O-C adsorption bands. Consequently, it is necessary to call upon the use of other analytical mean allowing the observation of reactions *in situ*.

High Pressure Liquid Chromotagraphy (HP-LC) [66], Raman spectroscopy [67], small angle X-ray scattering [68], gas chromatography [68], mass spectrometry [47], or the measurement of the interfacial tension at a water/alkane interface by pendant drop method [69] were used in this context. However, in many cases, these studies have also called upon Nuclear Magnetic Resonance spectroscopy (NMR) to obtain *in-situ* observations.

Indeed, more recently, most of the studies on reaction kinetics used experimental data obtained from NMR. Both ^{1}H, ^{13}C, and ^{29}Si NMR were successfully used to monitor the reactions of silanes

in solution [33], [35], [40], [69], [70], and in few cases other atoms such as Oxygen or Fluorine were used depending on the structure of the silane. While ^{1}H and ^{13}C NMR allow to follow-up the reaction of alkoxy groups through the consumption of water and the release of alcohol, ^{29}Si NMR is the only tool allowing the direct observation of the change of substituents on the silicon atom. Despites its low sensibility causing the need for concentrated solutions (up to 10% in silane), ^{29}Si NMR signal is very sensitive to neighbouring effects. It is therefore possible to separate the signals from pristine molecules, partially or completely hydrolyzed silanols, and siloxanes with different degrees of condensation [47]. In fact, it is known that the hydrolysis of silanes to silanols generally causes a slight down-field shift as the electronegativity of the oxygen decreases due to a greater electronegative character of the hydroxyl group compared to that of the alkoxy counterpart [36]. Furthermore, the condensation reactions of the silanols result in the replacement of Si-OH groups by Si-O-Si bonds. Such phenomenon is emphasized in the NMR spectrum by important up-field shifts due to the increase in electronegativity of the new link involving oxygen atom. These shifts yield quite distinct peaks corresponding to the various combinations of Si-O-Si bonds, as discussed above. The peaks attribution for various structures based on these assumptions was confirmed by experimental data obtained from other techniques [36], [60], [71]. As far as mixtures of silanes are concerned, ^{29}Si NMR was able to discriminate between cross- and self-condensation of the different monomers [45], [53], [64].

It is meaningful to note here that due to the necessity of using deuterated *nuclei* to acquire NMR spectra, the rates of reactions observed may be affected by this change in solvent composition. In fact, De Buyl and Kretschmer [69] observed differences between the reaction rate they observed using NMR data for γ-glycidoxylpropylsilane and those exposed in literature, from other techniques, and proposed that the deuterium isotope effect might explain the difference. This effect results in slowing down the reaction rates significantly. Additionally, this problem has also been addressed by Rankin and co-workers [30] who recommended avoiding the use of deuterated solvents whenever possible.

Finally, silane-born species having rather long relaxation time, many researchers have made use of spin relaxation agents, mostly chromium agents, in order to acquire enough signals for a good spectral resolution in short period of times thus increasing the time resolution of the method [31], [72]. However, doubts were pointed out on the impact of such agents on the silane reaction rates. In this context, Assink and Kay [73] showed that the addition of a chromium spin relaxation agent has no impact on the initial reaction kinetics of the silane solution under the conditions of the analysis.

Owing to the various analytical means available, and in particular the various methods developed with ^{29}Si NMR, the effects of several parameters on silane hydrolysis and condensation have been studied over the last decades.

I.D Parameters influencing alkoxysilanes reactions in solution

The alkoxysilane structure, the pH of the solution, the temperature, the silane concentration, and the type of the solvent were found to be the predominant parameters affecting the kinetic rates of hydrolysis and condensation of alkoxysilanes [4].

I.D.1 Influence of alkoxysilane structure

It was shown that the organic substituent has a great importance on the rates of both hydrolysis and condensation reactions. The role of the substituent is proposed to be related to the affinity between the silane and the medium, particularly in concerns of its polarity [36]. Also, it can be envisaged that the electronic and steric effects of the substituent can be used to qualitatively predict the relative rates of reaction of these compounds [74]. However, these trends can be greatly affected by reaction conditions, such as pH and solvent type. Therefore, the overall reaction conditions must be considered [71].

The rate of hydrolysis and condensation of various N-bearing alkoxysilanes was observed by Brochier-Salon and co-workers [33], [36], and various conclusions were presented, in particular on the importance of the position of the amine group borne by the organic moiety. In fact, it was shown that aminosilanes having one or three amine groups on their functional moiety behave very differently, as the former condenses to soluble species whereas the second forms insoluble aggregates.

Besides, in the case of a functional group undergoing chemical reactions in the medium, the kinetics of reactions of the silicon group may be affected. While studying the reactions of γ-glycidoxypropylsilane, de Buyl and Kretschmer [69] observed that the rate of hydrolysis of the silane was directly related to the kinetic of hydrolysis of the epoxy ring which occurs in slightly acidic conditions. From these results, the existence of specific interaction such as hydrogen bonding between the silanols and the formed diol was proposed. However, it was not possible to determine if these interactions were occurring through an intramolecular or an intermolecular mechanism.

It is possible to tailor the solution functionality by mixing silanes with different substituents, which has proven to be useful in the sol-gel process. Thus, for example, such mixtures made from an epoxysilane and amino-derivatives, were observed by Heitz [64], who reported that the hydrolysis reaction rate of the mixture was higher than those observed for each silane separately. However Prabakar and Assink [45] exposed that the cross-condensation reaction kinetics between alkyltriethoxysilanes and tetraethoxysilanes was intermediate to the rates of self-condensation of each silane.

As exposed previously, the hydrolysis reaction has been shown to follow a step-wise mechanism [2]. It was observed that the kinetics of each step is different and is order dependent. Indeed, whereas the first alkoxy group hydrolyzes rather slowly, the hydrolysis of the second group is faster and that of the third moiety proceeds even more rapidly [2], [18]. These observations have been ascribed to the consequence of an improvement of solubility of the partially hydrolyzed silane in the medium [39]. Furthermore, it has been demonstrated that larger alkoxy groups hydrolyzes more slowly [41]. Values reported in literature show that, in similar conditions, the hydrolysis of an ethoxy group is 5 to 10 times slower than that of a methoxy counterpart [41], [66], [71], [74].

In addition, the number of alkoxy groups also has a great importance. When alkoxy moieties are replaced by alkyl substituents, the hydrolysis rates of the remaining alkoxy groups are modified. Hook [71] stated that while the ethoxy group is a moderate electron withdrawer, the methyl group is a weak electron donor, hence the replacement of the former by the later is expected to cause an increase in negative charge at the silicon atom, thus increasing the protonation of the Si-O bonds. Consequently, the rates of hydrolysis of methyl substituted compounds are expected to be higher than that of the initial ethoxysilanes. Accordingly, Arkles and co-workers [66] have measured that the rate of hydrolysis of trimethylmethoxysilane is faster than that of dimethydimethoxysilane, which in turn is more rapid than that of trimethylmethoxysilane. Such findings were confirmed in other reports [29], [39]. In addition, the effect of alkoxy replacement by alkyl groups also impact the condensation rates, as described by Rankin and co workers [20], who showed that methyl substitution increases condensation rates, in opposition to findings on ethyl substitution [75].

I.D.2 Influence of pH

An abundant literature is available on the impact of pH on the hydrolysis and condensation reactions of silane coupling agent. Pratt [76] has measured the extent of the hydrolysis over a wide range of pH (from about 1 to 13). The observed rate constants fitted a V-shaped profile with a minimum at a pH value between 6 and 7. Furthermore, acid catalysis was observed to be specific to certain acids, whereas a general base catalysis occurred in the systems under scrutiny. This V-shaped profile was assessed for trialkoxy-, dialkoxy-, and monoalkoxysilanes by Pohl and Osterholtz [56] and was found to be in agreement with data reported in other studies and general textbooks [2], [8], [37], [40], [41], [77]. Erickson and Plueddemann [78] have proposed that the solution pH effectively controls both the hydrolysis and condensation reactions and have described general trends for the effect of both range of pH. According to these observations, alkoxysilanes rapidly undergo hydrolysis under slightly acidic conditions to form monomeric silanols and condense slowly to small oligomers. On contrary, at pH values above 7, the hydrolysis catalysis is maintained, but condensation reactions tend to proceed at very high rates. For what concerns condensation, the pH dependence reported in literature is also very high, with a minimum of

reaction rate at a pH close to 4. This minimum may vary slightly between silanes, due to the variations of substituents on the silicon. In addition, the pH of the solution was also reported to impact the formation of cyclic species. Indeed, the amount of 4-membered rings produced in acidic conditions was found to be higher that than that yielded by alkaline conditions [30].

From the applicative point of view, it is desired to produce reactive solutions with a high amount of silanol functions and as little condensed structures as possible. Thus, in regard of the findings presented here, the use of slightly acidic solutions with a pH close to 4 is preferred, in order to limit the kinetics of self-condensation while maintaining a high rate of hydrolysis.

I.D.3 Influence of temperature

The specific impact of temperature on hydrolysis was studied by Jiang and coworkers [28] who noticed a significant increase of hydrolysis rate as the temperature was raised. These results are in good agreement with those obtained while studying the hydrolysis and condensation kinetics of γ-glycidoxypropylsilane at three different temperatures, 26°C, 50°C and 70°C [69]. Interestingly, the rate of consumption of the hydrolyzed silane into T^1 structures was not impacted by the temperature, however further condensation into T^2 and T^3 was significantly accelerated.

I.D.4 Influence of concentration

As expected, the concentration of an alkoxysilane solution impacts both the hydrolysis and condensation rates [4]. The relationship between solution concentration and rate of hydrolysis was found to follow an exponential behavior by Jiang and coworkers who studied dioxane aqueous solutions of dimethyldimethoxysilane [40]. Besides, the condensation reaction was found to obey to second-order kinetic models by Osterholtz and Pohl [41]. In a mixture of silane, tripling the concentration resulted in an increased kinetic of condensation, while the general trends remained similar [64].

Ishida and coworkers proposed that the silanol/oligomers balance at equilibrium is dependent on the concentration [79], [80]. Indeed, aminopropylsilane solutions with very low concentration, below 0.15% w/w of silane, were shown to form solution comprising almost only monomeric triol structures. Above that concentration of 0.15%, an increase in the condensation products ratio was observed. Furthermore, moving the concentration of the solution above that transition value was shown to influence the amount of silane uptake by glass fibers [80].

In overall, most researchers agree on the fact that a low silane concentration increases the benefits of silane treatments. Osterholtz and Pohl [41] have proposed to use solution with concentrations below 1% by weight for what they describe as “typical organofunctional silanes”,

whereas others have proposed the use of concentrations ranging from 2% to 4% by weight [4], [35], [64].

I.D.5 Influence of solvent composition

The rates of reactions of silanes are strongly dependant on the medium used. In most cases, the hydrolysis of alkoxysilanes is commonly carried out in a mixture of water/alcohol solvents, owing to the generally good solubility of these compounds in such solvent [81].

The recent incitation of avoiding (or minimizing) the use of organic solvents leads to the apparition of investigations involving pure water or solvent-free silane treatments [69]. In this context, an extensive study was undertaken by Brochier-Salon and Belgacem [38], aiming at determining the kinetics of hydrolysis and condensation of alkoxysilane with various functional groups in mixed alcohol-water mixtures, with varied ratios. For most structures, the addition of water resulted in increasing both hydrolysis and condensation kinetics. Except for aminosilanes, for which the rate of the condensation reaction decreased. The impact of the water amount in solution had been previously discussed, but mostly for small concentrations. For instance, Peña-Alonzo [52] demonstrated that a stoichiometric reaction between water and alkoxy groups is necessary to reach a pseudo-equilibrium of hydrolysis before starting the condensation reaction. On another hand, limiting the amount of water allows a better control on the hydrolysis and the distribution of the species observed in the early stages of the reaction, which is sometimes needed in the sol-gel process to favour the formation of gels instead of aggregates [48].

The nature of the solvent not only impacts the kinetics of reactions, but also their extent of conversion. It was early stated by Grubb [61] that in protic solvents, such as water and alcohols, the condensation reactions from silanols to siloxanes approached equilibrium rather than completion. This may be related to the tendency of protic solvents to favour the solvolysis of silanes [40].

Finally, the presence in the solution of other compounds may impact the reactions of the silanes. Almanza-Workman and co-workers [13] described the impact of the addition of a cationic surfactant on the stability of a water dispersible commercial silane. The surfactant was shown to increase the shelf life of the bath by retarding the condensation of silanols. However, it was shown that over a critical surfactant concentration, the interactions between the silane and the surface on which the solution was applied were impacted, thus decreasing the overall treatment efficiency.

I.D.6 Catalysis

In addition to acid and base catalysis, some researchers have shown interest in the use of chemical catalysts to accelerate the hydrolysis reactions of some alkoxysilanes.

The impact of various catalysts including metal acetylacetonate and alkyl tin esters on the hydrolysis and condensation of a 1% γ-glycidoxypropylsilane and 4% water solution in ethanol was evaluated [31]. Optimal results were obtained for tin esters (dibutyltin dilaurate and dibutyltin diacetate), nevertheless the condensation rate was also increased by these catalysts. Metal acetonates were also successfully evaluated by Zhang with similar conclusions [82].

Triethylamine, (TEA) [35], [37], [48], [83] was also found to catalyse the competitive-consecutive self-condensation reaction of silanols. This reaction can be so fast that the formed silanols are not detected due to their rapid consumption [37]. Moreover, in presence of 2% TEA, non-aminosilanes were shown to have hydrolysis rate similar to that of aminosilanes, at the exception of octyltriethoxysilane (NOTES) for which a very large amount of catalyst was needed. In fact, in the case of NOTES, a quantity of tenfold more than that used for the other structures studied was added to reach similar kinetic rates. In all cases, the hydrolysis was followed by a very fast polycondensation of the silanols, leading to the formation of insoluble structures [35].

I.D.7 The special case of aminosilanes

Aminosilanes have been shown to display features otherwise uncommon in the family of alkoxysilane, due to the presence of at least one amine group on their functional moiety. First, these compounds have been found to be totally water soluble, most probably thanks to the presence of the hydrophilic amine function. Also, at their natural pH, which is in general close to 11~12, aminosilanes solutions have been shown to react very rapidly and reach an equilibrium state with formation of small hydrophilic aggregates [64]. However, further investigations have shown that a silane having three amine moieties behaved differently, forming insoluble aggregates in a mixture of 80% ethanol and 20% water [36]. When acetic acid is added to the reaction medium to reach a pH of 4, prior to the silane insertion, the resulting hydrolysed species are highly stable for solution concentrations up to 50% and the amount of condensed structures is very limited [1].

It was proposed that the very fast kinetics of aminosilanes in solution occur through a self-catalytic effect of the amine function on the silanes reactions [36]. Additionally, an extensive study on N-bearing alkoxysilanes solvolysis, hydrolysis and condensation was undertaken by Brochier-Salon and coworkers [33], in order to understand the specific relationship between the structure of aminosilanes and their exclusive features. The results of this work have highlighted the importance of the nature and position of the nitrogen bearing function in the structure of the silane. Indeed, it was reported that the solvolysis reactions between pristine silanes and an alcoholic anhydrous solvent is a step-wise mechanism and only occurs for γ-aminosilanes, i.e. molecules having an amine function attached on the third atom of their functional chain, if it is not hindered neither electronically, nor sterically. In addition it was also noticed that the reactivity of the amino function toward hydrolysis is lowered when the function is born by an atom localised more than 3 bonds away from the silicon. Moreover, the catalytic effect of certain aminosilane has been shown to

allow increasing the hydrolysis and condensation rates of other silane in the case of cross condensation of silane mixtures [64].

Regarding the stability of hydrolyzed aminosilane solutions, many cases have been reported. At low concentration, solutions of 0.2% or less w/w of monomeric silanetriol were reported to be stable over time [66], [80]. A recent work has shown that increasing the amount of water in a silane ethanolic solution allowed stabilizing more monomeric units, despite maintaining the very short hydrolysis time typical of these compounds [38]. Actually, the best results were obtained in purely aqueous solutions.

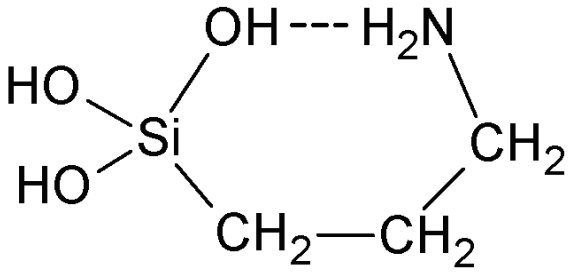

Figure I–11: γ-aminopropylsilanetriol internal hydrogen bonded six-member ring, based on [84].

Different mechanisms have been proposed to explain the stability of hydrolyzed aminosilanes in solution. Moses [84] proposed that the stabilization of γ-aminopropylsilanetriol occurs *via* the formation of an internally hydrogen bonded six-member ring, with partial proton transfer between the Si-OH moiety and the end amine function, thus involving the formation of a zwitterion as stabilized silanol molecule. The existence of such structures, represented in Figure I–11, was also mentioned by Chiang and coworkers [65], in view of their experimental results. These results furthermore refuted the existence of 5-membered rings comprising weak interactions between the amine moieties and the central silicon atoms. Finally, the cyclization of 3-membered or 4-membered rings, such as the structures mentioned in Figure I–10, has been proposed as a possible explanation to the high solubility of highly condensed aminosilane solutions, especially at low pH [1].

I.E Conclusions

It is commonly understood that in order to successfully apply silane treatments to modify the surface or the interfacial properties of materials, it is necessary to apply highly reactive silane solutions. Producing and maintaining such solutions with a maximum concentration of reactive species imposes to understand the mechanisms of the reactions occurring in the medium. These mechanisms are complex due to the number of step-wise, consecutive, and competitive reactions involved, in addition to the many solution variables that can control the kinetic rates of each reaction. Hence, in all cases, the process should be tailored according to time-resolved *in-situ* observations of the solution composition before any further optimization of the process itself.

List of references

[1] E. P. Plueddemann, *Silane coupling agents*. Springer, 1991.

[2] K. L. Mittal, *Silanes and other coupling agents*. VSP, 2000.

[3] R. Yang, Y. Liu, K. Wang, et J. Yu, « Characterization of surface interaction of inorganic fillers with silane coupling agents », *Journal of Analytical and Applied Pyrolysis*, vol. 70, n°. 2, p. 413-425, 2003.

[4] M.-L. Abel, R. D. Allington, R. P. Digby, N. Porritt, S. J. Shaw, et J. F. Watts, « Understanding the relationship between silane application conditions, bond durability and locus of failure », *International Journal of Adhesion and Adhesives*, vol. 26, n°. 1-2, p. 2-15, 2006.

[5] A. Parker, « A technical review on organosilanes and adhesion ».

[6] K. L. Mittal et A. Pizzi, *Adhesion promotion techniques*. CRC Press, 1999.

[7] A. C. Miller et J. C. Berg, « Effect of silane coupling agent adsorbate structure on adhesion performance with a polymeric matrix », *Composites Part A: Applied Science and Manufacturing*, vol. 34, n°. 4, p. 327-332, 2003.

[8] J. Weis et N. Auner, *Organosilicon chemistry V*. Wiley-VCH, 2003.

[9] P. Jutzi et U. Schubert, *Silicon chemistry*. Wiley-VCH, 2003.

[10] A. Pizzi et K. L. Mittal, *Handbook of adhesive technology*. CRC Press, 2003.

[11] A. Norström, H. Watson, B. Engström, et J. Rosenholm, « Treatment of E-glass fibres with acid, base and silanes », *Colloids and Surfaces A: Physicochemical and Engineering Aspects*, vol. 194, n°. 1-3, p. 143-157, 2001.

[12] S.-J. Park et J.-S. Jin, « Effect of silane coupling agent on interphase and performance of glass fibers/unsaturated polyester composites », *Journal of Colloid and Interface Science*, vol. 242, n°. 1, p. 174-179, 2001.

[13] A. M. Almanza-Workman, S. Raghavan, P. Deymier, D. J. Monk, et R. Roop, « Aqueous silane-surfactant co-dispersions for deposition of hydrophobic coatings onto pre-oxidized polysilicon », *Colloids and Surfaces A: Physicochemical and Engineering Aspects*, vol. 232, n°. 1, p. 67-75, 2004.

[14] G. Sèbe et M. A. Brook, « Hydrophobization of wood surfaces: covalent grafting of silicone polymers », *Wood Science and Technology*, vol. 35, n°. 3, p. 269-282, 2001.

[15] M. A. Tshabalala, P. Kingshott, M. R. VanLandingham, et D. Plackett, « Surface chemistry and moisture sorption properties of wood coated with multifunctional alkoxysilanes by sol-gel process », *Journal of Applied Polymer Science*, vol. 88, n°. 12, p. 2828-2841, 2003.

[16] N. Kim, D. H. Shin, et Y. T. Lee, « Effect of silane coupling agents on the performance of RO membranes », *Journal of Membrane Science*, vol. 300, n°. 1-2, p. 224-231, 2007.

[17] R. D. Jaeger et M. Gleria, *Inorganic polymers*. Nova Science Publishers, 2007.

[18] C. J. Brinker et G. W. Scherer, *Sol-gel science*. Gulf Professional Publishing, 1990.

[19] S. Sakka, *Sol-gel science and technology*. Springer, 2003.

[20] S. E. Rankin, C. W. Macosko, et A. V. McCormick, « Sol-gel polycondensation kinetic modeling: Methylethoxysilanes », *AIChE Journal*, vol. 44, n°. 5, p. 1141-1156, 1998.

[21] N. Re, « Kinetics of bicomponent sol-gel processes », *Journal of Non-Crystalline Solids*, vol. 142, p. 1-17, 1992.

[22] S. E. Rankin et A. V. McCormick, « Hydrolysis pseudoequilibrium: challenges and opportunities to sol-gel silicate kinetics », *Chemical Engineering Science*, vol. 55, n°. 11, p. 1955-1967, 2000.

[23] S. Sequeira, D. V. Evtuguin, I. Portugal, et A. P. Esculcas, « Synthesis and characterisation of cellulose/silica hybrids obtained by heteropoly acid catalysed sol-gel process », *Materials Science and Engineering: C*, vol. 27, n°. 1, p. 172-179, janv. 2007.

[24] A. Vainrub, F. Devreux, J. P. Boilot, F. Chaput, et M. Sarkar, « Sol-gel polymerization in alkoxysilanes: 29si nmr study and simulation of chemical kinetics », *Materials Science and Engineering B*, vol. 37, n°. 1-3, p. 197-200, févr. 1996.

[25] J. D. Wright et N. A. J. M. Sommerdijk, *Sol-gel materials*. CRC Press, 2001.

[26] C. J. Brinker et G. W. Scherer, « Hydrolysis and condensation II - Silicates », in *Sol-gel science: the physics and chemistry of sol-gel processing*, 5e éd., Gulf Professional Publishing, 1990, p. 97-234.

[27] S. Savard, L.-P. Blanchard, J. Léonard, et R. E. Prud'homme, « Hydrolysis and condensation of silanes in aqueous solutions », *Polymer Composites*, vol. 5, n°. 4, p. 242-249, 1984.

[28] H. Jiang, Z. Zheng, Z. Li, et X. Wang, « Effects of temperature and solvent on the hydrolysis of alkoxysilane under alkaline conditions », *Industrial & Engineering Chemistry Research*, vol. 45, n°. 25, p. 8617-8622, 2006.

[29] H. Schmidt, H. Scholze, et A. Kaiser, « Principles of hydrolysis and condensation reaction of alkoxysilanes », *Journal of Non-Crystalline Solids*, vol. 63, n°. 1-2, p. 1-11, 1984.

[30] S. E. Rankin et A. V. McCormick, « 29Si NMR study of base-catalyzed polymerization of dimethyldiethoxysilane », *Magnetic Resonance in Chemistry*, vol. 37, n°. 13, p. S27-S37, 1999.

[31] S. A. Torry, A. Campbell, A. V. Cunliffe, et D. A. Tod, « Kinetic analysis of organosilane hydrolysis and condensation », *International Journal of Adhesion and Adhesives*, vol. 26, n°. 1-2, p. 40-49, 2006.

[32] R. H. Glaser et G. L. Wilkes, « Structure property behavior of polydimethylsiloxane and poly(tetramethylene oxide) modified TEOS based sol-gel materials », *Polymer Bulletin*, vol. 19, n°. 1, p. 51-57, 1988.

[33] M. C. Brochier-Salon, M. Bardet, et M. N. Belgacem, « Solvolysis–hydrolysis of N-bearing alkoxysilanes: Reactions studied with 29Si NMR », *Silicon Chemistry*, vol. 3, n°. 6, p. 335-350, 2008.

[34] M. C. Brochier-Salon, G. Gerbaud, M. Abdelmouleh, C. Bruzzese, S. Boufi, et M. N. Belgacem, « Studies of interactions between silane coupling agents and cellulose fibers with liquid and solid-state NMR », *Magnetic Resonance in Chemistry*, vol. 45, n°. 6, p. 473-483, 2007.

[35] M. C. Brochier-Salon, P.-A. Bayle, M. Abdelmouleh, S. Boufi, et M. N. Belgacem, « Kinetics of hydrolysis and self condensation reactions of silanes by NMR spectroscopy », *Colloids and Surfaces A: Physicochemical and Engineering Aspects*, vol. 312, n°. 2-3, p. 83-91, 2008.

[36] M. C. Brochier-Salon, M. Abdelmouleh, S. Boufi, M. N. Belgacem, et A. Gandini, « Silane adsorption onto cellulose fibers: Hydrolysis and condensation reactions », *Journal of Colloid and Interface Science*, vol. 289, n°. 1, p. 249-261, 2005.

[37] R. Bel-Hassen, S. Boufi, M. C. Brochier-Salon, M. Abdelmouleh, et M. N. Belgacem, « Adsorption of silane onto cellulose fibers. II. The effect of pH on silane hydrolysis, condensation, and adsorption behavior », *Journal of Applied Polymer Science*, vol. 108, n°. 3, p. 1958-1968, 2008.

[38] M. C. Brochier-Salon et M. N. Belgacem, « Competition between hydrolysis and condensation reactions of trialkoxysilanes, as a function of the amount of water and the nature of the organic group », *Colloids and Surfaces A: Physicochemical and Engineering Aspects*, vol. 366, n°. 1-3, p. 147-154, 2010.

[39] K. A. Smith, « Polycondensation of methyltrimethoxysilane », *Macromolecules*, vol. 20, n°. 10, p. 2514-2520, 1987.

[40] H. Jiang, Z. Zheng, J. Xiong, et X. Wang, « Studies on dialkoxysilane hydrolysis kinetics under alkaline conditions », *Journal of Non-Crystalline Solids*, vol. 353, n°. 44-46, p. 4178-4185, 2007.

[41] F. D. Osterholtz et E. R. Pohl, « Kinetics of the hydrolysis and condensation of organofunctional alkoxysilanes: a review », *Journal of Adhesion Science and Technology*, vol. 6, p. 127-149, 1992.

[42] J. A. Deiters et R. R. Holmes, « Effect of entering and leaving groups on nucleophilic substitution reactions at silicon. A molecular orbital approach », *J. Am. Chem. Soc.*, vol. 109, n°. 6, p. 1692-1696, 1987.

[43] J. A. Deiters et R. R. Holmes, « Pathways for nucleophilic substitution at silicon. A molecular orbital approach », *J. Am. Chem. Soc.*, vol. 109, n°. 6, p. 1686-1692, 1987.

[44] T. M. Alam, R. A. Assink, et D. A. Loy, « Hydrolysis and esterification in organically modified alkoxysilanes: A 29Si NMR investigation of Methyltrimethoxysilane », *Chemistry of Materials*, vol. 8, n°. 9, p. 2366-2374, 1996.

[45] S. Prabakar et R. A. Assink, « Hydrolysis and condensation kinetics of two component organically modified silica sols », *Journal of Non-Crystalline Solids*, vol. 211, n°. 1-2, p. 39-48, 1997.

[46] B. Orel, R. Ješe, A. Vilčnik, et U. L. Štangar, « Hydrolysis and Solvolysis of Methyltriethoxysilane catalyzed with HCl or Trifluoroacetic acid: IR spectroscopic and surface energy studies », *Journal of Sol-Gel Science and Technology*, vol. 34, n°. 3, p. 251-265, 2005.

[47] F. Beari, M. Brand, P. Jenkner, R. Lehnert, H. J. Metternich, J. Monkiewicz et H. W. Siesler, « Organofunctional alkoxysilanes in dilute aqueous solution: new accounts on the dynamic structural mutability », *Journal of Organometallic Chemistry*, vol. 625, n°. 2, p. 208-216, 2001.

[48] J. K. Crandall et C. Morel-Fourrier, « Siloxanes from the hydrolysis of isopropyltrimethoxysilane », *Journal of Organometallic Chemistry*, vol. 489, n°. 1-2, p. 5-13, 1995.

[49] J. Chojnowski, S. Rubinsztajn, et L. Wilczek, « Acid-catalyzed condensation of model hydroxyl-terminated dimethylsiloxane oligomers - cyclization vs. linear condensation: intra-inter catalysis », *Macromolecules*, vol. 20, n°. 10, p. 2345-2355, 1987.

[50] Z. Zhang, B. P. Gorman, H. Dong, R. A. Orozco-Teran, D. W. Mueller, et R. F. Reidy, « Investigation of polymerization and cyclization of Dimethyldiethoxysilane by 29Si NMR and FTIR », *Journal of Sol-Gel Science and Technology*, vol. 28, n°. 2, p. 159-165, 2003.

[51] W. T. Grubb et R. C. Osthoff, « Kinetics of the polymerization of a cyclic dimethylsiloxane », *Journal of the American Chemical Society*, vol. 77, n°. 6, p. 1405-1411, 1955.

[52] R. Peña-Alonso, F. Rubio, J. Rubio, et J. Oteo, « Study of the hydrolysis and condensation of γ-Aminopropyltriethoxysilane by FT-IR spectroscopy », *Journal of Materials Science*, vol. 42, n°. 2, p. 595-603, 2007.

[53] J. Brus et J. Dybal, « Copolymerization of tetraethoxysilane and dimethyl(diethoxy)silane studied by 29Si NMR and ab initio calculations of 29Si NMR chemical shifts », *Polymer*, vol. 40, n°. 25, p. 6933-6945, 1999.

[54] P. Lux, F. Brunet, J. Virlet, et B. Cabane, « Combined DEPT 1D and INEPT DQF COSY 2D experiments in 29Si NMR spectroscopy of alkoxysilane polymers. 2—Applications of 29Si

NMR to polymerisation reactions in Dimethyldiethoxysilane. », *Magnetic Resonance in Chemistry*, vol. 34, p. 173-180, 1996.

[55] R. West, « Cyclic organosilicon compounds. II. Ring size and reactivity in the alkali-catalyzed hydrolysis of silanes », *Journal of the American Chemical Society*, vol. 76, n°. 23, p. 6015-6017, 1954.

[56] E. R. Pohl et F. D. Osterholtz, « Kinetics and mechanisms of condensation of alkylsilanols in aqueous solution », in *Silanes, Surfaces, and Interfaces*, Gordon and Breach., New-York: Leyden D. E., 1986, p. 481-500.

[57] J. Chojnowski, « The behaviour of the silanol function in polycondensation systems », in *Silicon-Containing Polymers*, Royal Society of Chemistry, Cambridge: Jones R. G., 1995, p. 59-72.

[58] M. Castellano, A. Gandini, P. Fabbri, et M. N. Belgacem, « Modification of cellulose fibres with organosilanes: Under what conditions does coupling occur? », *Journal of Colloid and Interface Science*, vol. 273, n°. 2, p. 505-511, 2004.

[59] C. M. Bertelsen et F. J. Boerio, « Linking mechanical properties of silanes to their chemical structure: an analytical study of γ-GPS solutions and films », *Progress in Organic Coatings*, vol. 41, n°. 4, p. 239-246, 2001.

[60] R. A. Assink et B. D. Kay, « Study of Sol-Gel Chemical Reaction Kinetics by NMR », *Annual Review of Materials Science*, vol. 21, p. 491-513, 1991.

[61] W. T. Grubb, « A rate study of the silanol condensation reaction at 25°C in alcoholic solvents », *Journal of the American Chemical Society*, vol. 76, n°. 13, p. 3408-3414, 1954.

[62] S. W. Kantor, W. T. Grubb, et R. C. Osthoff, « The mechanism of the acid- and base-catalyzed equilibration of siloxanes », *Journal of the American Chemical Society*, vol. 76, n°. 20, p. 5190-5197, 1954.

[63] W. T. Grubb et R. C. Osthoff, « Physical properties of organosilicon compounds. II. Trimethylsilanol and Triethylsilanol », *Journal of the American Chemical Society*, vol. 75, n°. 9, p. 2230-2232, 1953.

[64] C. Heitz, G. Laurent, R. Briard, et E. Barthel, « Cross-condensation and particle growth in aqueous silane mixtures at low concentration », *Journal of Colloid and Interface Science*, vol. 298, n°. 1, p. 192-201, 2006.

[65] C.-H. Chiang, H. Ishida, et J. L. Koenig, « The structure of [gamma]-aminopropyltriethoxysilane on glass surfaces », *Journal of Colloid and Interface Science*, vol. 74, n°. 2, p. 396-404, 1980.

[66] B. Arkles, J. R. Steinmetz, J. Zazyczny, et P. Mehta, « Factors contributing to the stability of alkoxysilanes in aqueous solution », *Journal of Adhesion Science and Technology*, vol. 6, p. 193-206, 1992.

[67] T. W. Zerda, I. Artaki, et J. Jonas, « Study of polymerization processes in acid and base catalyzed silica sol-gels », *Journal of Non-Crystalline Solids*, vol. 81, n°. 3, p. 365-379, 1986.

[68] C. J. Brinker, K. D. Keefer, D. W. Schaefer, R. A. Assink, B. D. Kay, et C. S. Ashley, « Sol-gel transition in simple silicates II », *Journal of Non-Crystalline Solids*, vol. 63, n°. 1-2, p. 45-59, 1984.

[69] F. de Buyl et A. Kretschmer, « Understanding hydrolysis and condensation kinetics of γ-Glycidoxypropyltrimethoxysilane », *The Journal of Adhesion*, vol. 84, n°. 2, p. 125, 2008.

[70] M. C. Brochier-Salon et M. N. Belgacem, « Hydrolysis-Condensation Kinetics of Different Silane Coupling Agents », *Phosphorus, Sulfur, and Silicon and the Related Elements*, vol. 186, n°. 2, p. 240-254, 2011.

[71] R. J. Hook, « A 29Si NMR study of the sol-gel polymerisation rates of substituted ethoxysilanes », *Journal of Non-Crystalline Solids*, vol. 195, n°. 1-2, p. 1-15, 1996.

[72] J. C. Pouxviel, J. P. Boilot, J. C. Beloeil, et J. Y. Lallemand, « NMR study of the sol/gel polymerization », *Journal of Non-Crystalline Solids*, vol. 89, n°. 3, p. 345-360, 1987.

[73] R. A. Assink et B. D. Kay, « Sol-gel kinetics I. Functional group kinetics », *Journal of Non-Crystalline Solids*, vol. 99, n°. 2-3, p. 359-370, 1988.

[74] R. Lindberg, G. Sundholm, G. Øye, et J. Sjöblom, « A new method for following the kinetics of the hydrolysis and condensation of silanes », *Colloids and Surfaces A: Physicochemical and Engineering Aspects*, vol. 135, n°. 1-3, p. 53-58, 1998.

[75] J. Sanchez, S. E. Rankin, et A. V. McCormick, « 29Si NMR kinetic study of tetraethoxysilane and Ethyl-substituted ethoxysilane polymerization in acidic conditions », *Industrial & Engineering Chemistry Research*, vol. 35, n°. 1, p. 117-129, 1996.

[76] K. J. McNeil, J. A. DiCaprio, D. A. Walsh, et R. F. Pratt, « Kinetics and mechanism of hydrolysis of a silicate triester, tris(2-methoxyethoxy)phenylsilane », *Journal of the American Chemical Society*, vol. 102, n°. 6, p. 1859-1865, 1980.

[77] G. Tesoro et W. Yulong, « Silane coupling agents: the role of the organofunctional group », *Journal of Adhesion Science and Technology*, vol. 5, n°. 10, p. 771-784, 1991.

[78] P. W. Erickson et E. P. Plueddemann, in *Composite materials*, New York: Academic Press., vol. 6, 1974: Plueddeman EP.

[79] H. Ishida, C.-H. Chiang, et J. L. Koenig, « The structure of aminofunctional silane coupling agents: 1. [gamma]-Aminopropyltriethoxysilane and its analogues », *Polymer*, vol. 23, n°. 2, p. 251-257, 1982.

[80] H. Ishida, S. Naviroj, S. K. Tripathy, J. J. Fitzgerald, et J. L. Koenig, « The structure of an aminosilane coupling agent in aqueous solutions and partially cured solids », *Journal of Polymer Science: Polymer Physics Edition*, vol. 20, n°. 4, p. 701-718, 1982.

[81] I. M. El-Nahhal et N. M. El-Ashgar, « A review on polysiloxane-immobilized ligand systems: Synthesis, characterization and applications », *Journal of Organometallic Chemistry*, vol. 692, n°. 14, p. 2861-2886, 2007.

[82] Z. Zhang, « Catalytic effect of Aluminum Acetylacetonate on hydrolysis and polymerization of Methyltrimethoxysilane », *Langmuir*, vol. 13, n°. 3, p. 473-476, 1997.

[83] G. R. Bogart et D. E. Leyden, « Investigation of Amine-catalyzed alkoxysilane-modified Cab-O-Sil by drift spectroscopy », *Journal of Colloid and Interface Science*, vol. 167, n°. 1, p. 18-26, 1994.

[84] P. R. Moses, L. M. Wier, J. C. Lennox, H. O. Finklea, J. R. Lenhard, et R. W. Murray, « X-ray photoelectron spectroscopy of alkylaminesilanes bound to metal oxide electrodes », *Anal. Chem.*, vol. 50, n°. 4, p. 576-585, 1978.

II. Materials and Methods

II.A Materials

The *in situ* NMR kinetics were carried out in deuterium oxide and ethanol-d_6. Deuterium oxide (D_2O) with a high purity grade (99.96% atom % D) and deuterated ethanol (CD_3-CD_2-OD, Ethanol-d_6 99.5 atom % D, anhydrous) were purchased from Sigma-Aldrich and used as received.

The organo-functional silanes used in this part of the work were: trimethylmethoxysilane (TMMS), dimethyldimethoxysilane (DMDMS), methyltrimethoxysilane (MTMS), methylvinyldiethoxysilane (MVDES), methylvinyldimethoxysilane (MVDMS), 3-aminopropyldimethylethoxysilane (APDMES), and 3-(2-amino-ethylamino)-propyltrimethoxysilane (DAMS). Their structure, formula, physical properties, purity, CAS number and suppliers are described in Table II-1.

For experiments in acidic media, a pH of 4 was obtained by adding an appropriate amount of glacial acetic acid. A research grade product from Sigma-Aldrich was used as received.

Name	Structure	Molecular formula	Molar weight (g/mol)	Density at 25°C (g/cm3)	Boiling point (°C)	Purity (%)	CAS Number	Distributor	Commercial Reference
Trimethylmethoxy-silane (TMMS)	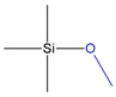	$C_4H_{12}OSi$	104,22	0,756	57	>97	[1825-61-2]	abcr GmbH & Co. KG - Karlsruhe - Germany	AB 111500
Dimethyldimethoxy-silane (DMDMS)	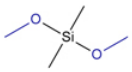	$C_4H_{12}O_2Si$	120,22	0,865	82	> 98 %	[1112-39-6]	Dow Corning, S.A. - Seneffe - Belgium	Z-6194
Methyltrimethoxy-silane (MTMS)		$C_4H_{12}O_3Si$	136,22	0,948	102	> 60 %	[1185-55-3]	Dow Corning, S.A. - Seneffe - Belgium	Z-6070
Methylvinyldimethoxy-silane (MVDMS)	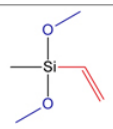	$C_5H_{12}O2Si$	132,22	0,881	104	> 95 %	[16753-62-1]	Dow Corning, S.A. - Seneffe - Belgium	Z-2349
Methylvinyldiethoxy-silane (MVDES)	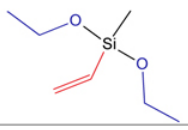	$C_7H_{16}O_2Si$	160,29	0,858	133	> 95 %	[5507-44-8]	Gelest, Inc. - Morrisville, PA - USA	SIV 9085.0
(3-Amino)-propyl-dimethylethoxysilane (APDMES)	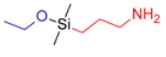	$C_7H_{19}NOSi$	161,32	0,857	78	> 95 %	[18306-79-1]	Gelest, Inc. - Morrisville, PA - USA	SIA 0603.0
3-(2-amino-ethylamino)propyl-trimethoxysilane (DAMS)	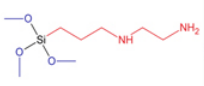	$C_8H_{22}N_2O_3Si$	222,36	1,02	264	> 98 %	[1760-24-3]	Dow Corning, S.A. - Seneffe - Belgium	Z-6094

Table II-1: List of the silanes studied by NMR spectroscopy and their properties. Functional groups are in red, whereas hydrolysable moieties are in blue.

II.B Methods

II.B.1 NMR Kinetics set-up

The silane was weighted directly into clean tubes containing the appropriate amount of deuterium oxide, or deuterium oxide / ethanol-d_6 mixture. The initial reaction time was fixed after the addition of the silane into the tube. The temperature was set at a constant value (25°C or 45°C) and stabilized in the sample chamber, before the insertion of the tube. The kinetic set up was carried out directly into the NMR tubes by following the variation of the relevant NMR signals. All experiments were made performing ^{29}Si NMR spectroscopy to follow the modification of the changes in the chemical environment of the central silicon atom of the molecule. Furthermore, to assess the validity of the method, ^{1}H- and ^{13}C-NMR spectra were also performed, in order to investigate the release of methanol during the hydrolysis reaction. All the spectra were acquired on Varian UNITY 400 and MERCURY 400 NMR spectrometers. For ^{29}Si, a 10 mm BB probe operating at 79.455 MHz was used to optimize the signal/noise ratio, in order to minimize the acquisition times, thus allowing to set-up the kinetics of relatively fast reaction. All chemical shifts were measured with a coaxial insert tube containing a tetramethylsilane (TMS) solution, as an external reference. The delays and pulses used allowed quantitative measurements (T_1 measurements by inversion-recovery method were previously performed). The spectral width was 12 kHz and the relaxation delay 100 s, with a proton decoupling applied only during the acquisition time, in order to avoid negative nOe. The number of scans was increased with kinetic reaction time.

II.B.2 ^{29}Si NMR study

The reactions were carried out in two different media: (i) Pure deuterium oxide was used as a model for a purely aqueous medium and; (ii) a solution of deuterium oxide and ethanol-d_6 (20:80 w/w) was used as aqueous alcoholic solvent. In both media, experiments were carried out at two different pH conditions: (i) at an unmodified pH; (ii) at a pH of 4 after the addition of an adequate volume of glacial acetic acid. It is important to note that the pH of experiments carried out without the addition of acetic acid varied depending on the silane used. For most structures, the pH of the pristine solution was that of the initial solvent, i.e. close to 7 for deuterium oxide, whereas for aminosilanes, the natural pH of the solution was measured at ~11,5.

Also, two different temperatures were used: (i) 25°C to simulate room temperature conditions, and (ii) 45°C to evaluate the impact of thermal activation on the reactions at a temperature close to that generally measured in the papermaking process.

The chemical shifts used for setting up the kinetics from the ^{29}Si-NMR spectra, allowing to establish the ratios of the different species, for monoalkoxysilanes, dialkoxysilanes, and trialkoxysilanes are given in Table II-2, Table II-3 and Table II-4 respectively.

	TMMS	APDMES
M^0_R	n.d.	n.d.
M^0_H	n.d.	17,5 to 18,5
M^1	n.d.	10,5 to 11,5
Cyclic structure	n.d.	7,5 to 8

Table II-2: Chemical shifts of the various structures in solutions for monoalkoxysilanes, in ppm

	DMDMS	MVDES	MVDMS
D^0_R	-1,0 to -1,5	n.d.	n.d.
D^0_H	-4,0 to -7,5	centered at -22	-16 to -22
D^1	-14,5 to -15,5	centered at -30	centered at -30
D^2	-22,0 to -29,0	centered at -40	centered at -41
Cyclic structure 1	centered at -12	centered at -32	centered at -32
Cyclic structure 2	centered at -19	n.d.	centered at -38

Table II-3: Chemical shifts of the various structures in solutions for dialkoxysilanes, in ppm

	MTMS	DAMS
T^0_R	-37 to -38	-41,5 to -43
T^0_H	-38,5 to -43	-39,5 to -41
T^1	-52 to -56	-48,5 to -51,5
T^2	-61 to -64	-57 to -60
T^3	-70 to -73	-66 to -69

Table II-4: Chemical shifts of the various structures in solutions for trialkoxysilanes, in ppm

Before starting the data collection, the validity of the ^{29}Si NMR method was confirmed by a complementary study using ^{1}H-NMR and ^{13}C-NMR, and following the kinetics of DAMS in a mixed ethanol/water medium, under unmodified pH conditions. The results of these experiments are not presented here, but the kinetics curves built on the basis of the spectra associated to the three nuclei were in good agreement.

III. Results and Discussion

In the following part, the results of an extensive NMR study on silane reactions in various conditions are presented. The first section is dedicated to the study of the impact of the solvent composition on these reactions, and is focused on only one silane. Then, a study involving the hydrolysis and condensation of various organosilanes in purely aqueous media is presented. Finally, the effect of various parameters, namely the pH, the temperature and the concentration are discussed, and some comparisons between silanes having slight structural differences are made.

III.A Impact of solvent composition on DAMS reactions

In many cases, both industrial applications and literature studies deal with the preparation of 1% or 2% w/w silane solutions in mixed alcohol-water mixtures [1-4]. The amount of water added in the medium is generally rather low, i.e., ranging from a molar ratio with respect to the amount of hydrolysable groups, to up to 20% w/w. However, in order to verify the feasibility of using organosilanes in papermaking applications, we decided to evaluate the behaviour of a silane in purely aqueous media and compare the results obtained to previously published data [5] associated with the same compound in a 80/20 w/w ethanol/water mixture. For both media, the impact of pH was evaluated, and all reactions were monitored by *in situ* ^{29}Si NMR spectroscopy for a period of 48 hours. It was decided to study the hydrolysis and self-condensation kinetics of a silane presenting a good solubility in both media, which could be a potential candidate for grafting cellulose surfaces. In this context, DAMS was chosen. Thus, all experimental and analytical conditions were chosen to allow quantitative comparison with results from the previous study which presented the reaction of a 10% w/w DAMS solution in alcoholic media at acidic pH.

The behaviour of a 10% w/w solution of DAMS in 80/20 w/w alcohol/water mixture in unmodified pH conditions is obtained from the ^{29}Si NMR spectra presented in Figure III–1 (a), from which the kinetics of formation and/or consumption of the different species are given in Figure III–2 (a). Under these conditions, the hydrolysis seems to be highly fast, as witnessed by the total consumption of alkoxy moieties before the first acquisition is performed, at a reaction time of 10 min (T^0_H moieties were not detected). At this moment, the concentration of T^1 species has already reached its maximum value and started to decrease, indicating that more condensed structures are formed. In fact, the condensation into T^2 and T^3 structures were already detected at such short time (t = 10 min). The concentration of T^3 species augmented regularly, until reaching an equilibrium value of 80%, after 20 hours of reaction. This equilibrium was observed most likely because of the condensation phenomenon being highly slowed down due to the lack of accessibility of some of the hydroxyl groups in the network.

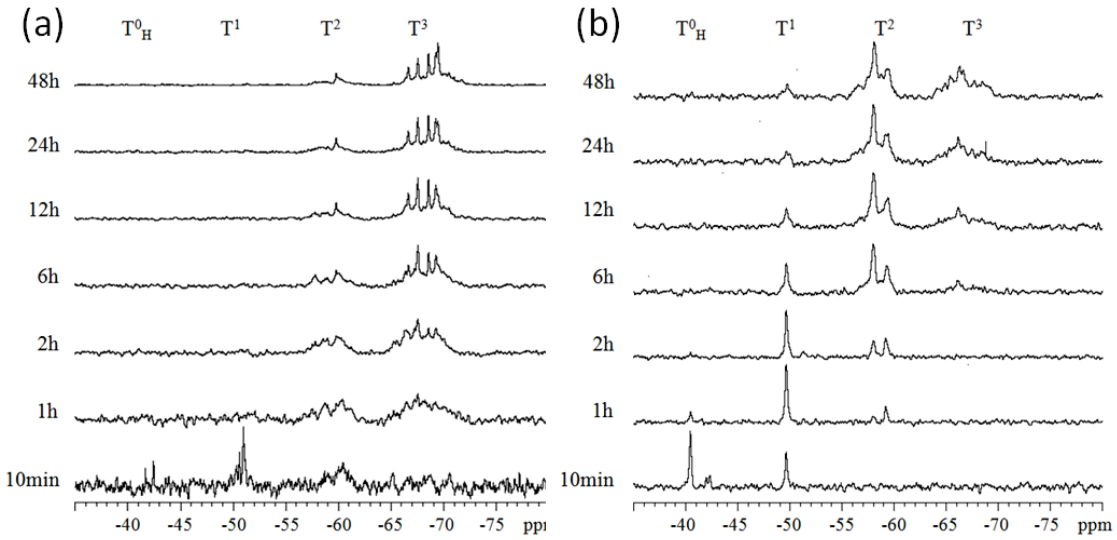

Figure III–1: ^{29}Si NMR spectra over time for a 10% DAMS alcoholic solution at 25°C, under (a) unmodified pH, (b) acidic pH

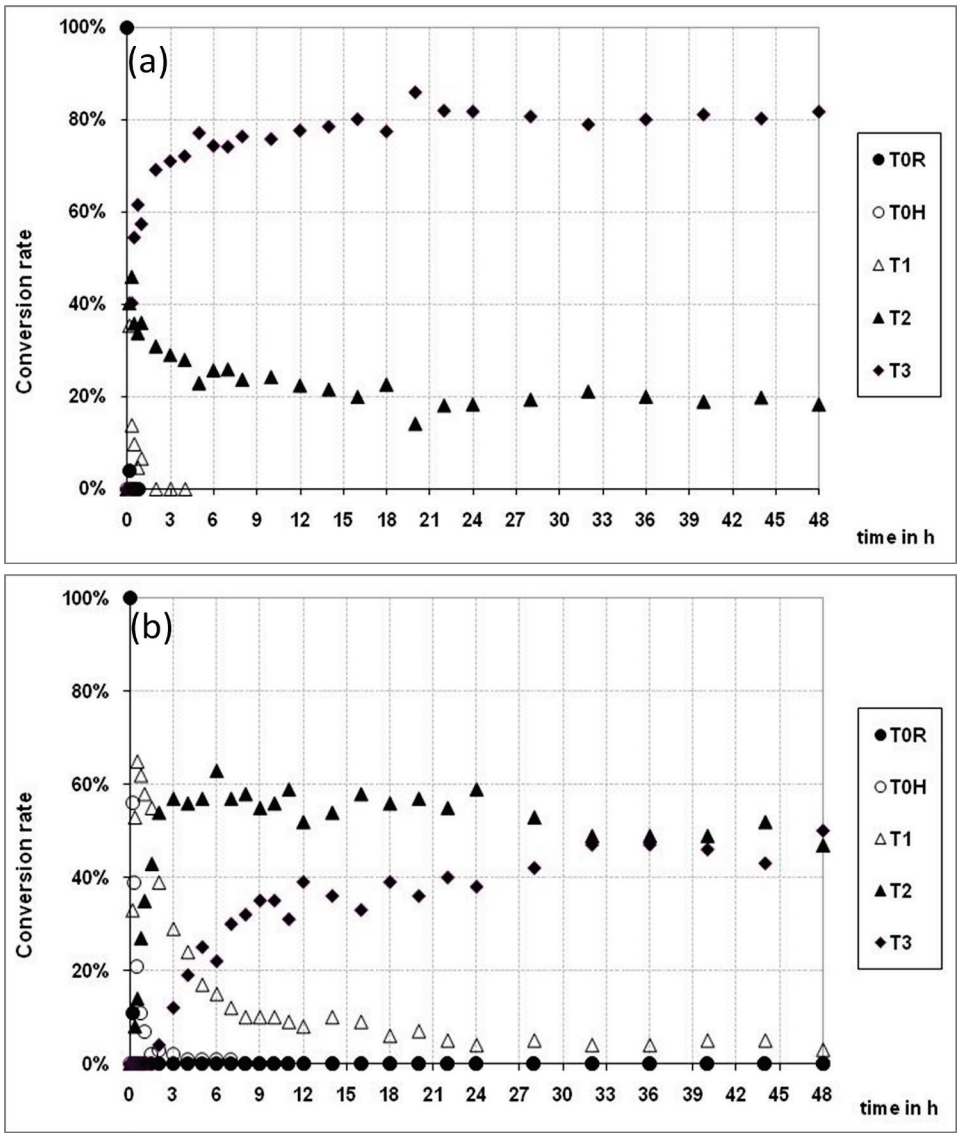

Figure III–2: Hydrolysis and self-condensation kinetics of 10% w/w DAMS in mixed ethanol/water solutions (80/20 w/w) at 25°C, as deduced from the ^{29}Si NMR spectra presented in Figure III–1, i.e. under (a) unmodified pH; (b) acidic conditions

The NMR study of the same reaction carried out under acidic conditions was investigated, as shown in the NMR spectra presented in Figure III–1 (b), and the deduced kinetic data presented in Figure III–2 (b). Under these conditions, the hydrolysis of DAMS was completed at t=20 min. The hydrolyzed structure T^0_H presents a maximum at 10 min, with a concentration of 56%. T^1 reaches an amount of 65% at 30 min, before starting to diminish. T^2 and T^3 appeared rapidly, respectively at 1 and 2 h. The concentration of the latter increased regularly, reaching 40 and 50% at 24 and 48h, respectively. Experiments carried out over 48h (not presented here) show that there is no equilibrium reached and that the reactions continue slowly toward a higher degree of condensation.

The kinetics under acidic pH conditions are in agreement with the literature data claiming for a protective role of acidic pHs against the self-condensation of hydrolyzed species. Indeed, the presence of acetic acid limited appreciably the T^0_H consumption kinetic. Actually, under acidic conditions, T^0_H species were present during the first 8 hours, whereas in the unmodified pH system, these species totally disappeared after less than 30 min.

Another set of experiments involved the study of the hydrolysis and self-condensation kinetics of DAMS carried out in pure water, under unmodified and acidic conditions.

For the unmodified pH, DAMS hydrolysis started immediately and was followed by self-condensation. The kinetics, deduced from the spectra introduced in Figure III–3 (a), are shown in Figure III–4 (a). For this experiment, we could not obtain data in the time interval between 24 and 44 hours due to a problem on the apparatus during acquisition. Initial silanes remained detectable up to 15 min, whereas totally condensed T^3 species already appeared at the very beginning of the reaction. Such features explain the small quantity of detected first formed T^0_H species. The condensation being very fast, few hydrolyzed species are available in the solution. Nevertheless, equilibrium seems to be reached between the various structures after one hour. Pristine silanes were totally hydrolyzed during the first 30 minutes whereas hydrolyzed uncondensed species reached a maximum content (around 12%) after 15 minutes and then their amount was stabilized between 5 and 7%. T^1 condensed species were present during the full range of the investigated experimental time. They reached an equilibrium value close to 13% after 1 hour, whereas T^2 species reached a maximum concentration of 50% after 15 minutes of reaction. Then their quantities declined to 40% after 1 hour. During the first hour of the reaction, the content of totally condensed species, T^3, increased to reach a value of around 41%. After one hour reaction, T^2 and T^3 species were the most abundant species in the reaction mixture, counting equal quantities of 40%.

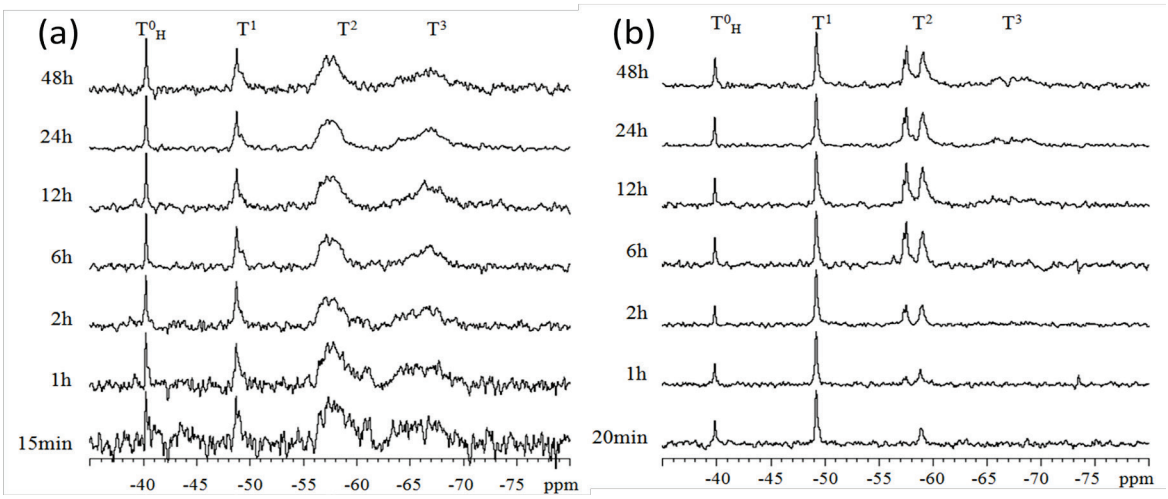

Figure III–3: ^{29}Si NMR spectra over time for a 10% DAMS purely aqueous solution at 25°C, under (a) unmodified pH, (b) acidic pH

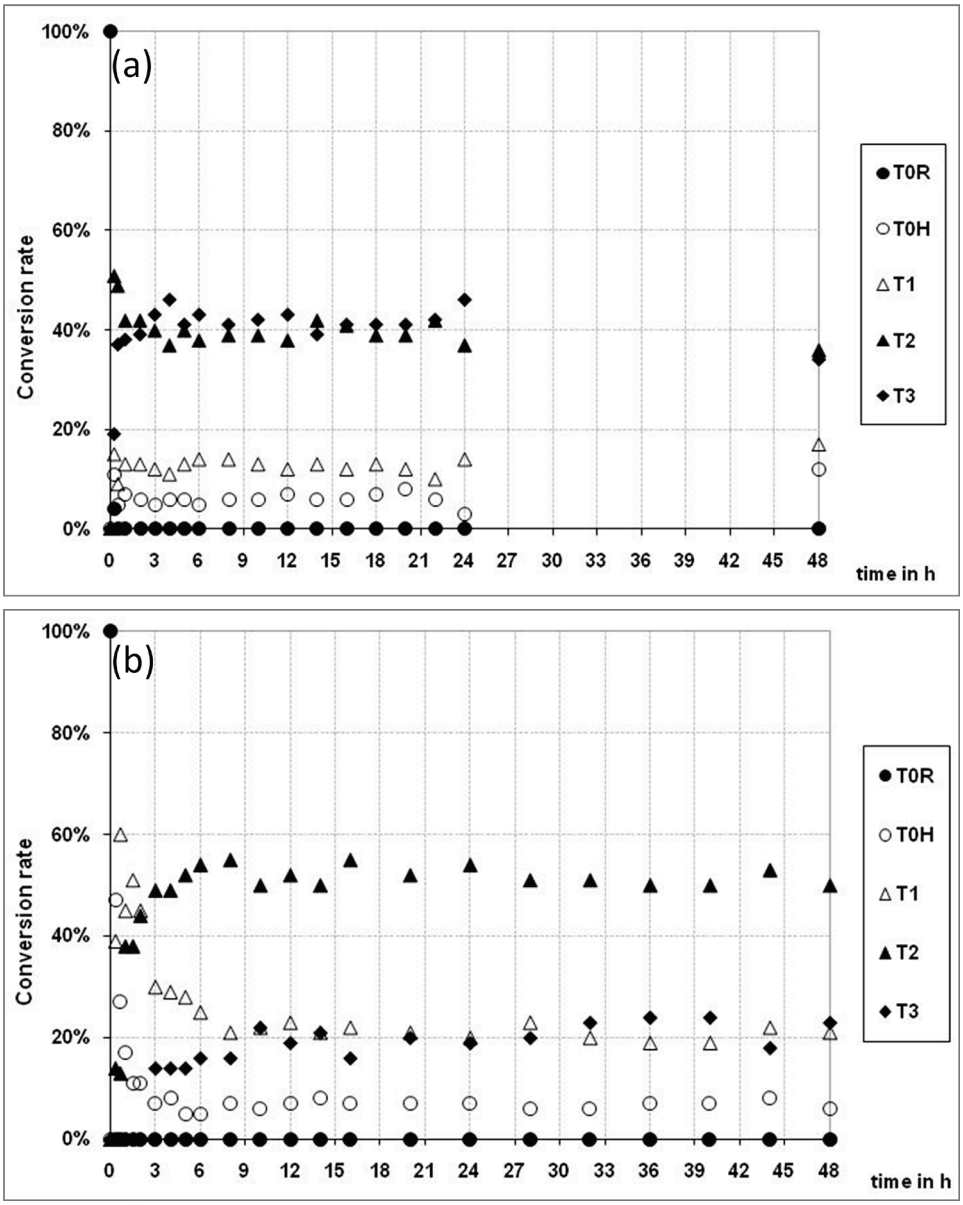

Figure III–4: Hydrolysis and self-condensation kinetics of a 10% w/w DAMS in pure water at 25°C, as deduced from the ^{29}Si NMR spectra presented in Figure III–3, i.e. under: (a) unmodified pH and (b) acidic conditions.

A very interesting finding is that, in pure aqueous medium, T^0_H structures are not totally consumed, even after 48 hours of reaction. Contrarily to what occurred in alcoholic medium, where, at the same pH, these structures were totally consumed before the first acquisition (10mn after solution preparation). So, as expected, the excess of water seems to displace the equilibrium to favour the hydrolysis reaction and to impede their condensation, at least in terms of kinetic rate. The total consumption of reactive species is not reached for long reaction times (48h). At the equilibrium, there are still small amounts of remaining silanol groups (close to 5%).

The spectra corresponding to the hydrolysis kinetics in pure water and under acidic conditions are shown in Figure III–3 (b), and the kinetic curves deduced from these are presented in Figure III–4 (b). The rate of the hydrolysis step was found to be very fast (almost immediate). Thus, after 20 minutes there are almost 50% of hydrolyzed silanes species (T^0_H) and 40 % of T^1 moieties present in the solution. The rest of the reaction mixture was composed of T^2 structures. The amount of T^0_H diminished rather rapidly and reached a value of 8% after 3h, whereas the content of T^2 structures increased slowly from 14 to 50%, between 20 min and 3h of reaction time. The apparition of totally condensed structures T^3 was delayed until the second hour of reaction and their amounts never reached more than 25%. After 9h, the reaction mixture displayed an equilibrium between the concentrations of the reactive species. Thus, the ratios of T^0_H, T^1, T^2 and T^3 in the reaction mixture were measured around 8, 20, 52 and 20%, respectively.

Noteworthy, for both experiments carried out in purely aqueous medium the time of complete disappearance of the uncondensed structures was not reached within the investigated range of time, 48 hours, which disagree with the common idea that the use of alcoholic solvents with a limited amount of moisture or water is the best way to control the self-condensation reactions of silanes. Indeed, it appears here, that in the case of an organofunctional silane bearing amine groups, the use of pure aqueous media leads to a better control of the condensation reactions and gives reactive mixture in which an equilibrium is set between the different reactive structures, and in which T^0_H moieties are available over long periods of time.

A detailed analysis of the ratio of T^0_H species at 24 and 48h, under unmodified pH in pure deuterium oxide shows a surprising increase (from 3 to 12%), after a full period of declining to reach a concentration of 3%. This unexpected trend could be explained by a reversible condensation reaction, occurring in aqueous medium. But it should be reminded that the silanol self-condensation is generally believed irreversible in organic solvent media under the conditions used here. So, further investigations on the reversibility of the reaction in pure water would be necessary to confirm the hypothesis. Another more probable explanation could be the formation of insoluble compounds, which would tend to segregate from the medium, thus becoming undetectable by the NMR spectrometer. In this case, the absolute ratio of T^0_H would be over-estimated. Such a

phenomenon, is most probably the main responsible of this result, as already reported previously [6]. Our data collected under acidic conditions in purely aqueous medium did not present such phenomenon. The protective effect of the acid against the formation of larger structures may have prevented the precipitation to occur.

Concerning the concentration of T^1 species, for the different reaction conditions, one can observe that in alcoholic media these structures were totally consumed or existed only in trace amounts, after a few hours. Whereas for both pH conditions in aqueous media, after 48 hours these structures had a content close to 15 and 20%, respectively, for unmodified and acidic pH. As T^3 structures are not suitable for grafting (since they do not bear OH functions anymore), the data show unambiguously that the purely aqueous reaction medium is much more favourable for the production of a reactive solution having available hydroxyls groups over a long period of time.

The SR parameter, plotted over time for the four reactions described in this section is presented in Figure III–5, which shows two different trends:

(i) The pH of the medium seems to be the predominant parameter during the first couple of hours of the reaction, for both alcoholic and pure water reaction solvent. Indeed, for both experiments in acidic conditions SR reached a maximum of almost 80% *versus* less than 40% for unmodified pH conditions. However, a less steep decline of SR over time is observed for the reaction carried out in purely aqueous medium under acidic pH, compared with the homologue system conducted in a water/alcoholic solvent.

(ii) Over longer periods, the SR parameter is maintained at a good level for the pure water solutions, compared to the alcoholic-based counterparts, indicating that the condensation reactions were limited, thus yielding a reactive mixture with appreciable potential reactivity.

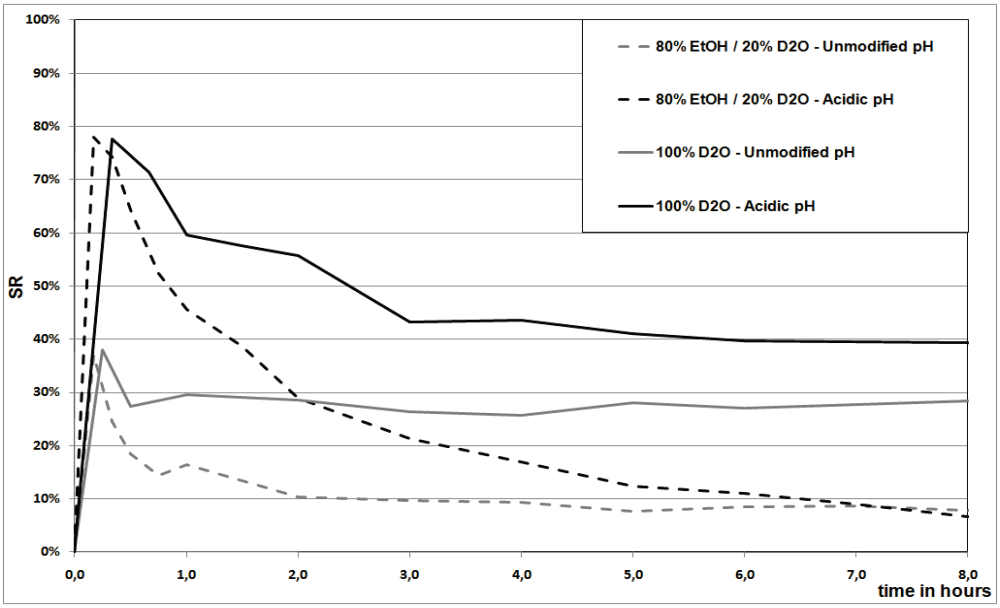

Figure III–5: Active Silanol Reactivity (SR) parameter, as a function of time over 8 hours, for different reaction conditions

As a conclusion, we can observe that DAMS hydrolysis and self-condensation reaction kinetics in water present noteworthy features compared to the ethanol/water solvent system. More specifically, it was shown unambiguously that the equilibrium is set between hydrolyzed and condensed species in pure aqueous media at acidic pH, a phenomenon which does not happen in organic solvent media, where monomeric hydrolyzed species (silanols) totally disappear. At unmodified pH conditions, the condensation results in insoluble structures. However, after 48 hours, the signal/noise ratio is still rather low, indicating that this phenomenon was not too significant. Here, the relative ratio of silanols in water is influenced by the pH, which is in agreement with the protective role of acidic media against self-condensation. Thus, the reactivity of DAMS water solutions is much higher than that of alcoholic solutions, whatever the pH and the solution age, as indicated by the SR parameter.

These findings are particularly interesting in view of using DAMS for the modification of natural fibres using conditions compatible with the papermaking industry process. Thus, based on these results, it was decided to carry out experiments on other silanes, in purely aqueous conditions only. Furthermore, for the experiments reported hereafter, only the SR curves will be shown in this manuscript.

The results presented in this section have been accepted for publication in an international peer reviewed journal. The reader interested is invited to consult Annex 1.

III.B Characterization of other silanes in aqueous medium

In order to provide a broad understanding on the specificities of reacting silanes in aqueous media, and the impact of the most relevant solution parameters (pH, temperature and concentration), an extensive study by ^{29}Si NMR was undertaken. Thus, allowing the determination of the best conditions for reacting silane coupling agents in view of their use for cellulosic substrates modification.

A few silane molecules were selected for this study. Their structures are given in Figure III–6. TMMS, DMDMS and MTMS were chosen in order to allow a comparison between structures having a simple inert core, while increasing the number of alkoxy groups. MVDMS and MVDES are both dialkoxy-vinylsilanes, the vinyl function is expected to improve the water solubility of both compounds, whereas the length of their alkoxy moieties is varied, allowing to investigate the effect of hydrolysable group length on the reactions in pure aqueous media. Finally, APDMES was chosen as a good candidate for a monoalkoxysilane with a good solubility in water, furthermore the presence of the amine group allowed to benefit from previous observations made on DAMS.

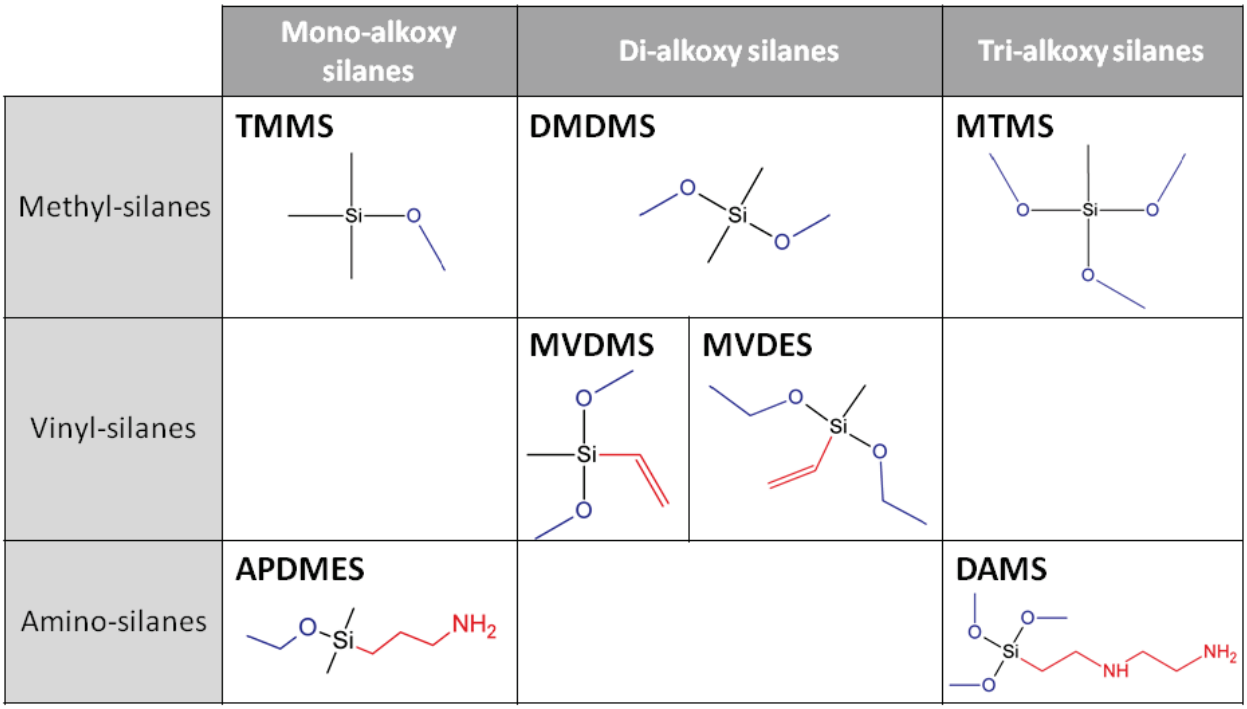

Figure III–6: Silane selection (hydrolysable groups in blue, functional groups in red)

		TMMS	DMDMS	MTMS	MVDES	MVDMS	APDMES	DAMS
pH = 4	Room temperature		200 mM 400 mM	400 mM		300 mM 400 mM	400 mM	10% w/w
	45°C		400 mM	400 mM	400 mM	400 mM	400 mM	
Unmodified pH	Room temperature	100mM	300 mM 400 mM	300 mM 400 mM		300 mM	400 mM	10% w/w
	45°C		400 mM	400 mM	400 mM	400 mM	400 mM	

Table III-1: NMR experiment list

The concentration used for experiments on DAMS in the previous section was set to 10% w/w of silane compared to the solvent, in order to allow comparison with a previous work. Nonetheless, this concentration does not represent typical conditions associated with the use of silanes. In fact, the silane concentration is generally closer to 1 or 2 % w/w. Hence, it was decided to minimize the concentration as much as possible, while maintaining a good time resolution in the ^{29}Si NMR spectra. Furthermore, it was decided to work at fixed molar concentrations for all the silanes, in order to exploit more properly the kinetics, which obey to molar concentration and allow comparison between silanes with different molar masses. In addition, this choice allows ensuring

that a similar amount of alcohol is released, and that a similar amount of potential grafting moieties are produced for silane with equal numbers of alkoxy moieties.

A good compromise for the concentration was found with a value of 400mM, which allows fast NMR acquisition. The list of the experiments performed, each comprising 48 hours of continuous *in-situ* data acquisition, is presented in Table III-1.

III.B.1 Alkylalkoxysilanes

For TMMS (structure recalled in Figure III–7), the solubility of the silane in aqueous media was not sufficient to acquire time resolved data, even at a concentration of 100 mM. Hence the behaviours of this compound could not be elucidated.

DMDMS (structure recalled in Figure III–7) is a dialkoxysilane. It was used at concentrations ranging from 200mM to 400mM. However, 400mM was very close to the upper limit of solubility of this compound in water. Thus the preparation of such solutions required a vigorous mixing during the first few minutes, before the acquisition of the NMR spectra could actually start. Some comments and observations, as well as the parameters of the experiments performed with DMDMS, are listed in Table III-2. From the comments listed here, it is already possible to observe that a loss of signal is enhanced by acidic conditions for this silane. This loss is associated with the formation of insoluble compounds which became undetectable by solution NMR spectroscopy.

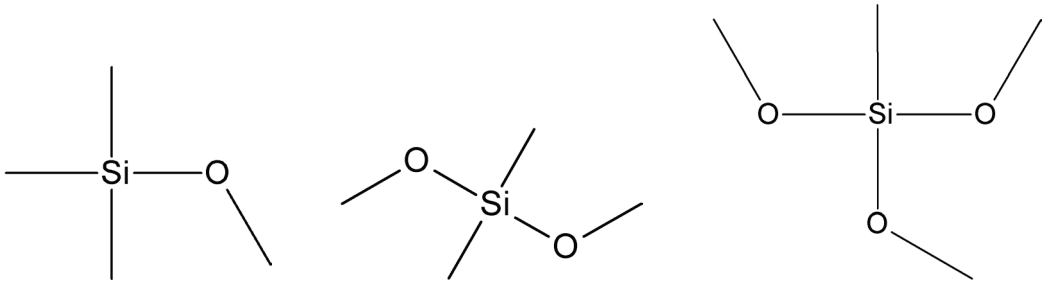

Figure III–7: Structures of TMMS, DMDMS, and MTMS.

For DMDMS, visual observations showed the formation of a haze in the solution, which became a clear liquid on top of the tube, hence indicating that water insoluble products with a lower density are formed. However, the detailed analysis of the various NMR spectra acquired allows to determine the time at which the phenomena started. Indeed, unusual features from a spectrum to another can indicate the existence of such phenomena. Such signs include the rise of the ratio of uncondensed structures when all unhydrolyzed species had been previously consumed. Also, the sudden loss of signal leading to a poor signal/noise ratio is a good indicator of the migration of studied structures out of the zone of observation, due to insolubility issues. Such observations will

be used all throughout this study in order to determine what part of our results is trustworthy and what part is not.

pH	*Temperature*	*Concentration*	*Comments*
pH = 4	25°C	200 mM	- 48h of acquisition - Slow phase separation occurs after 6h
		400 mM	- 16h of acquisition before loss of signal - Phase separation occurs rather rapidly after 4 hours - Presence of two different cyclic structures
	45°C	400 mM	- 12h of acquisition before loss of signal - Phase separation occurs rather rapidly after 2 hours - Presence of two different cyclic structures
pH = 7	25°C	300 mM	- 48h of acquisition - No phase separation - Slight presence of a cyclic structure but barely any D^2
		400 mM	- 48h of acquisition - No phase separation - No cyclic structure and very little D^2
	45°C	400 mM	- 48h of acquisition - Slow phase separation after 20h - Two cyclic structure and presence of few D^2 all troughout

Table III-2: DMDMS experiments

The SR curves obtained from the NMR data on DMDMS solutions in various conditions are presented in Figure III–8, for the first 10 hours of reaction. Longer durations of analysis are not presented here because of the uncertainties rising from the phase separation occurring in certain conditions. The duration of 10 hours will be used for the graphical analysis of the data issued from all the experiments detailed in this chapter. The impact of the different reaction parameters is discussed in the next sections.

pH	*Temperature*	*Concentration*	*Comments*
pH = 4	25°C	400 mM	- 24h of acquisition before signal loss - Phase separation after 8h
	45°C	400 mM	- 14h of acquisition before acquisition failure - Phase separation after 7h
pH = 7	25°C	300 mM	- 24h of acquisition before signal loss - Phase separation after 6h
		400 mM	- 20h of acquisition before signal loss - Phase separation after 6h
	45°C	400 mM	- 7h of acquisition before signal loss - Immediate phase separation

Table III-3: MTMS experiments

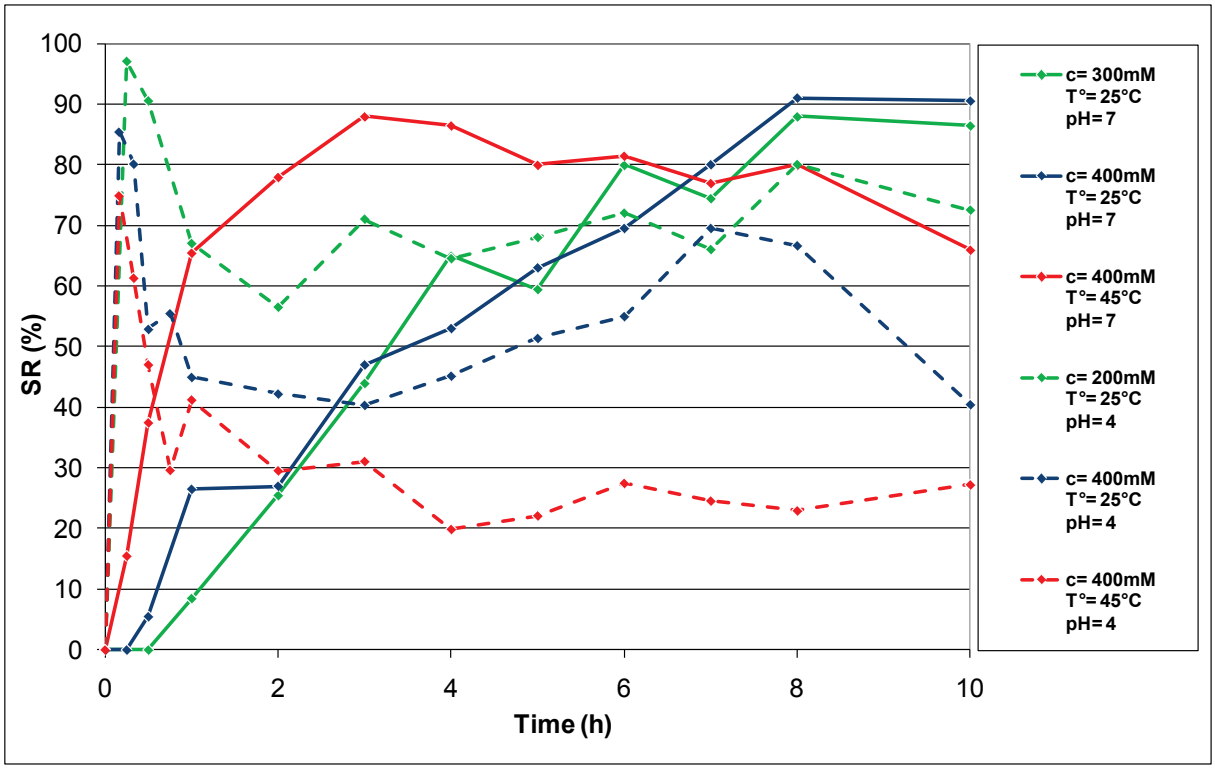

Figure III–8: SR Parameter as a function of time for reactions of DMDMS, at 200mM and 300mM, 25°C (green lines); 400mM, 25°C (blue lines); 400mM, 45°C (red lines). Continuous lines are for unmodified pH, whereas dashed lines are for pH=4

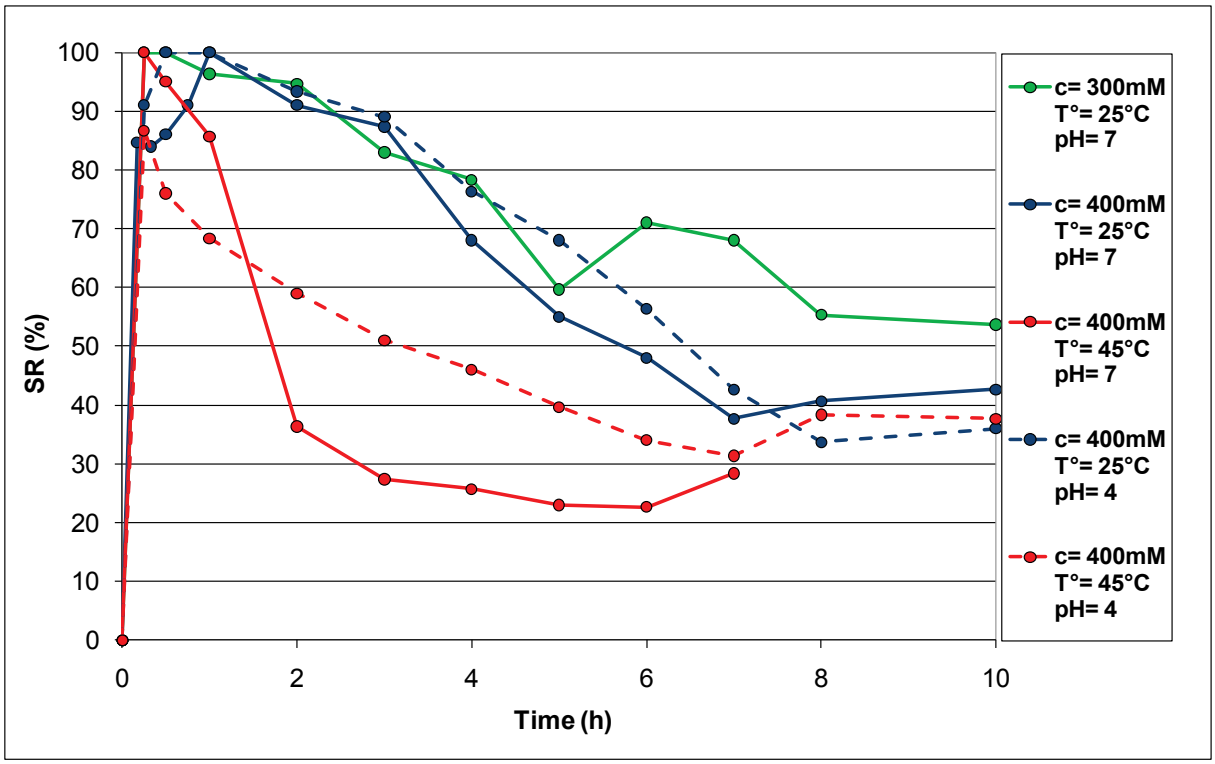

Figure III–9: SR Parameter over time for reactions of MTMS, at 300mM, 25°C (green line); 400mM, 25°C (blue lines); 400mM, 45°C (red lines). Continuous lines are for unmodified pH, whereas dashed lines are for pH=4

MTMS, has a structure (recalled in Figure III–7) very similar to DMDMS, with one of the methyl groups being substituted into a third methoxy group. For this silane, a few experiments were impacted by the formation of insoluble products, under the form of precipitates. The experiments performed on MTMS, as well as some observations stated during their conduction, are presented in Table III-3. Furthermore, Figure III–9 shows the SR curves for these experiments. For this silane, the phase separation observed corresponds to the precipitation of condensed structures, forming a white glue-like material, sticking to the sides and bottom of the NMR tubes.

III.B.2 Vinylalkoxysilanes

The two vinylsilanes studied here have a structure close to that of DMDMS. The only difference between DMDMS and MVDMS is the substitution of a methyl group in the former by a vinyl functional moiety in the latter. For MVDES, in addition, the methoxy groups have been replaced by ethoxy moieties. Observations on the outcome of the ^{29}Si NMR analyses on MVDES and MVDMS are presented in Table III-4 and Table III-5 respectively, whereas the SR curves for these silanes are shown in Figure III–11 and Figure III–12 below.

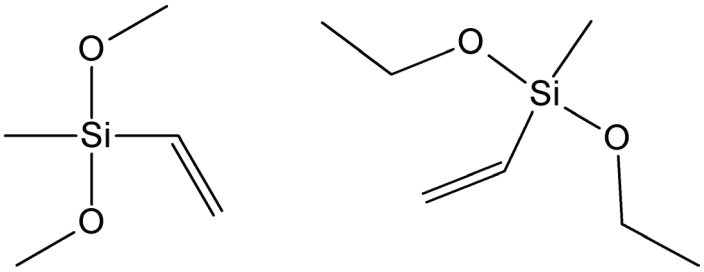

Figure III–10: Structures of MVDMS, and MVDES.

pH	*Temperature*	*Concentration*	*Comments*
pH = 4	45°C	400 mM	- 24h of acquisition before loss of signal - Phase separation occurs rapidly from t=0 - Presence of a cyclic structure
pH = 7	45°C	400 mM	- 20h of acquisition before loss of signal - Phase separation not clearly visible but strong signal loss - Neither cyclic structures nor D^2

Table III-4: MVDES experiments

For both MVDES and MVDMS (structures recalled in Figure III–10), phase separation was observed. However, the initial part of the kinetics was successfully acquired. It is observed that in the case of MVDES, the D^2 structures are formed and disappear very fast under acidic conditions, which indicated the occurrence of a phase separation. In neutral conditions, these structures are not observed at all however there is a clear loss of signal. Thus, it is supposed that such structures are formed in both conditions, with a difference that in a neutral pH, they precipitate before they can impact the analysis and appear on the graph, or their signal is mixed with the noise background. Like for alkoxysilanes, these data are further exploited hereafter.

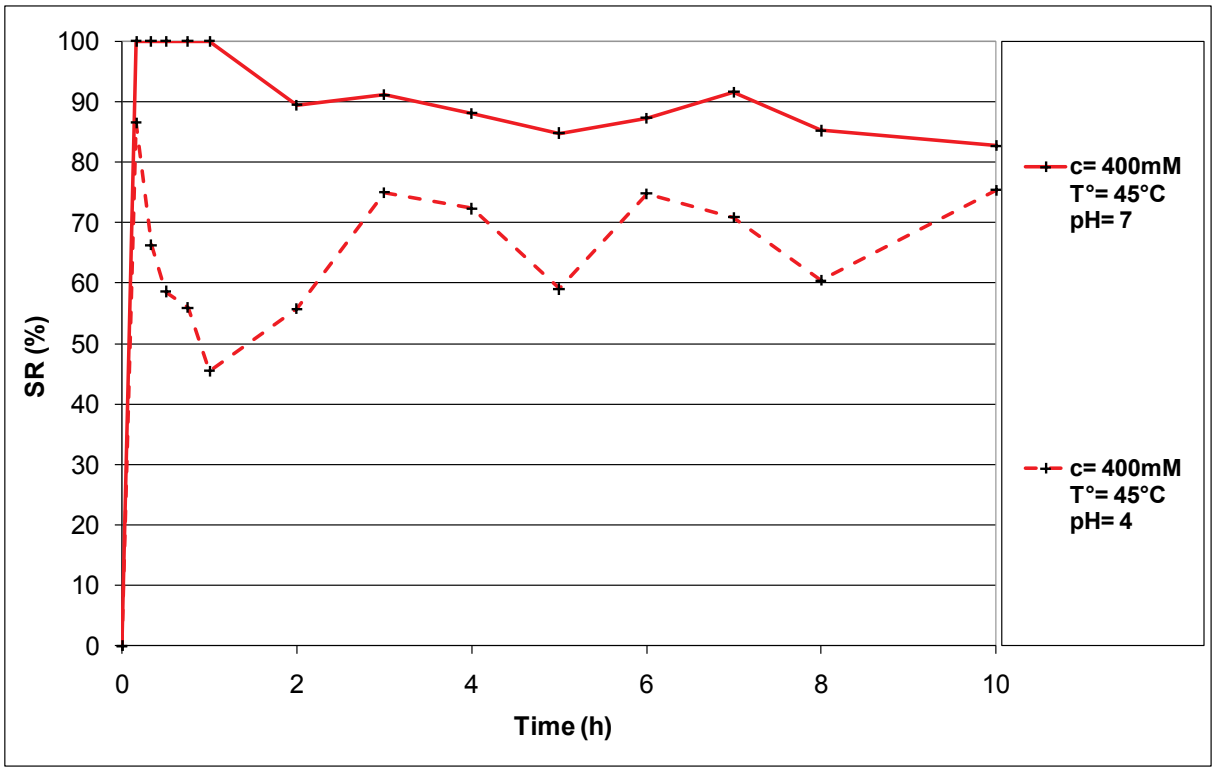

Figure III–11: SR Parameter over time for reactions of MVDES, at 400mM, 45°C. Continuous line is for unmodified pH, whereas dashed line is for pH=4

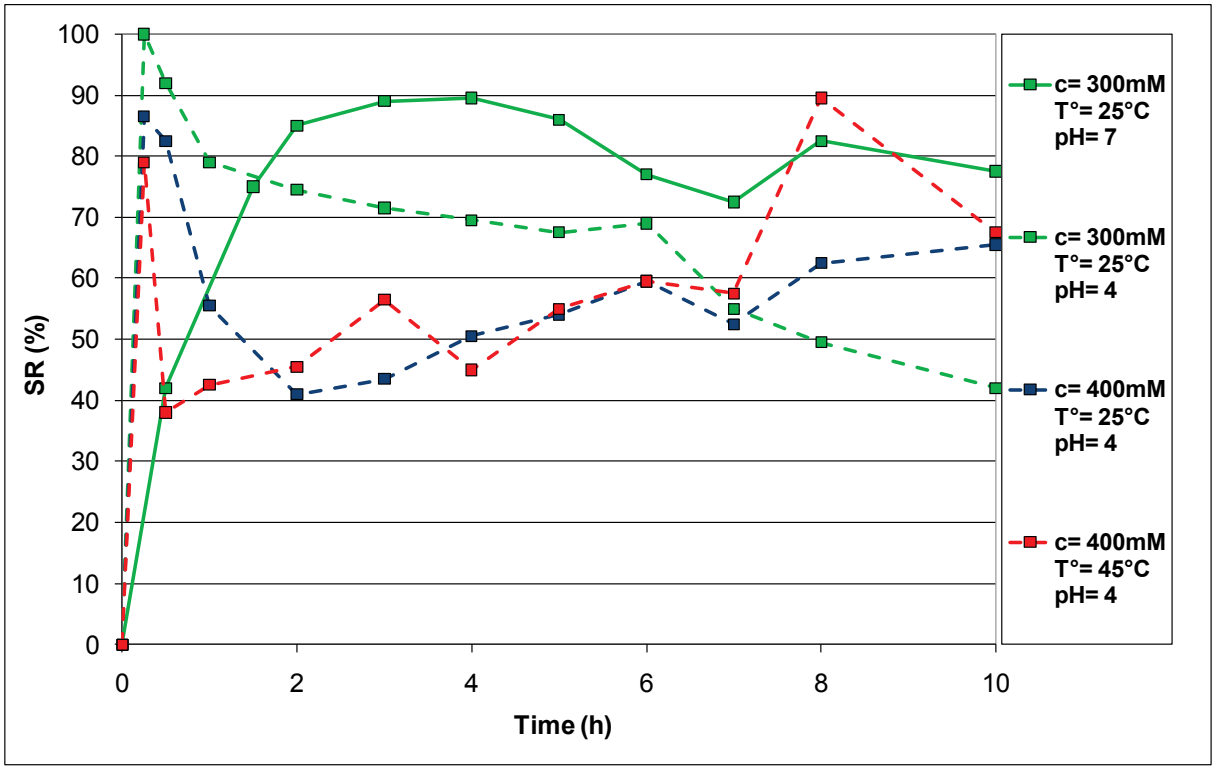

Figure III–12: SR Parameter over time for reactions of MVDMS, at 300mM, 25°C (green lines); 400mM, 25°C (blue line); 400mM, 45°C (red line). Continuous line is for unmodified pH, whereas dashed lines are for pH=4

pH	Temperature	Concentration	Comments
pH = 4	25°C	300 mM	- 48h of acquisition - Slow phase separation after 12h - Presence of a cyclic structure and D^2 appears after 10h
		400 mM	- 48h of acquisition - Phase separation after 3h - Presence of two cyclic structure and D^2 appears after 1h
	45°C	400 mM	- 48h of acquisition before loss of signal - Immediate and important phase separation - Presence of a cyclic structure
pH = 7	25°C	300 mM	- 48h of acquisition - No clear proof of separation - No D^2 structure
	45°C	400 mM	- 40h of acquisition - Very fast loss of signal did not allow to acquire quantitave data

Table III-5: MVDMS experiments

III.B.3 Aminoalkoxysilanes

For aminoalkoxysilanes, DAMS reactions have already been described in section III.A. DAMS investigations were carried out only at a concentration of 10% w/w, which corresponds to a molar concentration of 460mM, significantly higher than the 400mM used in this part of the study. Thus data on DAMS will not be further analyzed in this section.

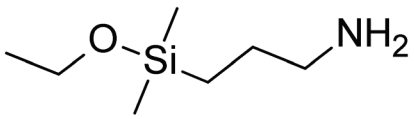

Figure III–13: Structure of APDMES.

pH	Temperature	Concentration	Comments
pH = 4	25°C	400 mM	- 48h of acquisition - No signal loss
	45°C	400 mM	- 48h of acquisition - No signal loss
pH = 11,5	25°C	400 mM	- 32h of acquisition before signal loss - Rapid apparition of a second phase with lower density - Early presence of a cyclic and M^1
	45°C	400 mM	- 24h of acquisition before signal loss - Rapid apparition of a second phase with lower density - Early presence of a cyclic and M1

Table III-6: APDMES experiments

Another aminosilane was chosen, namely APDMES (Structure recalled in Figure III–13). This molecule shows a high solubility in water and was studied at 400mM at both temperatures and both pH conditions. Noteworthy, the unmodified pH of APDMES solutions was measured and found to be around 11.5, which predicts that base catalysed reactions occur with this molecule in the absence of pH control. The data associated with APDMES analyses are presented in Table III-6, and the corresponding SR curves are shown in Figure III–14. Surprisingly, in unmodified pH conditions, the formation of a second liquid phase at the top of the tube was observed. This feature was not expected for this monoalkoxysilane since the possible formation of the dimer cannot produce an insoluble adduct. In order to try to understand the composition of this phase, the tube was vigorously agitated by the operator before being analyzed rapidly in the NMR apparatus again (data not presented here). This experiment showed that the upper phase is solely composed of APDMES in a conformation different than the expected M^0 and M^1, which are observed in the main phase. We therefore propose that this feature is explained by the formation of hydrogen bonded cyclic structures. However, we do not have supporting evidences allowing us to propose a more detailed structure for such compounds.

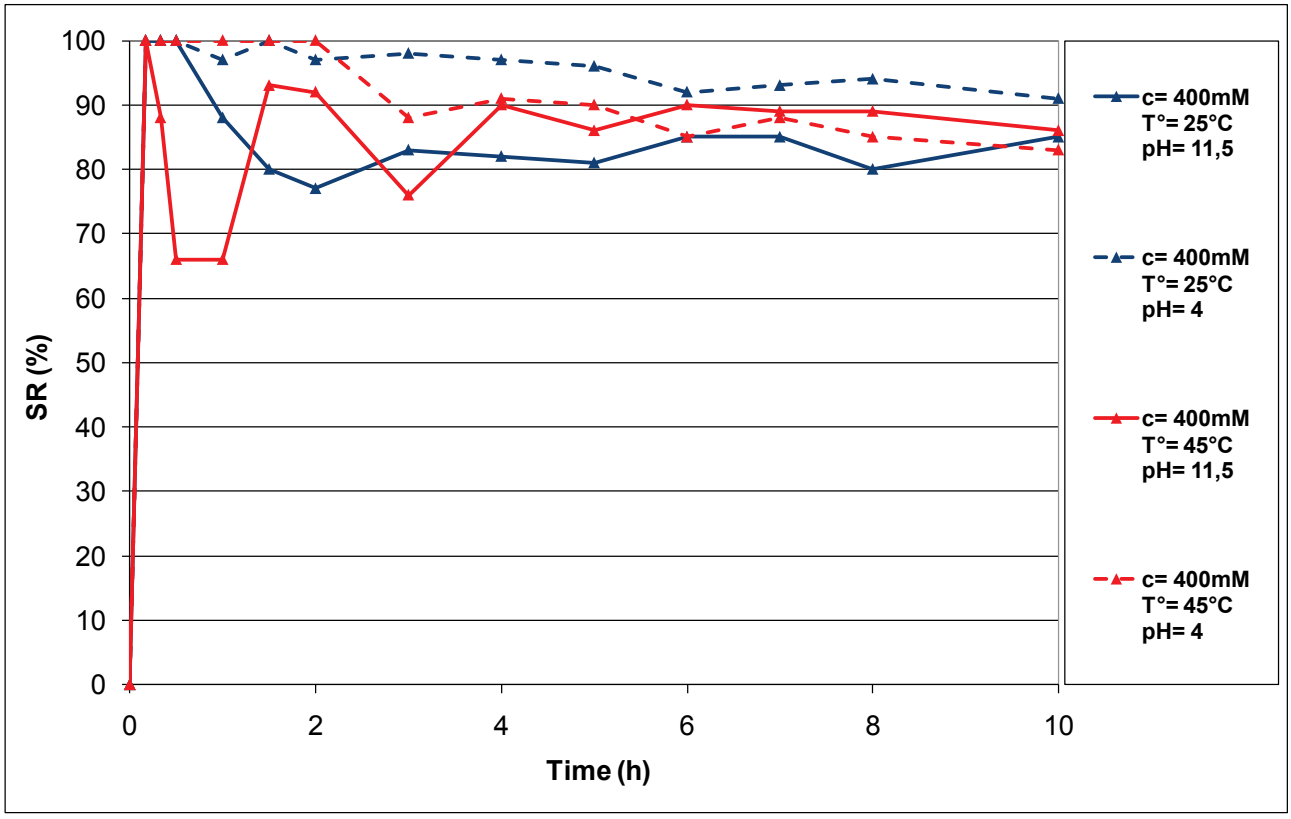

Figure III–14: SR Parameter over time for reactions of APDMES, at 400mM, 25°C (blue lines); 400mM, 45°C (red line). Continuous lines are for unmodified pH, whereas dashed lines are for pH=4

III.C Impact of pH

In order to provide a more relevant discussion on the effect of pH on the hydrolysis and the self-condensation reactions of our selected alkoxysilanes in purely aqueous media, the results have been divided between each family of silane considered.

III.C.1 Alkylalkoxysilanes

For DMDMS, the effect of pH was evaluated at a concentration of 400 mM, both at room temperature and at 45°C. However, based on experimental observations, we can only assess the validity of data before the apparition of phase separation: i.e. after 20 hours at pH=7. At pH=4, this phenomenon is observed after 2 hours at 45°C, and after 4 hours at 25°C. Comparative SR plots over the first 10 hours of reaction are presented in Figure III–15.

In neutral pH conditions, a rather slow and regular increase of SR over time is observed at 400mM and 25°C, with a maximum, about 90%, reached after 8 hours of reaction, indicating that a rather slow rate of hydrolysis is observed for DMDMS under these conditions. The self-condensation reactions are also limited by the slow release of hydrolyzed silanols, and have very slow kinetics. Actually, no totally condensed structures are observed at the end of the kinetic at t=48h; and a SR over 60% is maintained (data not presented here). In acidic media with the same concentration and temperature, a very fast hydrolysis was observed, providing a maximum SR of 85% after only a few minutes of acquisition. Nevertheless, a very fast self-condensation is observed too, giving birth to D^1, D^2 and cyclic structures, with significant ratios being reached very rapidly. A loss of the signal is associated with the formation of the more condensed species.

At a concentration of 400mM and a temperature of 45°C, as expected, the hydrolysis of the pristine silane is highly accelerated and a maximum of SR corresponding to a complete hydrolysis is attained after 3 hours. However, the formation of D^1 is also enhanced, and their content was higher than that obtained at 25°C, thus causing a decrease of SR over time. In acidic conditions, a maximum SR of 75% is reached after only a few minutes of acquisition. The observations are very similar with those attained at 25°C, except for the greater formation of condensed structure, causing a faster loss of signal.

Cyclic species were detected in significant quantities at acidic pH, for both temperatures. Whereas at pH=7, they were only detected at a temperature of 45°C.

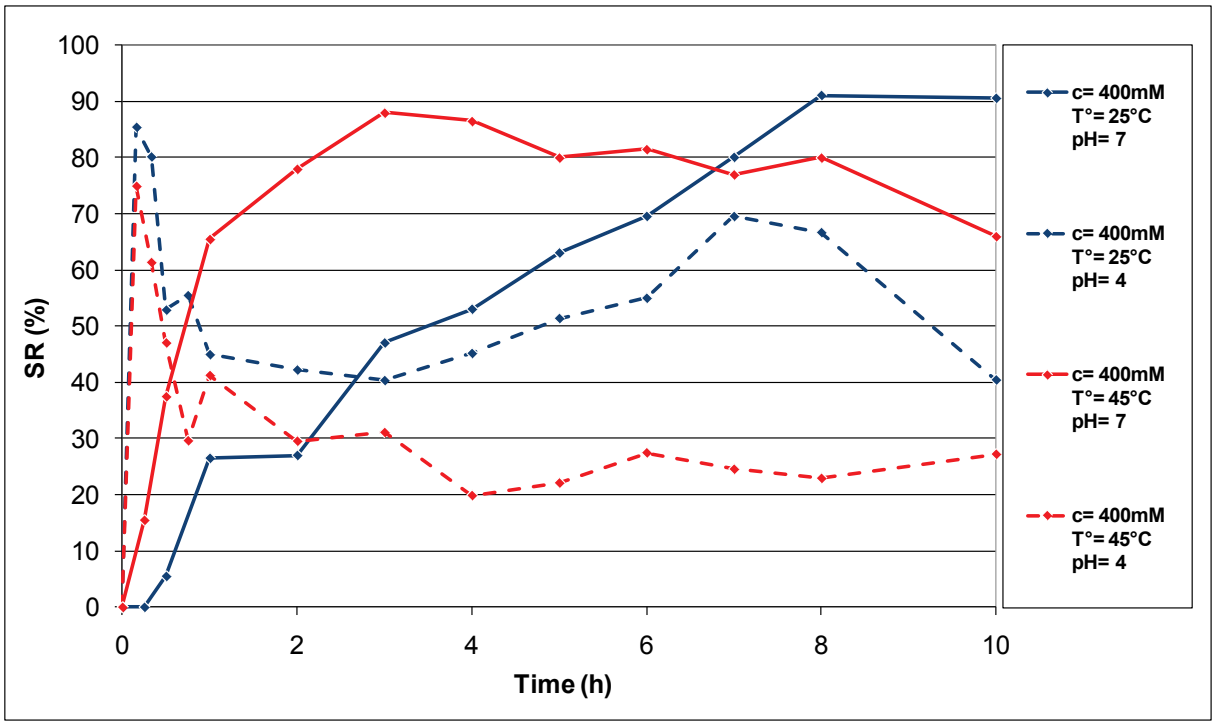

Figure III–15: SR curves for DMDMS, at 400mM, 25°C (blue lines); 400mM, 45°C (red lines). Continuous lines are for unmodified pH, whereas dashed lines are for pH=4

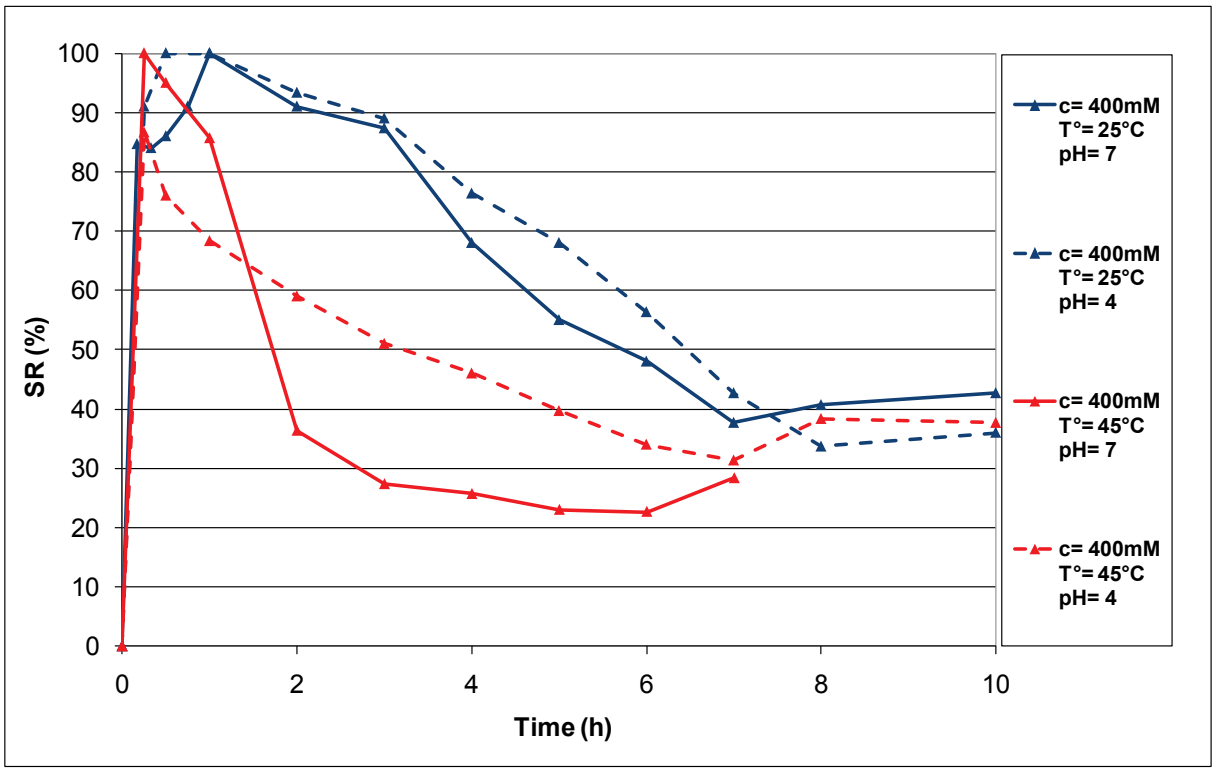

Figure III–16: SR curves for MTMS, at 400mM, 25°C (blue lines); 400mM, 45°C (red lines). Continuous lines are for unmodified pH, whereas dashed lines are for pH=4MTMS SR for pH

For MTMS, the effect of pH was also evaluated at a concentration of 400 mM, both at room temperature and at 45°C, as shown in Figure III–16. For all the conditions presented here, the precipitation of condensed structures started after a duration of reaction longer than 6 hours, except

for the experiment at pH=7 and 45°C, where the loss of signal associated to the precipitation was observed as soon as the experiment started.

At 25°C, at both pH and with a concentration of 400 mM similar behaviours are observed. The hydrolysis reaction is fast, giving birth to a peak of SR with a maximum reactivity of 100%, in a few minutes and in 1 hour, in acidic medium and in neutral medium respectively. In the latter medium, the rate of hydrolysis is the limiting factor. After reaching their maximum SR values, both solutions exhibit exactly the same features. A regular decrease of the solution reactivity is observed, leading to a decrease by more than 60% of the SR value. At 45°C, the maximum of SR is reached in a few minutes for both pH, with a maximum of 100% and about 85% at pH=7 and pH=4, respectively. Furthermore, in both conditions, the peak is immediately followed by a strong decrease of the SR parameter. However, in neutral pH, this decrease is slower than that observed in acidic medium, where a steep decline occurs right after the maximum peak. In acidic pH, the maximum of SR reached is lower, and the decline initiated faster, but it is much more regular and reaches an equilibrium value close to that of experiments at 25°C. Since the precipitation is observed at the very beginning of the experiment at pH=7, it is not really possible to draw any conclusion on the effect of pH at 45°C, except the confirmation that the hydrolysis reaction is fastened.

As a conclusion on the role of pH on alkylsilanes reactions in water, we can observe that an acidic pH greatly accelerates the hydrolysis kinetics. On one hand, for DMDMS, a lower pH was shown to enhance also the stabilization of cyclic structures and to accelerate strongly the formation of a second liquid phase associated to the condensation of silanols into water insoluble structures. On the other hand, for MTMS, a lower pH did not affect greatly the condensation kinetics at room temperature, and seemed to slow down greatly the formation of insoluble structures at 45°C.

In both cases, the use of acidic conditions allows enforcing a very fast hydrolysis phenomenon and should be favoured for applications where a fast reactivity is desired. On contrary, for applications where the shelf life is more important than the immediate reactivity, this study shows that there are no general rules and that the conditions should be chosen carefully depending on the structure used.

III.C.2 Vinylalkoxysilanes

The effect of pH on the reactivity of MVDES can only be discussed on one set of reaction conditions, namely: at 400mM and a temperature of 45°C. From the data presented in Figure III–17, it can be observed that, surprisingly, SR reaches a maximum at 100% at pH=7, and that this value is maintained over 1 hour before it starts to decrease slowly. On contrary of what happens at pH=4 where the maximum reached is less than 90% and where the decrease of SR is very brutal.

However, as stated previously, it is estimated that D^2 structures are formed very fast for both pH conditions, but their growth might be inhibited in acidic condition, thus avoiding their migration out of the analysis zone. In this case, the SR in neutral condition would be overestimated.

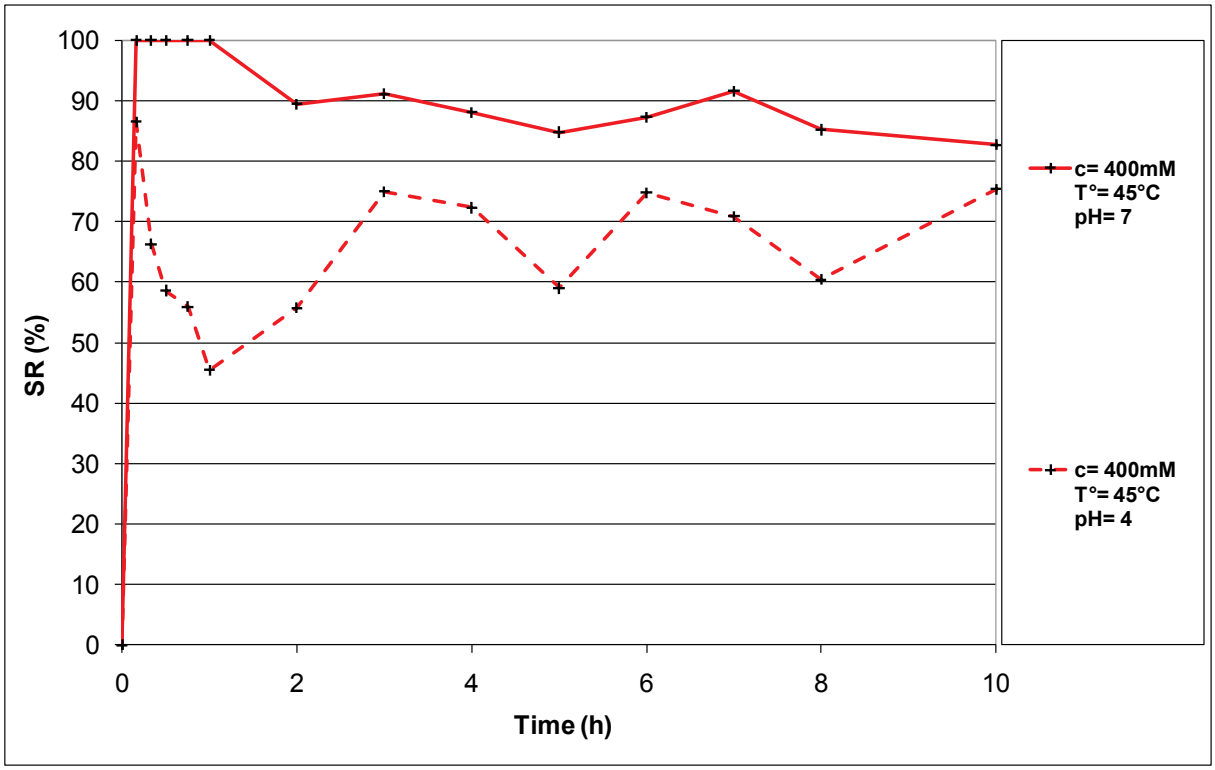

Figure III–17: SR curves for MVDES at a concentration of 400 mM and 45°C. Continuous line is for unmodified pH, whereas dashed line is for pH=4

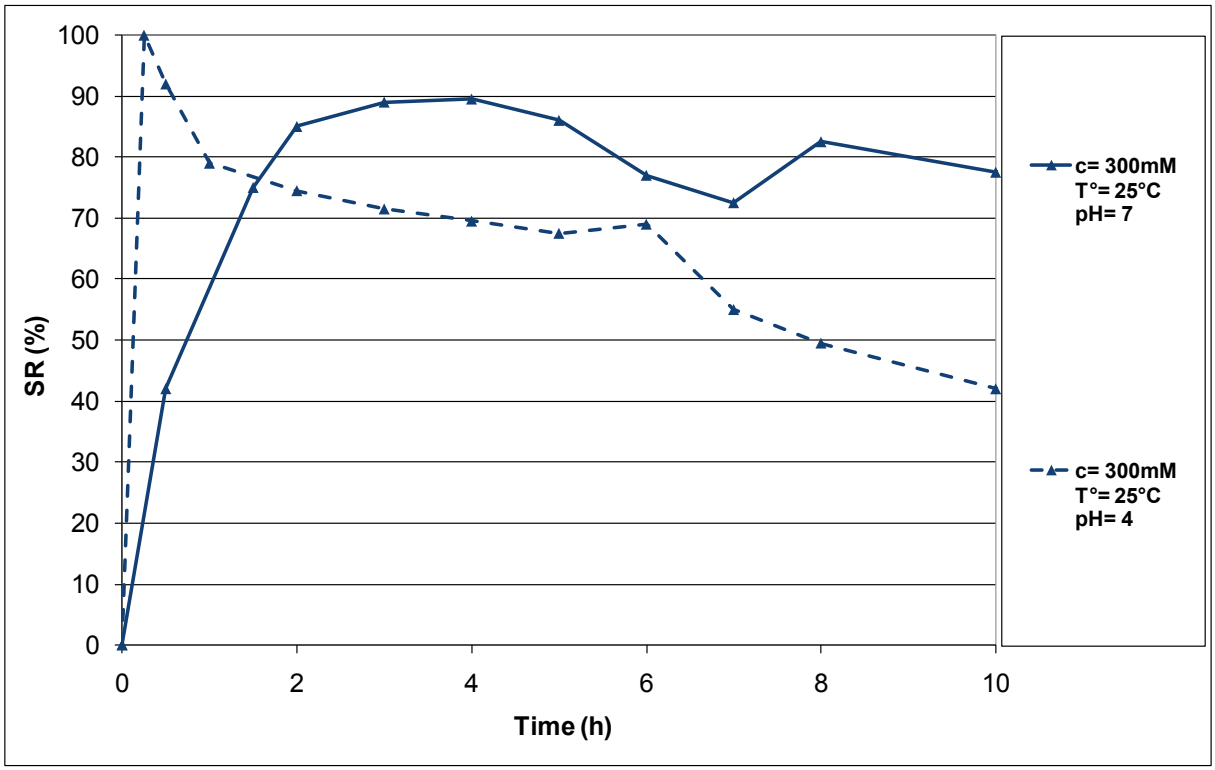

Figure III–18: SR curves for MVDMS, at 300mM. Continuous line is for unmodified pH, whereas dashed line is for pH=4

For MVDMS, it is only possible to compare the reactions carried out at different pH at a concentration of 300 mM, at 25°C. However, the results described in Figure III–18 have to be taken cautiously since the existence of a phase separation is observed early in the reaction. Despite of this lack of certainties, we can see that the behaviours are really different from each other. More specifically, at a pH=7, the SR value increases with time during the first 3 hours of reaction and reaches a plateau at 90%. This time of scale correlates perfectly with the end of the hydrolysis. After t=3h, this parameter decreases irregularly and very slowly, but since a significant loss of signal is observed, we suspect that condensed structures are formed, thus inducing inaccurate measurements. On contrary, at a pH=4, the SR value reaches a maximum of 100% in a few minutes and, immediately after, decreases abruptly.

In conclusion, for vinylalkoxysilanes, similarly to alkylalkoxysilanes, moving to an acidic pH strongly increases their hydrolysis at 25°C. For MVDES however, the effect of temperature seems to be in competition with that of pH and there is no clear tendency on the effect of pH, except the fact that an acidic pH facilitates the detection of condensed structures otherwise invisible.

III.C.3 Aminoalkoxysilanes

For DAMS, it was shown previously that an acidic pH allows maintaining a higher reactivity at the beginning of the reaction.

Figure III–19 shows the behavior of APDMES at a concentration of 400mM, both at 25 and at 45°C. For both temperatures, the behaviors are very similar (This Figure was duplicated from Figure III–14, for the reader's comfort). A common observation for all experiments is that the hydrolysis is completed very rapidly, independently of any reaction parameter. Then, the main difference between the experiments at pH=11.5 and their acidic counterparts is that in the formers, a second liquid phase was formed.

In conclusion, for aminoalkoxysilanes, the hydrolysis rate being enhanced in both pH media, a very high reactivity is obtained in all cases. However, an acidic pH has been shown to prevent the formation of insoluble structures, or to reduce their kinetic of formation, most probably through the protonation of the amine moieties. Hence for this family of compounds, the use of acidic solutions is recommended.

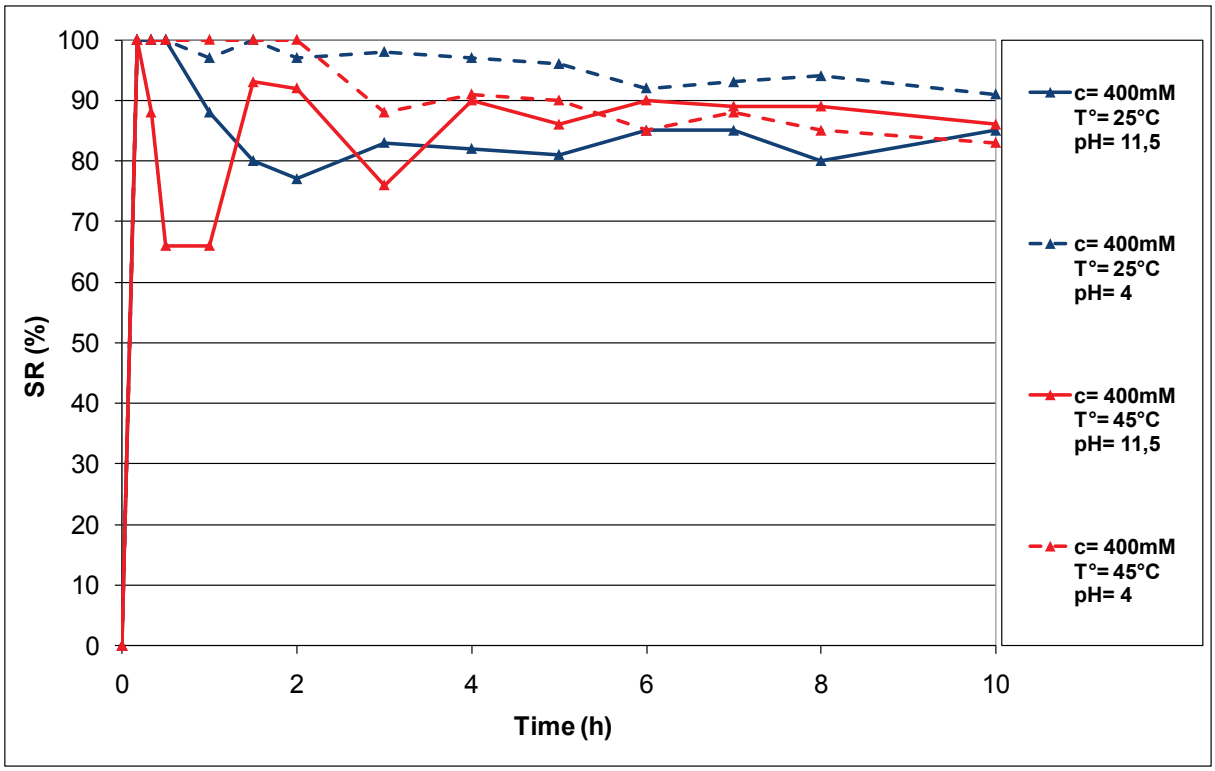

Figure III–19: SR curves for APDMES, at 400mM, 25°C (blue lines); 400mM, 45°C (red line). Continuous lines are for unmodified pH, whereas dashed lines are for pH=4

III.D Effect of temperature

III.D.1 Alkylalkoxysilanes

The effect of temperature on reactions involving DMDMS can be described from the data presented previously in Figure III–15. Data at 25°C and 45°C were obtained at a concentration of 400 mM, both in neutral and in acidic media.

In neutral pH and at 25°C, the SR value increases slowly with time, reaching a maximum value close to 90%, after 8 hours. Furthermore, the condensation reactions are very limited. While at a temperature of 45°C, the hydrolysis of the pristine silane is highly accelerated. A maximum of SR, corresponding to a complete hydrolysis, is attained after 3 hours. Also, the formation of D^1 is enhanced, causing a decrease of SR value over time. Besides, at a pH of 7, cyclic structures were detected in the NMR spectra only at 45°C

In acidic condition at 25°C, a very fast hydrolysis is observed, providing a maximum SR of 85% after only a few minutes of reaction. It is followed by very fast self-condensation reactions, giving birth to D^1, D^2 and cyclic structures. Also, a loss of signal is associated with the formation of condensed structures. At 45°C, a maximum SR of 75% is reached at the first moments of the reaction, and a rapid condensation is observed, leading to a steep decrease of the SR value.

For MTMS, the effect of temperature can be discussed for a concentration of 400 mM, at both pH, as presented in Figure III–16. As a reminder, for all conditions tested, the precipitation of condensed structures was initiated after more than 6 hours, except for the experiment at pH=7 and 45°C, where the loss of signal associated to the precipitation was observed as soon as the experiment started.

In neutral condition at 25°C, a maximum of solution reactivity is attained after one hour of reaction, due to the limited rate of hydrolysis. Then the SR value decreases steadily until reaching a value lower than 40%. After a few hours, the ratio of species in the solution reaches its equilibrium. However, precipitation phenomena were observed. At 45°C, the precipitation occurs very rapidly, and despite of a SR value reaching its maximum at 100%, the reactivity of the solution rapidly declines.

At acidic pH, the observations are very similar, except for the reaction at 25°C, for which the SR value reaches 100% after 30mn. As expected, the increase of temperature also causes an increased rate of formation of precipitate, and a fast decline of SR.

In conclusion, as expected, an increase of temperature is shown to increase the kinetics of both the hydrolysis and the self-condensation of the investigated alkylalkoxysilanes. However, differences were observed between DMDMS and MTMS. In particular, at neutral pH condition for DMDMS, an increase of the temperature was shown to diminish the duration of the hydrolysis step, hence allowing to reach a maximum of the SR value much earlier, while maintaining an acceptable condensation rate. However, for MTMS, the hydrolysis being already very fast, only the condensation is enhanced, thus shortening the span of life of the solution. In acidic conditions, the duration of the hydrolysis process is shortened. Finally, the impact of increasing the temperature to 45°C was negative for both silanes.

III.D.2 Vinylalkoxysilanes

For MVDES, it was not possible to dissolve the silane in water, at acceptable concentrations, at room temperature. Hence, NMR experiments were only performed at 45°C and it is not possible to discuss the effect of temperature on this molecule, except for saying that an increase of temperature from 25°C to 45°C allows to solubilize the compound at a concentration up to 400mM.

For MVDMS, the SR curves at both temperatures, for a concentration of 400mM in an acidic solution are presented in Figure III–20. For both experiments, a very fast hydrolysis reaction occurs, most probably because of the acidic character of the medium, and a maximum of SR is reached after 15mn. More specifically, at 25°C, a value over 85% is attained, whereas at 45°C, the peak is slightly below 80%. Unfortunately, at 45°C, a phase separation phenomenon is observed very

rapidly, traduced in the Figure by the unexpected rise of SR after t=30mn, despite all uncondensed species being already consumed.

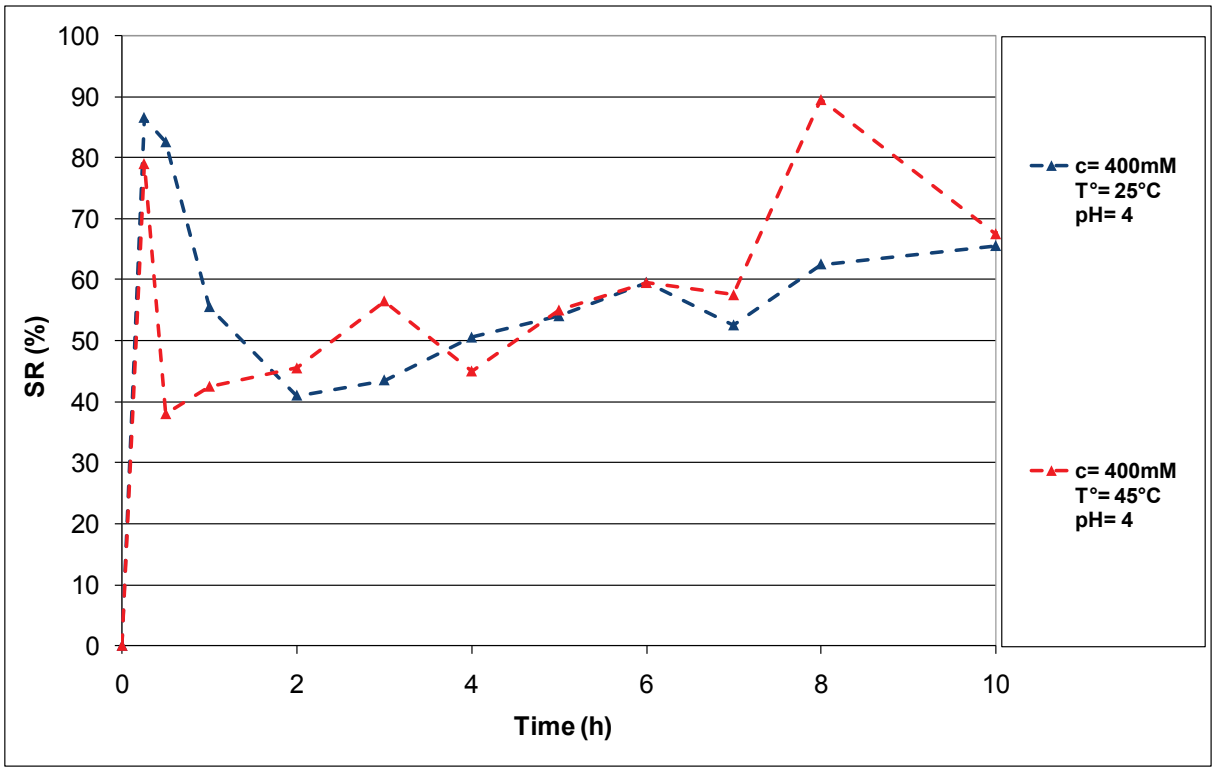

Figure III–20: SR curves for MVDMS at a concentration of 400 mM; at 25°C (blue line); and at 45°C (red line)

In conclusion, the experiments on vinylalkoxysilanes performed in our study do not allow the establishment of clear trends on the effect of temperature on the rates of hydrolysis and condensation of these compounds in purely aqueous media. However, based on the observations made during this study, it is expected that MVDMS will have a behavior very close to that of DMDMS, with a higher temperature enhancing both hydrolysis and condensation. For MVDES, the effect of the ethoxy moieties (reducing the solubility of the compound at 25°C) did not allow to make any comparison with other compounds.

III.D.3 Aminoalkoxysilanes

The effect of temperature on the reactions of APDMES at a concentration of 400 mM in both pH conditions can be discussed based on the data presented previously in Figure III–19.

For all experiments, the hydrolysis is completed immediately after the beginning of the reaction; hence the temperature has no effect on the time at which the maximum of SR value. Thus, a SR value of 100% is obtained in all cases.

At neutral pH, an increase in temperature induced an increase in the formation of insoluble structures, whereas in acidic condition no significant differences were observed between the two experiments.

Therefore, we shall conclude when dealing with aminoalkoxysilanes in purely aqueous media, that an increase of temperature does not have any positive outcome regarding the maximum of reactivity attained and the time at which it is reached. Also, in unmodified pH conditions, (pH of 11.5 here) the increase in the temperature enhances the formation of a second phase. Thus, with aminosilanes, the key parameter seems to be the pH rather than the temperature.

III.E Effect of concentration

In addition to the results already presented, a few experiments were performed at lower silane concentration, in order to allow the study of the effect of concentration on the hydrolysis and self-condensation reactions of the selected silanes in purely aqueous media.

III.E.1 Alkylalkoxysilanes

For DMDMS, the effect of concentration was evaluated at both pH conditions, at room temperature, as presented in Figure III–21. In neutral condition, very similar features are observed at concentrations of 300mM and 400mM, and there is no clear effect of lowering the concentration by 25%. At pH=4, changing the concentration from 400 mM to 200 mM did not modify the initial rate of hydrolysis, however a slight change was observed, as the maximum of SR value is slightly higher at 200 mM, i.e., over 95% instead of 85% for the concentration of 400 mM. After the maximum value is reached, the trends are very similar, however the solution with a lower concentration maintain a higher reactivity for a few hours (around 4 hours). Then, the formation of a second phase composed of condensed structures starts to take place thus affecting the ratio of the compounds in the reaction medium. Thus, at pH=4, the decrease in concentration seems to slightly stabilize the solution over time and reduce the kinetic of self-condensation.

The trialkoxysilane MTMS has been investigated at concentrations of 300 mM and 400 mM at 25°C under neutral pH conditions. The data, presented in Figure III–22, show that for both concentrations the hydrolysis is very fast, with an advantage to the lower concentration system for which a solution with a SR of 100% is achieved more rapidly. For reactions carried out at a higher concentration, some pristine silane existed in the solution until t=1h. Afterward, for both concentrations, SR decreases regularly with almost similar rates. The data suggest however that the condensation rate is slightly higher at 400 mM than at 300 mM, as witnessed by the faster decrease of the SR value.

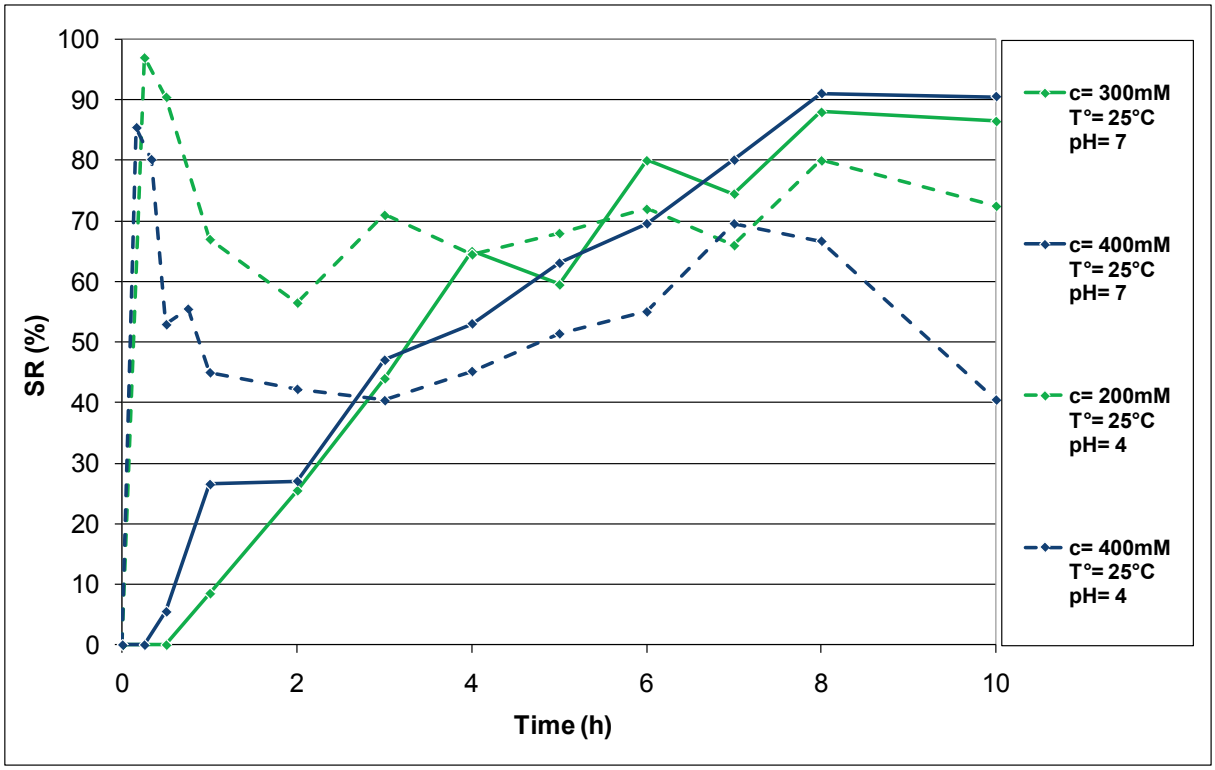

Figure III–21: SR curves for DMDMS at 25°C, at concentrations of 300 mM (green lines); and 400 mM (blue lines). Continuous lines are for unmodified pH, whereas dashed lines are for pH=4

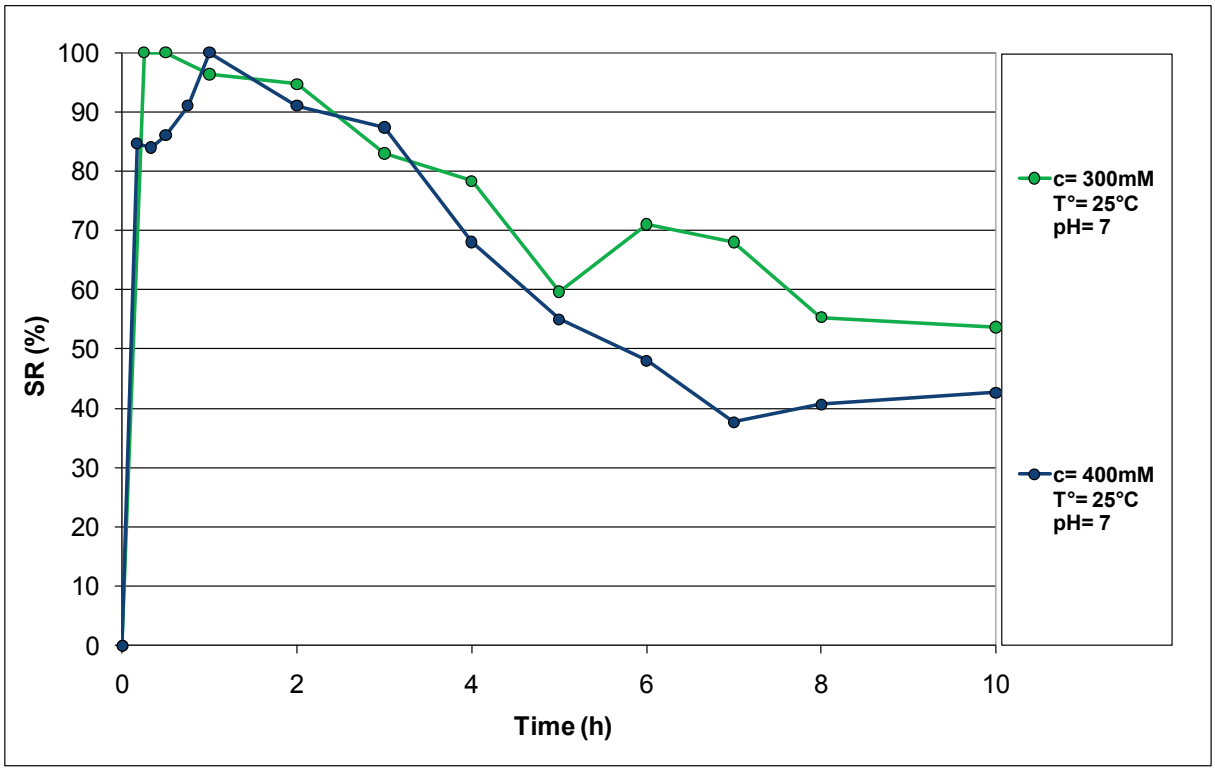

Figure III–22: SR curves for MTMS at concentrations of 300 mM (green line); and 400 mM (blue line). Both experiments at 25°C and pH=7

In conclusion, for alkylalkoxysilanes, the effect of the concentration on the initial reactivity of the silane seems to be non significant. But when considering the reactivity over longer durations, it seems that, as expected, an increase of silane concentration causes an increase of the self-condensation reaction rates.

III.E.2 Vinylalkoxysilanes

For a MVDMS solution at 25°C and under acidic pH, it is possible to observe the effect of concentration (for two systems: 400 mM and 300 mM), as presented in Figure III–23. The curves presented here show that, as expected, the fast rate of hydrolysis causing the steep increase of the initial SR value is not affected by the change in the concentration. However, like for DMDMS, at 300 mM the maximum of reactivity attained is 100%, against 85% for the higher concentration system (i.e., 400 mM). Likewise, the condensation leading to a decrease of the SR value is enhanced at 400 mM, because of the formation of insoluble structures.

Thus, the conclusions on the effect of the concentration for vinylalkoxysilanes are similar to those for alkylalkoxysilanes. An increase of silane content in the solution is detrimental for the reactivity of the solution over time, and does not impact much the initial hydrolysis rate.

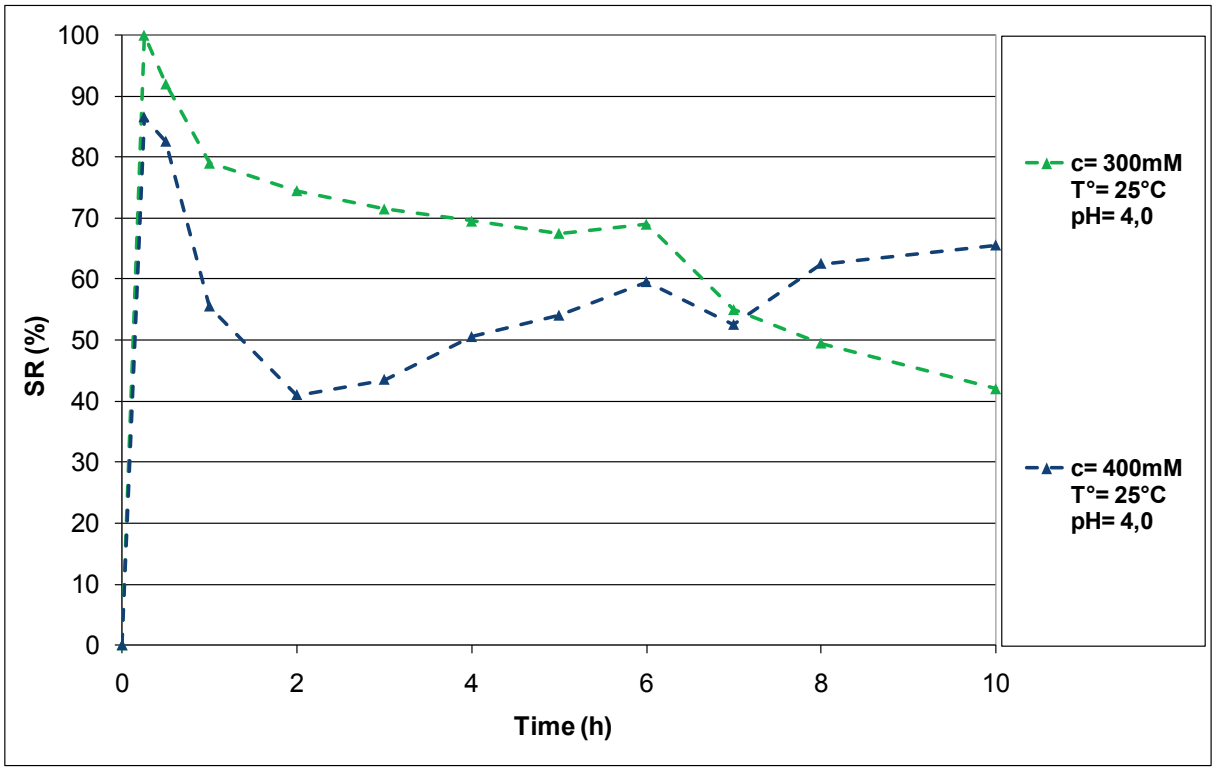

Figure III–23: SR curves for MVDMS at concentrations of 300 mM (green line); and 400 mM (blue line). Both experiments at 25°C and pH=4

III.E.3 Aminoalkoxysilanes

Unfortunately, we do not have enough data on APDMES to discuss the effect of concentration for this silane. However, it is most expected that the conclusions would be similar to those presented previously for other molecules, i.e. an increase of condensation with concentration, and no effect on hydrolysis, this reaction being already immediate for aminosilanes in the conditions of reaction used here.

III.F Effect of silane structure

Thanks to the experiments already presented for various silanes, and meant to understand the effect of solution parameters, it is also possible to perform some comparisons between molecules with slightly different structures reacted in otherwise similar conditions.

III.F.1 TMMS-DMDMS-MTMS

Regarding the comparison between TMMS, DMDMS and MTMS (structures recalled in Figure III–24), one can observe that the structure of the molecule is similar, with an increased number of methoxy substitutions on the core silicon atom. In fact, 1, 2 and 3 alkoxy moieties are respectively present in these structures in their pristine form. By comparing the reactions of these silanes in otherwise similar reaction conditions, it is possible to evaluate the effect of the number of alkoxy groups.

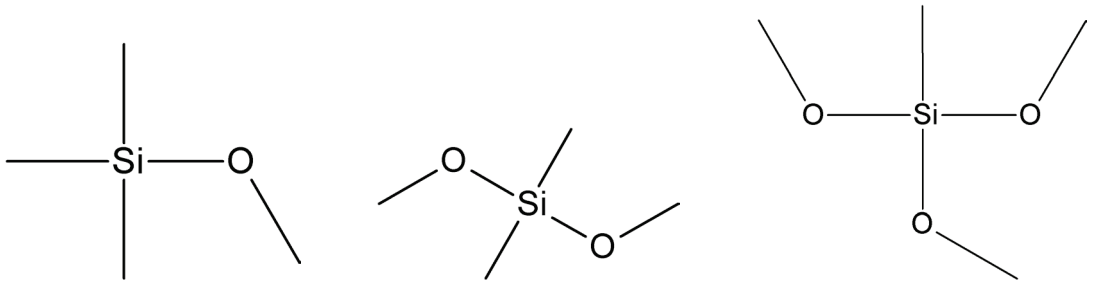

Figure III–24: Structures of TMMS, DMDMS, and MTMS.

It is reminded that TMMS could not be dissolved in water in sufficient quantities to allow NMR analyses. For DMDMS and MTMS, the results of reactions at similar conditions for both silanes are presented in Figure III–25 for experiments in neutral conditions, and in Figure III–26 for experiments at pH=4. In these figures, the reader is invited to look at lines with similar colours, in order to compare matching reactions on both silanes.

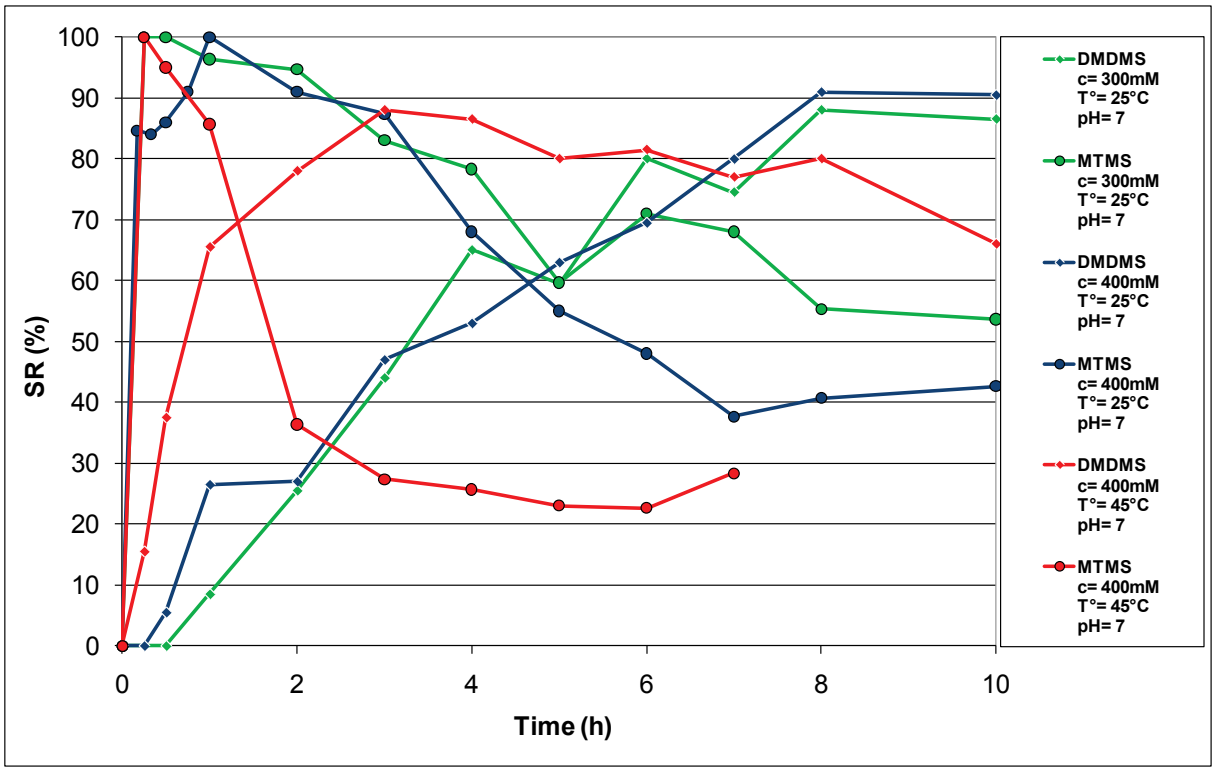

Figure III–25: SR curves for structural comparison between DMDMS (diamond marker) and MTMS (circle marker). At concentrations of 300 mM, 25°C (green lines); 400 mM, 25°C (blue lines); and 400mM, 45°C (red lines). All reactions in neutral pH conditions

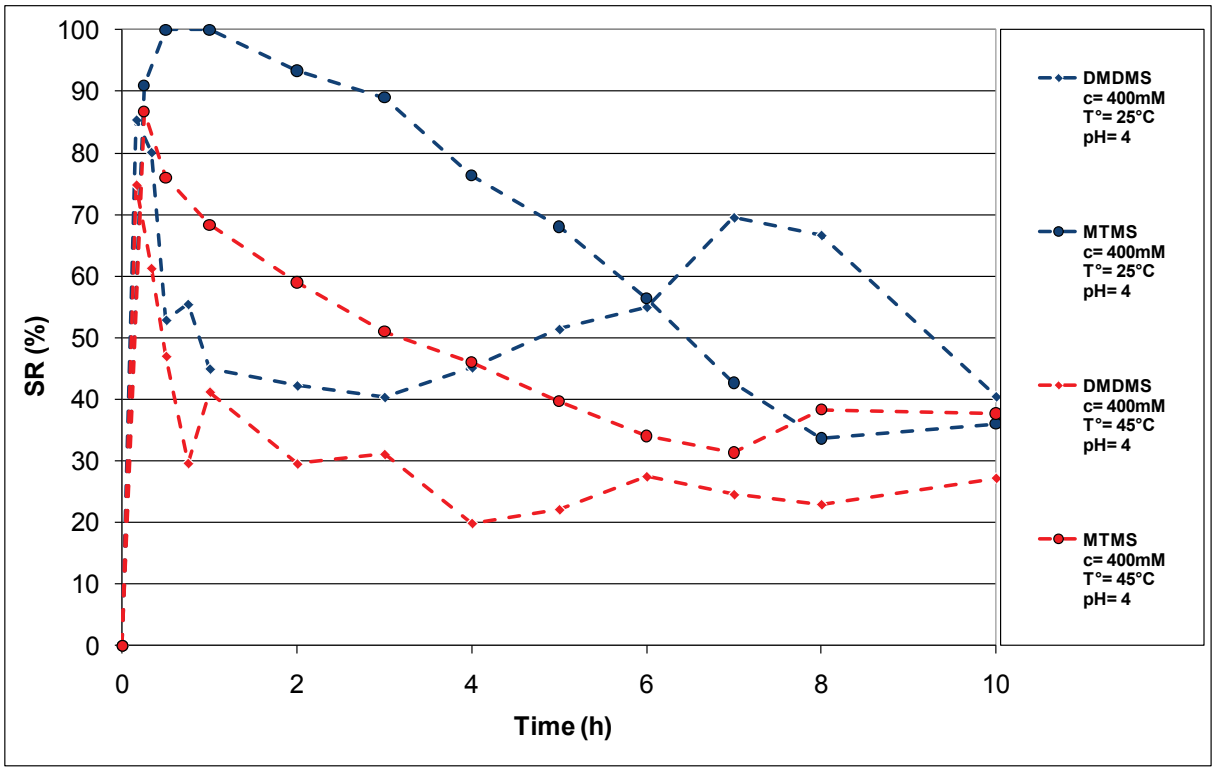

Figure III–26: SR curves for structural comparison between DMDMS (diamond marker) and MTMS (circle marker). At concentrations of 400 mM, 25°C (blue lines); and 400mM, 45°C (red lines). All reactions in acidic pH conditions

At pH=7, for all conditions, moving from two methoxy moieties to three, greatly influences the rate of the initial hydrolysis. For all conditions of DMDMS (diamond marker), the hydrolysis is completed after only a few hours, whereas for MTMS (circle marker), in all conditions, this reaction is rapidly completed, from a few minutes to one hour. However, MTMS clearly appears as being subjected to self-condensation reactions faster than DMDMS, and the formation of insoluble structures is carried out in more significant amounts.

At pH=4, the SR value reaches its maximum after a few minutes of reaction for all the conditions presented here. In opposition to the observations in neutral conditions, here, MTMS shows a better SR over time, compared to experiments with DMDMS in similar conditions, for the first few hours of the reaction.

As a conclusion, we can observe that the substitution of an alkyl moiety by an alkoxy group greatly influences the solubility of the silane in water, and allowed much faster hydrolysis rate, which is in agreement with literature data and attributed to the presence of the oxygen atom. Furthermore, this change of the structure has been shown to affect significantly the self-condensation reactions of the silane, but the trends observed for this point are dependant of solution parameters, such as the pH.

Noteworthy, only the role of methoxy groups can be discussed here, since we do not have data on ethoxy counterpart with varied number of alkoxy moieties. This point is very important since it was observed in our literature survey that methoxy groups are known to increase the solubility of a compound when they replace alkyl moieties. Whereas ethoxy groups provide a lower solubility than their methoxy counterparts. Thus, we can expect that an increased substitution by ethoxy groups would not lead to the same conclusions.

III.F.2 DMDMS-MVDMS

The only difference between DMDMS and MVDMS structures is the substitution of an alkyl moiety by a vinyl function. Hence, comparing these two molecules can provide valuable data on the effect of the vinyl function on the reactions of an alkoxysilane in water.

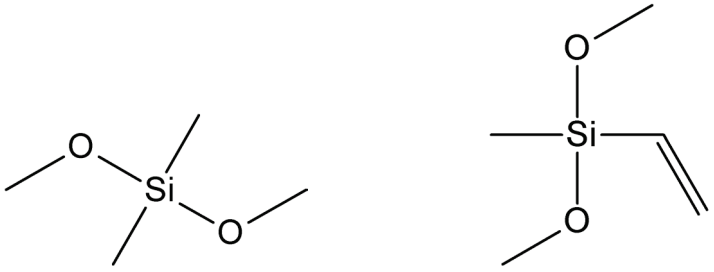

Figure III–27: Structures of DMDMS and MVDMS.

Relevant SR curves for DMDMS (diamond marker) and MVDMS (square marker) are shown in Figure III–28 for three different reaction conditions. For reactions at pH=7, 300 mM and 25°C, the main effect of the vinyl function seems to be an increased rate of hydrolysis, leading to a more steep rise of the SR value during the first three hours of the experiment. Otherwise, the maximum of SR value reached is similar for both silanes, i.e., about 90%. Very little D^2 moieties are observed in both cases. At acidic pH, there are no significant differences between the SR ratios of the two compounds in otherwise similar conditions during the first two hours of reaction. After this time, the effect of phase separation does not allow to draw clear cut conclusion on the observed trends.

Nevertheless, it appears that the presence of a vinyl function causes an improved hydrolysis rate in neutral conditions, and certainly an improved solubility of the compound in water. Nevertheless the vinyl group does not allow to avoid the formation of insoluble structures.

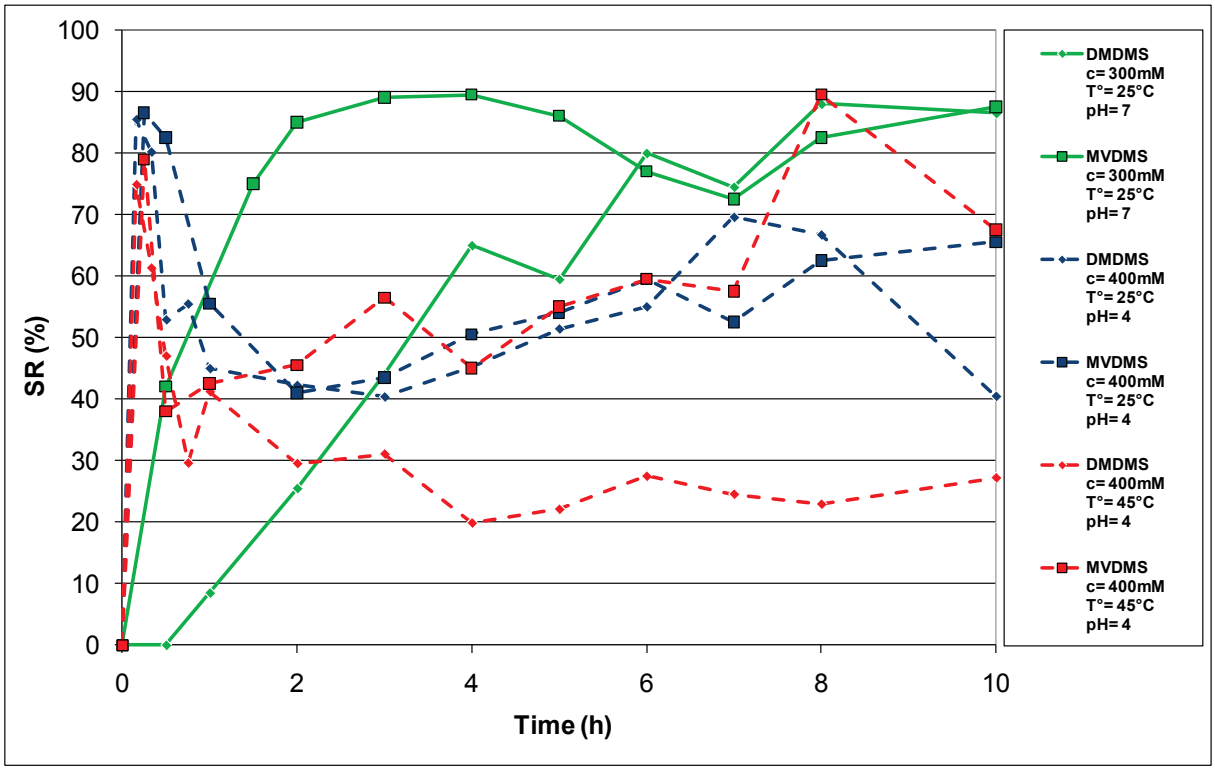

Figure III–28: SR curves for structural comparison between DMDMS (diamond marker) and MVDMS (square marker). At concentrations of 300 mM, 25°C (green lines); 400 mM, 25°C (blue lines); and 400mM, 45°C (red lines). Continuous lines are for unmodified pH, whereas dashed lines are for pH=4

III.F.3 MVDES-MVDMS

MVDMS and MVDES structures (which are recalled in Figure III–29) differ only by the nature of their alkoxy groups. Thus, a very interesting point for these two molecules is that after the hydrolysis reaction is completed, they give birth to the same silane-diol.

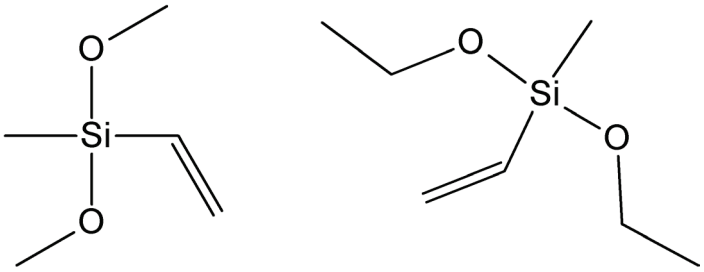

Figure III–29: Structures of MVDMS, and MVDES.

Figure III–30 shows the SR curves for MVDES (black cross marker) and MVDMS (square marker) for a reaction at a concentration of 400 mM, a temperature of 45°C and a pH set to 4. Unfortunately, these conditions of temperature and pH were already shown to greatly enhance the hydrolysis reaction and favour the formation of insoluble species. It was therefore not possible to acquire data on MVDES in other conditions of temperature. From the data presented here, a very similar behaviour is observed for both silanes, with a maximum of SR value close to 80~85% reached at the very beginning of the reaction, and followed by a steep decline of SR values by more than the half. The formation of insoluble structures is greatly enhanced in these conditions and does not allow discussing the rest of the curves, since the difference appearing on the curves correspond only to the part of silane structures remaining in the solution.

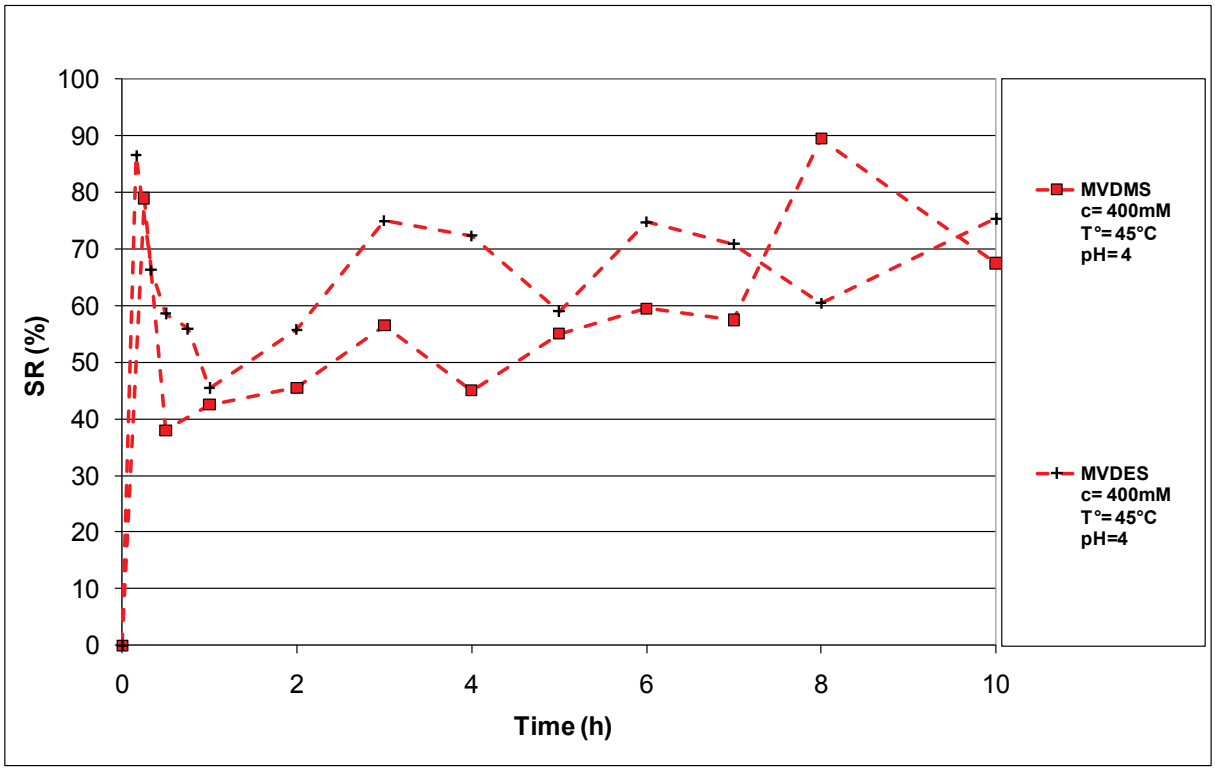

Figure III–30: SR curves for structural comparison between MVDMS (square marker) and MVDES (black cross marker) at a concentration of 400mM, pH=4 and T°=45°C

As a conclusion, the increased length of the alkoxy moieties does not impact significantly the reactions of the silane in water. However, the fact that MVDES could not be studied at lower temperature than 45°C is already a sign that the longer alkoxy moieties have a negative effect on the solubility of the compound.

IV. Conclusions and perspectives

The study presented in this chapter was focused on the analysis of the reactions of various alkoxysilanes in aqueous media by ^{29}Si NMR spectroscopy, with varied concentration, pH and temperature. It was shown that the use of purely aqueous media can provide solutions with increased reactivity or shelf life. Nevertheless, the study of some compounds, in such media, demonstrated that a purely aqueous medium can cause the rapid phase separation of the reacted silanes when the conditions are not carefully chosen. In particular, the functional group born by the silane was shown to play an important role.

In addition, the effects of different parameters were evaluated for three families of structures. In overall, the pH was proven to be the most important parameter to control, since an acidic pH allows the immediate formation of highly reactive solutions for all the silane molecules and the conditions tested. However, for some silanes, acidic conditions increased the formation of insoluble structures. Then, the temperature was found to enhance both the hydrolysis and the self-condensation reactions, with the major disadvantage of shortening shelf life for most experiments presented here. Finally, the concentration was demonstrated to have a slight effect on the hydrolysis reaction rate, even though this effect is negligible when compared with the impact of pH and temperature, for the range of concentrations tested. Another feature was also observed on the kinetic of self-condensation where a higher concentration accelerates the loss of reactivity of the solution over time.

However, with the perspective of using silanes for the modification of natural fibers in papermaking applications, the results presented here show unambiguously that all compounds, except TMMS, can be reacted in pure water to form highly reactive solutions with SR reaching values ranging from 75% to 100%.

Then, from a pragmatic point of view, it is confirmed that it is essential for our application to have time-resolved *in-situ* data, such as those presented here, for each silane used, in order to optimize the grafting process. From these data, it is possible to determine the best strategy of use for a given silane in aqueous medium. Thus, several parameters could be established, such as: the time for pre-hydrolysis before addition of the fibers when this step is needed, the control of the reaction parameters, the duration of reactivity of the solution, etc. The most valuable data obtained from this study are summarized in Table IV-1. These data will be used in the next parts of this work to optimize the reaction of silanes with cellulose pulp.

Silane	*pH*	*Concentration (mM)*	*Temperature (°C)*	*Highest SR (%)*	*Time at highest SR (hours)*	*Estimated duration of period with high reactivity*
TMMS	Solubility not sufficient for NMR analysis					
DMDMS	**4**	**200mM**	**RT**	95	0	~ 1 hour
		400mM	**RT**	85	0	~ 1 hour
		400mM	**45ºC**	75	0	~ 30 minutes
	7	**300mM**	**RT**	90	8	a few days
		400mM	**RT**	90	8	a few days
		400mM	**45ºC**	90	3	~ 10 hours
MTMS	**4**	**400mM**	**RT**	100	0	~ 2 hours
		400mM	**45ºC**	85	0	~ 6 hours
	7	**300mM**	**RT**	100	0	~ 6 hours
		400mM	**RT**	100	0	~ 6 hours
		400mM	**45ºC**	100	0	~ 2 hours
MVDES	**4**	**400mM**	**45ºC**	85	0	~ 30 minutes
	7	**400mM**	**45ºC**	100	0	a few hours
MVDMS	**4**	**300mM**	**RT**	100	0	~ 4 hours
		400mM	**RT**	85	0	~ 2 hours
		400mM	**45ºC**	80	0	~ 30 minutes
	7	**300mM**	**RT**	90	4	~ 6 hours
		400mM	**45ºC**	**Phase separation too fast to allow NMR acquisition before signal loss**		
APDMES	**4**	**400mM**	**RT**	100	0	days
		400mM	**45ºC**	100	0	days
	11,5	**400mM**	**RT**	100	0	a few hours
		400mM	**45ºC**	100	0	~ 1 hour

Table IV-1: NMR data summary

List of references

[1] N. Kim, D. H. Shin, et Y. T. Lee, « Effect of silane coupling agents on the performance of RO membranes », *Journal of Membrane Science*, vol. 300, n°. 1-2, p. 224-231, 2007.

[2] C. M. Bertelsen et F. J. Boerio, « Linking mechanical properties of silanes to their chemical structure: an analytical study of γ-GPS solutions and films », *Progress in Organic Coatings*, vol. 41, n°. 4, p. 239-246, 2001.

[3] S. A. Torry, A. Campbell, A. V. Cunliffe, et D. A. Tod, « Kinetic analysis of organosilane hydrolysis and condensation », *International Journal of Adhesion and Adhesives*, vol. 26, n°. 1-2, p. 40-49, 2006.

[4] A. Kretschmer et M. Backer, « Concentration dependence of the 1H- and 29Si-NMR chemical shifts of tetramethyldisiloxanediol in deuterated chloroform », *Journal of Organometallic Chemistry*, vol. 628, n°. 2, p. 233-240, 2001.

[5] M. C. Brochier-Salon, M. Bardet, et M. N. Belgacem, « Solvolysis–hydrolysis of N-bearing alkoxysilanes: Reactions studied with 29Si NMR », *Silicon Chemistry*, vol. 3, n°. 6, p. 335-350, 2008.

[6] M. C. Brochier-Salon, M. Abdelmouleh, S. Boufi, M. N. Belgacem, et A. Gandini, « Silane adsorption onto cellulose fibers: Hydrolysis and condensation reactions », *Journal of Colloid and Interface Science*, vol. 289, n°. 1, p. 249-261, 2005.

Chapter 2 - Silane adsorption on model surfaces

Table of contents

List of figures - 78 -
List of tables - 80 -
List of equations - 80 -
I. Study of silanes adsorption onto cellulosic substrates - 81 -
I.A Cellulose - 81 -
I.B Adsorption phenomena - 84 -
I.C Silanes adsorption - 87 -
I.D Quartz Crystal Microbalance (QCM) - 90 -
List of references - 96 -
II. Materials and Methods - 101 -
II.A Materials - 101 -
II.B Methods - 101 -
III. Results and Discussion - 105 -
III.A Silane adsorption onto cellulose sensors - 105 -
III.B Silane adsorption onto silica sensors - 124 -
IV. Conclusions and perspectives - 127 -
List of references - 128 -

List of figures

Figure I–1: Structure of cellulose - 80 -
Figure I–2: Typical decay curves of rigid and viscoelastic materials. - 92 -
Figure I–3: Example of a QCM-D apparatus - 93 -
Figure I–4: AT-cut quartz crystal for QCM, electrode side, above a sample chamber - 93 -
Figure III–1: 7th overtone frequency shift for repeated experiments on the adsorption of a 0.2% DAMS solution under unmodified pH, at 45°C, on silica quartzs. - 105 -
Figure III–2: APDMES structure. - 106 -
Figure III–3: 7th overtone Frequency and Dissipation shifts (primary vertical axis), and Sauerbrey modeling (secondary vertical axis) for the adsorption of 0.2% APDMES on a cellulose sensor, at a pH of 11.5, and a temperature of 45°C - 107 -
Figure III–4: Zoom on the -300s to +600s time period of Figure III–3. - 107 -
Figure III–5: Sauerbrey modeling of APDMES adsorption on cellulose sensors, under acidic pH, at 25°C. - 109 -
Figure III–6: Sauerbrey modeling of APDMES adsorption on cellulose sensors, under unmodified pH, at 25°C. - 109 -
Figure III–7: Sauerbrey modeling of APDMES adsorption on cellulose sensors, under acidic pH, at 45°C. - 110 -
Figure III–8: Sauerbrey modeling of APDMES adsorption on cellulose sensors, under unmodified pH, at 45°C. - 110 -
Figure III–9: Model representation of the cellulose sensors surface. - 112 -
Figure III–10: Estimation of APDMES amount adsorbed on average cellulose fibers (with a specific area of 3m²/g) after 30mn according to QCM model data, and theoretical values based on geometry considerations. - 114 -
Figure III–11: DAMS structure - 115 -
Figure III–12: Sauerbrey modeling of DAMS adsorption on cellulose sensors, under acidic pH, at 25°C and 45°C. - 116 -
Figure III–13: Sauerbrey modeling of DAMS adsorption on cellulose sensors, under unmodofied pH, at 25°C and 45°C. - 116 -
Figure III–14: Estimation of DAMS amount adsorbed on average cellulose fibers (with a specific area of 3m²/g) after 30mn according to QCM model data, and theoretical values based on geometry considerations - 118 -
Figure III–15: Possible paths for polyalkoxysilane grafting. (Source : [6]) - 119 -
Figure III–16: 7th overtone Sauerbrey modeling for all experiments on VDMES adsorption on cellulose sensors. - 121 -

Figure III–17: Estimation of VDMES amount adsorbed on average cellulose fibers (with a specific area of 3m²/g) after 30mn according to QCM model data, and theoretical values based on geometry considerations - 122 -

Figure III–18: Estimation of the amount of silane adsorbed on typical cellulose fibers after 30mn at a concentration of 0.4% under varied pH and temperature conditions for APDMES, DAMS and VDMES. - 123 -

Figure III–19: Example of an adsorption curve obtained for APDMES on silica quartz, under unmodified pH. - 125 -

Figure III–20: Example of an adsorption curve obtained for APDMES on silica quartz, under acidic pH. - 125 -

Figure III–21: Comparison of the estimated amount of silane adsorbed on typical cellulose fibers after 30mn for APDMES and DAMS, based on measurements on cellulose and on silica. - 126 -

List of tables

Table II–1: List of the silanes studied with the Quartz Crystal Microbalance, and their properties. Functional groups are in red, whereas hydrolysable groups are in blue. - 101 -

Table III–1: Key data on APDMES adsorption on cellulose model surfaces at varied pH, T°, and concentration - 113 -

Table III–2: Key data on DAMS adsorption on cellulose model surfaces at varied pH, T°, and concentration - 117 -

Table III–3: Key data on VDMES adsorption on cellulose model surfaces at varied pH, and temperature - 121 -

List of equations

Equation II–1: Sauerbrey equation [65] - 91 -

Equation II–2: Sauerbrey relation [66] - 92 -

I. Study of silanes adsorption onto cellulosic substrates

In order to modify a surface with organosilanes, the silane has to have a certain affinity with the surface, thus allowing the adsorption of the silane onto the surface to occur, before the chemical grafting can be envisaged. Hence, with the aim of maximizing or optimizing the amount of coupling agent retained on the surface after the silane treatment, it is necessary to evaluate the organosilane adsorption on cellulose, and how it is affected by reaction parameters.

Within such a context, it is essential to clearly understand the phenomenon of adsorption. Therefore, in the next sections, the chemistry of the substrate used in this work, cellulose, will be introduced, as well as the physical chemistry concepts behind adsorption. Also, the existing literature will be summarized, in regard of the adsorption of silanes onto various substrates, and more specifically onto cellulose. Finally, a very specific apparatus for the evaluation of adsorption will be introduced, the quartz crystal microbalance with dissipation (QCM-D).

I.A Cellulose

Cellulose is a natural polymer produced by plants and trees, along with other polysaccharides. This very abundant polymer, the most common vegetal biomass-based organic compound on Earth, is involved in the structural properties of wood. It is very widely used by man in several classical applications, such as textiles, building, etc. In addition, today, new areas of applications are emerging such as bio-fuels. The following sections summarize relevant data regarding cellulose described in general textbooks [1-5], and the reader interested on more specific topics, such as the synthesis, or the role of cellulose in nature, is invited to consult these references.

I.A.1 Structure, surface chemistry and reactivity of cellulose

The cellulose macromolecule is composed of β-D-(1-4)-glucopyranose units forming a linear homo-polysaccharide, as presented in Figure I–1. Cellulose coming from wood is generally found to have a degree of polymerisation varying from 5000 to 10000. More specifically, cellulose is a polymorphic material; with the native form being denominated cellulose I. This form is a mixture of two allomorphs, cellulose I_α (triclinic) and cellulose I_β (monoclinic) [6] which coexist naturally in wood. However, other structures of cellulose were synthesized and characterized by researchers, such as regenerated cellulose, giving birth to cellulose II, III, and IV.

Each glucopyranose unit involved in the structure of cellulose bears three hydroxyl moieties which are commonly considered as reactive groups. However, cellulose is a rather inert material in general, owing to the facts that it is usually highly crystalline, and that strong physical interactions exist between the polysaccharide chains [7]. Moreover, each hydroxyl moiety in the saccharidic unit presents a different reactivity, since factors such as the steric hindrance, or the electro-negativity of the closest atoms affect this hydroxyl reactivity [8].

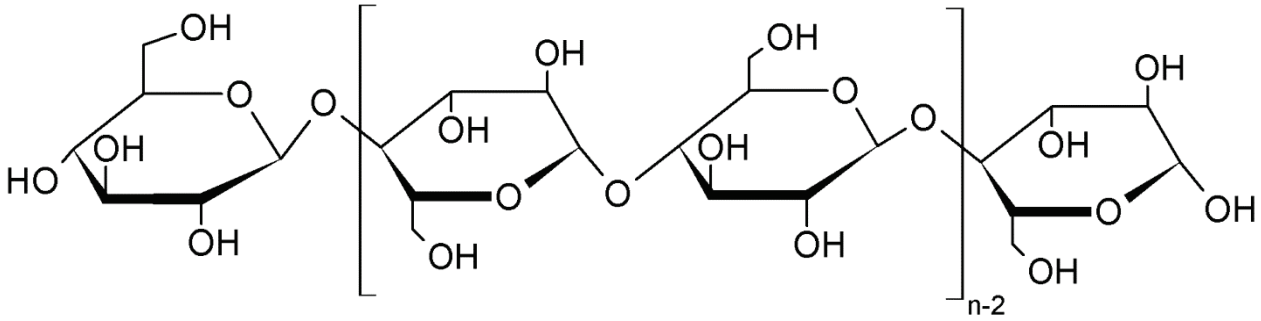

Figure I–1: Structure of cellulose

Cellulose is one of the most important constituent of wood fibers. The structure of wood fibers can be described, in a very rough approximation, as an empty cylinder with walls composed of different layers presenting varied chemical composition [5]. In overall, these walls are mostly composed of cellulose, and other natural polymers, giving the wood its mechanical properties. In the fibers walls, cellulose is organized in crystalline and amorphous regions [5]. The crystalline parts are composed of a few layers of cellulose molecules structurally organized, whereas the amorphous parts are made of layers with no specific organization. In wood fibers, the amorphous and crystalline regions are uniformly and randomly distributed [5]. Furthermore, it is known that the amorphous parts being more accessible than the crystalline ones to chemical agents; they are, consequently, more reactive [8].

For very small molecules, it is generally admitted that they can reach both the outer, and the inner wall of the fibers, as well as penetrate its porosity, and to a certain extent penetrate the surface, especially after the fibers have been left to swell in an adequate solvent [8]. Likely, in the case of chemical modification of cellulose through condensation of its hydroxyls, it is known that the heavier the grafting agent, the fewer sites are accessible on the cellulose surface [8].

It should also be noted that the structure of cellulose fibers is affected by its origin: differences of composition and structure are observed between wood species, and also in the same species it is known that fibers growing at different season have slightly different features. Even though native cellulose does not contain charged groups, a few carboxylic groups can be introduced during pulping and bleaching [9]. The surface charge of fibers from different species can differ, which may severely affect their reactivity with chemicals, but in overall cellulose fibers surfaces are negatively

charged. In addition to the charges formed during pulping and bleaching, cellulose fibers are negatively charged because of the presence of hemicelluloses, which carry carboxylic functions, easily ionizable in basic papermaking conditions.

I.A.2 Model cellulosic surfaces

Model surfaces are crucial for fundamental research on adhesion, and surface phenomena. The interest in the preparation of model cellulosic surfaces has been rapidly increasing over the last decade, most likely owing to the complex morphology of cellulosic fibres, which impacts negatively the capacity of scientists to perform analysis requiring flat surfaces, such as friction measurements, or Atomic Force Microscopy (AFM) studies.

At first, glass has been used as a model surface for cellulose, because of their similar hydrophilicity and acid/base character [10]. Very short time after, spin-coated cellulose surfaces have been used [11], with the advantage of being rather simple to prepare, with a well defined surface [12]. Also, well defined Langmuir-Blodgett deposited cellulose films were introduced as early as 1997 [13], [14], with the disadvantage of requiring a long preparation procedure. Cellulose spheres were used as AFM colloidal probes and have been used since 1997 [12]. Cast-coated films as well as cast-coated cellulose I were in use, as a model surface, in 2000 [12].

The main drawbacks of the techniques used for the preparation of model cellulose films are the lack of control of the thickness (especially for the preparation of thin films), the chemistry of the cellulose, which is often regenerated cellulose instead of native cellulose, or the roughness of the substrates prepared. In the 2000s, efforts were made for the improvement of preparation methods [10]. The spin-coating of dissolved cellulose solutions prior to their regeneration was strongly improved, allowing the preparation of films with thicknesses of 30~90nm [12], [15], and even as low as 20nm [16-18].

More recently, researchers have strived at preparing smooth films with very low thickness, from native cellulose. For this purpose, they prepared aqueous cellulose nano-crystals or nano-fibrils suspensions, and let the solvent evaporate in order to produce the films [19-21]. Such films present the advantage of having particularly low thicknesses and roughness, while maintaining the structure of Cellulose I. However, being composed of essentially crystalline parts, they do not allow taking into account the swelling behavior of cellulose fibers, and their reactivity is likely to be affected.

The preparation of model cellulosic surfaces being a very active field, where many findings were presented over the previous 20 years, a few reviews and books on the topic have been published in the latter years [22-24]. The reader is invited to consult such resources to find more details on the differences between the preparation techniques used and the surface properties of the ensuing films.

I.B Adsorption phenomena

I.B.1 Definition

Adsorption is a surface phenomenon corresponding to the attraction and bonding of particles (adsorbate) on a liquid or solid surface (adsorbent). A wide range of adsorbate can be considered, such as atoms, ions, molecules of gas, liquids, or dissolved solids.

The adsorption is driven by surface energy phenomena. Indeed, in the bulk of the adsorbent, the atoms are surrounded by other atoms, their bonding requirements to reach equilibrium being fulfilled, and hence atomic interactions are equal in all directions. However, atoms or molecules at the surface of a liquid or a solid are in contact with other atoms or molecules in the bulk underneath, but have very few neighboring particles in the phase above the surface. As a result, the molecules at the surface experience inward forces of attraction which give birth to surface tension. Because of these unbalanced forces, the surface is able to attract and retain particles with which it comes in contact, thus allowing the decrease of the overall free energy (G) of the system through an exothermic adsorption reaction.

During the adsorption, different mechanisms are involved, among which Van der Waals forces, hydrogen bonds, polarity, etc. The adsorption process is generally classified in one of these categories:

- Physi-sorption (Physical adsorption): When a particle adsorbs on a surface by Van der Walls forces, without formation of chemical bond between the adsorbate and adsorbent. This phenomenon involves low energies of bonding and is reversible.
- Chemi-sorption (Chemical adsorption) – When a particle adsorbs on a surface and forms chemical links, thus involving higher energies of bonding. Chemi-sorption is an irreversible phenomenon.
- Electrostatic interactions – In the case of charged surfaces, electrostatic interactions with charged adsorbate can tailor the repulsion/attraction phenomenon leading to the covering of the surface and the formation of ionic bonds [25].

Different parameters affect the adsorption phenomena and their extent, making them selective reactions:

- The specific surface of the adsorbent – When the specific surface increases, the amount of the adsorbed molecules increases.
- The temperature – When the temperature increases, the adsorption decreases, owing to the exothermicity of the adsorption reaction [26].

- The nature of the adsorbent – The size of the adsorbent, or its affinity with the medium, when adsorbing dissolved compounds, can affect its capacity to approach the surface.
- The pressure or concentration – An increase in pressure (gas) or concentration (liquid) causes a better adsorption since the number of chocks between the adsorbate molecules and the surface increases.
- The pH – The pH can impact the interactions between the adsorbate and the surface, especially if some groups can be ionized [27].

Various models were proposed to describe adsorption reactions, building the so-called "adsorption isotherms". Such isotherms are built by plotting the amount of adsorbate retained onto the adsorbent, after the equilibrium is reached, as a function of its pressure, for gases, or concentration, for liquids. In general the quantity of the adsorbate retained is normalized by the mass of the adsorbent, thus allowing the comparison of different materials and establishing the capacity of adsorption of the investigated materials. The most commonly used models for adsorption are the following [28]:

- Freundlich Adsorption Isotherm – This model, established in 1909 is based on an empirical equation, representing the isothermal variation of a quantity of adsorbate retained, by unit mass of solid adsorbent, and as a function of the gas pressure. This simple model is designed to describe the adsorption of gases on solids, and is known to fail at higher pressures.
- Langmuir Adsorption Isotherm – Developed in 1916, Langmuir's equation describes a semi-empirical model derived from a proposed kinetic mechanism, and allows relating the adsorption of a given adsorbate on a solid surface, as a function of the pressure or concentration of the medium surrounding it. The postulate on which the model is based is that a dynamic equilibrium exists between adsorbed gaseous molecules and the free gaseous molecules. However, this model is based on four assumptions. It is considered that (i) all the adsorption sites are equivalent (uniform surface); (ii) adsorbed molecules do not interact between each other (which is not respected by most organosilanes); (iii) a single mechanism drives all the observed adsorption phenomena; and (iv) at the maximum adsorption, only a monolayer is formed, meaning that only the available surface of the adsorbent can allow further adsorption. These conditions are rarely all satisfied, and more importantly, the forth condition does not allow to describe most of real-life situations, since several multi-layers absorption are often detected.
- BET theory – Named after its creators, Stephen Brunauer, Paul Emmett, and Edward Teller, who proposed it in 1938, this theory addresses most particularly the situations where multilayers are formed during adsorption. Thus, it is an extension of Langmuir's equation, based on five assumptions, namely: (i) the adsorption is limited to well-defined

sites of the sample surface (one per molecule); (ii) a molecule can act as a single adsorption site for a molecule of the upper layer; (iii) the upper layer of adsorbate is considered in equilibrium with the adsorbate phase, which means that the adsorption and desorption rates are similar; (iv) the desorption is a kinetically-limited process, which can only occur if heat is provided; and (v) at the saturation pressure of a gas, the molecule layer number tends to infinity, thus forming a liquid-like film at the surface of the investigated solid.

In addition, when considering the adsorption of compounds in solution, it is necessary to consider the DLVO theory, named after Derjaguin and Landau [29], and, Verwey and Overbeek [30]. This approach is based on the consideration that many interactions between particles in aqueous solutions could be explained by the result of Van der Waals forces, and electrostatic double-layer forces.

The reader interested in adsorption phenomena, and the interactions and forces involved in this physical chemistry field is invited to consult general textbooks on the topic [31-34], and more particularly the excellent and renowned work from Israelachvili [35].

I.B.2 Nature of the interactions involved in adsorption onto cellulose

Cellulose is a very complex substrate, involved in many industrial applications. Several researchers have shown interests on measuring the adhesion phenomena occurring at its surface. However, only more representative cellulose model surfaces could give accurate measurements and viable parameters. In this context, the work of Österberg's group is of a particular interest [13], [14], [22], [36-42].

In this work, interactions of cellulose surfaces with various components were evaluated. The interactions between cellulose surfaces and xylan surfaces were studied, and steric forces were found to dominate the interactions between these substances in aqueous solutions. Other factors like charge density, pH and electrolyte concentration were also shown to be relevant. The adhesion between cellulose surfaces in air was demonstrated to mainly depend on the contact area, and weak interactions (Van der Waals forces). The effect of a cationic polyelectrolyte on the forces exerted between two cellulose surfaces and/or between cellulose and mineral surfaces was also investigated. It appeared that, in the presence of a cationic polyelectrolyte, the forces at large distances were dominated by double-layer repulsion, whereas bridging attraction was observed in some cases. More particularly, the presence and magnitude of this force were dependent on the properties of the substrate surface. Owing to the negatively charged character of the cellulose, it was observed that electrostatic interactions were responsible for the adsorption of cationic compounds on the fibers surface.

I.B.3 Analytical means for adsorption evaluation

In order to evaluate the level and kinetics of adsorption of particles on a surface, various methods have been presented in literature.

Some researchers [13], [22], [38], [41], [42] focused their effort on measuring directly the forces on the surface, thanks to methods such as the interferometric Surface Force Apparatus (SFA), or the AFM colloidal-probe technique. Such measurements were also used to understand the interactions between cellulose and colloidal silica particles, or to quantify the Van der Waals interactions between regenerated cellulose surfaces in aqueous environments [11], [43], [44].

Other researchers focused on fitting experimental data with adsorption isotherm models [45-48], calling upon various quantitative techniques for measuring the adsorbate amount under selected conditions. Such techniques include Fourier Transform Infra-Red (FTIR) spectroscopy, chemical analyses (dosage), etc.

Finally, a few methods were proposed for *in-situ* measurements of the adsorption of a compound on a surface. Thus, Attenuated Total Reflection (ATR) – FTIR spectroscopy [49], radioactive marking and isotope detection techniques [50], and many other more or less exotic techniques were used. However, over the last decade, a tool allowing the determination of chemicals adsorption on model surfaces in aqueous environments has been used with an increasing interest. This tool, namely the Quartz Crystal Microbalance with Dissipation monitoring (QCM-D) has been used to study the adsorption of various particles on cellulose, including polyelectrolytes, surfactants, or enzymes [51-53]. The QCM-D plays a central role in the work described in this chapter; it will therefore be further described in section I.D.

I.C Silanes adsorption

Organosilanes coupling agents being extensively used in several industrial applications, the adsorption of these compounds on various substrates has been widely discussed in literature. Even though most of these studies take place on various inorganic substrates, some work was presented, performed on cellulosic materials.

I.C.1 Silanes adsorption onto inorganic substrates

Various inorganic materials were used as substrates for the adsorption of silane coupling agents, in the context of surface modification by grafting of several coupling agents. Thus, aminopropyltriethoxysilane (APS) adsorption onto a quartz surface has been monitored by X-Ray Photo-electron Spectroscopy(XPS) and found to obey to the Langmuir type [54]. Evidences were

given of partial protonation of the APS amine moiety in the used conditions. These studies were assessed by angular dependent XPS measurements which showed that the ammonium group was oriented towards the quartz substrate. APS was also used to modify diamond surfaces, with the aim of developing substrates for immobilizing biomolecules [55]. Here, the formation of APS multilayers with a controlled hardness, roughness, and capacity for immobilizing protein was reported. An AFM study revealed that the surface geometries and nanoscopic hardness of the multilayers on an oxygen-terminated diamond surface depended on the dielectric constant of the solvent; i.e., smaller is the constant, harder is the layer. Methanolic solutions of APS were used to impregnate nonwoven fabric and blocks of polyester [56]. An improved Langmuir adsorption rate equation, in which the diffusion rate for APS in methanol solution is introduced, was used to compare different conditions of adsorption on the substrates. The maximum rate of adsorption was observed for APS molecules deposited on the polyester surface. In another study, the use of APS for molecular layer deposition under an inert atmosphere, by a gas-phase technique, was described [57]. The surface densities of amino groups on silica surface were shown to decrease when the pretreatment temperature of the substrate was increased. Finally, the adsorption of APS aqueous solution on high surface area silica gel (Cab-O-Sil) and E-glass fibers was studied by FTIR [58]. It was found that the adsorbed aminosilane formed essentially a monolayer on silica and adsorbed as a multilayer on E-glass fibers. Moreover, the amine moiety of APS was shown to chemically interact with the glass surface.

Another very common silane often reported in the literature is γ-glycidoxypropyltrimethoxysilane (GPS). The effect of the water/methanol ratio, in the GPS solution, on the silane adsorption on aluminum surfaces was investigated, by means of X-ray Photoelectron Spectroscopy (XPS) and Time of Flight - Secondary Ion Mass Spectrometry (ToF-SIMS) [59]. XPS data indicated that the adsorption taking place from a solution containing methanol is less favorable than that occurring in pure water. Unexpected “inversion” of the adsorption isotherm plateau obtained for solutions containing 10% and 90% methanol, respectively, was observed. ToF-SIMS spectra variation for the fragment ions characteristic of the silane epoxy and silicon atom suggested a variation in the adsorption conformation. A correlation was obtained between the extent of hydrolysis, deduced from NMR data, and the intensities of specific fragments, as detected by ToF-SIMS. In a very different context, GPS was deposited onto silica colloids (20 nm diameter) suspended in a solution of isopropanol and water [60]. ^{29}Si NMR results indicated an adsorption limit of ~2.2 molecules of GPS monomer (or its repeating units, in the polymer built up from it) per nm² of silica surface after 24 h in suspension. However, for coatings dried at 100°C, FTIR data showed that surface silanols are further consumed as GPS is added beyond the adsorption limit in the suspension. The increased adsorption after drying has been proposed to be related to enhanced reaction rates and to drying-induced deposition onto the surfaces.

The competitive adsorption of methoxysilanes and amines with silica surfaces were investigated by a thin film infrared technique [61]. The mono-methoxysilane (TMMS) did not displace pre-

adsorbed triethylamine, whereas both di- and tri-methoxysilane (DMDMS, and MTMS, respectively) did. In the reverse sequence, the triethylamine displaced all three methoxysilanes on the surface.

The behavior of different silane molecules (octyltrihydroxysilane, aminopropyltrihydroxysilane, and thiolpropyltrihydroxysilane) adsorbed onto a zinc oxide surface in isopropanol was studied via molecular dynamics simulations, at 298K [62]. The silane molecules exhibited different behavior depending on the chemical nature of their tail. For Octyltrihydroxysilane, having a rather non-polar tail, most of the molecules had the three polar hydroxy groups of the head in contact with ZnO, with the non-polar tail remaining in the isopropanol phase. However, aminopropyltrihydroxysilane molecules, having a highly polar amine group, were found to be all orientated with two hydroxy groups as well as the amino group of the tail being in contact with the surface. The behavior of the thiolpropyltrihydroxysilane molecules was somehow intermediate, since the thiol moiety is not polar enough to induce a permanent contact to the polar surface, thus allowing the existence of two molecular orientations.

In overall, the various reports available show that depending on the conditions of deposition, the nature of the substrate, and the functionality of the silane, many different adsorption patterns can be observed.

I.C.2 Silanes adsorption onto cellulose

Up to date and to the best of our knowledge, only few papers have been published focusing on describing the adsorption, or adsorption isotherms of organosilanes onto cellulosic substrates, and most of them were published by our team.

The adsorption of five prehydrolyzed alkoxysilanes agents (γ-methacryloxypropyltrimethoxysilane (MPS), γ-aminopropyltriethoxysilane (APS), and γ-diethylenetriaminopropyltrimethoxysilane (TAS), γ-mercaptopropyltrimetoxysilane (MRPS), n-phenyl-γ-aminopropyltrimethoxysilane (PAPS)) onto the surface of cellulosic fibers in ethanol/water mixtures has been studied quantitatively [45]. The corresponding isotherms, obtained from FTIR and UV spectroscopy, show the formation of a monolayer followed by further adsorption, when increasing the concentration of the adsorbate. The nature of the silane's fourth substituent was shown to highly influence the adsorption behavior. Furthermore, the quantitative assessment performed for several silanes indicated that the adsorption of a mono- or multiple-layers of silanes is readily achieved, but that a simple extraction with ethanol allowed removing entirely these molecules, which were physically adsorbed to the substrate.

In another paper, the hydrolysis of MPS, APS, TAS, was carried out in ethanol/water solutions at different pH values, and variations in the solution composition were assessed by NMR spectroscopy [63]. MPS hydrolyzed in acidic media was successfully adsorbed onto a cellulose surface by physisorption, and the ensuing substrate was submitted to thermal treatment at 110~120°C under reduced pressure, in order to induce the formation of covalent bonds between the cellulose and the adsorbed coupling agent.

Finally, the adsorption isotherms of MPS and MRPS on cellulose fibers were established at neutral and acidic pH [46]. Under acidic conditions, for both silanes no detectable adsorption was detected, below an initial concentration of 20 mM (which corresponded to about 0.5% w/w of silane with respect to the cellulose). Then, the adsorption started and further addition of the silane yielded the appearance of multilayer adsorptions for both MPS and MRPS. Under neutral conditions, a continuous increase in the silane adsorption was observed, and a single plateau was observed for MRPS, whereas for MPS, multiple adsorption plateau were found. Such results were unexpected, since in acidic conditions over 80% of the silanol groups were present, while under neutral condition the silane hydrolysis was practically negligible. It was proposed that such results show that hydrolyzed silanol moieties are not indispensable to promote adsorption through hydrogen bonding with the hydroxyl groups of cellulose, but instead the adsorption of MPS might be driven by Van der Waals interactions.

Thus, it appears from these studies that, similarly to other substrates, the adsorption of silanes onto cellulose differs greatly depending on experimental conditions, such as pH, concentration, and also depending on the chemical structure of the fourth substituent of the silane coupling agent. Furthermore, no *in-situ* measurement of silane adsorption on cellulose surfaces was published up-to-date, more particularly in the case of purely aqueous silane solutions.

I.D Quartz Crystal Microbalance (QCM)

Recently, a new tool allowing the determination of adsorption kinetics on model surfaces became available. This tool is the quartz crystal microbalance with dissipation monitoring (QCM-D).

I.D.1 Description

The QCM is a very sensitive tool for the measurement of the deposition of adsorbates on a given surface. It provides extremely precise and useful data for scientists, and is a very versatile analysis tool thanks to the development of various model surfaces, and different apparatus configurations. The principle of functioning of the QCM is based on the piezoelectric effect, which corresponds to

the modification of the charge of certain materials in response to mechanical stresses. Crystal quartzes are the most commonly used piezoelectric substrates in QCM devices. When such substrates are submitted to alternating currents, oscillations are induced in the quartz. The frequency of oscillation of the quartz crystal depends mostly on the thickness of the crystal, in standard conditions of use, when the quartz thickness is modified, a change in frequency is observed. As particles are adsorbed or deposited on the surface of the crystal, its thickness increases; and consequently the frequency of oscillation decreases from its initial value. By accurately monitoring, in real time, the modification of the resonance frequency of a quartz crystal exposed to a solution, and its overtones, it is possible to plot the amount of adsorbate retained over time per unit area. The calculations for the conversion from a frequency shift to a mass are made using Sauerbrey's equation, following the main assumptions that the adsorbed material is: (i) evenly distributed, (ii) rigidly attached to the surface and (iii) small compared to the mass of the crystal. Such conditions are respected for small molecules such as silanes monomers or lowly-condensed oligomers.

The best agreement between the theory and experimental values is reached with planar, optically polished crystals for overtone orders between n = 5 and n = 13. At lower harmonics, energy trapping is insufficient and interferences have a great impact on the measurement, while at higher harmonics, side bands interfere with the main resonance [64].

The Sauerbrey equation, developed in 1959, allows to correlate the changes in the oscillation frequency of a piezoelectric crystal, with the mass deposited on it. Hence, the QCM is often considered as a gravimetric tool. The Sauerbrey equation is given as follows:

$$\Delta f = -\frac{2f_0^2}{A\sqrt{\rho_q \mu_q}}\Delta m$$

Equation I-1: Sauerbrey equation [65]

Where:

f_0 = Resonant frequency (Hz)

Δf = Frequency change (Hz)

Δm = Mass change (g)

A = Active piezoelectric crystal area (cm²)

ρ_q = Density of quartz (ρ_q = 2.648 g.cm^{-3})

μ_q = Shear modulus of quartz for an AT-cut crystal (μ_q = 2.947x10^{11} g.cm^{-1}.s^{-2})

The Sauerbrey equation was developed for oscillation in air, hence when measurements are performed in liquid, it is necessary to integrate, in Equation I-1, a decrease in the resonant frequency related to the viscosity. Also, when respecting the assumptions detailed above, Equation I-1 can be derived, for a sensor in a liquid, giving the Sauerbrey relation:

$$\Delta m = \frac{C\,\Delta f}{n}$$

Equation I-2: Sauerbrey relation [66]

Where:

Δm = Mass change ($g.cm^{-2}$)

Δf = Frequency change (Hz)

C = Resonator mass sensitivity ($g.cm^{-2}.Hz^{-1}$)

n = Overtone number

In addition to the measurement of mass or thickness of the adsorbed molecules, a new mode of analysis by QCM has become a standard over the last few years: the QCM-D. Indeed, as part of his doctoral work [66], Höök has shown that the absolute dissipation factor, D, of the QCM can be obtained with high accuracy and repetition rate. For this purpose, the author proposes to set the crystal to oscillation with a signal generator, and then disconnect the generator and record how the crystal oscillation decays on a digitizing oscilloscope. The recorded decay curve is then fitted to a sinusoidal dependency, and thus the resonant frequency and the dissipation factor are simultaneously obtained [67].

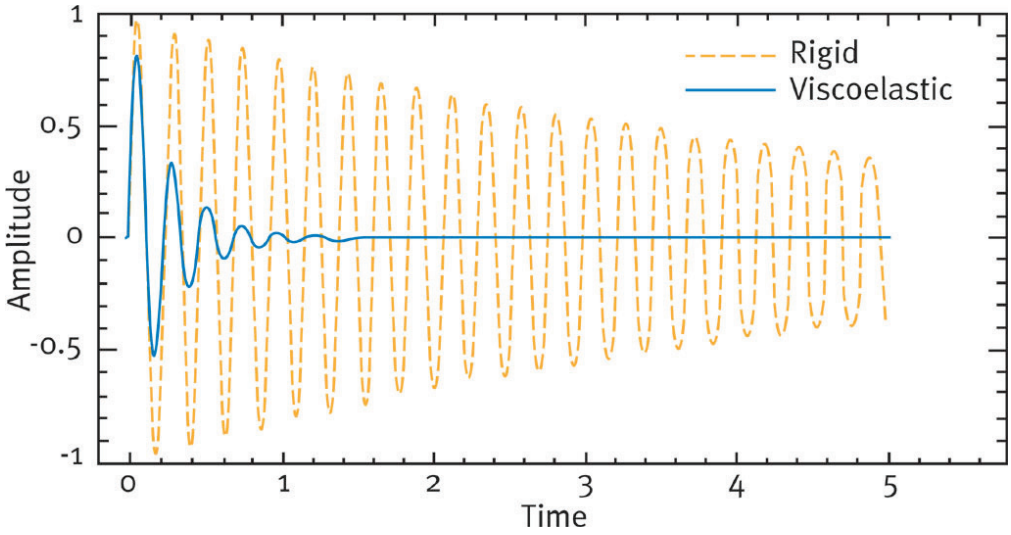

Figure I–2: Typical decay curves of rigid and viscoelastic materials. Source: http://www.q-sense.com

With this additional option, the QCM-D offers the possibility to analyze the viscous and elastic properties of adsorbed layers at the solid/liquid interface by measuring the dissipation energy, since

the decay rate depends on these properties. The change in the dissipation factor is equal to the difference between the dissipation factor of the crystal quartz before and after molecular adsorption. A very small difference of D is characteristic of thin rigid layers, whereas a large increase in D is a sign of a layer swollen by adsorbed solvent (See Figure I–2), eventually with long chains being oriented in the solvent direction instead of the surface.

Figure I–3: Example of a QCM-D apparatus (source http://www.q-sense.com)

Figure I–4: AT-cut quartz crystal for QCM, electrode side, above a sample chamber (source http://www.q-sense.com)

An example of a QCM-D apparatus is given in Figure I–3, where a control unit (large box) generates the oscillations and records the experimental data. The sample chamber (small pieces next to the generator) and a conditioning unit (medium size box) are also shown in this Figure. The latter unit allows to raise the temperature during the analysis, or to perform temperature ramps or cycles. A peristaltic pump used to control the solution flow in the sample chamber which has to be constant during the measurement is not shown in this image. This pump is particularly important, because higher flow may increase the surface forces exerted at the quartz/liquid interface, and hence affect the equilibrium at the interface. Figure I–4 presents the back side of an AT-cut quartz, where the electrodes are visible, above a QCM-D sample chamber. The quartz possesses two sides: the first one is under a constant stream of the adsorbate solution, whereas the second one (back side) is kept dry and connected to the data acquisition device.

Owing to such versatile capacities (*in-situ* mass/thickness characterization in real-time, and dissipation monitoring), and the increasing number of modified quartz substrates made commercially available (gold, steel, cellulose, silica, inox, etc.), the QCM-D technique has been at the center of many investigations lately: From proteins adsorption characterization onto specific substrates [68], to the study of organosilane monolayer formation on aluminum [69], to the evaluation of the viscoelastic properties of polyelectolytes on silica [70], and much more …

The fundamental principles of the quartz crystal microbalance (QCM) and its use in several domains are explained in various references, and the reader interested in more details on this technique and the various versions on the market is invited to consult such reviews [71], [72].

I.D.2 Literature review on QCM use for cellulose characterization

With the recent developments concerning the preparation of model cellulose surfaces by various methods, QCM-D was proven to be an efficient tool to characterize these new model surfaces. In this context, it was applied for the characterization of spin-coated cellulose model films obtained from an improved protocol, and to evaluate their value for swelling measurements [15].

In a similar way, silicon wafers covered by dissolved cellulose, using spin-coating, were analyzed with the QCM-D, in order to understand the adsorption of polyelectrolytes on these surfaces [52]. According to the QCM-D analysis, the cellulose films showed a pronounced swelling in water that took several hours to complete. Subsequent adsorption of polyelectrolytes onto the swollen cellulose films led to a release of water from the cellulose.

While working on the preparation of native cellulose model films (containing both amorphous and crystalline cellulose I) by spin-coating of aqueous cellulose nanofibril dispersions onto silica substrates, researchers used QCM-D in combination with AFM Force measurements to study the effects of nanofibril charge density, electrolyte concentration, and pH, on the swelling and the surface interactions of the model films [73]. The average thicknesses of the films were found to correspond to a monolayer of fibrils, and the root mean square roughness of the films was of the nanometers order. The model surfaces were stable in QCM-D swelling experiments, and the behavior of the nanofibril surfaces at different electrolyte concentrations and pH values correlated with other studies.

QCM-D was also used for the characterization of common papermaking additives adsorption on cellulose. In this context, the adsorption of cationic starch from aqueous electrolyte solutions onto model cellulose film has been investigated. The influences of the electrolyte composition and charge density of the cationic starch were examined [74]. The starch adsorbed following trends expected for polyelectrolyte adsorption on oppositely charged surfaces, although some exceptions were encountered. As an example, highly charged starch did not adsorb in a flat conformation even at low ionic strength. Also, the porosity of the film enabled the penetration of coiled starch molecules into the film at high electrolyte concentrations. While noticing differences in the adsorption behavior observed onto cellulose, in comparison to previous measurements on silica, the authors suggested that such differences could be explained by the difference of morphologies and acidities of the hydroxyl groups on the two surfaces.

QCM-D and cellulose model surfaces were used in order to describe the adsorption of a combination of cellulose nanofibrils and poly(amideamine) epichlorohydrin (PAE), as wet- and dry-strength additives [75]. The differences in fibril and polyelectrolyte adding strategies onto cellulose fibres were studied by comparing layer-structures and nano-aggregates formed by the nanofibrils

and PAE. The results showed that when PAE was first adsorbed on the model fiber surface, an uniform and viscous layer of nanofibrils could be adsorbed, whereas when the opposite sequence was used, a non-uniform and more rigid layer was adsorbed.

The interactions between films of cellulose and cellulase enzymes were monitored using a quartz crystal microbalance [53]. Real-time measurements of the coupled contributions of enzyme binding and hydrolytic reactions were fitted to a kinetic model. The obtained kinetics parameters were proven to be useful to discriminate the effects of incubation variables and to perform enzyme screening. From these results, QCM was demonstrated to be a relevant analysis method for tracking mass and morphological transformations due to enzyme activities.

Finally, QCM-D was used in our facilities with cellulose I model surfaces to compare the adsorption of silane-modified cationic starches onto cellulose, in comparison to commercial cationic starches [76].

To the best of our knowledge, there are no data available describing *in-situ* the adsorption of organosilanes from purely aqueous solutions onto cellulose model surfaces. Such data were needed to optimize our cellulose modification protocol, to understand the phenomena involved and to establish the structure of silane layers adsorbed from such solution. It was thus decided to undertake a study with QCM-D and commercially available cellulose I model surfaces. The results of which are presented hereafter.

List of references

[1] J. T. Marsh, *An introduction to the chemistry of cellulose*. Read Books, 2008.

[2] J.-L. Wertz, O. Bédué, et J. P. Mercier, *Cellulose science and technology*. EPFL Press, 2010.

[3] J. F. Kennedy, G. O. Phillips, et P. A. Williams, *Cellulose: structural and functional aspects*. Ellis Horwood, 1989.

[4] D. Klemm, *Comprehensive cellulose chemistry: Functionalization of cellulose*. Wiley-VCH, 1998.

[5] P. Vallette et C. de Choudens, *Le Bois, la pâte, le papier*, 2e éd. Centre technique de l'industrie des papiers, cartons et cellulose, 1989.

[6] D. L. Vanderhart et R. H. Atalla, « Native cellulose: a composite of two distinct crystalline forms. », *Science*, vol. 223, no. 4633, p. 283-285, 1984.

[7] L. Wågberg et G. Annergren, « Physicochemical characterization of papermaking fibres », in *Fundamentals of Papermaking Materials*, Pira international., UK: Baker, C.F., 1997, p. 1-82.

[8] J. A. Trejo-O'Reilly, « Synthèse d'agents de couplage, réactions de greffage en surfacede fibres cellulosiques et propriétés d'interface fibres-matrices dans des matériauxcomposites à base de polystyrène », Institut Nationale Polytechnique de Grenoble, 1997.

[9] D. Eklund et T. Lindström, *Paper chemistry: an introduction*. DT Paper Science Publications, 1991.

[10] J. Stiernstedt, « Interactions of cellulose and model surfaces », Chemical Science and Engineering, KTH, 2006.

[11] R. D. Neuman, J. M. Berg, et P. M. Claesson, « Direct measurement of surface forces in papermaking and paper coating systems », *Nordic Pulp and Paper Research Journal*, vol. 8, no. 1, p. 096-104, 1993.

[12] S. Gunnars, L. Wågberg, et M. A. Cohen Stuart, « Model films of cellulose: I. Method development and initial results », *Cellulose*, vol. 9, no. 3, p. 239-249, 2002.

[13] M. Holmberg, J. Berg, S. Stemme, L. Ödberg, J. Rasmusson, et P. Claesson, « Surface force studies of Langmuir–Blodgett cellulose films », *Journal of Colloid and Interface Science*, vol. 186, no. 2, p. 369-381, 1997.

[14] E. Poptoshev, A. Carambassis, M. Österberg, P. M. Claesson, et M. W. Rutland, « Comparison of model surfaces for cellulose interactions: elevated pH », in *Surface and Colloid Science*, Springer Berlin Heidelberg., vol. 116, Berlin, Heidelberg: Valdemaras Razumas, Björn Lindman and Tommy Nylander, 2001, p. 79-83.

[15] S. Fält, L. Wågberg, E.-L. Vesterlind, et P. T. Larsson, « Model films of cellulose II – Improved preparation method and characterization of the cellulose film », *Cellulose*, vol. 11, no. 2, p. 151-162, 2004.

[16] E. Kontturi, P. C. Thüne, et J. W. Niemantsverdriet, « Novel method for preparing cellulose model surfaces by spin coating », *Polymer*, vol. 44, no. 13, p. 3621-3625, 2003.

[17] E. Kontturi, P. C. Thüne, et J. W. (Hans) Niemantsverdriet, « Cellulose model surfaces simplified preparation by spin coating and characterization by X-ray photoelectron spectroscopy, infrared spectroscopy, and atomic force microscopy », *Langmuir*, vol. 19, no. 14, p. 5735-5741, 2003.

[18] E. Kontturi, T. Tammelin, et M. Oesterberg, « Cellulose - Model films and the fundamental approach », *Chemical Society Reviews*, vol. 35, p. 1287-1304, 2007.

[19] C. Aulin, S. Ahola, P. Josefsson, T. Nishino, Y. Hirose, M. Sterberg et L. Wagberg, « Nanoscale cellulose films with different crystallinities and mesostructures - Their surface properties and interaction with water », *Langmuir*, vol. 25, n°. 13, p. 7675-7685, 2009.

[20] C. Aulin, E. Johansson, L. Wågberg, et T. Lindström, « Self-Organized Films from Cellulose I Nanofibrils Using the Layer-by-Layer Technique », *Biomacromolecules*, vol. 11, n°. 4, p. 872-882, 2010.

[21] C. D. Edgar et D. G. Gray, « Smooth model cellulose I surfaces from nanocrystal suspensions », *Cellulose*, vol. 10, n°. 4, p. 299-306, 2003.

[22] M. Österberg, L.-E. Enarsson, et L. Wågberg, « Interactions at cellulose model surfaces », in *Encyclopedia of Surface and Colloid Science, Second Edition*, Taylor & Francis, 2007, p. 1-19.

[23] E. D. Cranston et D. G. Gray, « Model cellulose I surfaces: A review », in *Model Cellulosic Surfaces*, vol. 1019, American Chemical Society, 2009, p. 75-93.

[24] M. Roman, *Model cellulosic surfaces*, American Chemical Society., vol. 1019. USA: Maren Roman, 2010.

[25] L. Ferrari, J. Kaufmann, F. Winnefeld, et J. Plank, « Interaction of cement model systems with superplasticizers investigated by atomic force microscopy, zeta potential, and adsorption measurements », *Journal of Colloid and Interface Science*, vol. 347, n°. 1, p. 15-24, 2010.

[26] S. Giraudet, P. Pré, et P. Le Cloirec, « Modeling the temperature dependence of adsorption equilibriums of VOC(s) onto activated carbons », *Journal of Environmental Engineering*, vol. 136, n°. 1, p. 103, 2010.

[27] J. Gavoille et J. Takadoum, « Study of surface forces dependence on pH by atomic force microscopy », *Journal of Colloid and Interface Science*, vol. 250, n°. 1, p. 104-107, 2002.

[28] K. Y. Foo et B. H. Hameed, « Insights into the modeling of adsorption isotherm systems », *Chemical Engineering Journal*, vol. 156, n°. 1, p. 2-10, 2010.

[29] B. Derjaguin et L. Landau, « Theory of the stability of strongly charged lyophobic sols and of the adhesion of strongly charged particles in solutions of electrolytes », *Acta Physico Chemica URSS*, vol. 14, p. 633, 1941.

[30] E. J. W. Verwey et J. T. G. Overbeek, *Theory of the stability of lyophobic colloids*, Elsevier. Amsterdam: , 1948.

[31] R. J. Silbey, R. A. Alberty, et M. G. Bawendi, *Physical chemistry*. Wiley, 2005.

[32] P. W. Atkins et J. D. Paula, *Atkins' Physical chemistry*. Oxford University Press, 2010.

[33] J. Lyklema, *Fundamentals of interface and colloid science*. Academic Press, 2000.

[34] F. Galembeck, *Surface and colloid science*. Springer, 2004.

[35] J. N. Israelachvili, *Intermolecular and Surface Forces, 3rd Ed.*, Academic Press. 2010.

[36] M. Österberg, J. Laine, P. Stenius, A. Kumpulainen, et P. M. Claesson, « Forces between Xylan-coated surfaces: Effect of polymer charge density and background electrolyte », *Journal of Colloid and Interface Science*, vol. 242, n°. 1, p. 59-66, 2001.

[37] N. Maximova, M. Österberg, K. Koljonen, et P. Stenius, « Lignin adsorption on cellulose fibre surfaces: Effect on surface chemistry, surface morphology and paper strength », *Cellulose*, vol. 8, n°. 2, p. 113-125, 2001.

[38] M. Österberg, « On the interactions in cellulose systems : surface forces and adsorption », dissertation, KTH, 2000.

[39] M. Österberg, « The effect of a cationic polyelectrolyte on the forces between two cellulose surfaces and between one cellulose and one mineral surface », *Journal of Colloid and Interface Science*, vol. 229, n°. 2, p. 620-627, 2000.

[40] P. M. Claesson, E. Poptoshev, E. Blomberg, et A. Dedinaite, « Polyelectrolyte-mediated surface interactions », *Advances in Colloid and Interface Science*, vol. 114-115, n°. 0, p. 173-187, 2005.

[41] M. Holmberg, R. Wigren, R. Erlandsson, et P. M. Claesson, « Interactions between cellulose and colloidal silica in the presence of polyelectrolytes », *Colloids and Surfaces A: Physicochemical and Engineering Aspects*, vol. 129-130, n°. 0, p. 175-183, 1997.

[42] M. Österberg et P. M. Claesson, « Interactions between cellulose surfaces: effect of solution pH », *Journal of Adhesion Science and Technology*, vol. 14, n°. 5, p. 603-618, 2000.

[43] S. M. Notley, B. Pettersson, et L. Wågberg, « Direct measurement of attractive van der Waals' forces between regenerated cellulose surfaces in an aqueous environment », *Journal of the American Chemical Society*, vol. 126, n°. 43, p. 13930-13931, 2004.

[44] I. L. Radtchenko, G. Papastavrou, et M. Borkovec, « Direct force measurements between cellulose surfaces and colloidal silica particles », *Biomacromolecules*, vol. 6, n°. 6, p. 3057-3066, 2005.

[45] M. Abdelmouleh, S. Boufi, A. Ben Salah, M. N. Belgacem, et A. Gandini, « Interaction of silane coupling agents with cellulose », *Langmuir*, vol. 18, n°. 8, p. 3203-3208, 2002.

[46] R. Bel-Hassen, S. Boufi, M. C. Brochier-Salon, M. Abdelmouleh, et M. N. Belgacem, « Adsorption of silane onto cellulose fibers. II. The effect of pH on silane hydrolysis, condensation, and adsorption behavior », *Journal of Applied Polymer Science*, vol. 108, n°. 3, p. 1958-1968, 2008.

[47] G. M. Nishioka, « Adsorption/desorption of water on glass fiber surfaces », *Journal of Non-Crystalline Solids*, vol. 120, n°. 1-3, p. 34-39, 1990.

[48] M. Shirazi, T. G. M. van de Ven, et G. Garnier, « Adsorption of modified starches on pulp fibers », *Langmuir*, vol. 19, n°. 26, p. 10835-10842, 2003.

[49] S. J. Hug, « In-situ Fourier transform infrared measurements of Sulfate adsorption on Hematite in aqueous solutions », *Journal of Colloid and Interface Science*, vol. 188, n°. 2, p. 415-422, 1997.

[50] J. A. Kafalas et H. C. Gatos, « Apparatus for the direct measurement of adsorption on solid surfaces from liquids », *Review of Scientific Instruments*, vol. 29, n°. 1, p. 47, 1958.

[51] C. Aulin, I. Varga, P. M. Claesson, L. Wagberg, et T. Lindstrom, « Buildup of polyelectrolyte multilayers of Polyethyleneimine and microfibrillated cellulose studied by in situ dual-polarization interferometry and quartz crystal microbalance with dissipation », *Langmuir*, vol. 24, n°. 6, p. 2509-2518, 2008.

[52] L.-E. Enarsson et L. Wågberg, « Polyelectrolyte adsorption on thin cellulose films studied with reflectometry and quartz crystal microgravimetry with dissipation », *Biomacromolecules*, vol. 10, n°. 1, p. 134-141, 2009.

[53] X. Turon, O. J. Rojas, et R. S. Deinhammer, « Enzymatic kinetics of cellulose hydrolysis: A QCM-D study », *Langmuir*, vol. 24, n°. 8, p. 3880-3887, 2008.

[54] D. Kowalczyk, S. Slomkowski, M. M. Chehimi, et M. Delamar, « Adsorption of aminopropyltriethoxy silane on quartz: an XPS and contact angle measurements study », *International Journal of Adhesion and Adhesives*, vol. 16, n°. 4, p. 227-232, 1996.

[55] Y. Amemiya, A. Hatakeyama, et N. Shimamoto, « Aminosilane multilayer formed on a single-crystalline diamond surface with controlled nanoscopic hardness and bioactivity by a wet process », *Langmuir*, vol. 25, n°. 1, p. 203-209, 2009.

[56] K. Kurematsu, M. Wada, et M. Koishi, « Kinetic studies on silane coupling molecular adsorption on polyester surface », *Journal of Colloid and Interface Science*, vol. 109, n°. 2, p. 531-541, 1986.

[57] S. Ek, E. I. Iiskola, L. Niinistö, J. Vaittinen, T. T. Pakkanen, J. Keränen et A. Auroux, « Atomic layer deposition of a high-density Aminopropylsiloxane network on silica through sequential reactions of γ-Aminopropyltrialkoxysilanes and water », *Langmuir*, vol. 19, n°. 25, p. 10601-10609, 2003.

[58] C.-H. Chiang, H. Ishida, et J. L. Koenig, « The structure of [gamma]-aminopropyltriethoxysilane on glass surfaces », *Journal of Colloid and Interface Science*, vol. 74, n°. 2, p. 396-404, 1980.

[59] M.-L. Abel, R. Joannic, M. Fayos, E. Lafontaine, S. J. Shaw, et J. F. Watts, « Effect of solvent nature on the interaction of -glycidoxy propyl trimethoxy silane on oxidised aluminium surface: A study by solution chemistry and surface analysis », *International Journal of Adhesion and Adhesives*, vol. 26, n°. 1-2, p. 16-27, 2006.

[60] M. W. Daniels et L. F. Francis, « Silane adsorption behavior, microstructure, and properties of Glycidoxypropyltrimethoxysilane-modified colloidal silica coatings », *Journal of Colloid and Interface Science*, vol. 205, n°. 1, p. 191-200, 1998.

[61] L. D. White et C. P. Tripp, « An infrared study of the amine-catalyzed reaction of methoxymethylsilanes with silica », *Journal of Colloid and Interface Science*, vol. 227, n°. 1, p. 237-243, 2000.

[62] A. Kornherr, S. Hansal, W. E. G. Hansal, J. O. Besenhard, H. Kronberger, G. E. Nauer et G. Zifferer, « Molecular dynamics simulations of the adsorption of industrial relevant silane molecules at a zinc oxide surface », *The Journal of Chemical Physics*, vol. 119, n°. 18, p. 9719, 2003.

[63] M. C. Brochier-Salon, G. Gerbaud, M. Abdelmouleh, C. Bruzzese, S. Boufi, et M. N. Belgacem, « Studies of interactions between silane coupling agents and cellulose fibers with liquid and solid-state NMR », *Magnetic Resonance in Chemistry*, vol. 45, n°. 6, p. 473-483, 2007.

[64] S. Goka, K. Okabe, Y. Watanabe, et H. Sekimoto, « Multimode quartz crystal microbalance », *Japanese Journal of Applied Physics*, vol. 39, n°. Part 1, No. 5B, p. 3073-3075, 2000.

[65] G. Sauerbrey, « Verwendung von Schwingquarzen zur Wägung dünner Schichten und zur Mikrowägung », *Zeitschrift für Physik A Hadrons and Nuclei*, vol. 155, n°. 2, p. 206-222, 1959.

[66] F. Höök, « Development of a novel QCM technique for protein adsorption studies », Doctoral thesis, Chalmers University of Technology, 2004.

[67] M. Rodahl, F. Höök, A. Krozer, P. Brzezinski, et B. Kasemo, « Quartz crystal microbalance setup for frequency and Q-factor measurements in gaseous and liquid environments », *Review of Scientific Instruments*, vol. 66, n°. 7, p. 3924, 1995.

[68] F. Höök, M. Rodahl, P. Brzezinski, et B. Kasemo, « Energy dissipation kinetics for protein and antibody−antigen adsorption under shear oscillation on a quartz crystal microbalance », *Langmuir*, vol. 14, n°. 4, p. 729-734, 1998.

[69] D. G. Kurth et T. Bein, « Quantification of the reactivity of 3-Aminopropyl-triethoxysilane monolayers with the quartz-crystal microbalance », *Angewandte Chemie International Edition in English*, vol. 31, n°. 3, p. 336-338, 1992.

[70] T. Tammelin, J. Merta, L.-S. Johansson, et P. Stenius, « Viscoelastic properties of cationic starch adsorbed on quartz studied by QCM-D », *Langmuir*, vol. 20, n°. 25, p. 10900-10909, 2004.

[71] F. Wudy, C. Stock, et H. J. Gores, « Measurement methods - Electrochemical: Quartz microbalance », in *Encyclopedia of Electrochemical Power Sources*, Amsterdam: Elsevier, 2009, p. 660-672.

[72] C. K. O'Sullivan et G. G. Guilbault, « Commercial quartz crystal microbalances – Theory and applications », *Biosensors and Bioelectronics*, vol. 14, n°. 8-9, p. 663-670, 1999.

[73] S. Ahola, J. Salmi, L.-S. Johansson, J. Laine, et M. Österberg, « Model films from native cellulose nanofibrils. Preparation, swelling, and surface interactions », *Biomacromolecules*, vol. 9, n°. 4, p. 1273-1282, 2008.

[74] K. S. Kontturi, T. Tammelin, L.-S. Johansson, et P. Stenius, « Adsorption of cationic starch on cellulose studied by QCM-D », *Langmuir*, vol. 24, n°. 9, p. 4743-4749, mai. 2008.

[75] S. Ahola, M. Österberg, et J. Laine, « Cellulose nanofibrils - Adsorption with poly(amideamine) epichlorohydrin studied by QCM-D and application as a paper strength additive », *Cellulose*, vol. 15, n°. 2, p. 303-314, 2008.

[76] C. Guézénnec, « Master Thesis : Study of the modification of cationic starch by organosilanes and its product adsorption on cellulosic substrates », 2009, Grenoble.

II. Materials and Methods

II.A Materials

All experiments were carried out using Ultra-pure water (Millipore water: 18 MΩ/cm) produced by an ultra-pure water production device (Elix 3 UV, MIlli-Q GradientA10, Nihon Millipore Ltd.).

The organo-functional silanes used in this part of the work were: 3-aminopropyldimethylethoxysilane (APDMES), 3-(2-amino-ethylamino)-propyltrimethoxysilane (DAMS) and vinyldimethylethoxysilane (VDMES). Their formula, physical properties, purity, CAS number and distributor are described in Table II-1.

For experiments in acidic media, a pH of 4 was obtained by adding an appropriate amount of glacial acetic acid to the solutions prior to the silane addition. A research grade product from Sigma-Aldrich was used as received.

Name	Structure	Molecular formula	Molar weight (g/mol)	Density at 25°C (g/cm3)	Boiling point (°C)	Purity (%)	CAS Number	Distributor	Commercial Reference
(3-Amino)-propyl-dimethylethoxysilane (APDMES)	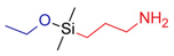	$C_7H_{19}NOSi$	161,32	0,857	78	> 95 %	[18306-79-1]	Gelest, Inc. - Morrisville, PA - USA	SIA 0603.0
3-(2-amino-ethylamino)propyl-trimethoxysilane (DAMS)	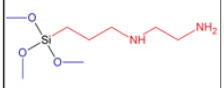	$C_8H_{22}N_2O_3Si$	222,36	1,02	264	> 98 %	[1760-24-3]	Dow Corning, S.A. - Seneffe - Belgium	Z-6094
Vinyldimethyl-ethoxysilane (VDMES)	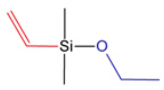	$C_6H_{14}OSi$	130,26	0,79	99	> 95 %	[5356-83-2]	Gelest, Inc. - Morrisville, PA - USA	SIV 9072.0

Table II-1: List of the silanes studied with the Quartz Crystal Microbalance, and their properties. Functional groups are in red, whereas hydrolysable groups are in blue.

II.B Methods

II.B.1 Quartz Crystal Microbalance set-up

Silane adsorption on model surfaces was studied using the Quartz Crystal Microbalance with Dissipation monitoring device, from Q-Sense, Gothenburg, Sweden. A Q-Sense E1 instrument was used, allowing the measurements of frequency and dissipation shifts related to the adsorption of the silanes on model surfaces under controlled flow and temperature conditions. The QCM measures simultaneously the changes in the frequency and the dissipation of the quartz sensor at the fundamental frequency of 5 MHz, and at its overtones of 15, 25, 35, 45, 55 and 75 MHz.

Two types of quartz were used in this study in order to describe the adsorption features of a given silane on hydroxyl-rich surfaces representing cellulose fibres.

As a model cellulose surface, we used quartz crystals which were spin-coated by the supplier with native micro-fibrillated cellulose, composed of crystalline cellulose I and amorphous cellulose. The fibrils diameter was measured around 5 to 6 nm by the supplier. According to the data furnished, the characteristics of the sensors are the following [1]:

- Cellulose thickness: ~ 6 nm
- Surface roughness: 3-4 nm (Root Mean Square roughness according to AFM)
- Adhesive layer composition: Poly(ethylene imine)
- Reference: QSX 334.

Unfortunately, the exact quantity of cellulose is not given by the supplier and therefore for our further calculations we will give plausible assumptions.

Silica quartz crystals were also used as an alternative hydroxyl bearing surface. The reference of these sensors is QSX 303.

The experimental conditions to set-up the adsorption kinetics were set as follow:

For the cellulose sensors, a preliminary step was added: they were immersed into a solution corresponding to the reference of the experiment (pure solvent, or solvent and acetic acid) overnight, allowing the cellulose of the sensor to swell, which avoids such an effect during the measurement [2]. Then, for all the sensors, the quartz were placed in the reaction chamber and the pump was set on in order to allow a constant flow of pure solvent. After the stabilization of all frequency and dissipation signals, the acquisitions were started, and after a few minutes of acquisition, in order to build the baseline, the silane was added to the medium. After a transfer time of 45s (at the selected flow), the silane solution attained the sensors surface, and the time was set to zero. The silane solution flow on the sensor was maintained constant throughout all the analysis duration, which varied from 30mn to several hours. After that, the silane solution was replaced by a pure solvent solution in order to observe the desorption of weakly adsorbed compounds from the surface, and finally the acquisition was stopped. For all experiments, the same flow was used, and similar rinsing protocols were performed.

Noteworthy, the transfer time of the solution into the system tubes was measured using a protocol from the supplier of the QCM device. After the acquisition, the system was rinsed alternatively with ethanol and water, several times, and the sensors were immersed in ethanol and surfactant (sodium dodecyl sulphate) baths for 5 minutes each, before being thoroughly rinsed with ultra pure water and being dried under a flow of nitrogen gas.

II.B.2 QCM study

The experiments were performed at varied pH, temperature, and concentration for each silane.

The pH was either left unmodified, or set to a pH of 4, such as described in the previous section dealing with NMR studies. For both aminosilanes, the unmodified pH was measured and found to be around 11.5 after the addition of the silane in the solution, whereas for VDMES, the unmodified pH of the solution corresponded to that of the ultra pure water which was measured to be close to 6.

The temperature of the solution was set either at 25°C or at 45°C depending on the experimental conditions required. The QCM device's sensor chamber could be thermo-stated. However, previous work from our team [3], in conditions similar to those used in this work, has shown that when the difference of temperature between the incoming flow and the target temperature is more than a few degrees, the regulation is not sufficient, and artefacts related to the temperature can affect the measurement. Thus, for all experiments, the flasks containing the solvent or the silane solutions were maintained in a water bath at the target temperature.

Three silane concentrations were used: 0.1, 0.2 or 0.4%. The concentrations used are very low in comparison to those used in the NMR study, because of the extreme sensitivity of the QCM device, for which the recommended concentrations vary from 0.01% to less than 1%.

Also, in order to ensure significant results, various verifications were made prior to any data collection and exploitation. Firstly, it was verified that there was no difference of response between the 5 sensors that we used for these experiments, by repeating an experiment with similar conditions on each sensor. This test was carried out at both temperatures, and using both the lowest and the highest concentrations used in our study. Secondly, the repeatability of the measure was evaluated by duplicating the experiments in the same way on a single sensor.

II.B.3 Data treatment

The data obtained for each QCM measurement are presented in the form of a datasheet containing columns of data corresponding to the various shifts measured by the apparatus over time, as well as, the temperature. These datasheets were first treated using the appropriate software provided with the instrument, namely *QTools*. Using this software, an offset was applied to all relevant columns of the data, in order to set all frequency and dissipation shifts at zero at the time corresponding to the moment when the silane solution reaches the sensor.

Then, the values of frequency shifts were compared to those of dissipation shift. It appears that for all experiments performed on silanes, the dissipation shift was not significant in regard to the frequency shift, thus indicating that the adsorbed layers were thin and did not retain a significant amount of water molecules in between the adsorbed molecules. This is a logical finding since the

deposition of monomeric silanes, or small condensed polysiloxanes is not expected to retain water, in contrast to large polymeric molecules, such as starch, for which viscoelastic modelling is needed to fit the data. In our case, the low values of dissipation shift indicated that the Sauerbrey equation is relevant to the treatment of our data. Hence, for all files, the Sauerbrey equation was applied directly into *QTool* on all the frequency shift columns, and the file was then exported into a format compatible with *Microsoft Excel*®.

Finally, the adsorption curves were plotted from the data obtained after applying the Sauerbrey equation, and the obtained curves from the different overtones were compared for all the experiments in order to assess which overtone presented the most regular behaviours throughout all our experiments (i.e., to avoid the presence of certain interferences on the overtone). In our case, it was arbitrarily decided to use the 7^{th} overtone to compare all our data. Thus, the data analysis was concluded by plotting the curves, and comparing relevant data of the 7^{th} overtone for each of our files.

III. Results and Discussion

In this chapter, the results of the QCM study of silane adsorption on model surfaces will be presented in two main parts. In the first part, the adsorption kinetics of APDMES, DAMS and VDMES onto cellulose will be discussed and compared. Then the second part of this chapter will briefly present the results of experiments carried out on silica sensors, and compare them with the data obtained with cellulose sensors. Finally, the most relevant data found in this study will be summarized in a concluding section.

III.A Silane adsorption onto cellulose sensors

Cellulose sensors obtained by spin-coating of native cellulose on quartz QCM sensors were used to evaluate the adsorption kinetics of silanes under different conditions.

III.A.1 Assessment of method reliability

In order to assess the validity of the experimental protocol used in this study and to determine the standard deviation of the QCM method, selected experiments were repeated five times at two different concentrations (0.2 and 0.4%), both with APDMES and DAMS, either on the same sensor, or varying among sensors of a same type, both with silica and cellulose sensors.

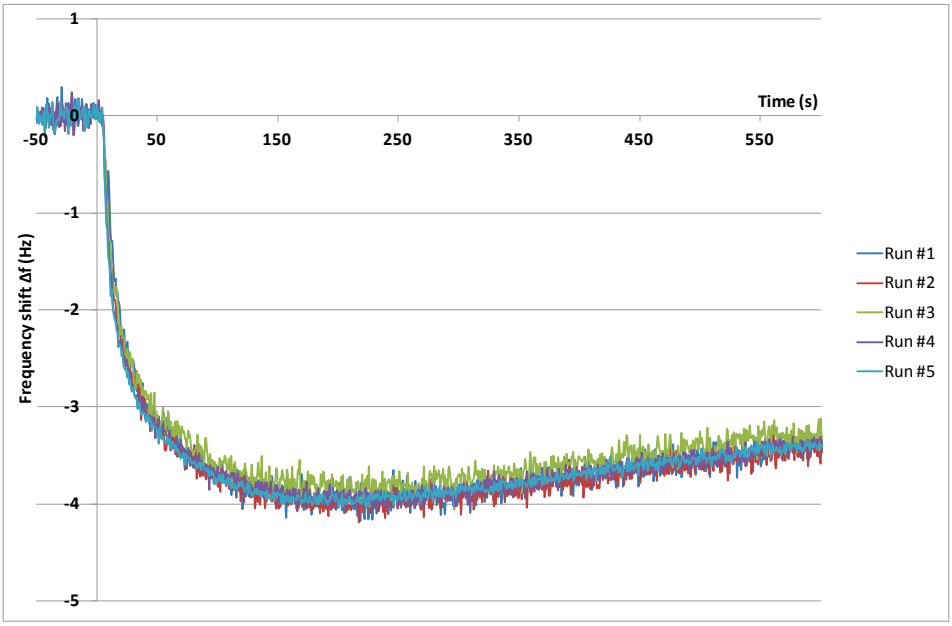

Figure III–1: 7th overtone frequency shift for repeated experiments on the adsorption of a 0.2% DAMS solution under unmodified pH, at 45°C, on silica quartzs.

For each of these series of experiment, the data were treated and compared on the 7th overtone, in order to determine the standard deviation of the sensor response. Two criteria were observed: the amount of silane adsorbed estimated through the Sauerbrey equation after an initial step in the adsorption curve, and the corresponding time at that point.

Regarding the maximum of amount adsorbed, it was found that the results were equivalent, between the different sensors and/or on a same sensor. Also, for both silanes, the results were found to be similar, and a good accuracy was found under the conditions tested. Actually, the concentration was observed to be the only critical parameter in estimating the standard deviation, and our data show that this deviation was found in all case to be between 5% and 10% of the measured value, as illustrated in Figure III–1. Indeed, this figure shows, for repeated experiments, the 7th overtone frequency shift obtained when adsorbing DAMS from a 0.2% w/w aqueous solution, under unmodified pH, at a temperature of 45°C. For the data presented on this Figure, 5 experiments were performed, using 3 different silica quartz sensors. Hence showing a good correlation on the results obtained on a same sensor after it has undergone our washing procedure, and between different sensors. Similar results were observed on cellulose coated sensors. Thus, for all our results, error bars of 10%, with respect to the measured values, will be used as an estimate of the standard deviation.

On the topic of the time at which the initial step of adsorption ended, two observations were made. First, this delay was relatively short in comparison with the length of the complete measurement duration, since such a phenomenon occurred after only a few minutes of the experiments, in all cases. And also, this criterion was found to vary too much to be a meaningful parameter of comparison: standard deviations ranging between 25% and over 60% for certain experiments were found. Thus, it was decided that this data will not be further exploited.

III.A.2 Adsorption of APDMES on cellulose model surfaces

In order to determine how silanes adsorb onto cellulose fibers, to what extent, and how long the contact time between the solution and the fibers should be, a wide study by QCM was initiated on model cellulose surfaces.

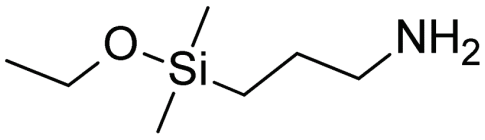

Figure III–2: APDMES structure.

An example of the data, obtained from the adsorption of APDMES (see structure in Figure III–2) on a cellulose coated-sensor, is shown in Figure III–3. In this Figure, both the frequency shift (blue curve) and the dissipation shift (red curve) are plotted over time on the primary vertical axis, for duration of almost 4 hours. In addition, the adsorbed mass per areal unit (black curve), obtained by using the Sauerbrey equation on the frequency shift, is plotted on the secondary vertical axis. Also,

time zero is set at the moment when the silane solution reaches the sensor. The data for the five minutes preceding the beginning of the adsorption are plotted, showing stable frequency and dissipation values. At t=3h30, the silane solution was replaced by a pure solvent solution, in order to accomplish the rinsing operation, and the data acquisition was continued for 10 minutes.

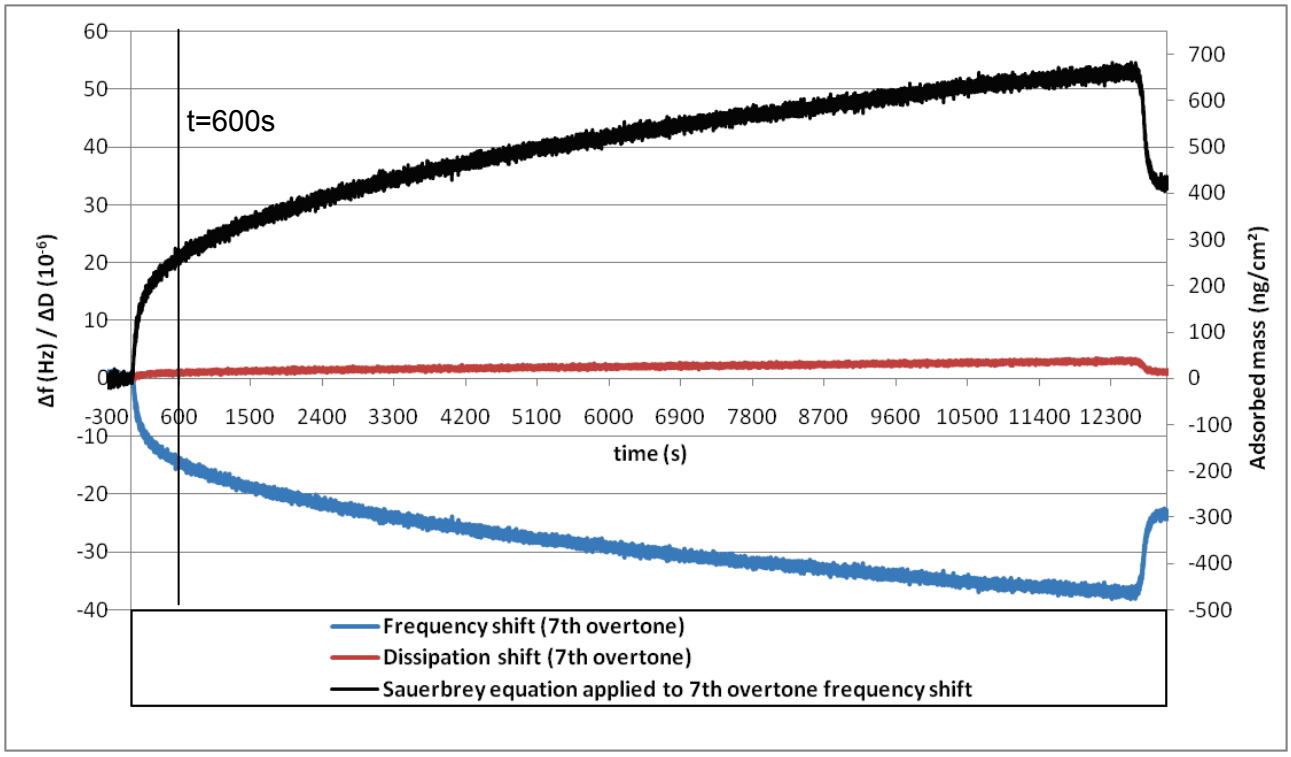

Figure III–3: 7th overtone Frequency and Dissipation shifts (primary vertical axis), and Sauerbrey modeling (secondary vertical axis) for the adsorption of 0.2% APDMES on a cellulose sensor, at a pH of 11.5, and a temperature of 45°C

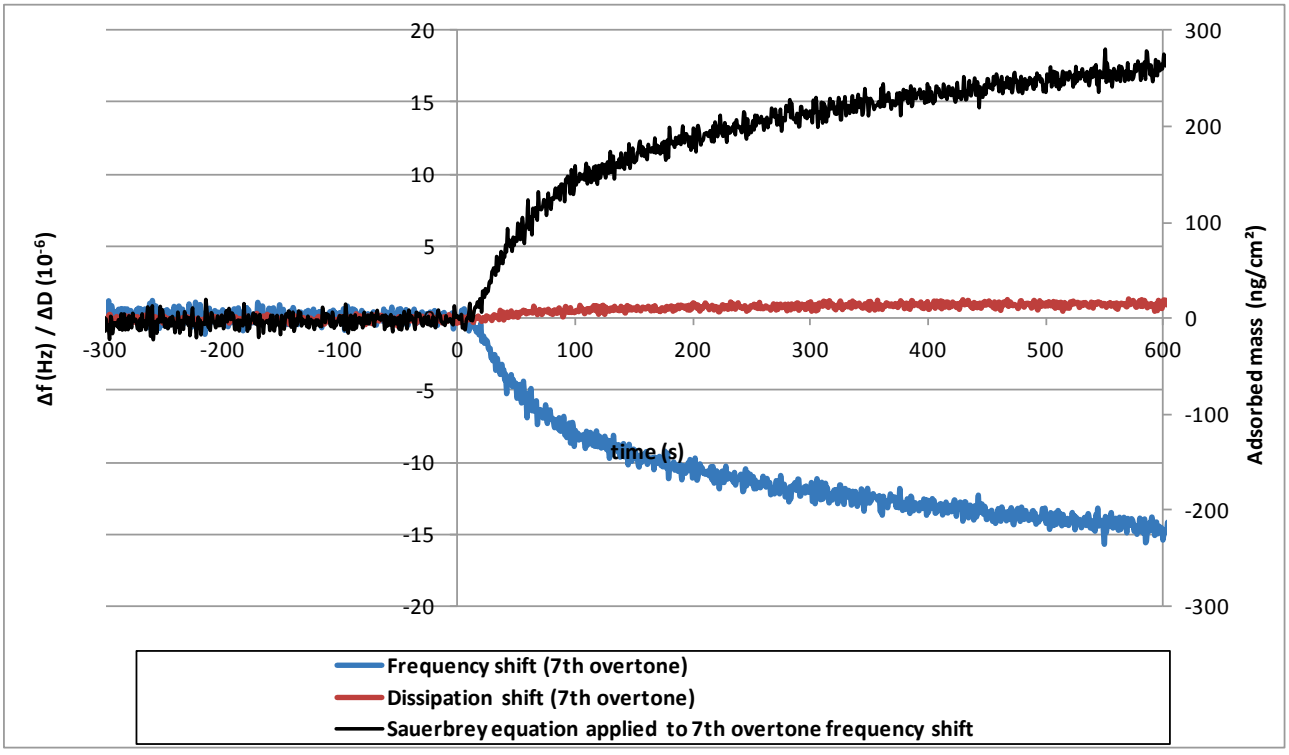

Figure III–4: Zoom on the -300s to +600s time period of Figure III–3.

As shown on Figure III–3, the adsorption of the silane on the cellulose is initiated very rapidly, as soon as the silane solution is in contact with the sensor, and the overtone frequency shifts rapidly to lower values. Besides, even though a very slight dissipation shift is observed, it is clearly negligible compared to the frequency shift. If we look at the overall shape of the frequency shift curve, it appears that an initial step of rapid adsorption occurs in the first few minutes of the experiment. This step lasts approximately 600s here (see the vertical line on Figure III–3), and at that time a value of 270 ng of silane adsorbed per square centimeter of substrate is reached. This zone of the curve is more clearly shown in Figure III–4.

After this rapid initial adsorption, more silane continues to adsorb on the sensor, in a less steep way, with a slope slightly decreasing over time. After 30mn and 3 hours, adsorbed amount values of 365 and 640 ng/cm² were reached, respectively. Concerning the dissipation, the shift increases in a more linear way compared to that of the frequency. It seems that some molecules of water are weakly attached to the amine moieties of the silane and plays a role in the amount of adsorbed product. However, the very small dissipation shifts clearly shows that the molecules are adsorbed in a very thin and uniform layer, thus indicating their small quantities and the negligible effect they may play.

Finally, the rinsing step initiated at t=12400s allowed to remove part of the silane adsorbed, but not all of it. According to this observation, it seems that at least one layer of silane is adsorbed on the model cellulose surface with rather strong interactions, whereas a part of the silane that adds over time is very weakly adsorbed onto the surface. In order to remove that more strongly attached silane, it was necessary to use ethanol solutions, as described in the method section above (data not presented here, due to the strong effect of the change in solution on the values measured).

The data treatment procedure presented here for a 0.2% APDMES solution in unmodified pH conditions at a temperature of 45°C was performed for all the other experiments related to APDMES adsorption onto cellulose surface. Thus it was possible to determine for each condition an estimated value of adsorbed silane per unit of surface over time, and the slope of the adsorption curve after the end of the initial adsorption. For the latter parameter, the adsorption values used were taken at t=700s, a time at which the initial step was finished under all experimental conditions, and at t=1800s. It was decided to use this latter value (i.e. 30 minutes) as a representative value of the contact time that we have used for modification of cellulose pulps by organosilanes.

All the curves representing the adsorption of APDMES on cellulose model surfaces under various conditions are given in Figure III–5, Figure III–6, Figure III–7, and Figure III–8, where the Sauerbrey modelings of the 7^{th} overtone frequency shift of each experiment are shown. More specifically Figure III–5 presents this modeling for three different concentrations, namely 0.1, 0.2, and 0.4% w/w, at room temperature, under acidic conditions. Figure III–6 shows the counterparts of

these data, under unmodified pH. And Figure III–7 and Figure III–8 present the experiments carried out at 45°C, under acidic and unmodied pH respectively.

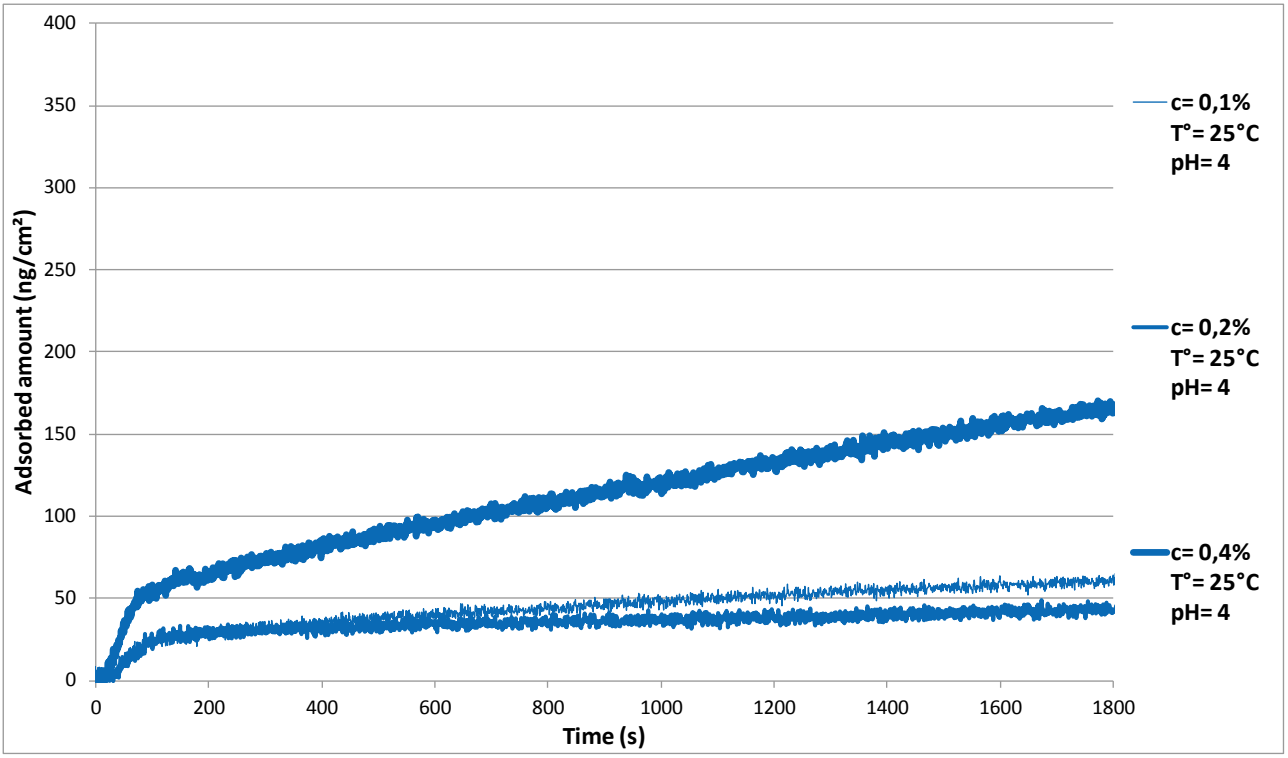

Figure III–5: Sauerbrey modeling of APDMES adsorption on cellulose sensors, under acidic pH, at 25°C.

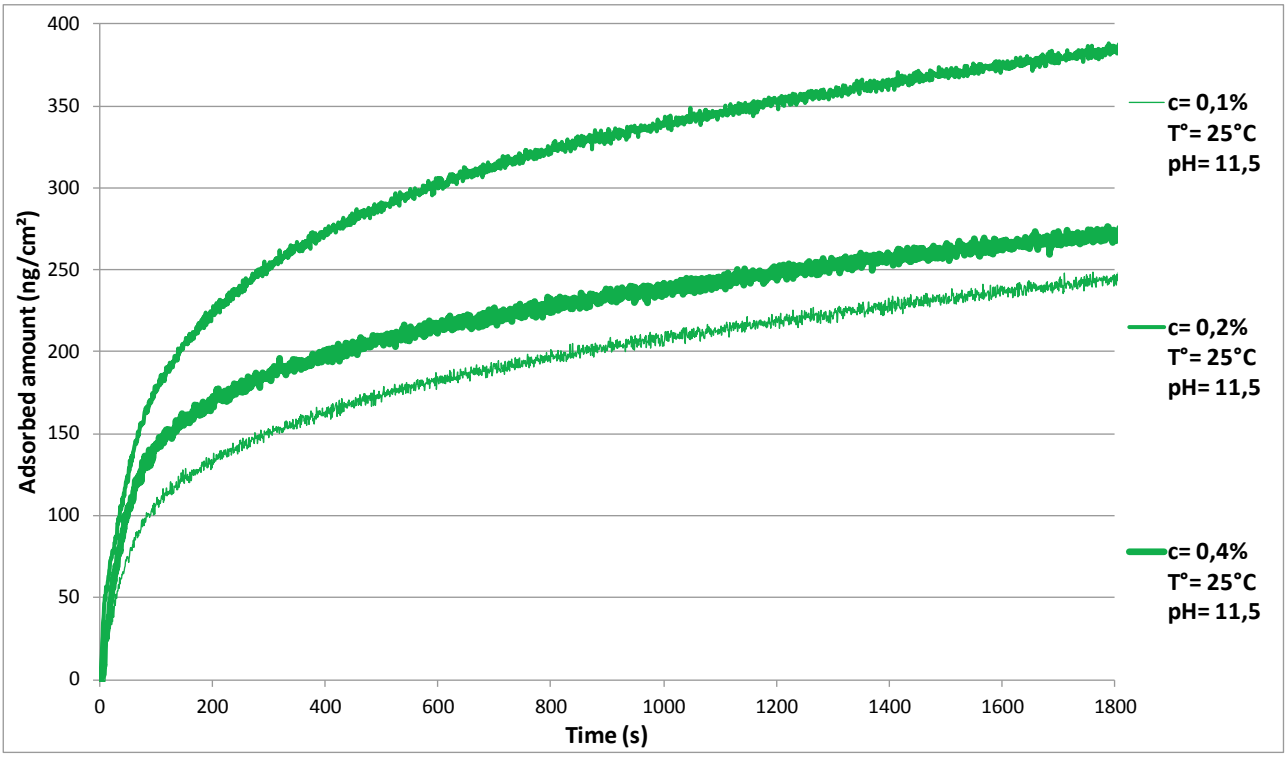

Figure III–6: Sauerbrey modeling of APDMES adsorption on cellulose sensors, under unmodified pH, at 25°C.

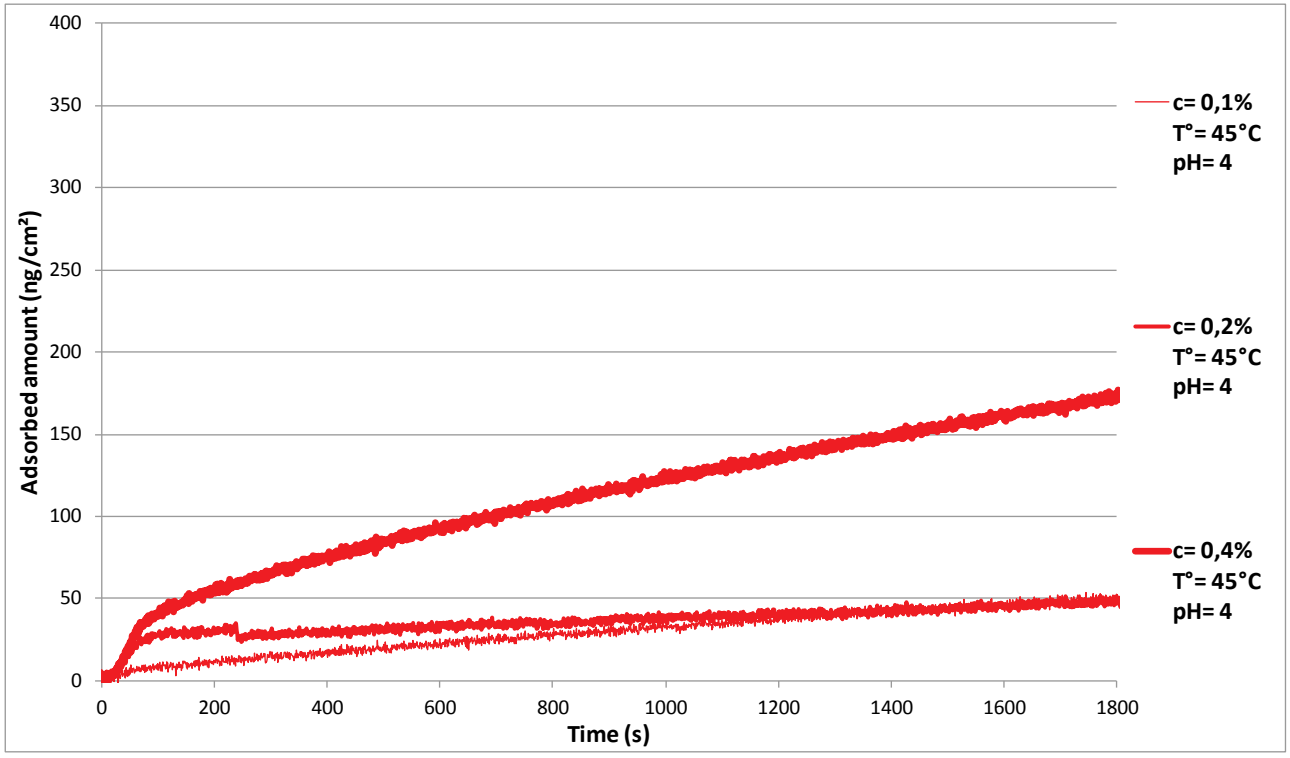

Figure III–7: Sauerbrey modeling of APDMES adsorption on cellulose sensors, under acidic pH, at 45°C.

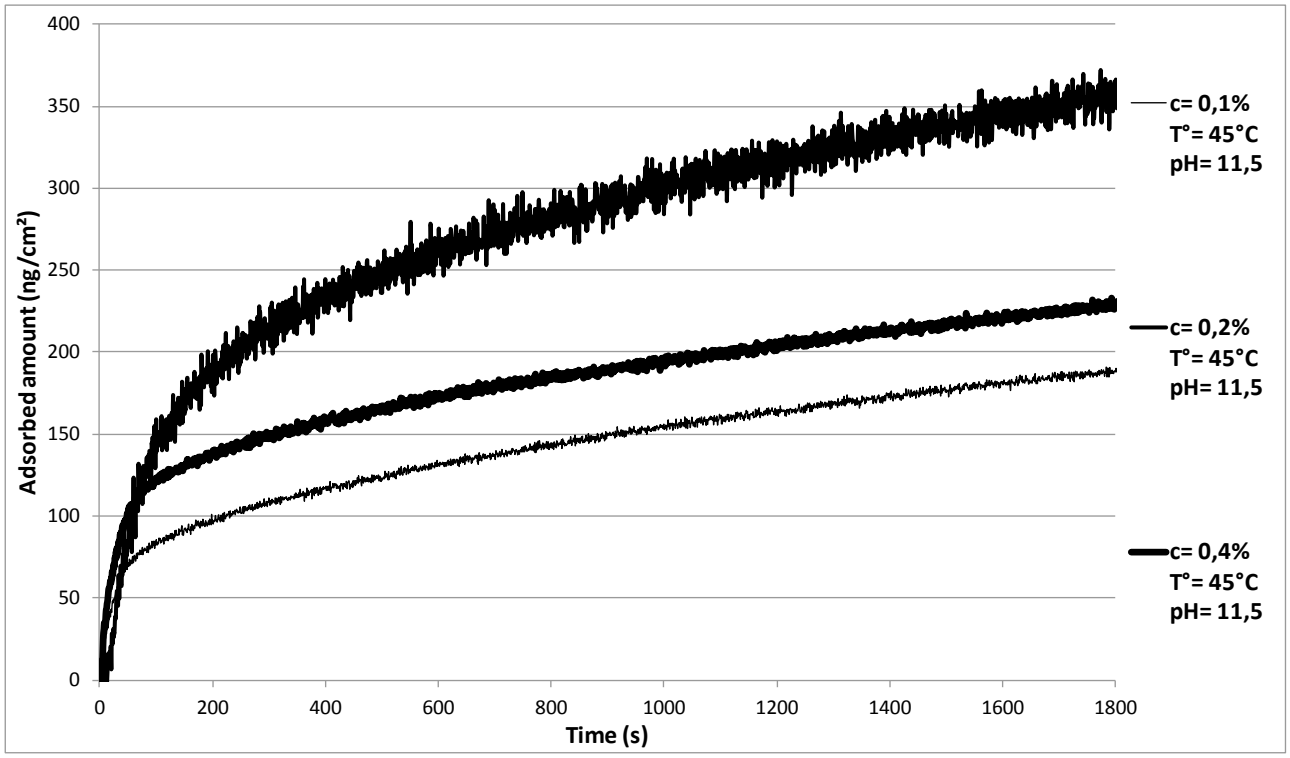

Figure III–8: Sauerbrey modeling of APDMES adsorption on cellulose sensors, under unmodified pH, at 45°C.

As exposed in these Figures, for all the conditions used here, the adsorption of APDMES onto cellulose started by a first rather quick step, followed by a slower but contineous increase in

adsorbed amount onto the surface. A first observation is that the most important factor impacting the amount of the adsorbed silane onto cellulose surface is the pH of the solution. Indeed, at pH=4 (Figure III–5 and Figure III–7), all the experiments reported here resulted in lower levels of adsorption than any experiment carried out at the pristine pH of the silane solution, namely 11,5. Actually, the experiments at pH 4 showed almost no impact of the temperature, and the differences between concentration of 0.1% and 0.2% were found to be not significant. At this pH, only the experiments carried out at 0.4% were found to result in a significantly higher adsorption, reaching values twice as high as the experiments at lower concentrations at the end of the initial adsorption, and up to three times higher after 30 minutes. The values of adsorbed mass reported in Table III-1, obtained from the experimental curves after use of the Sauerbrey equation, also show that the slope of the secondary adsorption is higher for experiments at 0.4%. In order to explain the lower adsorptions observed at low pH, it is necessary to remind the reader that the pH chosen here, is very close to the isoelectric point of cellulose [4], and that the cations (ammonium) formed after the addition of acetic acid into the medium are very likely to shield the negative charge of the cellulose surface.

At pH=11.5 (Figure III–6 and Figure III–8), different features are observed. Here, the temparature has an important impact on the amount of APDMES adsorbed. Increasing the temperature results in a lower level of adsorption, both at the end of the initial step, and after 30 minutes. Furthermore, the changes in concentration are more important, and an increase from 0.1 to 0.2% w/w in silane causes a sigificant increase in adsorption.

In addition, at this pH, an unexpected phenomenon is observed: the level of adsorption reached are higher at a concentration of 0.2% than at 0.4%, for both temperatures (This features does not appear clearly in Figure III–8 where the stronger noise/signal ratio of the experiment at 0.2% gives a false impression of increased line thickness.). This result was confirmed with repeated experiments. A possible explanation for such a feature is that at 0.4%, the competition between homo-condensation and adsorption is significantly increased, and since the condensed M^1 structures have no more silanols available for adsorption, they do not impact significantly the surface.

Table III-1 summarizes the data obtained for all the experiments on APDMES adsorption onto cellulose sensors described above. For each testing conditions, the mass of silane adsorbed (in ng per square centimeter of the sensor) is given at t_i, which corresponds to the end of the initial adsorption, and at t=30mn. The equivalent silane amount, calculated from the adsorbed mass, is also given in this table, in nmol/cm². A very important fact here is that the molar mass used for our calculations is not that of the pristine silane, but that of the hydrolyzed compound. Indeed, under the conditions used, our silanes coupling agents are completely hydrolyzed, and owing to the excess of water present, they are not expected to have undergone condensation reactions. Thus, the molar mass used for the hydrolyzed APDMES is: 133.26 g/mol.

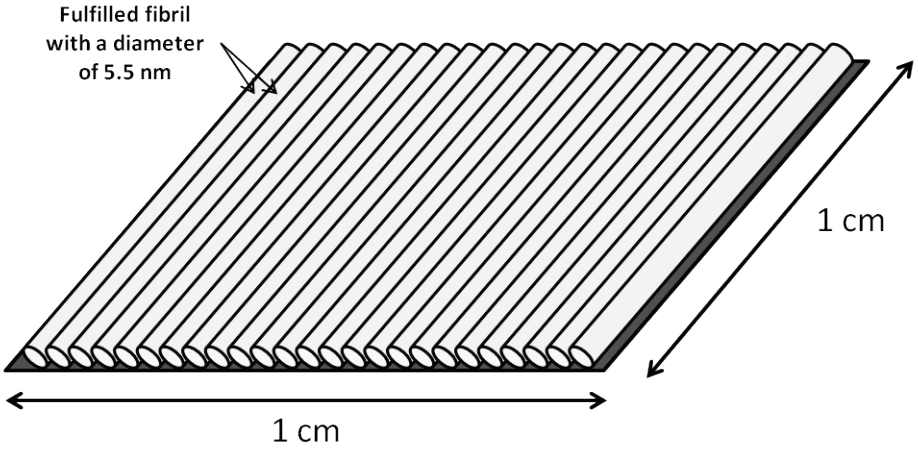

Figure III–9: Model representation of a unit surface area on the cellulose sensors surface.

In addition, for each adsorbed mass, another value is introduced, named the "Equivalent amount retained". This value corresponds to the mass of silane that would be retained on the surface of a typical cellulose pulp, with a specific area of 3 m²/g. In order to estimate this value, it is necessary to take into consideration the specific surface topography of cellulose sensors, which are made of cylinder shaped cellulose nanofibrils. Such sensors have a more important specific surface area than that of flat silica sensors. In order to evaluate this specific area, we have decided to use a simple model, where the cellulose fibrils are represented by perfect fulfilled cylinders aligned on the sensor surface, as depicted in Figure III–9. The diameter for these cylinders was set to 5.5 nm, since the cellulose fibrils used for the sensors coating have been reported to have diameters of 5 to 6 nm mostly [1]. The surface of the top and bottom of the cylinders was not taken into account; however we considered that the outer wall was completely accessible to our coupling agent. We obtain a specific surface area of 3.1416 cm² per square centimeter of sensor. So, in order to evaluate the amount retained on a typical pulp, we divide 3m² by these 3.1416 cm² and multiply this result by the amount of silane retained on 1cm² of the sensor at that time.

Necessary calculations were performed in order to present the result of our modeling as a mass of silane retained per gram of a typical pulp substrate ($mg_{silane}/g_{cellulose}$). The results presented in the table confirm the large differences in adsorption observed under varied pH conditions.

In addition, this table includes the slopes observed on our experimental curves after the initial adsorption. These values are representative of the kinetic of adsorption during this range of time of the experiment. As expected, these values are smaller under low pH conditions.

Temperature (°C)	*pH*	*Silane concentration (%)*	*Adsorbed mass at t_1 (ng/cm²)*	*Silane amount at t_1 (nmol/cm²)*	*Equivalent amount retained at t_1 (mg/$g_{cellulose}$)*	*Slope after initial adsorption*	*Adsorbed mass at t=30mn (ng/cm²)*	*Silane amount at t=30mn (nmol/cm²)*	*Equivalent amount retained at t=30mn (mg/$g_{cellulose}$)*
25°C	4	0,1	25	0,188	0,239	0,0166	61	0,458	0,583
		0,2	28	0,210	0,267	0,0103	46	0,345	0,439
		0,4	66	0,495	0,630	0,0575	165	1,238	1,576
	11,5	0,1	145	1,088	1,385	0,0508	245	1,839	2,340
		0,2	302	2,266	2,884	0,0576	384	2,882	3,667
		0,4	205	1,538	1,958	0,0482	273	2,049	2,607
45°C	4	0,1	7	0,053	0,067	0,0236	52	0,390	0,497
		0,2	30	0,225	0,286	0,0127	55	0,413	0,525
		0,4	50	0,375	0,477	0,0596	170	1,276	1,623
	11,5	0,1	105	0,788	1,003	0,0444	188	1,411	1,795
		0,2	230	1,726	2,196	0,0856	365	2,739	3,485
		0,4	160	1,201	1,528	0,0475	228	1,711	2,177

Table III-1: Key data on APDMES adsorption on cellulose model surfaces at varied pH, T°, and concentration

In order to confirm our approach, a second model was used. This model is based on a theoretical modelling of adsorption, from a geometrical point of view. In this approach, in order to evaluate the amount of silane corresponding to a complete mono-layer coverage of the surface, we used the software Marvin [5], and its geometry module, and calculated the molecular surface area covered by the grafted APDMES fragment. More precisely, we were interested in the projection area given by the software, which is obtained by calculating the molecular Van der Waals Surface Area (molecular VSA). The atomic Van der Waals Surface Area (VSA) surface corresponds to the surface obtained when considering the shape of each atom as a sphere where the radius is equal to the van der Waals's radius of the atom. When summing all the "available VSA" in a molecule, meaning the VSA which is not shared with another atom, the molecular VSA is obtained. The software provided two estimations of the projection area of the molecule, a minimum projection area and a maximum projection area, which for APDMES are equal to 29 and 48 square angstroms respectively. Based on the average from these values, equal to 38.5 square angstroms, we calculated the number of molecules needed to cover a square centimeter of a cellulose sensor surface (=3.1416 cm² as discussed above). Using the same method as for Table III-1, we estimated the theoritical amount of silane needed to complete a monolayer on one gram of a cellulose pulp having a specific area of 3m²/g, and found a value of 1.724 mg/$g_{cellulose}$.

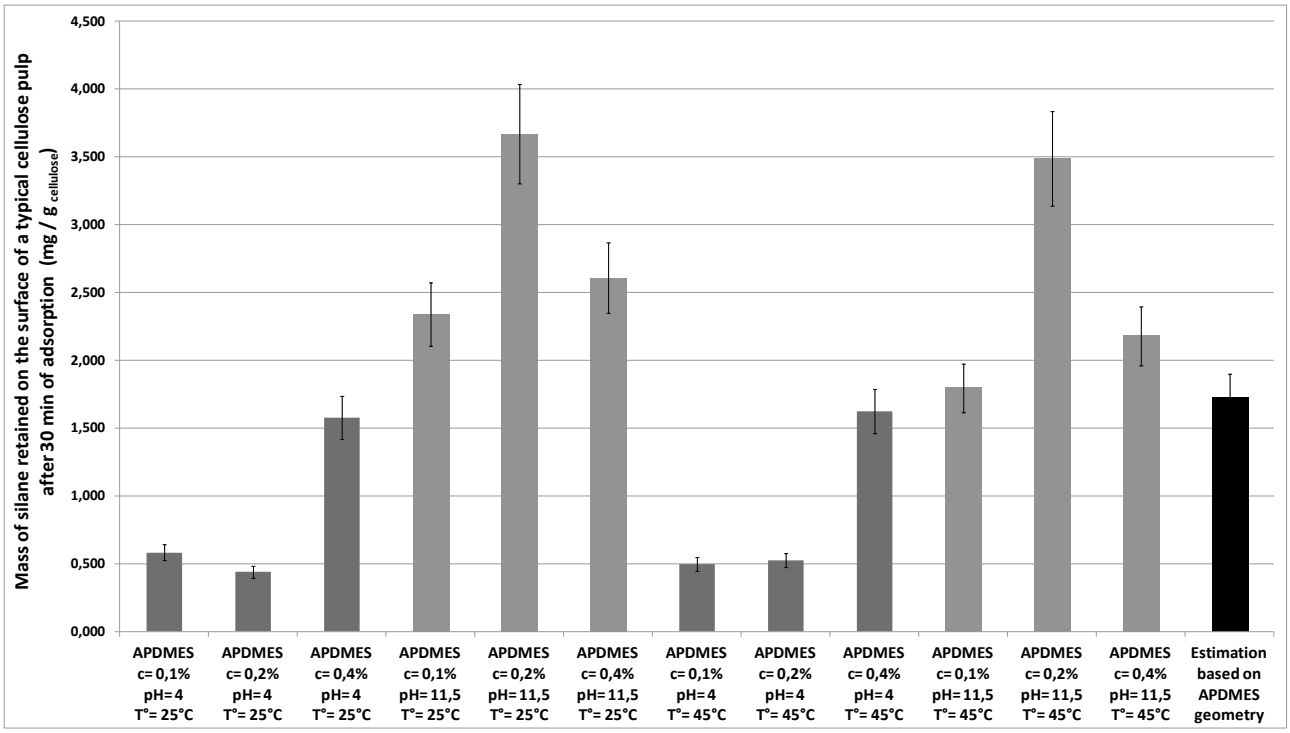

Figure III–10: Estimation of APDMES amount adsorbed on average cellulose fibers (with a specific area of 3m²/g) after 30mn according to QCM model data, and theoretical values based on geometry considerations.

The adsorption values obtained from our experimental data and from our geometry-based model are compared in Figure III–10, with standard deviations of 10% shown by error bars. These data confirm that the difference of adsorption at pH=4 for concentration of 0.1% and 0.2%, at both temperatures, are not significant. The adsorption level reached after 30mn for these experiments are much lower than the theoretical amount needed to build a monolayer on the surface. Under acidic conditions, only the experiments carried out with a concentration of silane of 0.4% allow reaching an adsorption equivalent to a monolayer after 30mn. For all the experiments carried out under alkaline conditions, the level of adsorption reached after 30mn is equivalent to, or above, the mass considered as necessary to fulfill a monolayer of silane. More particularly, at a concentration of 0.2%, it would seem that, after 30mn, already two layers are formed. In addition, it appears that at unmodified pH conditions, the differences observed between experiments at 25°C and at 45°C are barely significant. It shall be reminded that in all cases, the adsorption was shown to continue for durations much longer than the 30 minutes of our observation, and higher levels adsorb over time, leading to sufficient amount to cover the surface completely in all cases.

These are very encouraging findings, confirming that the approach we used with the QCM apparatus provides results comparable (in the same order of magnitude) to those of the theoretical approach.

As a conclusion, this part of the study focusing on the adsorption of APDMES on cellulose model surfaces investigated by mean of a quartz crystal microbalance has allowed the determination of optimized conditions for the adsorption of this compound. An increase in temperature was shown

to have a slightly negative impact on the adsorption, whereas the addition of acetic acid to the solution clearly affected negatively the adsorption. However, even though unmodified pH conditions are shown to favor the amount of compound adsorbed onto the surface, it shall be reminded that acidic conditions were shown to favor the reactivity of the silane solution over time.

The results obtained here on a mono-alkoxy aminosilane are very encouraging for the demonstration of the capacity of hydrolyzed silane solutions to modify the surface properties of cellulose. However, it is necessary to compare these data with those obtained for a polyalkoxysilanes, bearing amine functionalities as well, in order to be able to discuss the effect of the self-condensed structures on the adsorption. Also, since the amine function borne by the silane might play an important role in the adsorption observed, through the existence of hydrogen bonds with the hydroxyl moieties of the cellulose; it is also necessary to compare these results with those of a silane having a less reactive functional moiety.

III.A.3 Adsorption of DAMS on cellulose model surfaces

In addition to the work presented on APDMES, another aminosilane was studied by mean of QCM, namely DAMS, whose structure is recalled in Figure III–11. This trialkoxysilane has a functional moiety containing two amine functions, and also bears three hydrolysable groups, which were shown to hydrolyze very rapidly in presence of water. A very important difference between APDMES and DAMS is that the latter is able to form poly-condensed units, which are still reactive, whereas the former can only form dimers unable to graft onto cellulose.

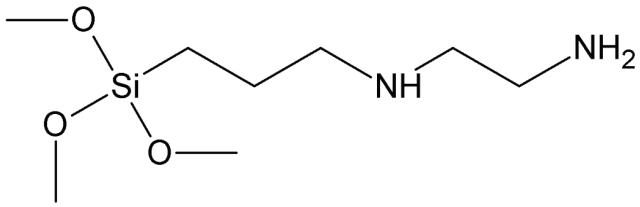

Figure III–11: DAMS structure

The adsorption curves obtained for DAMS adsorption on cellulose sensors, presented in Figure III–12 and Figure III–13, are very similar in shape to those obtained for APDMES. For all experiments, a fast adsorption was completed after periods of time ranging from 5 to over 10 minutes, and then more compounds adsorbed onto the surface with a slower rate. The main data for all the experiments carried out with DAMS onto cellulose sensors are given in Table III-2. Similar reaction conditions were used in terms of pH and temperature. However, regarding the concentration, no experiments were carried out at 0.1% for DAMS. Indeed, since it has been shown for APDMES that the difference between concentrations of 0.1 and 0.2% were not particularly significant, it was chosen to not perform these experiments here.

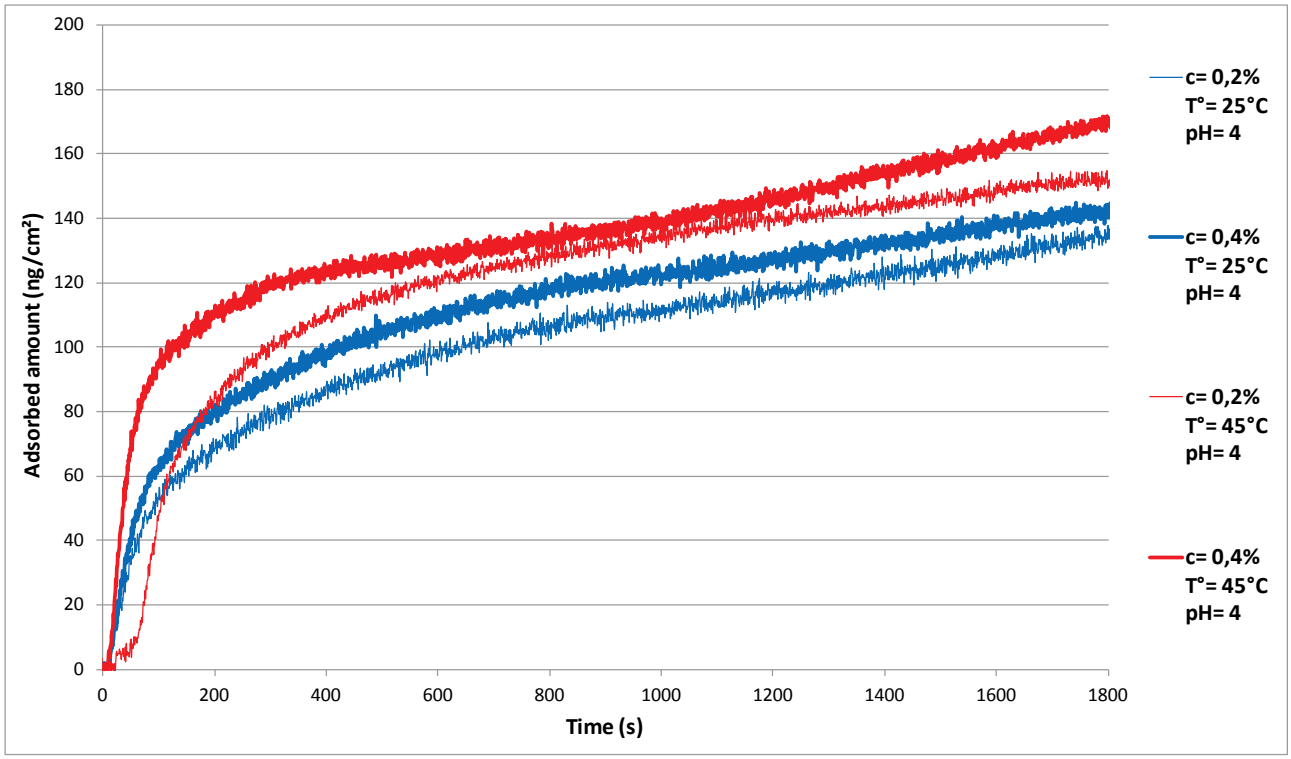

Figure III–12: Sauerbrey modeling of DAMS adsorption on cellulose sensors, under acidic pH, at 25°C and 45°C.

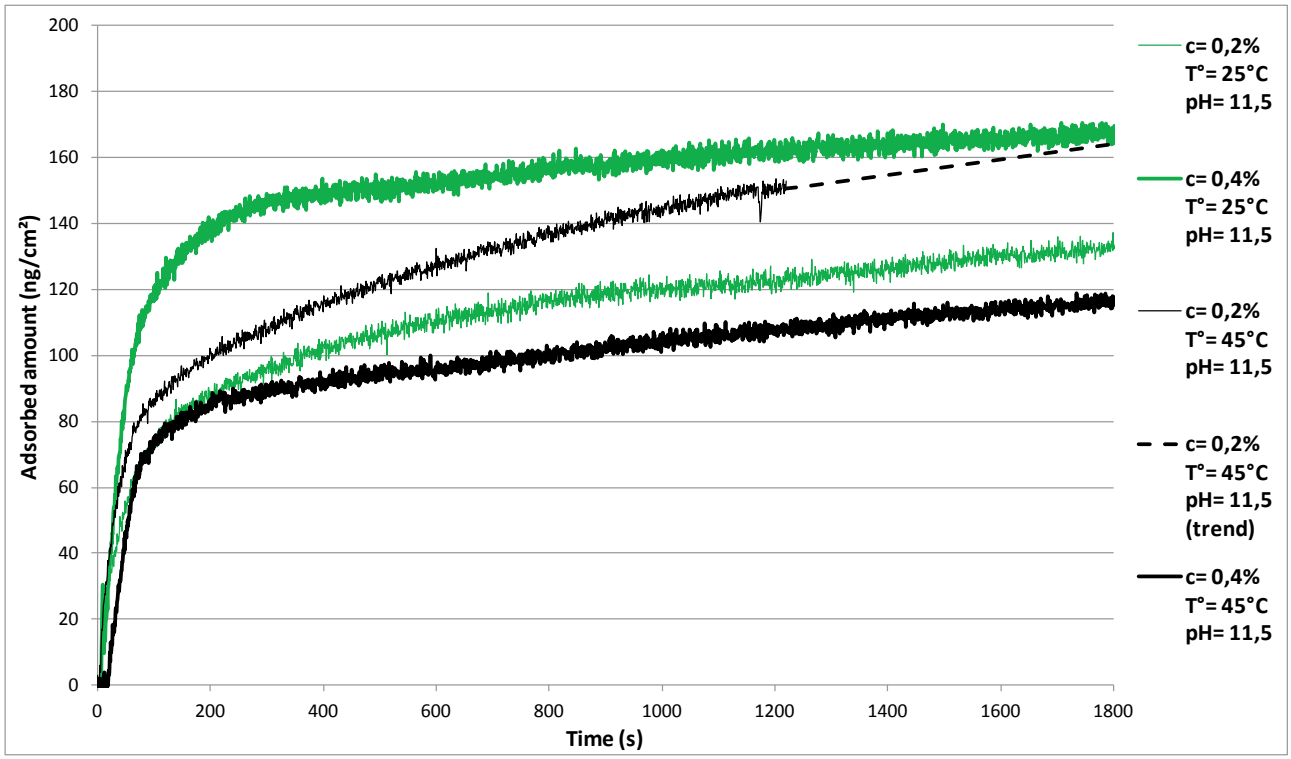

Figure III–13: Sauerbrey modeling of DAMS adsorption on cellulose sensors, under unmodofied pH, at 25°C and 45°C.

As shown by the data, after the initial adsorption step, the levels of adsorption reached are quite similar for most of the conditions used, with the exception of the experiments at 0.4% of silane, with a pH of 11.5, which showed a clear difference. At 25°C, the maximum of DAMS adsorption is obtained, whereas at 45°C the DAMS adsorption reached its minimum. In overall, at 25°C, higher amount are adsorbed at alkaline pH, whereas at 45°C, alkaline conditions give birth to lower adsorptions. This feature could be explained by the data obtained by NMR spectroscopy, which showed that in acidic conditions, self-condensation of DAMS-born silanols is limited compared to what is observed at the natural pH (alkaline) of the silane solution. Hence, the higher mass adsorbed under alkaline conditions at room temperature can be described through the adsorption of more condensed structures on the surface. At higher temperature conditions, it has been shown that the condensation reactions are greatly favored, causing the formation of more condensed structures whose reactivity is greatly diminished due to the lower amount of hydroxyls available, and the steric hindrance of such molecules. Thus, at this temperature the self-condensation might be more detrimental to the adsorption than at 25°C. Then, at higher temperature, the protective role of pH on self-condensation might prevent the formation of insoluble structures, and positively affect the level of silane adsorbed onto the sensor. The increase in concentration from 0.2% to 0.4% did not resulted in a significantly different level of adsorption for all experiments at pH=4, most likely due to the protonation effect on the amine, as discussed for APDMES.

Temperature (°C)	*pH*	*Silane concentration (%)*	*Adsorbed mass at t_1 (ng/cm²)*	*Silane amount at t_1 (nmol/cm²)*	*Equivalent amount retained at t_1 (mg/g $_{cellulose}$)*	*Slope after initial adsorption*	*Adsorbed mass at t=30mn (ng/cm²)*	*Silane amount at t=30mn (nmol/cm²)*	*Equivalent amount retained at t=30mn (mg/g $_{cellulose}$)*
25°C	4	0,2	96	0,533	0,917	0,0326	135	0,749	1,289
		0,4	103	0,571	0,984	0,0282	144	0,799	1,375
	11,5	0,2	110	0,610	1,050	0,0207	133	0,738	1,270
		0,4	144	0,799	1,375	0,0103	166	0,921	1,585
45°C	4	0,2	116	0,643	1,108	0,0274	160	0,888	1,528
		0,4	115	0,638	1,098	0,0336	171	0,949	1,633
	11,5	0,2	105	0,582	1,003	0,0398	165	0,915	1,576
		0,4	85	0,471	0,812	0,0154	115	0,638	1,098

Table III-2: Key data on DAMS adsorption on cellulose model surfaces at varied pH, T°, and concentration

The data were treated in a similar way as that presented in the previous section. The adsorbed mass, as well as the corresponding silane amount and the estimated amount of silane that would adsorb on a pulp having a specific area of 3m²/g are given in Table III-2. The hydrolyzed monomeric DAMS molecule used for our model, here, has a molar mass of 180.28 g/mol.

The slopes of the adsorption curves after the initial step are rather similar in acidic condition, independently on the concentration and the temperature. However, under alkaline conditions, for each temperature, the slope decreases at least by 50% when the concentration is doubled. We

suggest here that the rate of self-condensation, being increased with the concentration, is the responsible of this feature.

The theoretical amount of DAMS needed to form a complete mono-layer coverage of the surface was estimated using the same method as previously described. The minimum and the maximum projection area of the completely hydrolysed monomeric unit were found to be respectively equal to 27 and 59 square angstroms, and an average value of 43 square angstroms was used. We estimated the theoritical amount of silane needed to complete a monolayer on one gram of a typical cellulose pulp to be 2.089 $mg/g_{cellulose}$. However, this model does not take into account the existence of already self-condensed silanes potentially attached to the surface, which would have a much more important projection area (as an exemple, a dimer has a projection area ranging between 46 and 100 square angstroms).

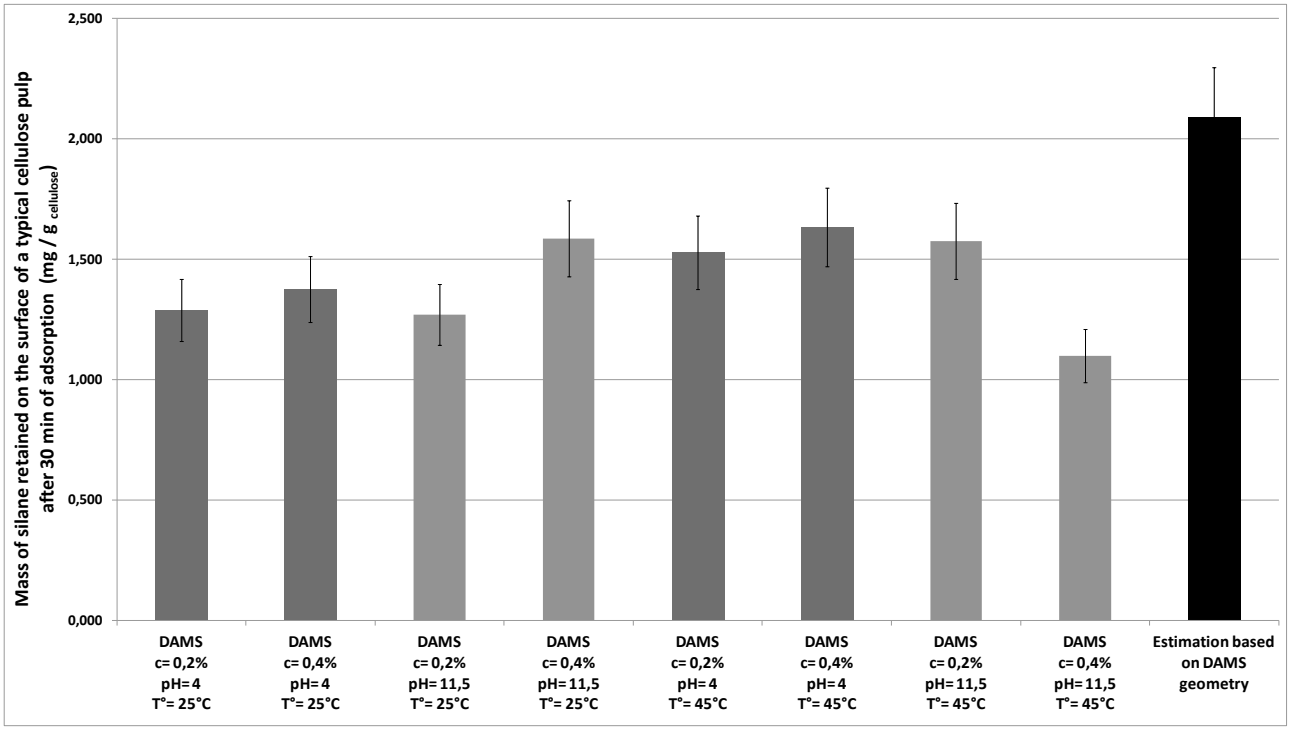

Figure III–14: Estimation of DAMS amount adsorbed on average cellulose fibers (with a specific area of 3m²/g) after 30mn according to QCM model data, and theoretical values based on geometry considerations

From the data presented in Figure III–14, it appears that for all the conditions tested, after 30mn of contact, the values obtained are very similar, and much more homogeneous than the values observed for APDMES. As indicated from the error bars, the difference of amount adsorbed between these different conditions are not clearly significant, and only qualitative observations arise. For all conditions, the mass of silane that would be retained on one gram of a typical cellulose pulp is slightly below the mass needed to cover the the surface with a monolayer, according to our model. As the adsorption continues after that period of time, it is expected that more silane adsorbs.

Thus, for this silane, we observe that a very wide set of parameters provides similar results in term of adsorbed mass. Nonetheless, this finding should be considered carefully, since it is possible

to adsorb similar masses of compound, from very different structures. Indeed, it is possible to form a full layer of silane units or dimers uniformly spread on the surface (condensation onto substrate), or to form a layer with a few polysiloxane attached (vertical polymerization) and contributing to the same mass, as sketched in Figure III–15. Since the first case presents a more homogeneous surface structure and composition, it is expected to be more favorable to modify the surface chemistry of cellulose fibers; hence, for DAMS, one shall gives preference to reaction conditions limiting the self-condensation, i.e. a lower temperature, limited concentration, and an acidic pH.

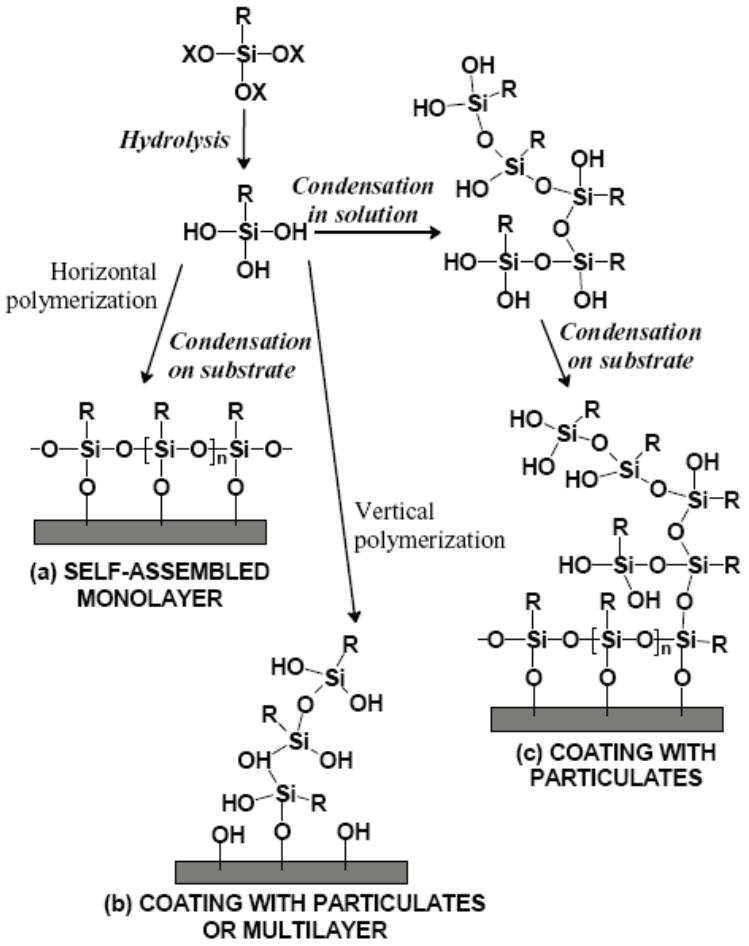

Figure III–15: Possible paths for polyalkoxysilane grafting. (Source : [6])

As a conclusion, the data exposed here show that a DAMS solution adsorbs readily onto a model cellulose surface, and that the dependance on pH, T and C is lower for this polyalkoxysilane compared to its monoalkoxysilane homologue. Thus, it appears that the self-condensation reaction, to which DAMS is subjected, impacts the nature of the layer of silane adsorbed onto the surface.

III.A.4 Adsorption of VDMES on cellulose model surfaces

In order to relieve the uncertainties raised by the presence of amine functions on APDMES and DAMS, on their adsorption behaviors, experiments were carried out on a monoalkoxysilane with a less reactive functional group. Our choice was set on VDMES, a vinyl-monoalkoxysilane, whose solubility in water was expected to be higher than alkyl-alkoxysilanes. However, the solubility of this compound was not sufficient to allow studying it by NMR in order to determine its kinetics of hydrolysis and self-condensation. Thus, we estimated that this compound might have reaction kinetics rather close to those of MVDES, a dialkoxysilane with one additional alkoxy substitution, which was studied by NMR in the previous chapter of this work. So, for experiments at the natural pH of the solution, at temperatures of 25 and 45°C, pre-hydrolysis times of 3 and 8 hours were applied respectively. For experiments at pH=4, no pre-hydrolysis was applied.

Experiments were carried out at concentrations of 0.2% and 0.4%, but even after a few hours of acquisition, no frequency shift could be detected at concentrations of 0.2%. Thus, only experiments at a concentration of 0.4% in silane are reported here.

As displayed in Figure III–16, the most important parameter influencing the adsorption of the silane on the sensor during the first period of the experiment is the pH. The data obtained from these curves are presented in Table III-3. For both experiments at the natural pH of the silane solution, i.e. pH=6, a very small amount (a few ng/cm²) of the compound adsorbs right after t=0, and then, nothing happens until t=600~800 seconds, when more compounds starts to adsorbs regularly onto the sensors surface over time, with a very slow kinetic. Most likely, this phenomenon is related to the time needed for the hydrolysis of the silane in the conditions used. It is possible that the durations of the pre-hydrolysis needed here has been underestimated, and that the moment at which the adsorption phenomenon starts indicates that the hydrolysis of the silane takes place in the medium. The temperature did not appear to be significant here, however it should be reminded that at 45°C, the duration of pre-hydrolysis was shortened from 8 h to 3 hours, thus even though the curves seems to match perfectly, the kinetics are not strictly similar; nonetheless, the adsorption rate are found to be rather similar after the moment the adsorption starts.

At pH=4, the features observed are very similar to those observed for APDMES and DAMS. A short period of fast adsorption is followed by a continued adsorption with a slow rate. The levels of adsorbed amount of silane attained after the initial adsorption step are similar at both temperatures. However at 45°C, the adsorption rate after the initial period is found to be more important than that reached at 25°C.

After 30 minutes of adsorption, the amount retained on the sensor varies, from slightly above 20 ng/cm² under unmodified pH, to as much as 40, and 70 ng/cm² under acidic pH conditions, as detailed in Table III-3.

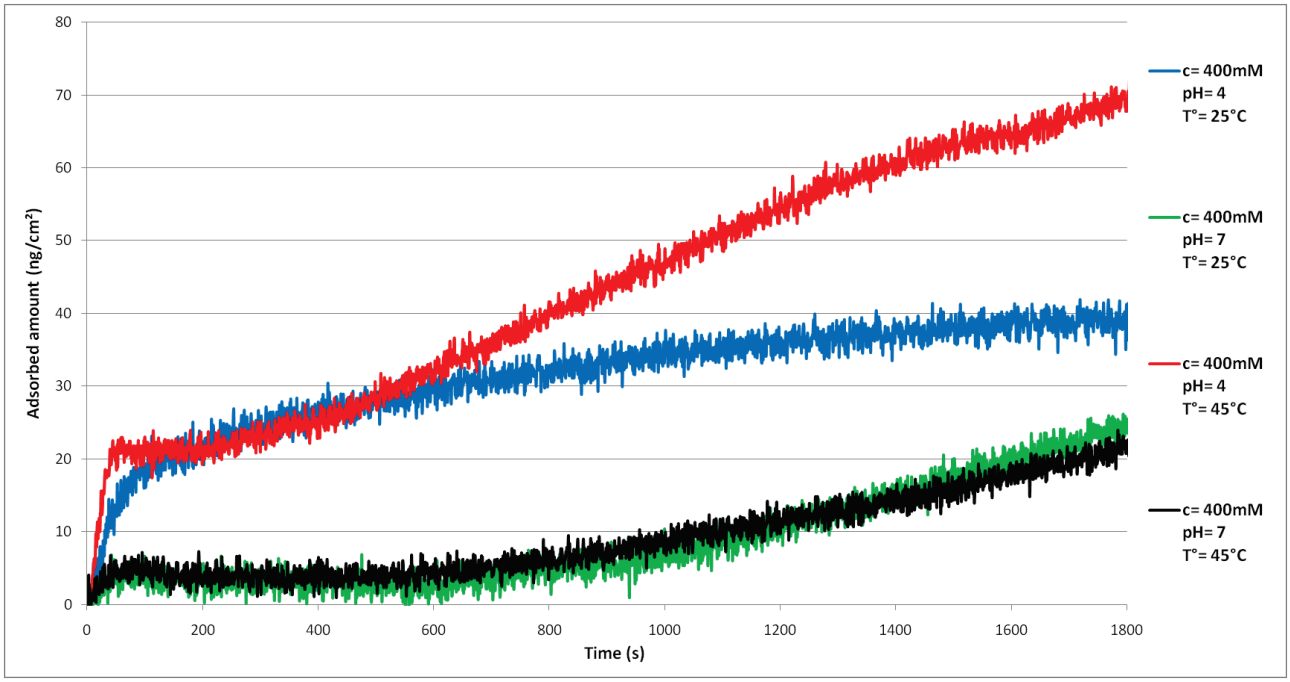

Figure III–16: 7th overtone Sauerbrey modeling for all experiments on VDMES adsorption on cellulose sensors.

Temperature (°C)	*pH*	*Silane concentration (%)*	*Adsorbed mass at t_1 (ng/cm²)*	*Silane amount at t_1 (nmol/cm²)*	*Equivalent amount retained at t_1 ($mg/g_{cellulose}$)*	*Slope after initial adsorption*	*Adsorbed mass at t=30mn (ng/cm²)*	*Silane amount at t=30mn (nmol/cm²)*	*Equivalent amount retained at t=30mn ($mg/g_{cellulose}$)*
25°C	4	0,4	22	0,215	0,210	0,0075	40	0,391	0,382
	11,5	0,4	3	0,029	0,029	0,0200	24	0,235	0,229
45°C	4	0,4	20	0,196	0,191	0,0305	70	0,685	0,668
	11,5	0,4	5	0,049	0,048	0,0163	22	0,215	0,210

Table III-3: Key data on VDMES adsorption on cellulose model surfaces at varied pH, and temperature

The minimum and the maximum projection area of hydrolysed VDMES were estimated by software analysis to be respectively equal to 28 and 34 square angstroms. Thus, the theoretical amount of VDMES needed to form a complete mono-layer coverage of the surface of a cellulose pulp with a specific area of 3m²/g was estimated at a value of 1.642 $mg/g_{cellulose}$. That model value is compared to those from experimental data in Figure III–17.

For all conditions, it appears that after a contact time of 30 minutes between the substrate and the silane solution, the amount adsorbed are very low in comparison to that estimated to be necessary for the formation of a monolayer. The low amount of silane adsorbed onto the surface from VDMES, in comparison to APDMES, clearly show that the amine function of the latter plays a very important role in its adsorption. However, the data presented in this section confirm that even hydrolyzed silanes with very low reactivities adsorb readily onto cellulose in purely aqueous media.

Even though the rather small amount of coupling agent retained indicates that the affinity between the adsorbate and the adsorbent is not very high, these experiments confirm that it is necessary for an alkoxysilane to be hydrolyzed to adsorb readily onto cellulose [7], and that at acidic pH the adsorption kinetic of such compounds is enhanced.

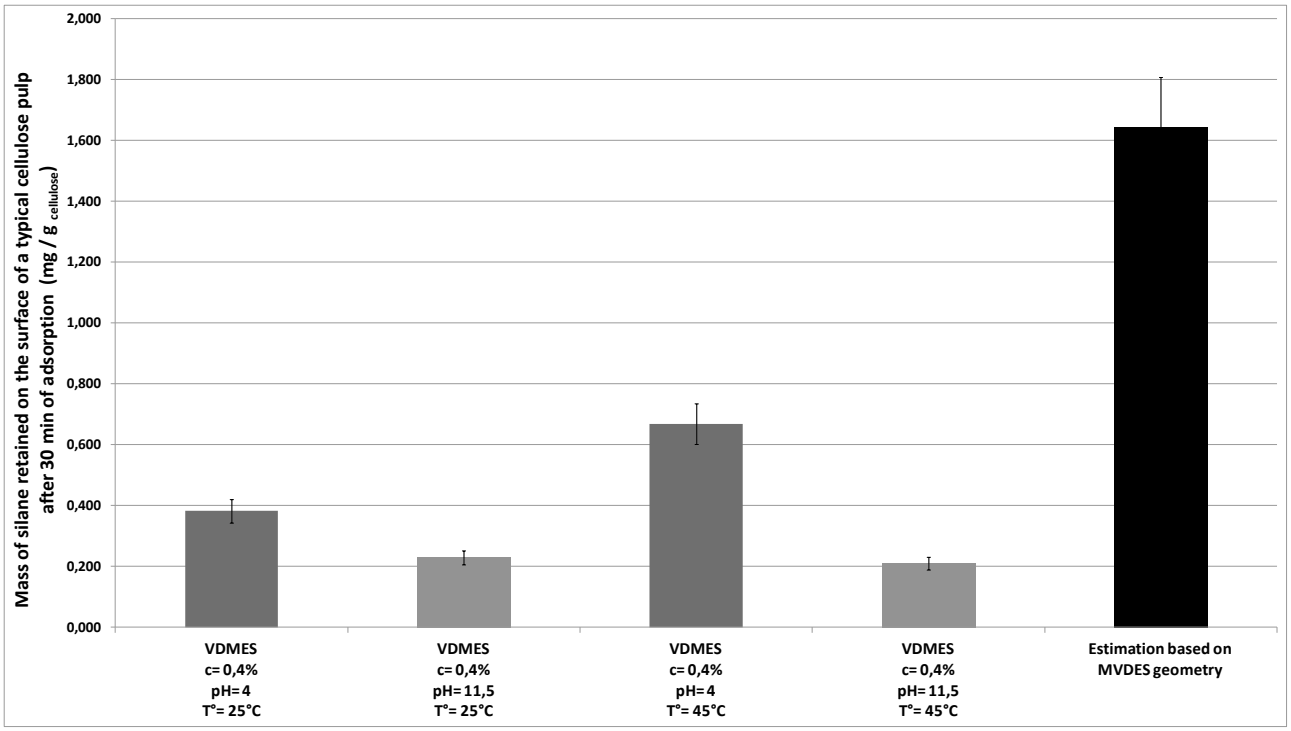

Figure III–17: Estimation of VDMES amount adsorbed on average cellulose fibers (with a specific area of 3m²/g) after 30mn according to QCM model data, and theoretical values based on geometry considerations

III.A.5 Influence of the silane structure on the adsorption onto cellulose

The estimated levels of silane adsorbed on regular cellulose fibers after 30 minutes of contact between the surface and the solution for our three silanes are compared in Figure III–18.

An overview of this figure shows that APDMES is the molecule for which the highest adsorbed amounts are obtained, under most conditions, whereas it would be expected that a higher mass of DAMS would be retained. Nonetheless, both APDMES and DAMS present more important amount of silane retained than VDMES. Which is in agreement with our postulate that the amine functions, borne by the formers coupling agents, act in favor of their adsorption onto cellulose surfaces.

Regarding the general features of each silane, it is observed here that the values obtained for APDMES span over a wide range, i.e., from about 1.5 to over 2.5 mg of silane per gram of substrate. On contrary, for DAMS, the values are contained into an interval going from about 1.1 to slightly over 1.6 mg/g. For VDMES, very few experiments could be carried out, it is therefore difficult to compare it with other silanes, but from the data obtained, it seems that rather large

difference are observed between the different conditions. Thus, it would be interesting, for future studies, to compare the difference of adsorption levels between mono-, di- and trialkoxysilanes, with similar functionalities, in order to determine if the ability of a silane to form small polymeric structures affects the extent to which its adsorption can vary under different conditions.

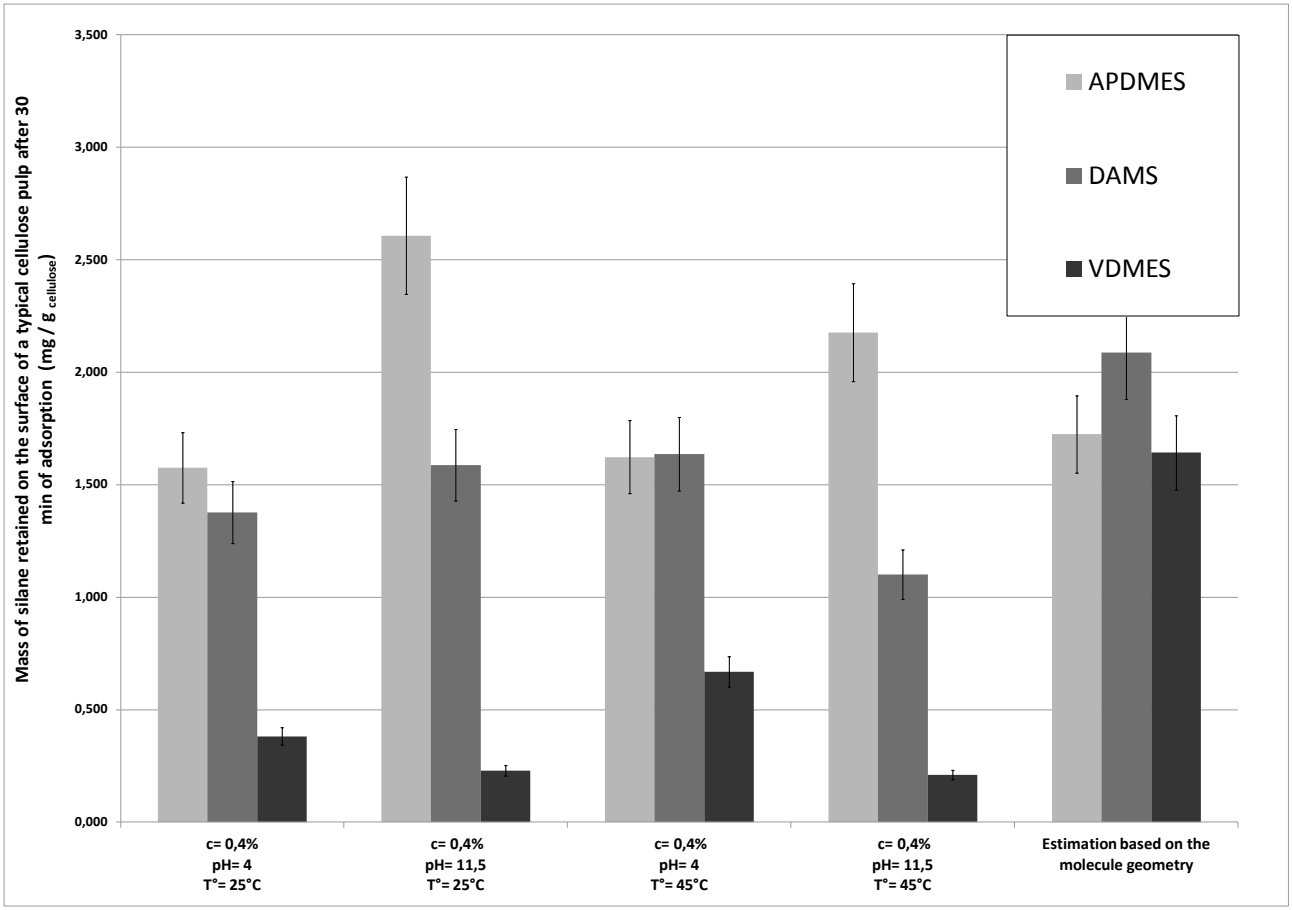

Figure III–18: Estimation of the amount of silane adsorbed on typical cellulose fibers after 30mn at a concentration of 0.4% under varied pH and temperature conditions for APDMES, DAMS and VDMES.

For all the experimental values presented here, it is reminded that they were discussed based on a model representation of the cellulose sensors surface. This model is based on an extreme condition, since we consider perfectly arranged rigid cylinders as the fibrils. However, the fibrils are more likely to be more flexible than rigid cylinders, and their arrangement might not be as perfect. Also, we considered the whole area of the cylinders sides in our model, whereas it is likely that fibrils are in contact with each other, with the area in contact being slightly swollen by water, thus forming a dense gel-like structure not available for adsorption. If these considerations better fit reality, then the value taken as the specific surface area of the cellulose sensors (3.1416 $cm^2_{cellulose}/cm^2_{sensor}$) has been overestimated. As a consequence, the amount of silane retained would be underestimated. Nonetheless, this impacts the discussion regarding the formation of a complete monolayer or eventually multilayers, but it has no impact on the comparisons discussed between different conditions of adsorption, or between molecules.

In overall, for the experiment where the highest amount of silane was retained (APDMES, 0.2%, 25°C, under unmodified pH), an amount of 0.028 mmol of silane, per gram of substrate, would be retained on a typical pulp. However, this amount only concerns the amount of silane retained onto the surface, measured on cellulose nanofibrils which have a very close surface, and no porosity. On a typical pulp where the surface is porous, such small coupling agents are expected to penetrate the surface and be retained in the fiber as well as on its surface. Thus, the amount of silane necessary to modify such pulps shall be considered as much higher than that value. Also, since most modifications made in this work are performed at a pulp concentration of 10g/L, it is likely that the concentrations in silane shall be kept close to a few mmol/L at least.

III.B Silane adsorption onto silica sensors

In order to compare the data obtained onto model cellulose surfaces with another hydroxyl bearing surface, silica sensors were used as a model surface. A few experiments were carried out on APDMES and DAMS, however the number of experiments had to be limited, since the silica sensors were shown to be highly sensitive to the pH of the solution. In particular, it was shown that, at the natural pH of the aminosilane solutions, the silica was attacked and that the surface degraded over time, which resulted in an increase of frequency partially compensating the negative frequency shift due to the silane adsorption, as exposed in Figure III–19. Thus, it was decided to focus only on the experiments carried out under acidic conditions (pH=4), and at 25°C. For both silanes, concentrations of 0.1, 0.2 and 0.4% were evaluated.

The adsorption curves obtained from these experiments were found to be quite similar to those presented on cellulose, at the initial times of the kinetic. In each case, a fast initial adsorption step occurred at the very beginning of the experiment. However, unlike on cellulose surfaces, a plateau was reached after that initial step, and almost no further adsorption occurred, for both silanes.

The estimated amount of silane adsorbed after 30 minutes on regular cellulose fibers are exposed in Figure III–21. Since the silica surfaces used on the sensor are supposedly perfectly flat (AT-cut crystals), the specific area of these sensors is not modified. Unlike that of cellulose coated sensors, which we considered to have a specific surface area of 3.1416 cm^2/cm^2_{sensor}, as detailed previously. That difference in specific surface area has been taken into account for the values presented in this figure. For DAMS, as the experiments at 0.1% onto cellulose sensors were not carried out for reasons previously described, the differences of response between the different sensors can be compared for only two concentrations.

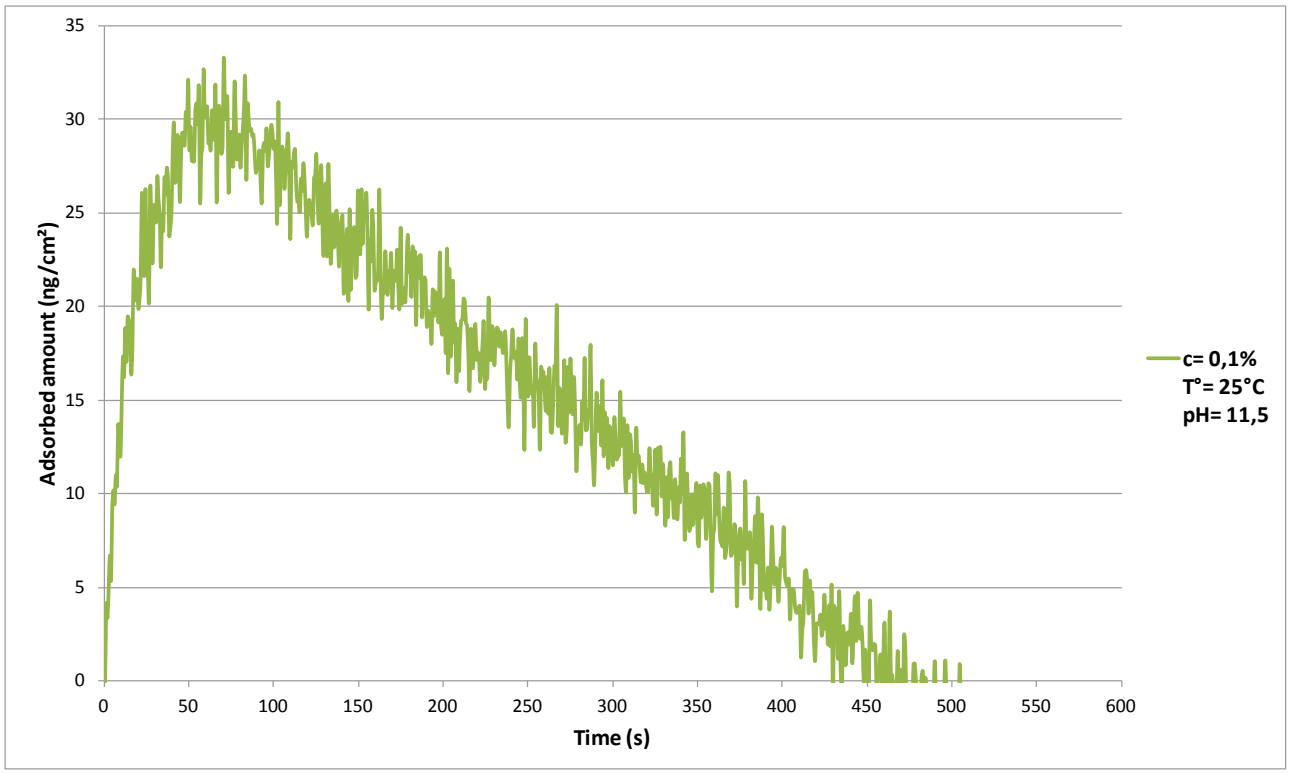

Figure III–19: Example of an adsorption curve obtained for APDMES on silica quartz, under unmodified pH.

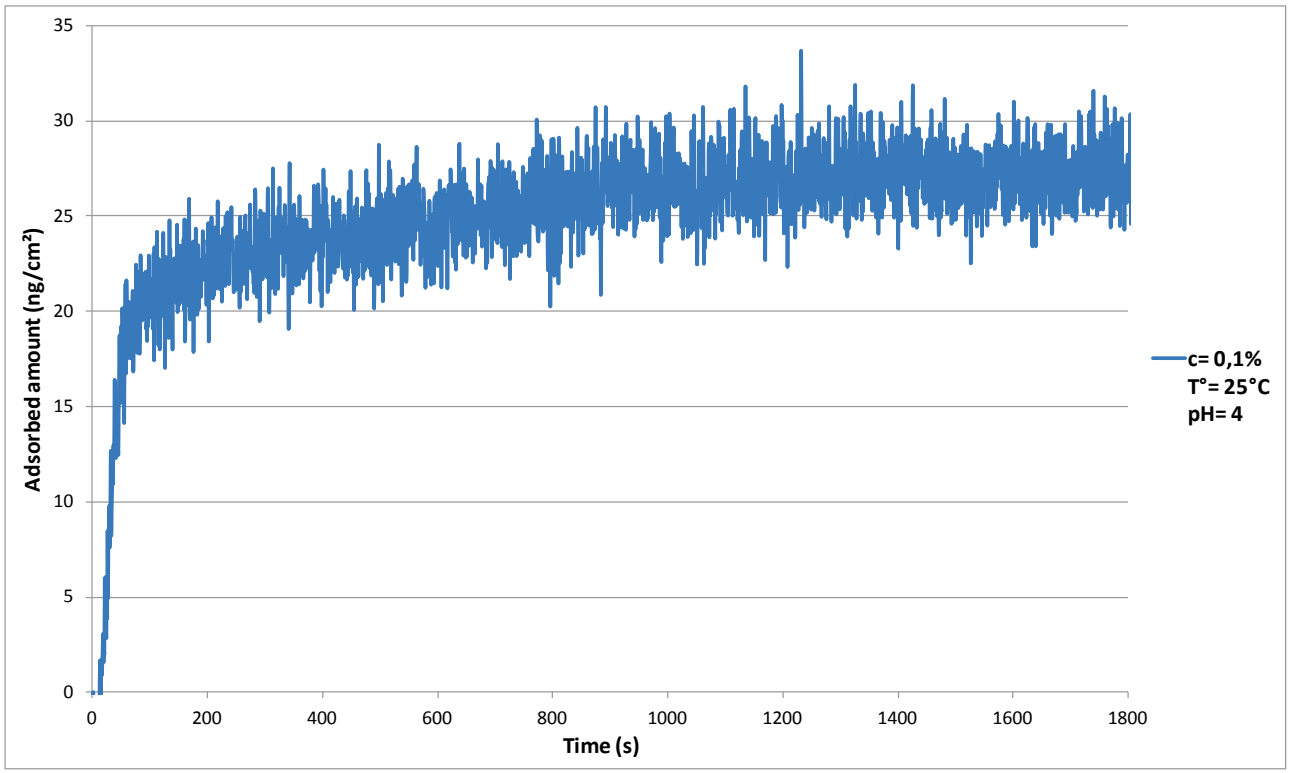

Figure III–20: Example of an adsorption curve obtained for APDMES on silica quartz, under acidic pH.

The first observation is that for all experiments, the values obtained on the two substrates are of similar magnitude, thus confirming that silanes adsorb on both OH-rich surfaces in similar ways. However, the amounts adsorbed on silica are systematically higher than those adsorbed onto cellulose. Two explanations can be proposed for this feature. First, it is possible that the specific surface area retained for the cellulose sensors has been over-estimated, thus impacting negatively the evaluation of the amount of silane retained on this substrate. Or, the affinity of the silane coupling agents toward the more acidic silica hydroxyls [7] could impact the adsorption onto these surfaces, as compared to cellulose. The differences in adsorption observed are more important for DAMS than for APDMES.

Another remark is that for silica sensors, the amount of silane retained increases clearly with the solution concentration, for both silanes. Unlike what was observed for APDMES on cellulose, where an increase to 0.4% can lower the adsorption under certain conditions.

Actually, the most significant difference between the two surfaces might be the fact that onto cellulose, the adsorbed amount continues to rise, a phenomenon which was not detected on silica substrate. To explain this feature, we propose to take the structure of cellulose into account. Indeed, whereas silica is a crystalline material, cellulose is an organic polymeric material. Even though the fibrils used for the sensors preparation are not porous like fiber walls, it is known that they adsorb water. Thus, indicating that a certain level swelling occurs. Hence, we propose that this difference in behavior comes from the adsorption of more water, or silane, penetrating into the cellulose layer structure gradually over time.

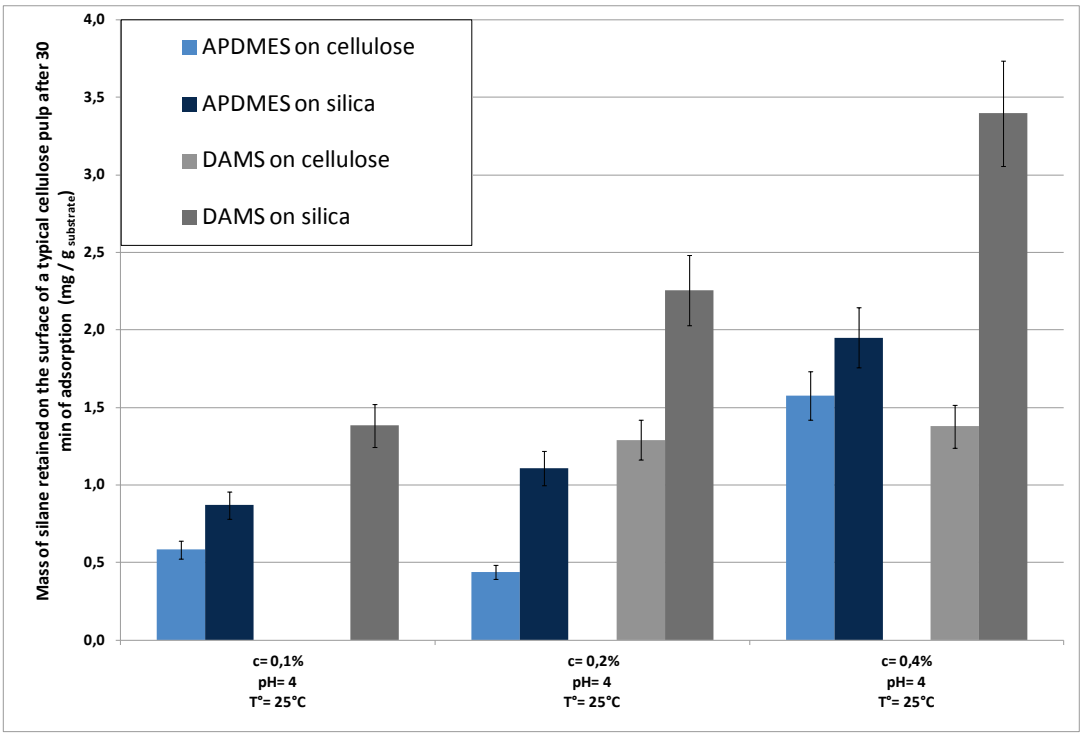

Figure III–21: Comparison of the estimated amount of silane adsorbed on typical cellulose fibers after 30mn for APDMES and DAMS, based on measurements on cellulose and on silica surfaces.

IV. Conclusions and perspectives

As a conclusion, we shall remark that the work exposed here is very original, since to the best of our knowledge, the *in-situ* measurement of organosilanes adsorption onto cellulose has never been reported previously.

Indeed, the approach presented here had been helpful in determining the kinetics and the extent of the adsorption of three different silanes onto cellulose model surfaces. It was shown unambiguously that hydrolyzed silanes adsorb onto cellulose fibers, within a few minutes of contact time between purely aqueous silane solution and the surface. Furthermore, this result was extended to model silica surfaces. Also, the effect of different parameters, namely the concentration, the temperature and the pH, was discussed. And it was shown that the studied silane molecules behaved differently depending on their functional moiety and the number of their hydrolyzable groups.

Finally, the experimental values obtained from our analyses were compared with a simple theoretical model, built in order to establish the amount of molecules needed to provide a complete surface coverage. Also, the results presented here indicate that pulp modifications (at a pulp concentration of 10g/L) should be carried out with silane concentrations close to a few mmol/L.

List of references

[1] M. Pääkkö, M. Ankerfors, H. Kosonen, A. Nykänen, S. Ahola, M. Österberg, J. Ruokolainen, J. Laine, P. T. Larsson et T. Lindström, « Enzymatic hydrolysis combined with mechanical shearing and high-pressure homogenization for nanoscale cellulose fibrils and strong gels », *Biomacromolecules*, vol. 8, n°. 6, p. 1934-1941, 2007.

[2] S. Ahola, P. Myllytie, M. Österberg, T. Teerinen, et J. Laine, « Effect of polymer adsorption on cellulose nanofibril water binding capacity and aggregation », *BioResources*, vol. 3, n°. 4, p. 1315-1328, 2008.

[3] C. Guézénnec, « Master Thesis : Study of the modification of cationic starch by organosilanes and its product adsorption on cellulosic substrates », Grenoble, 2009.

[4] J. C. Roberts, *Paper chemistry*. Chapman & Hall, New-York, USA: Blackie, 1996.

[5] « Marvin – ChemAxon – Toolkits and desktop applications for cheminformatics ». [Online]. Available: http://www.chemaxon.com/products/marvin/. [Accessed: 14-juin-2011].

[6] A. M. Almanza-Workman, S. Raghavan, P. Deymier, D. J. Monk, et R. Roop, « Aqueous silane-surfactant co-dispersions for deposition of hydrophobic coatings onto pre-oxidized polysilicon », *Colloids and Surfaces A: Physicochemical and Engineering Aspects*, vol. 232, n°. 1, p. 67-75, 2004.

[7] M. Castellano, A. Gandini, P. Fabbri, et M. N. Belgacem, « Modification of cellulose fibres with organosilanes: Under what conditions does coupling occur? », *Journal of Colloid and Interface Science*, vol. 273, n°. 2, p. 505-511, 2004.

Part 3: Silane-cellulose interaction

Table of contents

List of figures - 134 -
List of tables - 135 -
I. Literature review - 136 -
I.A Cellulose fibers chemical modifications - 136 -
I.B Cellulose fibers modifications by organosilanes - 137 -
I.C Surface modifications characterization - 138 -
List of references - 142 -
II. Materials and Methods - 145 -
II.A Materials - 145 -
II.B Methods - 146 -
III. Results and Discussion - 149 -
III.A Development of a suitable extraction method - 149 -
III.B Multi-scale characterization of the silane-cellulose interface - 152 -
III.C ToF-SIMS study - 160 -
IV. Conclusions and perspectives - 178 -
List of references - 179 -

List of figures

Figure II–1: Experimental drying set-up. - 147 -
Figure III–1: Structure of APDMES. - 149 -
Figure III–2: SEM-EDX: Comparison of organic solvents for APDMES removal by ASE, after thermal treatment. - 150 -
Figure III–3: SEM-EDX: Comparison between ASE and classical Soxhlet extraction for the removal of freshly deposited APDMES. - 150 -
Figure III–4: SEM-EDX: Comparison between ASE and Soxhlet extraction for APDMES removal after thermal treatment. - 151 -
Figure III–5: SEM-EDX characterization for the APDMES sample series. - 153 -
Figure III–6: SEM-EDX characterization for the VDMES sample series. - 154 -
Figure III–7: SEM-EDX characterization for the DAMS sample series. - 154 -
Figure III–8: ^{29}Si CP/MAS Solid NMR spectra for APDMES modified fibers. - 156 -
Figure III–9: ^{29}Si CP/MAS Solid NMR spectra for VDMES modified fibers. - 156 -
Figure III–10: ^{29}Si CP/MAS Solid NMR spectra for DAMS modified fibers. - 157 -
Figure III–11: XPS spectrum of the reference unmodified sample. - 158 -
Figure III–12: XPS spectrum of APDMES treated fibers. - 158 -
Figure III–13: ToF-SIMS spectra in the positive ion mode (m/z=0 to 200) of (A) Savoyeux sample; (B) Pristine fibers handsheet; (C) APDMES modified fibers handsheet. - 162 -
Figure III–14: ToF-SIMS spectra in the negative ion mode (m/z=0 to 200) of (A) Savoyeux sample; (B) Pristine fibers handsheet; (C) APDMES modified fibers handsheet. - 163 -
Figure III–15: ToF-SIMS spectra in the positive ion mode (m/z=0 to 200) of (A) a non-silanized sample; and (B) an APDMES modified sample. Both samples being prepared with the improved protocol. - 164 -
Figure III–16: Relative intensities at m/z(-) = 26 and 28, corresponding to CN^- and Si^- respectively. - 166 -
Figure III–17: Comparison between the O/C ratio obtained by XPS, and the OH^-/CH^- ratio obtained by ToF-SIMS. - 166 -
Figure III–18: Comparison between the N/Si ratio obtained by XPS, and the CN^-/Si^- ratio obtained by ToF-SIMS. - 167 -
Figure III–19: ToF-SIMS spectra in the positive ion mode (m/z = 0 to 200) of (A) a non-silanized sample; and four APDMES modified samples, where (B) is neither thermally treated nor extracted; (C) is thermally treated but not extracted; (D) is not thermally treated but is extracted; and (E) is both treated and extracted. - 168 -

Figure III–20: Variation of the m/z(+) 116/133 ratio for APDMES treated samples. - 170 -
Figure III–21: Variations of the relative intensity of peaks m/z(+) = 30, 116, 133, 148, 174 and 190 on APDMES-treated samples analyzed by ToF-SIMS. - 171 -
Figure III–22: Relative intensities at m/z(-) = 26 (corresponding to CN^-) and 28 (corresponding to Si^-) for VDMES treated samples. - 173 -
Figure III–23: Relative intensities at m/z(-) = 26 (corresponding to CN^-) and 28 (corresponding to Si^-) for DAMS treated samples. - 175 -
Figure III–24: OH-/CH- ratio for VDMES treated samples. - 175 -
Figure III–25: Relative intensities for potential APDMES-related secondary ions at m/z(+) = 116, 133, 148, 174 and 190 on DAMS treated samples. - 177 -
Figure III–26: Relative intensities for characteristic DAMS peaks at m/z(+) = 30, 44 and 56 on DAMS treated samples. - 177 -

List of tables

Table II–1: List of the silanes and their properties. Functional moieties are in red, whereas hydrolysable groups are in blue. - 145 -
Table III–1: Atomic composition of the surface of the samples deduced from XPS measurements. - 159 -
Table III–2: Peak attribution proposed for peaks at m/z(+) = 30, 73, 116, 133 and 190 on APDMES-treated samples analyzed by ToF-SIMS. - 169 -

I. Literature review

The characterization of the adsorption of silane coupling agents on cellulose surfaces, from aqueous solutions, was described in the previous chapter. However, the occurrence of such a phenomenon does not yield necessarily a chemical bonding. Since a covalent grafting is required to ensure durable properties of the modified fibers and the paper made thereof, it is necessary to broaden the study initiated in the previous chapter, and discuss the nature of the interactions involved in our system. For this purpose, this part starts with a review on the interaction between cellulose and silane coupling agents, and then it focuses on surface characterization techniques.

I.A Cellulose fibers chemical modifications

The chemical modification of cellulose fibers by various methods has been widely reported in literature, and in extensive reviews and books [1-6] focused on the topic.

Many authors have investigated the use of cellulose as reinforcements in composite materials [7]. For this purpose, it is important to ensure a strong fiber-matrix interface, in order to guarantee an effective stress transfer between the matrix and the fibers. Increasing the adherence between these two phases can be achieved by modifying the surface properties of the fibers, as a function of the matrix chemistry [3]. In such a context, the use of polymerization techniques have been widely described [1], since modifications achieved from polymeric chains will favor entanglements and inter-diffiusion between the surface of the modified fibers, and the matrix [3].

The surface modification of various cellulosic materials, in heterogeneous conditions, using different oligomeric or polymeric grafting agents bearing anhydride or isocyanate reactive groups was described [8]. The success of these chemical modifications was assessed by FTIR, SEM and XPS. Another study depicted the modification of various cellulosic substrates including powders, fibers and sheets with isocyanates bearing an alkenyl function [9]. In a second step, the free radical polymerization of styrene or methyl methacrylate was carried out in the presence of these modified cellulosics and yielded continuous fibre-matrix composites. Our team also reported the use of diisocyanate agents to modify the surface of cellulose in toluene, thus allowing the grafting of poly-ε-caprolactone chains with different molecular weights [10]. In addition to chemical characterizations by elemental analysis, attenuated total reflexion–FTIR, or XPS, contact angle measurements were performed and proved the conversion of the substrates to a totally apolar surface. The modification of microfibrillated cellulose by poly-ε-caprolactone *via* ring-opening polymerization was also reported [11].

Other methods were depicted for the cellulose surface modification, such as the grafting of succinic or maleic acid groups [12], or the use of modest amounts of octadecanoyl and dodecanoyl chloride [13], under specific solvent conditions. The activation of the fibers surface by N,N'-carbonyldiimidazole was also described [14], as a pre-treatment allowing to further react with diamine or triamine compounds. The other terminal amino groups remained available for reactions with an aliphatic amine through a urea linkage. In another study [15], esterification reactions with various acyl chlorides (acetyl, butyryl, or valeryl), and etherification reactions with ethyl iodide, on steam-exploded flax were reported. These modifications gave birth to cellulose fibers with unchanged structure and morphology, carrying the desired chemical groups on their surface. Finally, the esterification of cellulose fibers with fatty acid chlorides of different chain length in both swelling and non-swelling solvents was described [16]. In this work, the authors used XPS in combination with ToF-SIMS experiments to assess the occurrence of the chemical reaction between the cellulose hydroxyls, and the grafting agents.

In addition to these various modifications of cellulose, the use of organosilanes grafting agents to modify cellulosic substrates has been reported, as detailed in section I.B.

I.B Cellulose fibers modifications by organosilanes

The modification of cellulosic products by organosilanes has been attempted by various teams. They often used organic solvent-based mixtures, as reaction medium. In this context, DAMS and MTMS coupling agents were used, and the formation of chemical bonds between both silanes and the cellulosic materials used was established [2], using diffuse reflectance-FTIR, and diffuse reflectance ultraviolet-visible spectroscopy. Regarding the reactions involving the aminosilane, the authors reported that a fraction of the amino groups reacted with the cellulosic substrate. 3-aminopropyltriethoxysilane and 3-glycidoxypropyltrimethoxysilane were also used to modify microfibrillated cellulose [17]. The surface modifications were confirmed using FTIR, XPS, environmental-SEM and contact angle measurements. These modifications gave birth to materials with hydrophobic characters. The treatment allowed increasing the adhesion between the microfibrils and an epoxy matrix, thus providing better mechanical properties to the final composite materials. More recently, the preparation of amino-bearing cellulose paper after modification with APS in ethanol-water media was reported [18]. The authors assume that the silane is covalently bonded to the cellulose, as supported by FTIR measurements. Such modified papers are used for alkaline-catalysis applications, and show enhanced hydrophobicity and mechanical properties.

In addition, several years ago, our group initiated a research activity based on the grafting of cellulose fibers [19-30]. Most of the studies were performed with the aim of valorizing cellulose fibers as reinforcing materials in organic matrices. However, the reaction mechanisms taking place

during such a surface modification are then not necessarily similar to those occurring when coupling classical inorganic-based materials. Thus, our previous works have shown that the reaction between cellulose and alkoxysilane can take place, only if the following several grafting steps are respected, namely: (i) the grafting agent is previously hydrolyzed; (ii) the resulting hydrolyzed silanol-bearing intermediates are adsorbed at the cellulose surface; (iii) the formed cellulose/silane complexes are isolated from the liquid phase by centrifugation and filtration; (iv) the obtained solid phase is dried and thermally treated; and (v) the ensuing dry grafted cellulose is Soxhlet extracted, in order to remove the physically adsorbed non-reacted molecules, before being used and/or characterized.

In these studies [19-30], the optimal conditions at which silane coupling agents could react with cellulose were established. It was shown that, in all cases, the presence of the grafting agent was detected at the end of the reaction and after the removal of the non-reacted graft molecules. However, exclusively trialkoxy-silanes were studied, and the use of tri-functional reagent does not give clear-cut evidence about the formation of covalent bonds with cellulose (Si-O-Cellulose bond). In fact, as trialkoxysilanes undergo self-condensation reactions, insoluble three-dimensional networks are formed. These macromolecular architectures cannot be removed by solvent extraction and could form a sleeve of cross-linked macromolecules around cellulose fibers, which would be detected by all analytical means. Consequently, the existence of such structures would not necessarily mean that silanes are chemically bonded to the fibers. Furthermore, most of the work reported concerned modifications carried out in a mixture of ethanol and water. It is envisaged that the reactions carried out in purely aqueous media could yield different structures. Finally, the reaction of the silane may depend on the polarity of the solvent.

Thus, there is a lack of knowledge on the interactions between cellulose and silanes. Even though strong evidences support the generally accepted idea that a covalent bonding is possible between the silanol moieties and cellulose hydroxyls, it is necessary to acquire more data on this topic. For this purpose, it seems crucial to use molecules which cannot form tridimensional networks, and surface specific analytical means.

I.C Surface modifications characterization

Most of the techniques used for surface characterization are based on probes, used to irradiate the surface and provoke the emission of component-specific signals from the surface. Various probes such as photons, electrons or ions are used, each having their advantages and drawbacks. Therefore, it is often necessary to use more than one technique, in order to gain a complete understanding of the surface. The number of the molecular layers composing the surface of any material is commonly considered as few unities. Thus, only the first top nanometer is playing a real role on the surface properties.

Several techniques are available to ascertain the properties of the material surface. Some of them concern topographical and optical aspects, like roughness, porosity, gloss, etc., while some others give idea about the chemical composition. In this family, there are direct analyses giving a very precise insight on the chemical structure of the surface (XPS, Tof-SIMS), whereas the other ones give indirect information, such as wetting and energy (contact angle). The depth of analysis is specific to each technique. Only the first family dealing with techniques giving a direct insight on the chemical composition of the surface will be described. They are mostly based on spectroscopic features, such as Attenuated Total Reflection Fourier Transform Infra Red (ATR-FTIR), Energy Dispersive X-ray Spectroscopy (EDX), X-ray Photoelectron Spectroscopy (XPS), Time-of-Flight Secondary Ion Mass Spectrometry (ToF SIMS).

I.C.1 Attenuated Total Reflection Fourier Transform Infrared spectroscopy

Infrared spectroscopy is a technique based on the capacity of a given matter of absorbing electromagnetic bands, in the wavelength region of 2.5 to 25 µm. Infrared radiations induce several modes of motions in molecules (mainly: vibration, stretching and rotation). The absorption of infrared light is characterized by the Lambert-Beer Law. However, infrared spectra are usually presented by a plot of the percentage of transmission *versus* the wavenumber in cm^{-1}. A typical IR spectrum is therefore recorded from about 4 000 to about 400 cm^{-1}.

This technique gives information about functional groups present at the surface of the solid under study. The major drawback of this technique is associated to its high depth of analysis (about 3 microns).

Attenuated Total Reflectance FTIR spectroscopy is a variety of classical FTIR technique devoted to the surface. At each reflection, the light beam penetrates the sample to a depth of a few microns and is absorbed at the characteristic absorption frequencies. The key element of the technique is the ATR accessory, which is composed by a crystal. The most commonly used crystal is made from Zinc Selenide.

Unfortunately, a drawback of FTIR for the analysis of silane modification of substrates is the presence of overlapping bands impacting the region where silicon-related bands are observed.

I.C.2 Energy Dispersive X-ray spectroscopy

Energy Dispersive X-ray spectroscopy is generally carried out in a Scanning Electron Microscope, it is thus also know as SEM-EDX. In the SEM, the scanned electron beam used to produce images of the sample interacts with the surface and charges it. Ionized atoms can relax by electron shell-to-shell transitions, which lead to either X-ray emission or Auger electron ejection. The X-rays emitted are characteristic of the elements present ar the surface of the sample, at the µm

scale. This technique benefits from a very good lateral resolution, and allows mapping the composition of a sample rapidly over a rather large area. Nonetheless, it also suffers from its large depth of analysis, which is the cause of a lack of sensitivity to extreme surface modifications.

I.C.3 X-ray Photoelectron Spectroscopy

The emergence of X-ray Photoelectron spectroscopy (or Electron Spectroscopy for Chemical Analysis) could be considered as a significant progress, since the depth of analysis associated with this technique is less than 10 nm. XPS is a technique that gives low- (or wide) and high-resolution spectra. The first spectra lead to the determination of the elemental composition, empirical formula, whereas the second ones allows the deconvolution of the peaks corresponding to each atom, thus enabling to ascertain the chemical and electronic states of the elements, under scrutiny. XPS spectra are obtained by irradiating the surface by X-rays, which provoke the ejection of photoelectrons. The kinetic energy and the number of electrons ejected from the surface under investigation are measured.

XPS requires ultra high vacuum (UHV) conditions and detects all elements having an atomic number (Z) higher than 3. It, therefore, cannot detect only hydrogen (Z = 1) and helium (Z = 2). The detection limits for most of the elements are in the range of 1/1000. Higher resolutions are possible (1 ppm), but require very long collection time.

I.C.4 Time-of-Flight Secondary Ions Mass Spectrometry

Time-of-Flight Secondary Ions Mass Spectrometry (ToF-SIMS) gives information about the upper molecular layers (about 1 nm, depth). ToF-SIMS is one of the most surface-sensitive analytical techniques. It is based on bombarding the surface by a pulsed ion beam, which provokes the emission of atoms, molecular fragments, atomic ions, molecular ions, electrons, etc., from the very outermost surface of the sample. A part of the emitted species exist thus as ions, and are qualified as secondary ions, which are then directed into a mass analyser , i.e. a time of flight analyser. Their time-of-flight is measured and their mass/charge (m/z) ratio is determined. The modern time-of-flight analysers (using reflectrons or Trift electrostatic analysers) allows a high m/z resolution (mass accuracy in the <10 mamu range). The detected m/z cover a wide range of values, i.e., 0-10,000. Traces of elements could be detected as low as the ppm/ppb range. The main drawback of the technique is that severe matrix effects make data quantification particularly difficult.

A ToF-SIMS instrument is composed by the main following parts: (i) An ion gun (primary ions), among the used elements are Ga, Cs, Bi, Au, etc.; (ii) A chamber hosting the samples; (iii) A system generating an ultrahigh vacuum, aiming at increasing the free path of bombarding (primary)

and liberated (secondary) ions in the flight path; (iv) the flight path using electrostatic analyzers to allow a high m/z resolution, or a reflecting mirror; and (v) the time-resolved counting system.

I.C.5 Relevant studies on silane grafting characterization

With the development of modern engineered surfaces (self-assembled monolayers, chemically or physically modified surfaces), it becomes more and more essential to use very sensitive analytical means [31]. Secondary Ion Mass Spectroscopy (SIMS) methods are particularly fitted to provide information at the sub-nanometer level. More particularly, Time of Flight-SIMS (ToF-SIMS) has been used by some researchers to investigate the modifications of substrates with organosilanes. In this context, Wang and coworkers [32-35] carried out an extensive work on the use of ToF-SIMS, both in static and scanning mode, to study E-glass fiber surfaces modification with γ-aminopropyltriethoxysilane (APS). The existence of a chemical bond between the silane deposit and the E-glass fibers was confirmed, thanks to the observation of relevant peaks. In addition, the migration of aluminum elements from the fiber toward the interphase was observed. The reactions of hydrolyzed APS and an epoxy resin with the same fibers were also studied by ToF-SIMS, in combination with XPS. Also, the surface contamination of the as-received, apparently non-silanised or non-coupled, E-glass fibers by a "patchy" monolayer of APS was demonstrated thanks to the high surface sensitivity of these techniques. After the treatment of the fibers with hydrolyzed silane solutions, the formation of multilayers of APS on the fibers surface with the amino groups at the outer surface was observed. APS was also used [36] to prepare amine-modified glass slides, which were characterized using ToF-SIMS and XPS. In this study, it appears that the level of oxidation of the amine surface groups impacts greatly the intensity of emission of certain fragments in ToF-SIMS. This is particularly important as the treatment to which our samples are subjected may modify that level of oxidation.

Finally, the bonding of APDMES molecules deposed by chemical vapor deposition on silicon dioxide was recently evaluated by ToF-SIMS [37]. Interestingly, the analysis showed the presence of fragments containing both nitrogen and oxygen, despite such fragments being absent from the silane structure. The authors suggest that such fragments may have resulted from amino groups ionically bonded to substrate's silanols through $NH_2^+/^-OSi$ interactions.

List of references

[1] D. Roy, M. Semsarilar, J. T. Guthrie, et S. Perrier, « Cellulose modification by polymer grafting: a review », *Chem. Soc. Rev.*, vol. 38, n°. 7, p. 2046-2064, 2009.

[2] M. C. Matías, M. U. De La Orden, C. González Sánchez, et J. Martínez Urreaga, « Comparative spectroscopic study of the modification of cellulosic materials with different coupling agents », *Journal of Applied Polymer Science*, vol. 75, n°. 2, p. 256-266, janv. 2000.

[3] J. George, M. S. Sreekala, et S. Thomas, « A review on interface modification and characterization of natural fiber reinforced plastic composites », *Polymer Engineering & Science*, vol. 41, n°. 9, p. 1471-1485, 2001.

[4] M. N. Belgacem et A. Gandini, « Surface modification of cellulose fibres », *Polímeros*, vol. 15, p. 114-121, 2005.

[5] D. Klemm, *Comprehensive cellulose chemistry: Functionalization of cellulose*. Wiley-VCH, 1998.

[6] M. N. Belgacem, *Monomers, Polymers and Composites from Renewable Resources*. Elsevier, 2008.

[7] A. K. Bledzki et J. Gassan, « Composites reinforced with cellulose based fibres », *Progress in Polymer Science*, vol. 24, p. 221-274, mai. 1999.

[8] J. A. Trejo-O'Reilly, J.-Y. Cavaille, et A. Gandini, « The surface chemical modification of cellulosic fibres in view of their use in composite materials », *Cellulose*, vol. 4, n°. 4, p. 305-320, déc. 1997.

[9] V. R. Botaro et A. Gandini, « Chemical modification of the surface of cellulosic fibres. 2. Introduction of alkenyl moieties via condensation reactions involving isocyanate functions », *Cellulose*, vol. 5, n°. 2, p. 65-78, juin. 1998.

[10] O. Paquet, M. Krouit, J. Bras, W. Thielemans, et M. N. Belgacem, « Surface modification of cellulose by PCL grafts », *Acta Materialia*, vol. 58, n°. 3, p. 792-801, févr. 2010.

[11] H. Lönnberg, L. Fogelström, L. Berglund, E. Malmström, et A. Hult, « Surface grafting of microfibrillated cellulose with poly([epsilon]-caprolactone) - Synthesis and characterization », *European Polymer Journal*, vol. 44, n°. 9, p. 2991-2997, sept. 2008.

[12] P. Stenstad, M. Andresen, B. Tanem, et P. Stenius, « Chemical surface modifications of microfibrillated cellulose », *Cellulose*, vol. 15, n°. 1, p. 35-45, févr. 2008.

[13] D. Pasquini, M. N. Belgacem, A. Gandini, et A. A. da S. Curvelo, « Surface esterification of cellulose fibers: Characterization by DRIFT and contact angle measurements », *Journal of Colloid and Interface Science*, vol. 295, n°. 1, p. 79-83, mars. 2006.

[14] S. Alila, A. M. Ferraria, A. M. Botelho do Rego, et S. Boufi, « Controlled surface modification of cellulose fibers by amino derivatives using N,N'-carbonyldiimidazole as activator », *Carbohydrate Polymers*, vol. 77, n°. 3, p. 553-562, 2009.

[15] M. Baiardo, G. Frisoni, M. Scandola, et A. Licciardello, « Surface chemical modification of natural cellulose fibers », *Journal of Applied Polymer Science*, vol. 83, n°. 1, p. 38-45, 2002.

[16] C. S. R. Freire, A. J. D. Silvestre, C. Pascoal Neto, A. Gandini, P. Fardim, et B. Holmbom, « Surface characterization by XPS, contact angle measurements and ToF-SIMS of cellulose

fibers partially esterified with fatty acids », *Journal of Colloid and Interface Science*, vol. 301, n°. 1, p. 205-209, 2006.

[17] J. Lu, P. Askeland, et L. T. Drzal, « Surface modification of microfibrillated cellulose for epoxy composite applications », *Polymer*, vol. 49, n°. 5, p. 1285-1296, 2008.

[18] H. Koga, T. Kitaoka, et A. Isogai, « In situ modification of cellulose paper with amino groups for catalytic applications », *Journal of Materials Chemistry*, vol. 21, n°. 25, p. 9356, 2011.

[19] M. N. Belgacem et A. Gandini, « The surface modification of cellulose fibres for use as reinforcing elements in composite materials », *Composite Interfaces*, vol. 12, n°. 1, p. 41-75, 2005.

[20] A. Gandini et M. N. Belgacem, « Physical & chemical methods of fiber surface modification », in *Interface engineering of natural fibre composites for maximum performance*, Woodhead Publishing Limited., Cambridge, U.K.: Nikolaos E. Zafeiropoulos, 2011, p. 3-42.

[21] M. N. Belgacem, M. C. Brochier-Salon, M. Krouit, et J. Bras, « Recent advances in surface chemical modification of cellulose Fibres », *Journal of Adhesion Science and Technology*, vol. 25, n°. 6-7, p. 661-684, 2011.

[22] M. Abdelmouleh, S. Boufi, M. N. Belgacem, A. P. Duarte, A. B. Salah, et A. Gandini, « Modification of cellulosic fibres with functionalised silanes: Development of surface properties », *International Journal of Adhesion and Adhesives*, vol. 24, n°. 1, p. 43-54, 2004.

[23] M. Abdelmouleh, S. Boufi, A. Ben Salah, M. N. Belgacem, et A. Gandini, « Interaction of silane coupling agents with cellulose », *Langmuir*, vol. 18, n°. 8, p. 3203-3208, 2002.

[24] R. Bel-Hassen, S. Boufi, M. C. Brochier-Salon, M. Abdelmouleh, et M. N. Belgacem, « Adsorption of silane onto cellulose fibers. II. The effect of pH on silane hydrolysis, condensation, and adsorption behavior », *Journal of Applied Polymer Science*, vol. 108, n°. 3, p. 1958-1968, 2008.

[25] M. C. Brochier-Salon, M. Abdelmouleh, S. Boufi, M. N. Belgacem, et A. Gandini, « Silane adsorption onto cellulose fibers: Hydrolysis and condensation reactions », *Journal of Colloid and Interface Science*, vol. 289, n°. 1, p. 249-261, 2005.

[26] M. C. Brochier-Salon, G. Gerbaud, M. Abdelmouleh, C. Bruzzese, S. Boufi, et M. N. Belgacem, « Studies of interactions between silane coupling agents and cellulose fibers with liquid and solid-state NMR », *Magnetic Resonance in Chemistry*, vol. 45, n°. 6, p. 473-483, 2007.

[27] M. Castellano, A. Gandini, P. Fabbri, et M. N. Belgacem, « Modification of cellulose fibres with organosilanes: Under what conditions does coupling occur? », *Journal of Colloid and Interface Science*, vol. 273, n°. 2, p. 505-511, 2004.

[28] M. C. Brochier-Salon, P.-A. Bayle, M. Abdelmouleh, S. Boufi, et M. N. Belgacem, « Kinetics of hydrolysis and self condensation reactions of silanes by NMR spectroscopy », *Colloids and Surfaces A: Physicochemical and Engineering Aspects*, vol. 312, n°. 2-3, p. 83-91, 2008.

[29] M. C. Brochier-Salon, M. Bardet, et M. N. Belgacem, « Solvolysis–hydrolysis of N-bearing alkoxysilanes: Reactions studied with 29Si NMR », *Silicon Chemistry*, vol. 3, n°. 6, p. 335-350, 2008.

[30] M. C. Brochier-Salon et M. N. Belgacem, « Competition between hydrolysis and condensation reactions of trialkoxysilanes, as a function of the amount of water and the nature of the organic group », *Colloids and Surfaces A: Physicochemical and Engineering Aspects*, vol. 366, n°. 1-3, p. 147-154, 2010.

[31] F. Chérioux, B. Gauthier-Manuel, J. Eccles, T. Grenut, et M. Briant, « SIMS as a subnanometer probe: A new tool for chemical profile analysis of grafted molecules », *Applied Surface Science*, vol. 253, n°. 14, p. 6140-6143, 2007.

[32] D. Wang, F. R. Jones, et P. Denison, « A ToF-SIMS study of the incorporation of aluminium into the silane coating on e-glass fibres », *Catalysis Today*, vol. 12, n°. 4, p. 375-383, 1992.

[33] D. Wang et F. R. Jones, « ToF-SIMS and XPS study of the interaction of aminosilanised E-glass fibres with epoxy resins. Part I: Diglycidyl ether of bisphenol S », *Composites Science and Technology*, vol. 50, n°. 2, p. 215-228, 1994.

[34] D. Wang, F. R. Jones, et P. Denison, « ToF-SIMS and XPS study of the interaction of hydrolysed -aminopropyltriethoxysilane with E-glass surfaces », *Journal of Adhesion Science and Technology*, vol. 6, n°. 1, p. 79-98, 1992.

[35] D. Wang et F. R. Jones, « ToF-SIMS and XPS studies of the interaction of silanes and matrix resins with glass surfaces », *Surface and Interface Analysis*, vol. 20, n°. 5, p. 457-467, 1993.

[36] M. Jasieniak, S. Suzuki, M. Monteiro, E. Wentrup-Byrne, H. J. Griesser, et L. Grøndahl, « Time-of-Flight Secondary Ion Mass Spectrometry study of the orientation of a bifunctional diblock copolymer attached to a solid substrate », *Langmuir*, vol. 25, n°. 2, p. 1011-1019, 2009.

[37] F. Zhang, K. Sautter, A. M. Larsen, D. A. Findley, R. C. Davis, H. Samha et M. R. Linford, « Chemical vapor deposition of three aminosilanes on silicon dioxide: Surface characterization, stability, effects of silane concentration, and Cyanine dye adsorption », *Langmuir*, vol. 26, n°. 18, p. 14648-14654, 2010.

II. Materials and Methods

II.A Materials

II.A.1 Chemicals

Three organosilanes were used, namely: methylvinyldiethoxysilane (MVDES), 3-aminopropyldimethylethoxysilane (APDMES), and 3-(2-amino-ethylamino)-propyltrimethoxysilane (DAMS). The most relevant data about these chemicals, including their structure, formula, physical properties, purity, CAS number and suppliers, are described in Table II-1.

For modifications carried out in acidic media, a pH of 4 was obtained by adding an appropriate amount of glacial acetic acid, using a research grade product from Sigma-Aldrich, as received. Solvent extractions were performed using various organic solvents, namely : acetone, chloroform, cyclohexane, dichloromethane, and ethanol. These solvents were all research grade products obtained from Sigma-Aldrich and were used as received.

Name	Structure	Molecular formula	Molar weight (g/mol)	Density at 25°C (g/cm3)	Boiling point (°C)	Purity (%)	CAS Number	Distributor	Commercial Reference
(3-Amino)-propyl-dimethylethoxysilane (APDMES)		$C_7H_{19}NOSi$	161,32	0,857	78	> 95 %	[18306-79-1]	Gelest, Inc. - Morrisville, PA - USA	SIA 0603.0
3-(2-amino-ethylamino)propyl-trimethoxysilane (DAMS)	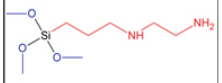	$C_8H_{22}N_2O_3Si$	222,36	1,02	264	> 98 %	[1760-24-3]	Dow Corning, S.A. - Seneffe - Belgium	Z-6094
Vinyldimethyl-ethoxysilane (VDMES)	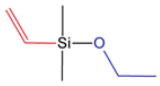	$C_6H_{14}OSi$	130,26	0,79	99	> 95 %	[5356-83-2]	Gelest, Inc. - Morrisville, PA - USA	SIV 9072.0

Table II-1: List of the silanes and their properties. Functional moieties are in red, whereas hydrolysable groups are in blue.

II.A.2 Cellulose fibers

The fibers used originate from a 100% softwood dry Kraft pulp, refined at 32°SR. Before modification, the dry pulp was disintegrated, and re-pulped at a consistency close to 1.5% in deionized water, using a Lhomargy pulper at 3000 rpm during 10 minutes at room temperature. The consistency of these suspensions was increased (up to 10~12%) by removing excess water, before storage. The modification was performed with suspensions having concentrations of 10g/l.

II.B Methods

II.B.1 Pulp modification

The preparation of the silane solution was performed by first weighing the necessary amount of water in a plastic beaker, under constant magnetic stirring. In addition, for experiments under acidic conditions, the necessary amount of acetic acid was added. Then, the needed amount of silane coupling agent was added and the solution was vigorously stirred. When required, the solution was left under constant stirring for the necessary length of pre-hydrolysis before the next step. Once a reactive aqueous silane solution was obtained, the thick fiber pulp was added and the mixture was vigorously stirred in order to obtain an homogeneous slurry at 10g/l. This slurry was left under gentle stirring for 30mn, which was chosen as a contact-time for the silane treatment for all our experiments. After that, the modified fibers were used to prepare handsheets, following the method described hereafter.

II.B.2 Handsheet formation

Laboratory paper samples were prepared using a retention handsheet former. Retention handsheets were produced with a basis weight close to 110 g/m², following the relevant sections of the standard T205-sp06 from TAPPI [1]. This operation can be summarized as follows: (i) after the pulp preparation (both silane modified and pristine pulps were used), an amount of pulp containing 3 g of dry fibers was introduced in the upper tank of the retention handsheet former; (ii) water was added to reach a concentration of 3g/L; (iii) the pulp was mixed during 50s at 800rpm (This step allows a rather homogeneous distribution of the fibers into the sheet without creating high interfacial shear stress on the fibers surface, which may remove the adsorbed silanes.); (iv) then the mix was poured on the wire; and (v) finally the handsheet was formed after the water drainage.

In the classical protocol for handsheets formation, the samples are then placed in a vacuum dryer operated at 92°C for 10mn. However, preliminary trials have shown that this process causes the removal of most of the silane adsorbed onto the sample. Consequently, we modified the drying protocol reported in the standard T205-sp06. Best results were obtained when the handsheets were placed between “Savoyeux” sheets and left under moderate pressure to dry at room temperature.

Since analysis carried out by ToF-SIMS showed a significant surface contamination from the savoyeux, as detailed in part III.C.1 of this chapter, another drying protocol was applied to a part of our samples. For the samples destined to be characterized by ToF-SIMS and XPS analysis, it was necessary to find a way of drying the samples without direct contact with ‘savoyeux’ sheets. Thus, the wet handsheets were left to dry at room temperature while preventing the deposition of any dusts on their surface. This experimental drying set-up is schematized in Figure II–1. All objects and

accessories used, as well as all surfaces of the hood used were thoroughly washed with ethanol before the sample drying, in order to minimize the risk of contamination.

After drying, selected samples were thermally treated at 110°C for 1 hour, in order to achieve the chemical reaction of the silane onto the fiber surfaces.

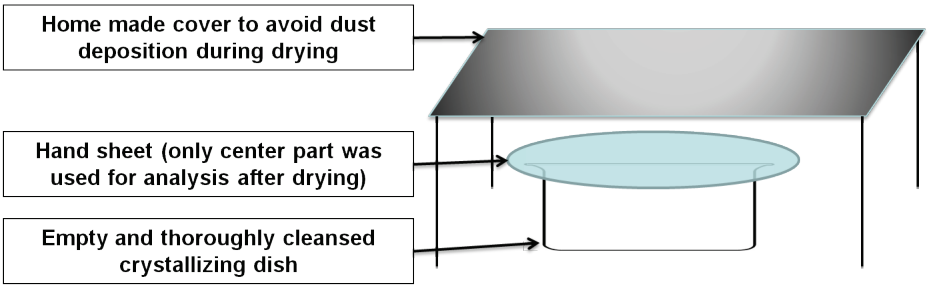

Figure II–1: Experimental drying set-up.

II.B.3 Solvent extractions

Two different protocols were used for solvent extractions. First, an Accelerated Solvent Extractor (ASE), ASE-150 from Dionex, was used. This apparatus uses a combination of elevated temperatures and pressure with common solvents to increase the efficiency of the extraction process. The apparatus was set to perform extraction cycles with a duration of 15mn. Most of the time, two cycles of extractions were performed. However, for some samples, the process was limited to one cycle. Classical Soxhlet extractions were also performed. The duration of the extraction was varied from 2 to 40 hours. In all cases, after the extraction, the samples were left to rest overnight in a vacuum dessicator, in order to remove any adsorbed solvent molecules.

II.B.4 SEM-EDX

Qualitative SEM-EDX spectra were obtained on a Quanta 200 environmental scanning electron microscope from FEI, in the low vacuum mode (at a pressure of 1.0 Torr i.e. 133 Pa). Under these conditions, it was not necessary to metal-coat our samples before analysis, hence avoiding the impact of such a coverage on the analysis outcome.

The sample composition analyses were performed under a beam current of about 2.0 mA, and an accelerating voltage of 15 kV, with an analysis duration set to 120s. A Bruker SSD detector with a 10 mm² active area was placed to collect photons at a take-off angle of 35°. The samples were placed at the optimal working distance of 10 mm. The data analysis was carried out using the software Spirit (v1.07.04) provided by PGT.

II.B.5 XPS

The X-ray photoelectron spectroscopy (XPS) experiments were performed with a XR3E2 apparatus from Vacuum Generators, UK. This apparatus is equipped with a monochromated MgKα X-ray source (1253.6 eV) and operating at 15 kV under a current of 20 mA. Samples were placed in an ultra high vacuum chamber (10^{-8} mbar) with electron collection by a hemispherical analyzer at an angle of 90°. These measurements were carried out at least in triplicate. The differences between the various values obtained are discussed in the experimental section below.

II.B.6 ToF-SIMS

The ToF-SIMS experiments were performed with a PHI TRIFT III apparatus from Physical Electronics. The apparatus was operated with a pulsed 22 keV Au+ ion gun (ion current of 2 nA) rastered over a 300 µm×300 µm area. Ultra high vacuum ($5x10^{-10}$ Torr) prevailed in the analysis chamber during acquisition. The spectra were acquired under static conditions, applying a primary ion dose density (PIDD) not higher than 10^{12} ions/cm². An electron gun was operated in pulsed mode at low electron energy for charge compensation.

Data analysis was performed on the WinCadence software (v4.4.0.17), provided by Physical Electronics. Mass calibration was performed on hydrocarbon secondary ions and all data were exported to Microsoft Excel® before further analysis. Then, the data were normalized to the total intensity minus $H^{+/-}$ intensity because of its low reproducibility. The mean and standard deviations were calculated from three measurements on different areas of each sample.

II.B.7 Solid-NMR

Solid-state ^{29}Si CP/MAS NMR measurements were carried out using a Bruker Avance 400 spectrometer operating at 79.490 MHz. The samples were placed in 7 mm ZrO_2 rotors. Magic angle spinning was performed at a spinning rate of 4 kHz. All the spectra presented were recorded using a combination of cross-polarization, high-power proton decoupling and magic angle spinning (CP/MAS) methods. A 25 kHz spectral width, a 5 s repetition time, a 3.5 ms contact time and a proton decoupling field equivalent to 33 kHz were used. The ^{29}Si scale was calibrated with the signal from the external standard M_8Q_8 (at -109.80 ppm). The ^{1}H radiofrequency field strength was set to give a 90° pulse duration of around 3.8 µs.

III. Results and Discussion

This work intends to establish if there is any reaction between the silanol hydroxyl moieties borne by hydrolyzed organosilanes, and cellulose hydroxyl functions. It also aims at establishing if there is an occurrence of chemical links between those groups, with or without a thermal post-treatment. The experimental work started with the evaluation of various solvent extraction protocols through SEM-EDX analyses, in order to assess that unretained silane could effectively be removed from cellulose fibers. Then, it focused on elucidating the nature of the interaction between the cellulose and the coupling agent. This part consists of a multi-scale approach based on SEM-EDX, Solid-NMR, XPS and ToF-SIMS experiments, and involves two different mono-functional alkoxysilanes, an aminosilane and a vinylsilane, as well as an amine-bearing trialkoxysilane.

III.A Development of a suitable extraction method

With the aim of assessing that ungrafted silane molecules could be removed from our cellulosic substrate by solvent extraction, and define a proper protocol for such extractions, various tests were performed, for the mono-alkoxysilane APDMES (Figure III–1), thus making sure to avoid the formation of insoluble polysiloxane networks. All samples were analyzed by SEM-EDX, and the qualitative spectra obtained are compared hereafter.

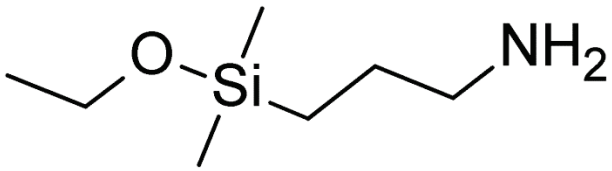

Figure III–1: Structure of APDMES.

In ethanol-based solutions, it was previously shown [2], [3] that the bonding of organosilanes onto cellulose can occur only if the samples have been subjected to a thermal treatment. Here the thermal treatment for 1h at 110°C was applied to ADPMES-modified fibers. Then, the ensuing fibers were subjected to extraction by various organic solvents, with different polarity, using an Accelerated Solvent Extractor (ASE) for two successive extraction cycles of 15mn. The SEM-EDX spectra of the different samples are shown in Figure III–2, and compared with the spectra of the unextracted modified fibers. It appears that for all the solvents, the spectra are qualitatively similar.

The signal associated with silicon atom is identical for all thermally treated samples. The extraction removed very little or nothing of the silane. It may also be considered that the ASE apparatus, and the short cycles used, are not good enough to remove such ungrafted compounds. Since qualitatively comparable results were obtained with all the solvents tested, it was decided to focus on only one of them for the rest of this study, namely acetone.

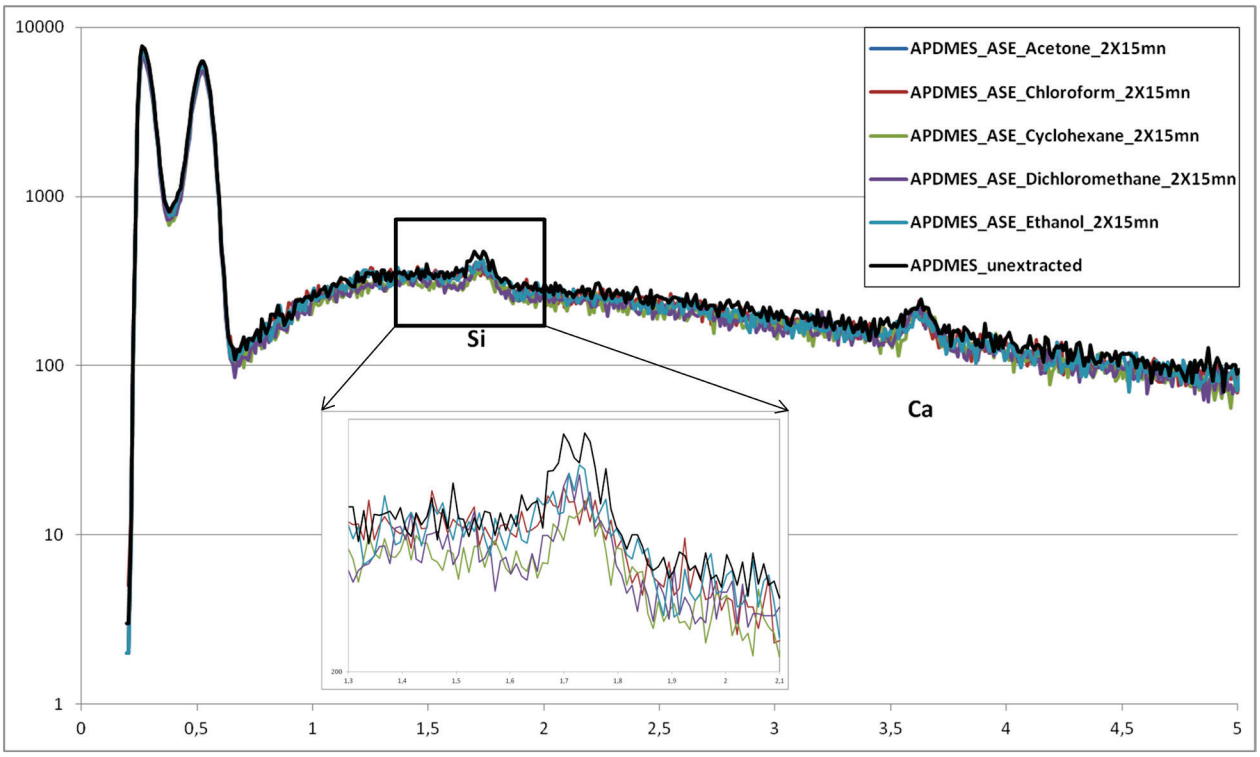

Figure III–2: SEM-EDX: Comparison of organic solvents for APDMES removal by ASE, after thermal treatment.

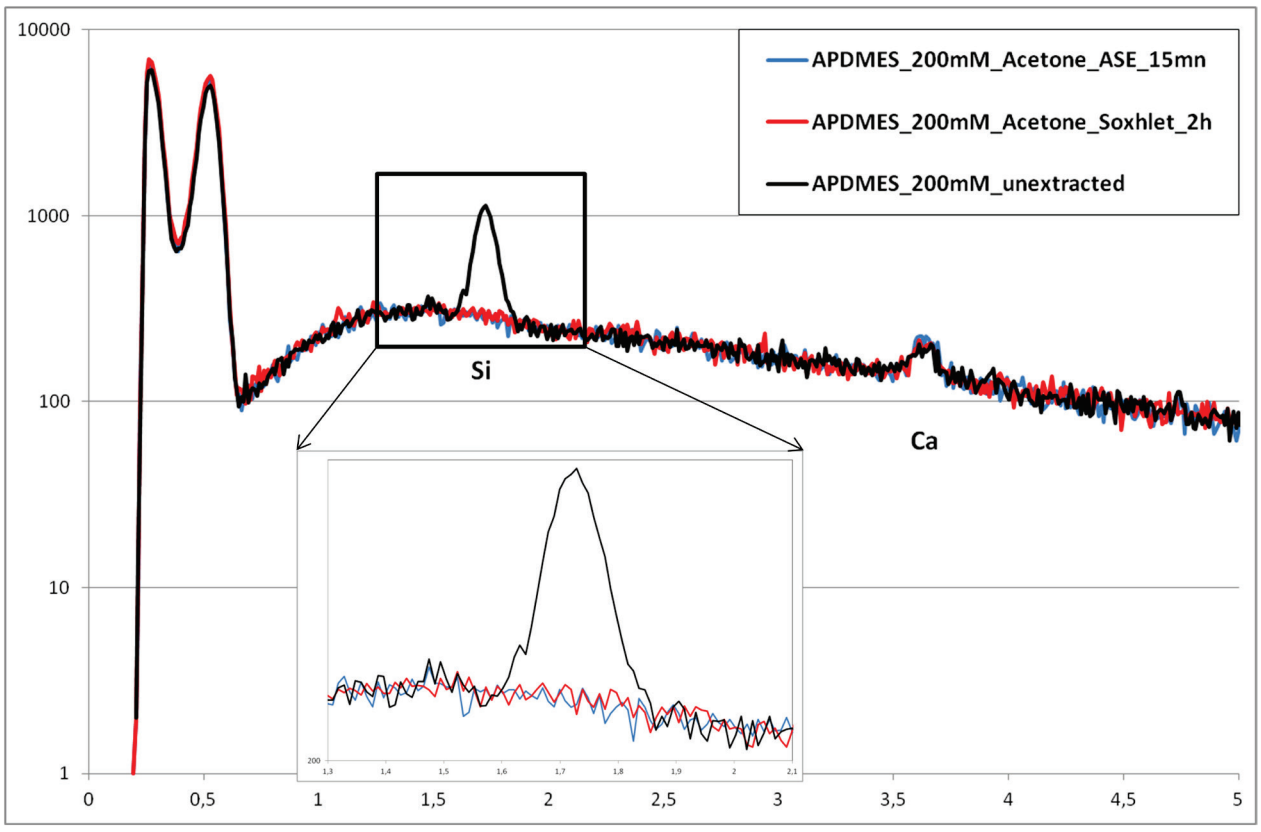

Figure III–3: SEM-EDX: Comparison between ASE and classical Soxhlet extraction for the removal of freshly deposited APDMES.

With the aim of verifying that ungrafted molecules can be effectively removed from paper, new samples were prepared. Handsheets from unmodified fibers were produced, and samples were taken from these handsheets. Then, a reactive APDMES solution at a concentration of 200mM was prepared, and drops of 150µL were deposited on the handsheets samples. A reference sample was left to dry at room temperature and remained unextracted, while two samples were washed with acetone just after the drop deposition. The first sample underwent a classical Soxhlet extraction during two hours, whereas the second sample was submitted to a single cycle of 15mn in the ASE apparatus. The SEM-EDX spectra of these three samples are compared in Figure III–3. It is shown unambiguously here that both methods of acetone extraction allow the removal of freshly deposited silanes from the cellulose fibers.

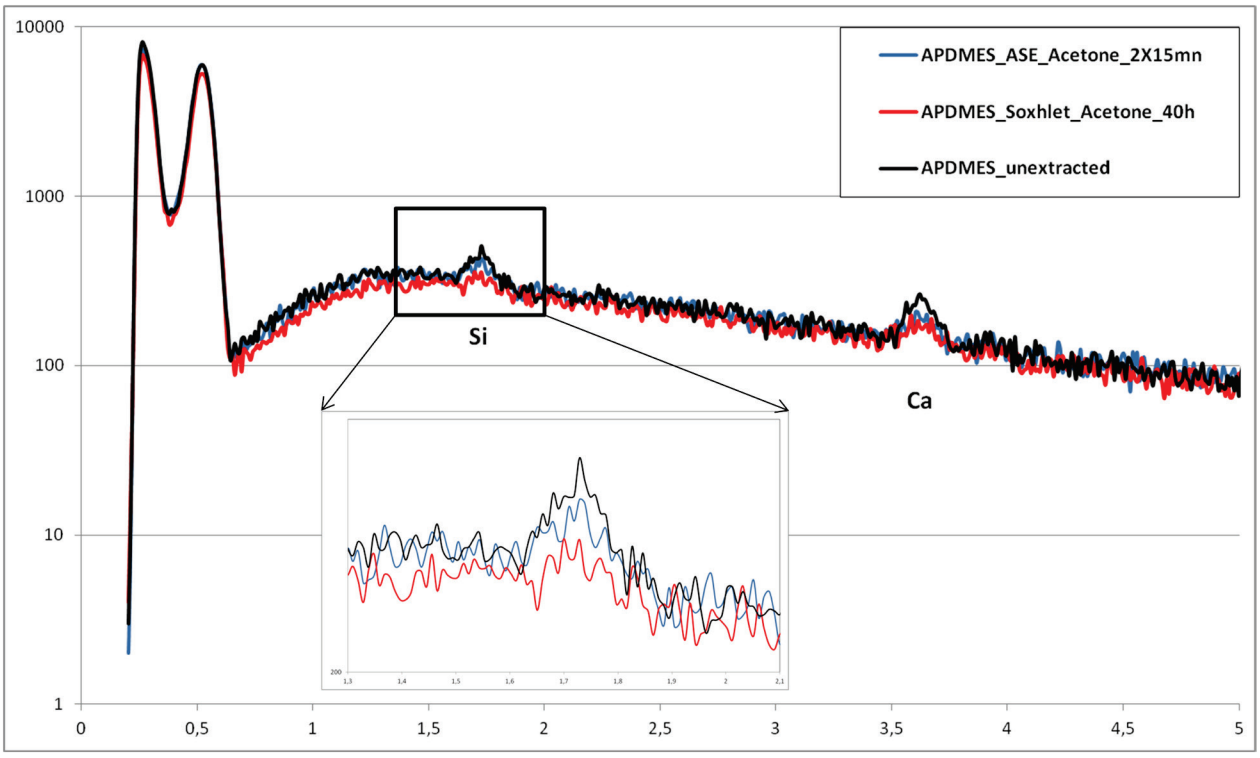

Figure III–4: SEM-EDX: Comparison between ASE and Soxhlet extraction for APDMES removal after thermal treatment.

Since acetone was found to remove ungrafted silane molecules, it was decided to compare the two-cycle ASE extraction protocol with a longer classical Soxhlet extraction on thermally treated samples. For this purpose, such thermally treated modified samples were Soxhlet extracted with acetone for 40 hours. Samples were taken out of the Soxhlet extractor every eight hours. As the SEM-EDX spectra of the samples taken at t=8, 16, 24, 32, and 48h exhibited similar features, only the latter one is presented in Figure III–4, in comparison with the spectra of unextracted modified fibers, and that of the ASE extracted modified fibers.

It appears that the accelerated extraction protocol allows obtaining qualitatively similar results in comparison to a traditional Soxhlet extraction performed over 40 hours. In both cases, little or no silane was removed from the samples.

The various experiments presented above allow drawing the following conclusions: (i) It has been established that it is possible to remove unreacted monoalkoxysilane molecules with acetone. Thus, for all future experiments where an extraction is needed, a protocol based on two cycles of ASE extraction with acetone will be used. (ii) Also, it has been demonstrated that the silane-cellulose interaction created after the thermal treatment is resistant to a wide variety of organic solvents.

III.B Multi-scale characterization of the silane-cellulose interface

Several samples were prepared from three types of modified fibers: (i) APDMES-; (ii) MVDES-; and (iii) DAMS-modified fibers. In addition, ungrafted control samples were prepared, and submitted to the same treatments as those made on modified samples. Two treatments were considered, namely the thermal treatment (1h at 110°C), and the solvent extraction (2 cycles of acetone extraction with an ASE apparatus). Thus, for each type of fibers, four samples were produced: (i) a sample which has neither been thermally treated, nor extracted; (ii) a sample which has been thermally treated, but not extracted; (iii) a sample which has been solvent extracted without prior thermal treatment; and (iv) a sample which has been thermally treated, and then solvent extracted.

III.B.1 SEM-EDX

In order to verify the presence of silicon in our modified fibers, SEM-EDX spectra were acquired with all our samples. Figure III–5, Figure III–6, and Figure III–7, show, respectively, the EDX spectra of APDMES-, VDMES- and DAMS-treated samples.

For APDMES-modified fibers (Figure III–5), it appears that: (i) silicon is detected in significant amount in the sample which was not submitted to any treatment; (ii) qualitatively, it comes out that both thermally treated samples show a similar amount of silicon, slightly inferior to the non-treated sample; and (iii) as expected, the sample which has undergone a solvent extraction without prior thermal treatment shows the smallest amount of silicon in the sample.

From these results, it appears that a part of the adsorbed silane is lost during the thermal treatment, but that the rest of the grafting agents are strongly attached to the cellulose. Also, it is interesting to observe that for the sample left to dry at room temperature, a part of the adsorbed silane has been able to form probably covalent bonds with the cellulose.

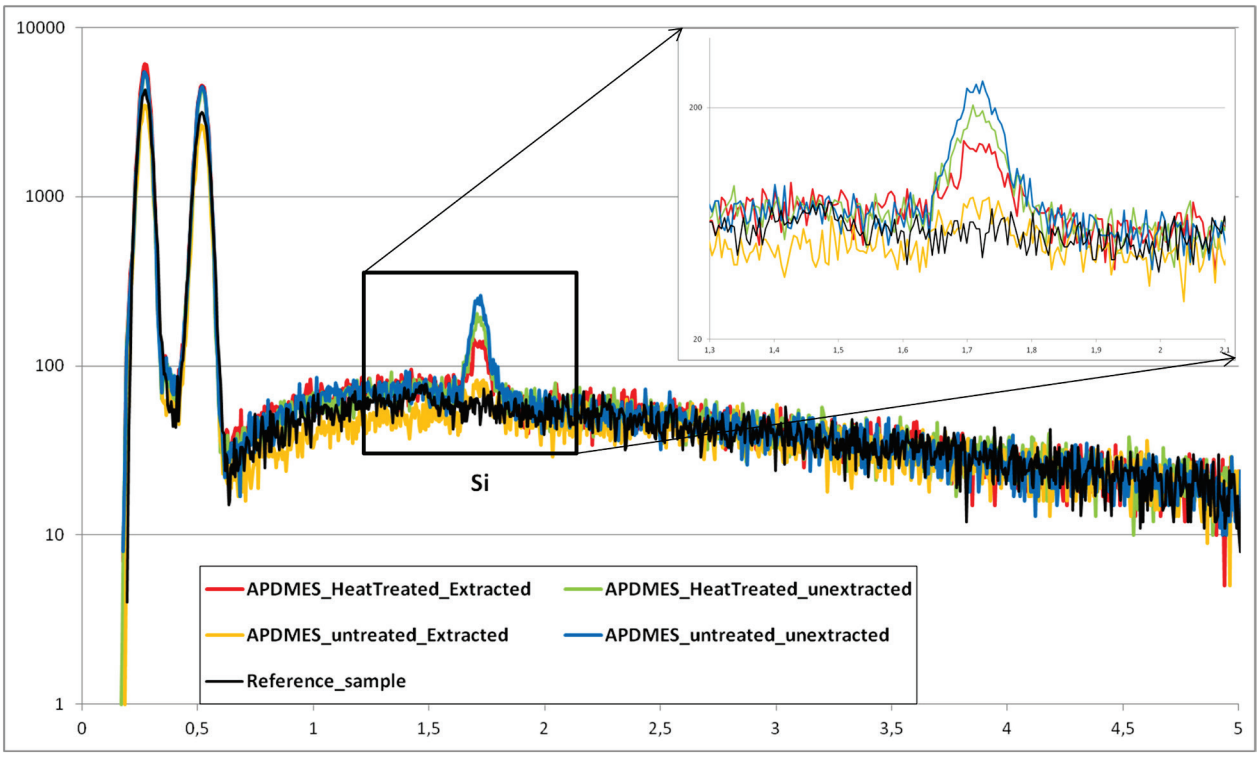

Figure III–5: SEM-EDX characterization for the APDMES sample series.

For VDMES-treated fibers, it is shown in Figure III–6 that silicon is not detected on any of the samples. The peak appearing in the spectra corresponds to Aluminum, which most likely originated from the sample holder. As it was shown in our QCM study that this compounds adsorbs on cellulose even though in much smaller quantities than APDMES, it is possible that the sensitivity of the SEM-EDX analysis used is not sufficient to detect the silicon from this silane. Indeed, the depth of analysis of SEM-EDX is about 1 µm, which is quite big for surface characterization. It is then necessary to investigate this series of samples with more sensitive tools before drawing conclusions.

Finally, the spectra for DAMS modified fibers are exposed in Figure III–7. It appears that the silicon element is detected in rather large quantities in all the modified samples, thus confirming that DAMS adsorbs readily on cellulose and react with it and/or homo-polymerize.

The analyses performed by SEM-EDX clearly show that: (i) APDMS molecules surely react with cellulose; (ii) DAMS is retained at the surface of cellulose, but its high number of functions (three) do not allow concluding if its presence at the surface arises from covalent bonding or results from a simple physical adsorption; and (iii) VDMES does not interact with the cellulose substrate.

It is, therefore, necessary to pursue our investigations in order to give further characterization.

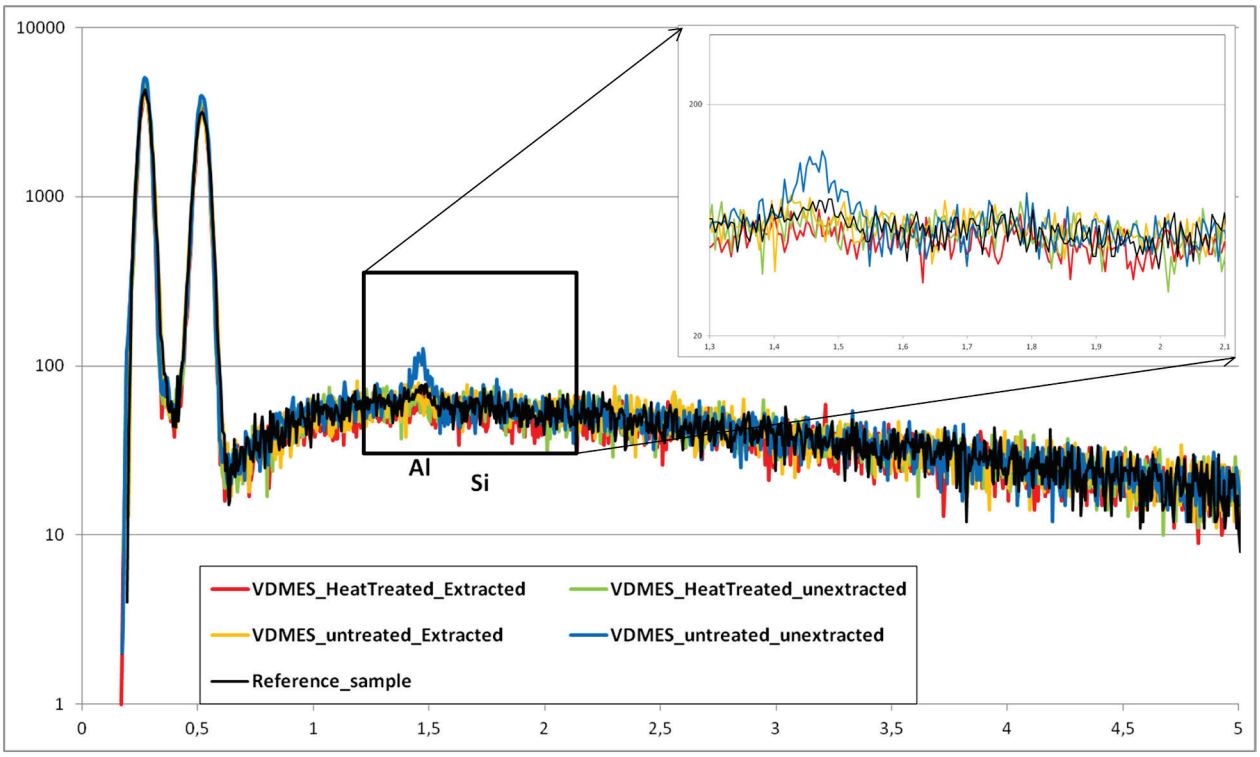

Figure III–6: SEM-EDX characterization for the VDMES sample series.

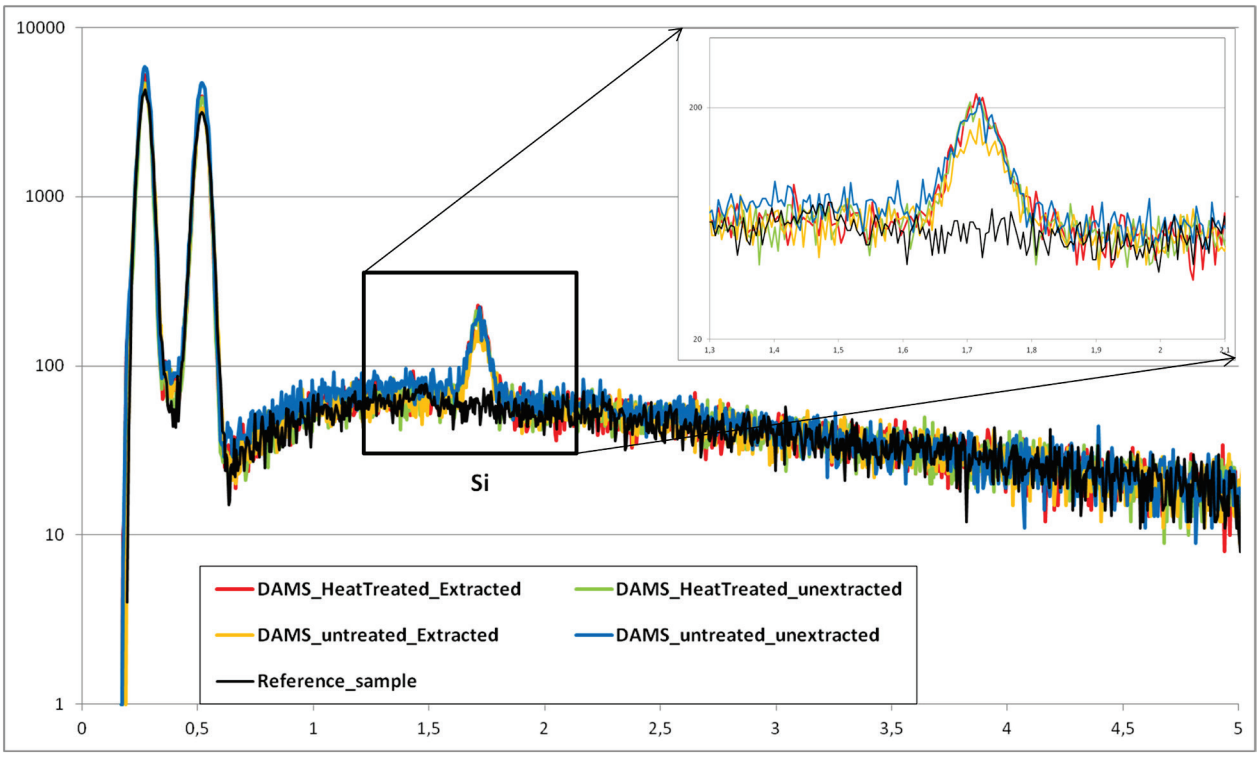

Figure III–7: SEM-EDX characterization for the DAMS sample series.

III.B.2 Solid NMR

With the aim of understanding the structure of the silane layer retained onto cellulose fibers, we have used the samples having undergone a thermal treatment followed by a solvent extraction to perform solid-NMR analyses. The samples were disintegrated, and the powders obtained were used to fill solid-NMR rotors.

The peak attribution was realized based on the data previously described in the first chapter of this dissertation. Indeed, even though the chemical shifts of a same structure slightly vary between liquid-NMR and solid-NMR, the attributions are almost similar. This slight shift is due to the solvent effect (liquid) and to the difference of the calibration method. In liquid-NMR, chemical shifts are given as displacements in regard to the signal of TMS, which is used to set the zero of the scale, whereas in solid-NMR the calibration is based on the peaks of the external standard M_8Q_8 (at 109.80 ppm). Between the liquid and solid spectra of a same compound, a difference of chemical shifts of 2 to 3 ppm is generally accepted. Thus it is possible to use the data obtained in our liquid NMR study to identify the peaks appearing in the spectra presented in this part of the work.

For APDMES modified fibers, the spectrum presented in Figure III–8 was obtained after 22 hours of acquisition. Two peaks are observed, with the first one being centered close to 10 ppm, whereas the second appeared at around 18 ppm. The former peak corresponds to condensed M^1 dimers, whereas the latter is attributed to uncondensed $M^0{}_H$ species. The latter signal can arise either from hydrolyzed silanes adsorbed on cellulose, or from molecules grafted to the substrate. It is observed that despite the rather long acquisition time, the noise/signal ratio is not very good. Furthermore, the peaks have an important width, which is a sign of a complex environment for the silicon atoms under scrutiny.

The existence of two peaks is rather surprising, since a proper solvent extraction method was used in order to remove all ungrafted material from the paper, before its disintegration. More specifically, all dimers were expected to be removed after such treatment. A first hypothesis to explain this feature is to consider that the solvent extraction has failed. Another hypothesis is to consider that cellulose fiber walls are porous and that a part of the silane might have been trapped in such porosity and resisted the solvent extraction. Indeed, it is important to consider the fact that the solid-NMR technique is a bulk analysis method, and hence it has access to a part of the matter that the electron beam used as a probe for our SEM-EDX analyses cannot reach, since the depth of analysis of SEM-EDX is limited at the micron scale.

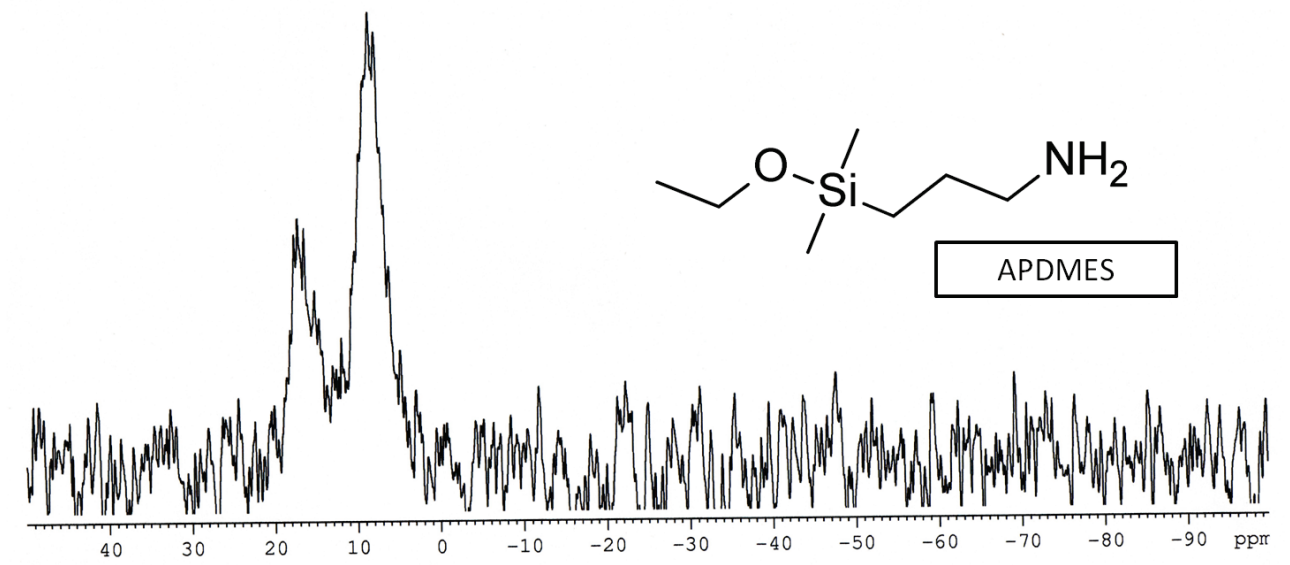

Figure III–8: ^{29}Si CP/MAS Solid NMR spectra for APDMES modified fibers.

For the second monoalkoxysilane used in this work, VDMES, the acquisition time lasted for 72 hours. However, despite this extended analysis duration, there is no sign of the presence of silicon on the spectrum, as presented in Figure III–9. This feature is not totally unexpected since it was shown in the previous part of this work that very little VDMES adsorbs onto cellulose over time. Since NMR analyses the bulk of the material, the contribution of the single silicon atom of each silane molecule might be too small to be detected with this analytical mean.

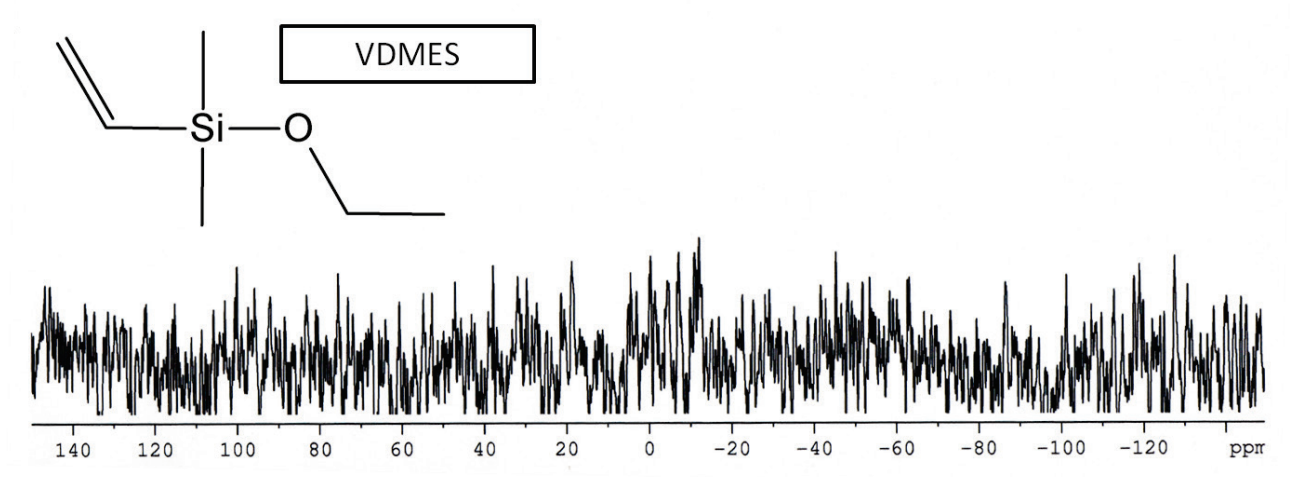

Figure III–9: ^{29}Si CP/MAS Solid NMR spectra for VDMES modified fibers.

Finally, Figure III–10 shows the spectrum obtained after 22 hours of signal collection for DAMS-modified fibers. This spectrum shows the presence of a large amount of completely condensed T^3 structures, as witnessed by the large peak centered around -68 ppm. In addition, a significant part of

T^2 structures is observed, as shown by the peak centered around -57 ppm. Finally, the T^1 peak does not appear clearly.

Owing to the important width of the peaks observed, and their overlapping, it is not possible to determine the ratio of the various structures detected.

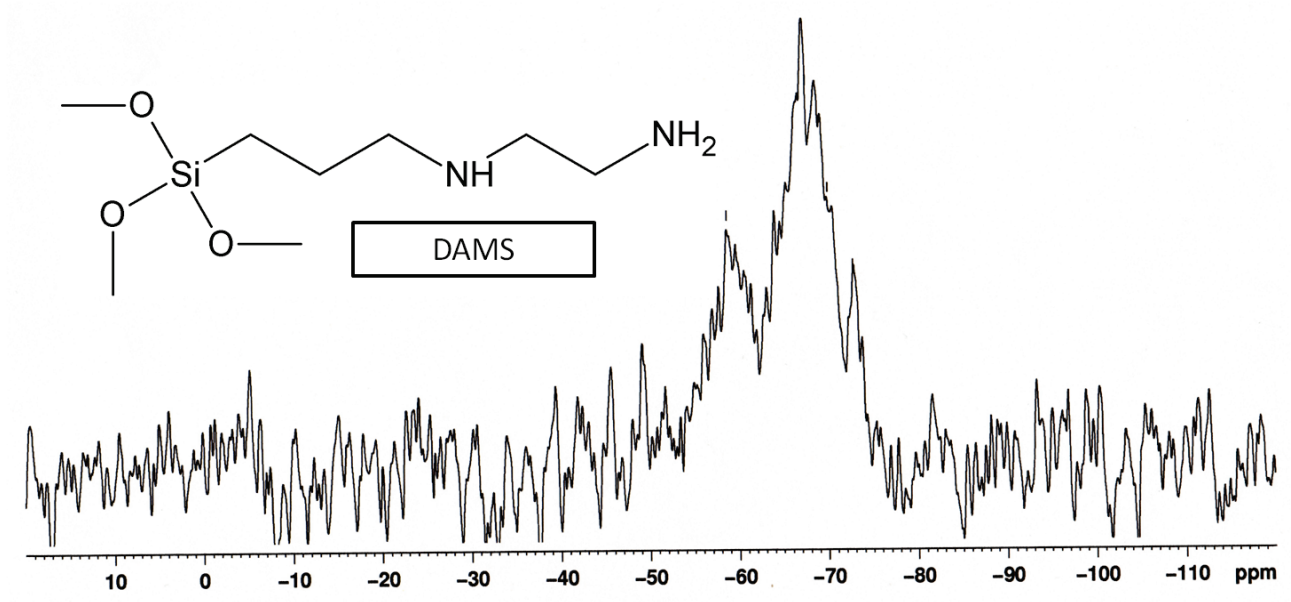

Figure III–10: ^{29}Si CP/MAS Solid NMR spectra for DAMS modified fibers.

The use of ^{29}Si solid-NMR as a technique to follow the grafting of silanes onto cellulose has the great advantage of tracking the presence of silicon in a material which usually does not have any. However, since this tool analyzes the bulk of the sample, it is difficult to obtain a good signal/noise ratio under acceptable data collection durations. Indeed, the surface of the fibers, where we expect the silane to be retained in greater amounts, represents only a small portion of the samples weight. Nonetheless, despite this evident drawback, it was possible to confirm the presence of two silanes of our selected molecules onto cellulose modified fibers after they had been solvent extracted.

Unfortunately, the results obtained do not allow to be very accurate regarding the chemical state of the atoms under scrutiny. Thus it was decided to use surface-specific analytical means, in order to enhance the contribution of the top surface atomic layers in our analyses.

III.B.3 XPS

The use of XPS to ascertain the efficiency of grafting showed to be a very powerful technique, allowing to detect the various changes occurring at the modified sample surfaces.

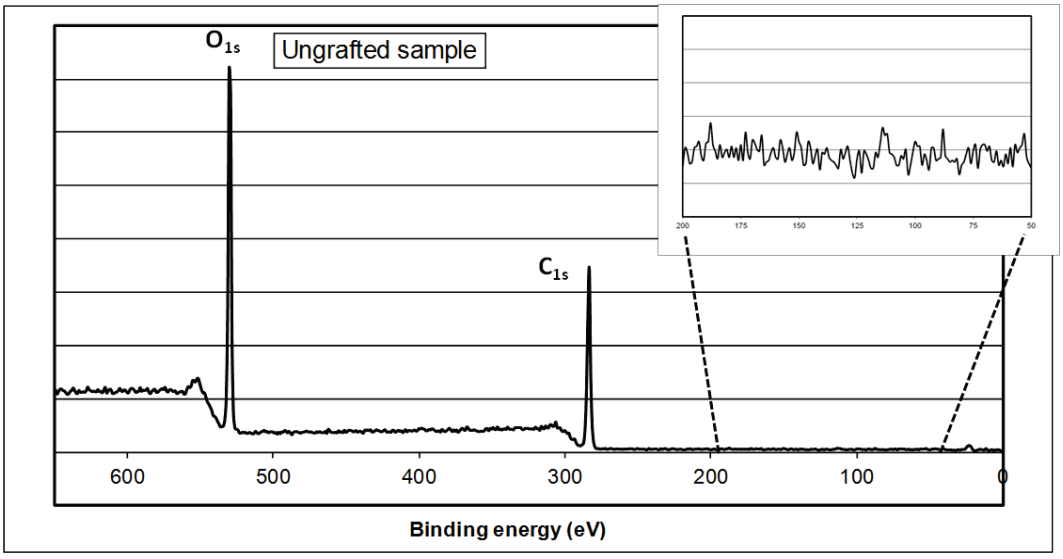

Figure III–11: XPS spectrum of the reference unmodified sample.

In our case, the main changes occurring during the modification are associated with the presence of new atoms borne by the grafting agent, namely: silicon for the three silane coupling agents and nitrogen for those bearing nitrogen atoms (DAMS and APDMES). The wide spectra of the surface of all the samples were recorded. As expected, for the unmodified paper sheets, the spectra showed the presence of two main atoms, as depicted in Figure III–11. The corresponding peaks were situated at 285 and 531 eV, and attributed to carbon and oxygen atoms, respectively.

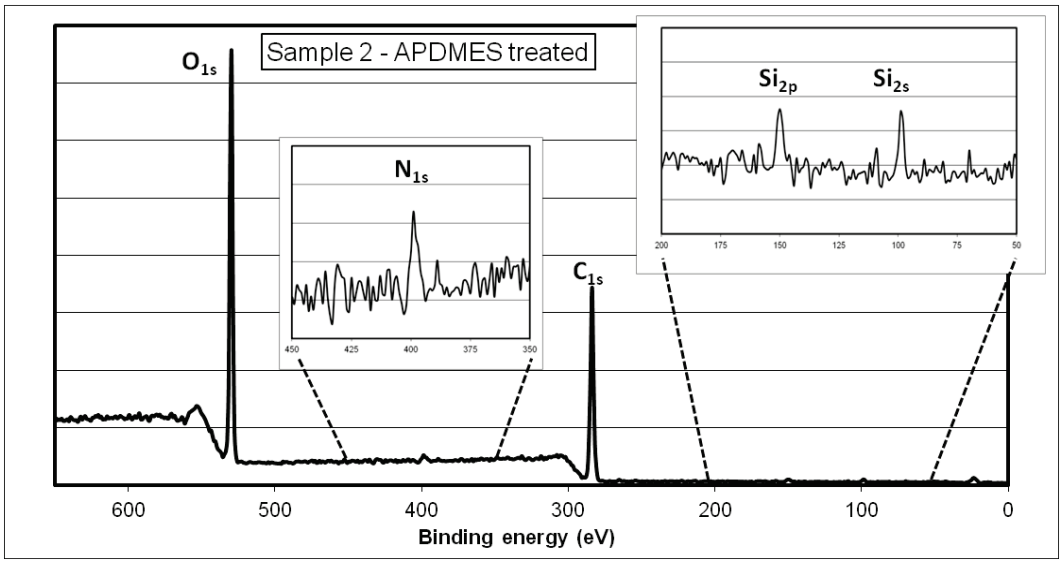

Figure III–12: XPS spectrum of APDMES treated fibers.

The alkoxysilane-modified samples, however, displayed the appearance of three additional signals, namely: (i) a new peak at around 398 eV, corresponding to nitrogen for DAMS- and APDMES-treated samples; and (ii) two other additional bands at 102 and 150 eV, corresponding to

Si_{2s} and Si_{2p} silicon atoms, respectively, which were observed for the three series of samples. The spectrum of an APDMES-treated sample is given in Figure III–12, as an example.

Sample number	Treatment			Atom composition (in %)				Atomic ratio	
	Silane	Heat	Extraction	C	O	N	Si	O/C	N/Si
1	*None*	*yes*	*yes*	60,6	39,4	0,0	0,0	0,65	-
2	*APDMES*	*no*	*no*	59,8	38,0	1,3	0,9	0,64	1,56
3		*yes*	*no*	60,4	37,6	1,2	0,8	0,62	1,41
4		*no*	*yes*	59,6	39,7	0,5	0,2	0,67	2,70
5		*yes*	*yes*	60,5	38,2	0,8	0,6	0,63	1,33
6	*VDMES*	*no*	*no*	61,2	38,0	-	0,3	0,62	-
7		*yes*	*yes*	59,3	39,9	-	0,2	0,67	-
8	*DAMS*	*no*	*no*	66,1	32,3	1,2	0,4	0,49	2,79
9		*yes*	*yes*	61,7	35,7	1,5	1,1	0,58	1,29

Table III-1: Atomic composition of the surface of the samples deduced from XPS measurements.

Table III-1 reports the surface atomic composition of the samples studied, as deduced from the XPS measurements. Several remarks could be deduced from these data.

First, these results show, qualitatively speaking, that the adsorption of all three silanes takes place at the surface of cellulosic fibers. A very interesting observation, here, is that for the first time in this study, the presence of VDMES onto fibers modified with this coupling agent has been detected. However, the atomic composition deduced from the XPS measurements show that the level of silicon is particularly low, in regard of that observed on samples modified by other silanes. Furthermore, the standard deviations observed between the measurements were higher for VDMES-modified samples, suggesting that the retention of this silane is not very regular on the surface.

Then, it also appears from our data that mono-alkoxysilanes remain at the surface after solvent extractions (experience #4, #5, #7 and #9), even without thermal treatment (experience #4). As already reported [2], the extraction of the unheated samples (experience #4) removed the major part of the adsorbed silane molecules and the detected amount is very low.

From the molecular structures of APDMES and DAMS, the theoretical ratio between N and Si atoms is equal to 1 and 2, respectively. The ratio deduced from the experiments is slightly higher but remains acceptable (except for experience #4 and #9), if one takes into account the low quantities of the grafting agents under quantification.

Theoretically, pure cellulose exhibits two peaks in the full XPS spectra: Carbon and Oxygen, with an O/C ratio of 0.83 [4]. Here, this ratio is lower for the reference samples, because of the presence of C-rich molecular segments at the surface of the solids under study, as previously reported [4]. After grafting, this ratio is expected to decrease, but, in reality it remains very close to

that of the reference, i.e., within the experimental error. This ratio decreases significantly only for DAMS-grafted samples. This could be rationalized by the fact that DAMS contains a higher number of CH_2 units.

Owing to the important standard deviation observed, it was not possible the high resolution spectra acquired on our samples.

As a conclusive remark, XPS appears as a very useful tool for the detection of silane adsorbed or grafted onto cellulose fibers. This technique allowed to confirm the remarks previously deduced from SEM-EDX and solid-NMR experiments, and detect the retention of VDMES molecules, which could not be characterized by the previous, less surface-sensitive, techniques. In addition, thanks to XPS measurements, it was possible to deduce the atomic composition of the top surface layers of the fibers and provide a first estimation of the amount of silane retained. Nonetheless, the amount of silicon or nitrogen present in these few layers is very low, as expected, and did not provide enough data to characterize the structures present at the surface. Hence, it is necessary to call upon an even more precise analytical technique, in order to analyze only the top layer of the surface.

III.C ToF-SIMS study

In the frame of this study focusing on the use of organosilanes to modify cellulose fibers, we have called upon various techniques such as Energy Dispersive X-ray Spectroscopy or X-ray Photoelectron Spectroscopy. However these techniques have a depth of analysis close to 1µm for the former, and around 10nm for the latter. Hence, these analytical mean are not perfectly fitted for the analysis of a surface modification limited to the extreme surface of a material.

ToF-SIMS (Time of Flight Secondary Ion Mass Spectrometry), in opposition, is a technique specifically designed to analyze the extreme surface of a material, from one to a few atomic layers. It is a mass spectrometry analysis of elemental and molecular signatures emitted from the surface following the bombardment of the sample using a limited number ($< 10^{12}$ ions/cm^2) of primary ions (here, 22 keV Au+). Using such a technique, it is possible to find direct evidences of the formation of a silane-cellulose bond. For this purpose, the detection of a fragment containing both the silane, or part of it, and cellulose, would provide a clear-cut to answer our scientific question. Nonetheless, the extreme sensitivity of ToF-SIMS can also give clues about the structure of the surface under study, and allow to distinguish of the the effect treatments on the surface composition.

The ToF-SIMS study performed in this work has been divided into two main parts. To begin with, a first set of experiments was aimed at determining if our samples were relevant for ToF-SIMS characterization, and verifying if our process was causing the presence of contaminants on the surface, which would hinder ToF-SIMS analysis. Based on the results of this first part, the sample preparation protocol was improved. Then, a second set of experiments was designed to

analyze the samples made from the improved protocol; the same samples that were characterized by XPS, and SEM-EDX. This second set included samples made from APDMES-, VDMES- and DAMS-treated fibers.

III.C.1 Determination of surface contamination

The nature of our substrate, i.e. paper from cellulose fibers, might cause difficulties for the analysis, as the method of analysis induces the accumulation of positive charges (related to primary ions) at the surface of insulating samples like cellulose. Even if a metal grid in contact with the sample and bombardment using low energy electrons are used to face this problem, it could be insufficiently efficient on some samples. Hence it was decided to verify if we could analyze modified cellulose samples in good conditions. Furthermore, a specificity of our process is that the surface modification is performed on the fibers before the handsheets are prepared. During the fabrication of the handsheets, a contact with a paper specifically used for this purpose (commonly named "Savoyeux") is needed. As this process could be the source of some contamination at the top surface of the handsheets, we have decided to use this first set of ToF-SIMS experiments to assess the quality of our surfaces. In this context, 3 samples were analyzed: (i) a piece of Savoyeux; (ii) a handsheet of unmodified cellulose having undergone the same treatments as the modified sample (heat treatment and solvent extraction); and (iii) a handsheet made of cellulose fibers modified with APDMES.

A first observation is that it was possible to analyze modified cellulose samples by ToF-SIMS analysis. Similarly to the XPS analyses described previously, no significant outgasing hindering the analysis was observed, and if pumping took a longer time than that observed for dry samples, it was considered as affordable. Furthermore, the use of a metal grid and of low energy electrons appeared efficient in neutralizing charge effects. Although the surface of our samples are not totally flat (which could deteriorate slightly the mass resolution), the identification of secondary ions was acceptable. Hence, it is acknowledged that ToF-SIMS is a relevant analysis technique for the study of samples such as the ones that were submitted for analysis during this session.

The first set of spectra, presented in Figure III–13 shows the positive ions fragments from m/z=0 to 200, whereas the second set of spectra (Figure III–14) displays the data acquired in the negative mode for the same m/z region.

Regarding the analyses in positive mode, as observed in Figure III–13, the secondary ions detected at the top surface of the three different samples are very similar. The same characteristic fragments are observed on each sample, at m/z(+) = 15, 29, 43, 57, 73, 85 and 97. Also each sample

present fragments at m/z(+) = 147 and 149, even though the relative intensity between these two peaks somewhat differs among samples.

In the negative mode, as presented in Figure III–14, the detected peaks are again very similar and the relative intensities between peaks are comparable. The characteristic fragments are observed at m/z(-) = 25, 45, 59, 71, 87 and 101.

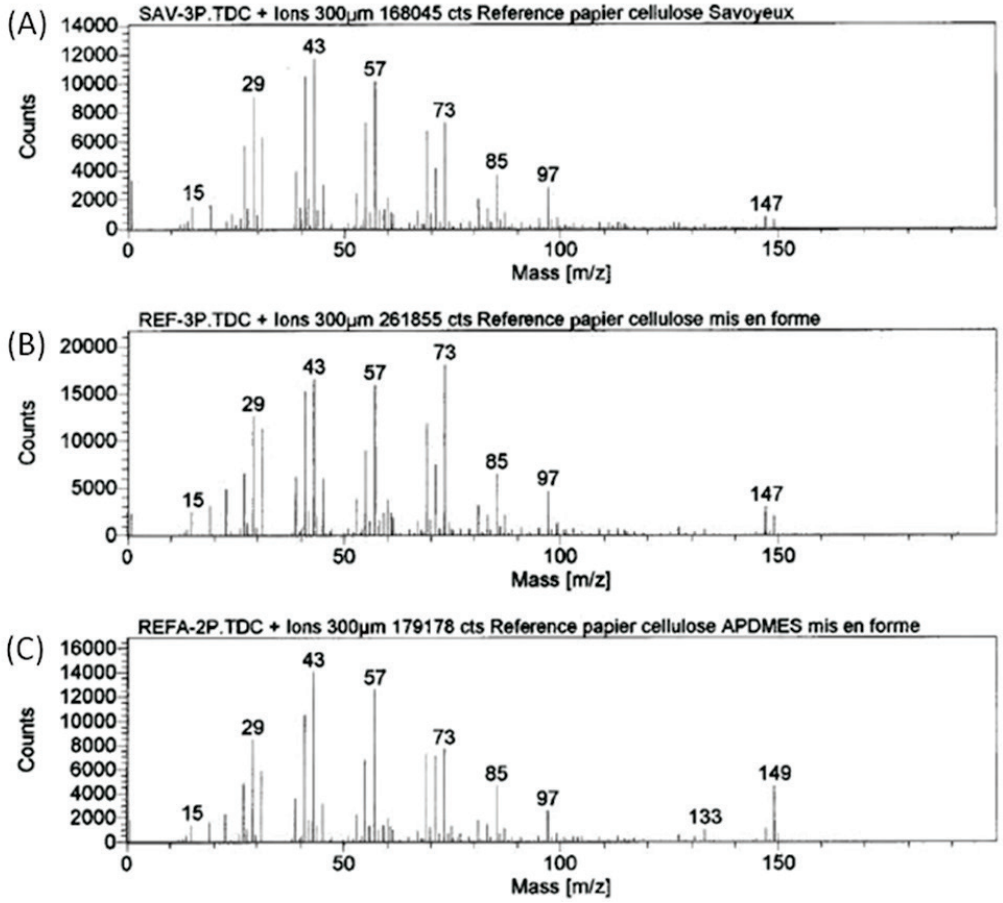

Figure III–13: ToF-SIMS spectra in the positive ion mode (m/z=0 to 200) of (A) Savoyeux sample; (B) Pristine fibers handsheet; (C) APDMES modified fibers handsheet.

At low m/z, for both positive and negative ion modes, the detected ions are very similar for all the samples. They are mostly cellulose characteristic peaks such as the secondary ions detected at m/z(+) = 57 (corresponding to $C_4H_9^+$), 115 (corresponding to $C_8H_3O^+$), 127 (corresponding to $C_6H_7O_3^+$) and 135 (corresponding to $C_6H_{15}O_3^+$) as well as at m/z(-) = 45 (corresponding to $C_2H_5O^-$), 59 (corresponding to $C_2H_3O_2^-$), 71 (corresponding to $C_3H_3O_2^-$), 87 (corresponding to $C_3H_3O_3^-$), 101 (corresponding to $C_4H_5O_3^-$) and 113 (corresponding to $C_5H_5O_3^-$). This is consistent with literature data [5].

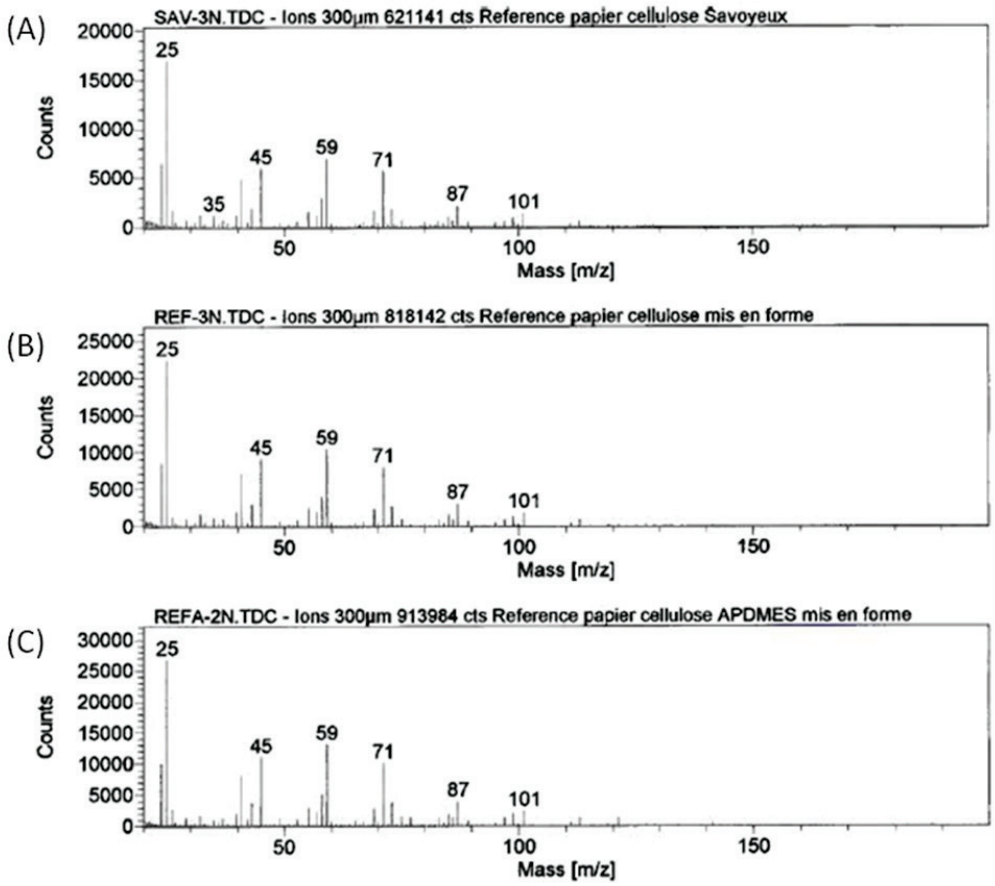

Figure III–14: ToF-SIMS spectra in the negative ion mode (m/z=0 to 200) of (A) Savoyeux sample; (B) Pristine fibers handsheet; (C) APDMES modified fibers handsheet.

The main comment regarding the comparison of the data comes from the surprising similarity between all the samples. It is mostly a surface of pure cellulose even though some unexpected fragments are detected. They could be issued from the pollution of the surfaces by polydimethylsiloxanes (PDMS) (secondary ions detected at m/z(+) = 73 (corresponding to $C_3H_9Si^+$), 133 (corresponding to $C_3H_9Si_2O_2^+$) and 147 (corresponding to $C_5H_{15}Si_2O^+$), or phthalates (secondary ions detected at m/z(+) = 149 (corresponding to $C_8H_5O_3^+$). The detection of these pollutants is unexpected in the samples prepared from the cellulose fibers used in this work. However, the Savoyeux sample is a commercial product used as received, and it is possible that such pollutants are used in its preparation. Since the Savoyeux is used during the drying step of the handsheet preparations, the results could be explained as follows: when the two Savoyeux are removed from the samples, a surface layer of the Savoyeux could remain on the samples. If that layer is not removed during the washing step, the top surface of all the cellulose samples prepared using this technique may be similar to that of a Savoyeux sample.

In order to verify this hypothesis, it was decided to prepare a new unmodified sample, as well as a new APDMES-treated sample, with an adapted protocol. This protocol involved a difference in the preparation of the handsheet. Thus, after the sheet was formed, it was recovered from the wire using powder-free nitril gloves, with the aim of limiting contaminations. The handsheets were then

left to dry under atmosphere and protected from possible pollution from surrounding atmosphere, as described in section II.B.2 of this chapter.

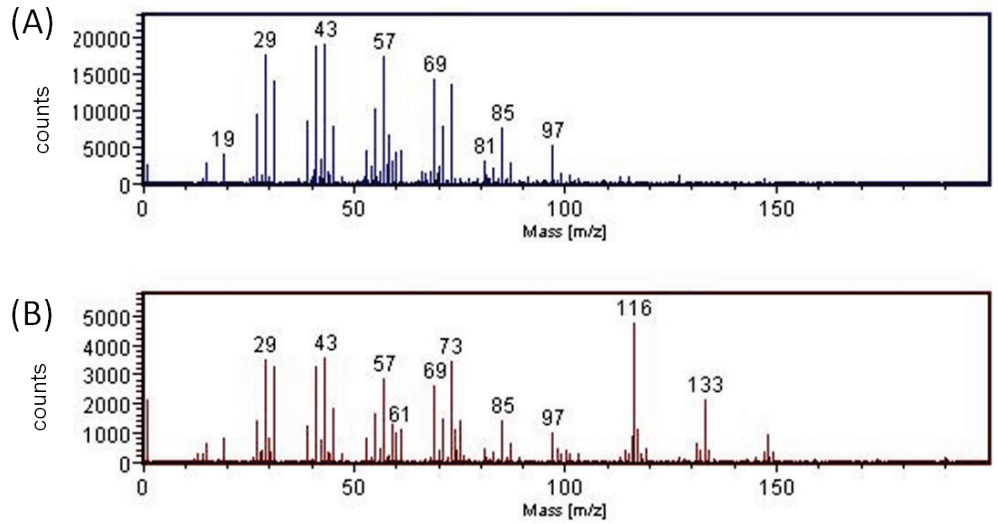

Figure III–15: ToF-SIMS spectra in the positive ion mode (m/z=0 to 200) of (A) a non-silanized sample; and (B) an APDMES modified sample. Both samples being prepared with the improved protocol.

The spectra of these new samples are displayed in Figure III–15. It appears that the new protocol avoided the contamination of the samples. Indeed, the characteristic peaks resulting from the contact with the Savoyeux, as well as the peaks for PDMS and phthalates are not present in a significant amount in the new samples. The reference sample still clearly shows the peaks previously attributed to cellulose, whereas on the APDMES modified sample, new characteristic fragments are detected, at m/z(+) = 116, and 133. Other analyses carried out on APDMES-treated samples and the attributions of these two peaks are further discussed in the next section.

With these evidences of the interest of ToF-SIMS analysis to investigate our cellulose surfaces, as well as with the introduction of a new protocol of handsheet preparation allowing to make samples with a good surface quality, it was decided to perform more experiments on silane-modified celluloses having undergone varied treatments.

III.C.2 Surface characterization of APDMES treated fibers

The ToF-SIMS spectra of a blank sample, and four different APDMES-modified samples (namely (i) without thermal treatment or solvent extraction; (ii) with thermal treatment but without extraction; (iii) without thermal treatment but solvent extracted; and (iv) both with thermal treatment and solvent extraction) were acquired both in the positive and negative ion modes.

At low m/z, for both positive and negative ion modes, the cellulose characteristic peaks are detected. They correspond to the secondary ions previously described, and remain the most important components of the spectra.

In the positive ion mode, the elementary peak of silicon is detected at m/z(+) = 28 (corresponding to Si^+), as expected in presence of silane. In the negative ion mode, the elementary peaks, such as m/z(-) = 12 (corresponding to C^-) or 16 (corresponding to O^-), do not show large variations. However, elementary peaks corresponding to the signature elements of APDMES (nitrogen and silicon), are present in the spectra at m/z(+) = 26 and 28, corresponding to CN- and Si- respectively. It was chosen to represent the variations of these two close peaks to illustrate the impacts of the silane modification, and the various treatments, on the extreme surface composition. Both peaks present much more important contributions to the normalized intensity after the modification, as witnessed by the data presented in Figure III–16.

From this Figure, the relative intensities of characteristic peaks for nitrogen and silicon are shown to follow the same trends depending on the treatments to which the APDMES-treated samples are subjected.

In addition, it has been observed previously [6] that the ratio of the intensities of atomic oxygen and carbon peaks (respectively, OH^- and CH^-) measured in static SIMS correlates well with the O/C ratio measured by XPS. In fact, XPS has shown that the O/C ratio was not affected by the modification, despite the fact that APDMES functionalization should have added only carbon atoms to the cellulose structure. Thus, we have compared these two ratios in Figure III–17, which points out that the ToF-SIMS analyses display a change in the oxygen/carbon ratio for the modified samples, except for the one having undergone a solvent extraction without being thermally treated. The ratio diminution for these samples confirms that the elemental composition of the surface layer has been modified by the silane treatment. The difference of results between the two techniques could be easily rationalized by the extreme sensitivity of ToF-SIMS technique and the associated very low depth of analysis (around 1 nm). In fact, the XPS technique which investigates the top dozen layers of the material, does not show a modification of the atomic composition, whereas ToF-SIMS, which focuses on the top layer only, show significant differences. This may indicate that the silane modification of the cellulose occurs in higher quantities at the extreme surface of the fibers (probed specifically by ToF-SIMS), and that the penetration of the silane in the fiber wall is limited. However, it is well know that chemicals as small as those used here are able to penetrate the fiber wall.

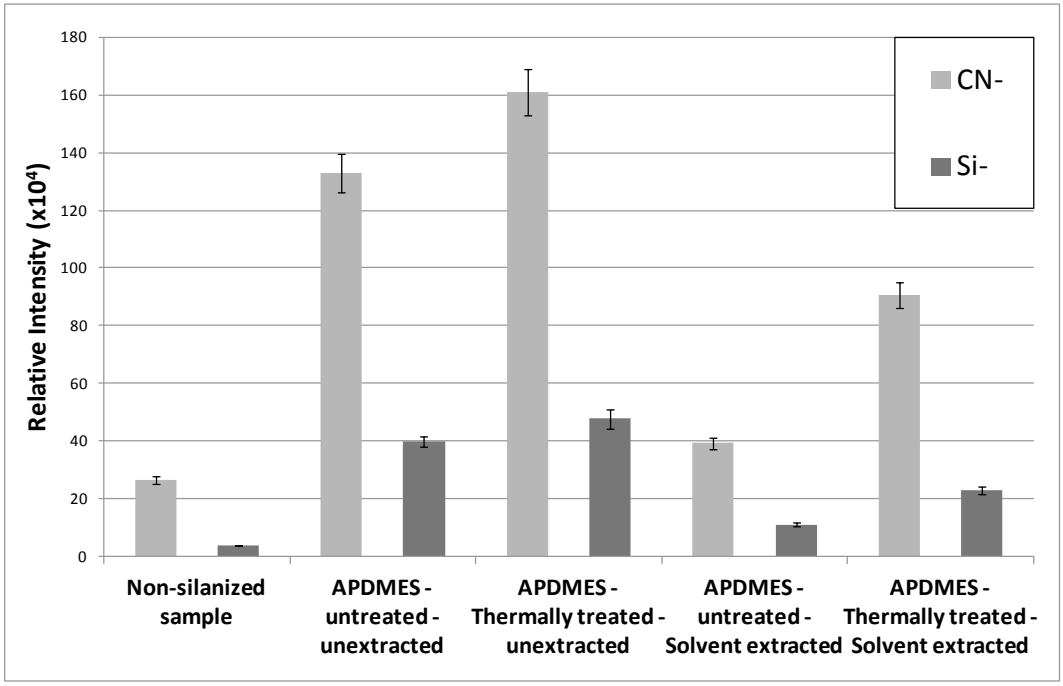

Figure III–16: Relative intensities at m/z(-) = 26 and 28, corresponding to CN^- and Si^- respectively.

As discussed earlier, the O/C ratio observed by XPS is close to 0.65, instead of the 0.83 deduced from the cellulose structure. The value obtained for the OH^-/CH^- ratio varies between 1.8 and 2.3, which may seem surprising. However, it is important to consider the fact that the values obtained by ToF-SIMS do not represent in any case a quantitative measurement of the surface composition. Rather, it is the variation observed between the different samples which is meaningful with this technique.

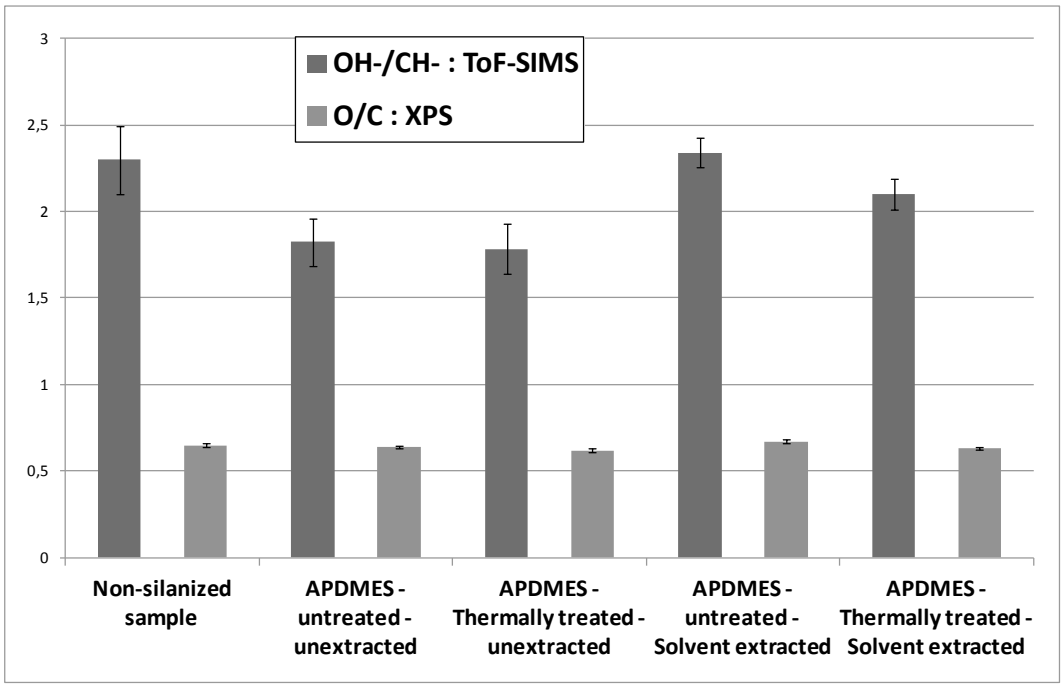

Figure III–17: Comparison between the O/C ratio obtained by XPS, and the OH^-/CH^- ratio obtained by ToF-SIMS.

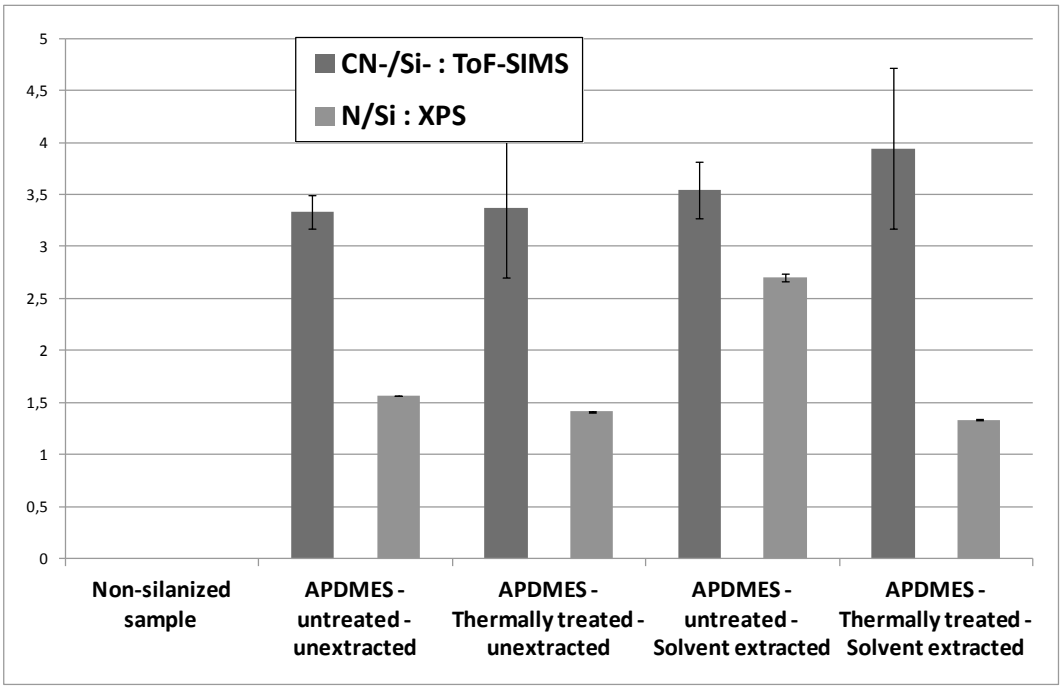

Figure III–18: Comparison between the N/Si ratio obtained by XPS, and the CN^-/Si^- ratio obtained by ToF-SIMS.

A similar comparison between the CN^-/Si^- ratio obtained by ToF-SIMS and the N/Si ratio observed by XPS is presented in Figure III–18. This observation allows confirming that the unlikely N/Si ratio observed by XPS for the untreated, solvent extracted sample is certainly due to a measurement problem. Thus, it seems that XPS overestimated the amount of nitrogen atoms in that sample. The ToF-SIMS analysis does not show significant differences between the ratio of the N^- and Si^- containing signatures from samples obtained after different treatments on APDMES-treated fibers. This observation is expected since neither the heat treatment nor the solvent extraction which were performed on our samples are expected to cleave the silane molecule and remove only a part of it.

From the variation of the ratio of CN^- and Si^-, as exposed in Figure III–16, it appears that the thermal treatment has very little effect on the surface composition, if not followed by a solvent extraction. On the other hand, a solvent extraction diminishes the amount of silane-related fragments significantly in all cases. However, if the solvent extraction is preceded by a thermal treatment, it is shown that the amount of material removed from the surface is lowered. As expected, the thermal treatment allows retaining an higher amount of silane.

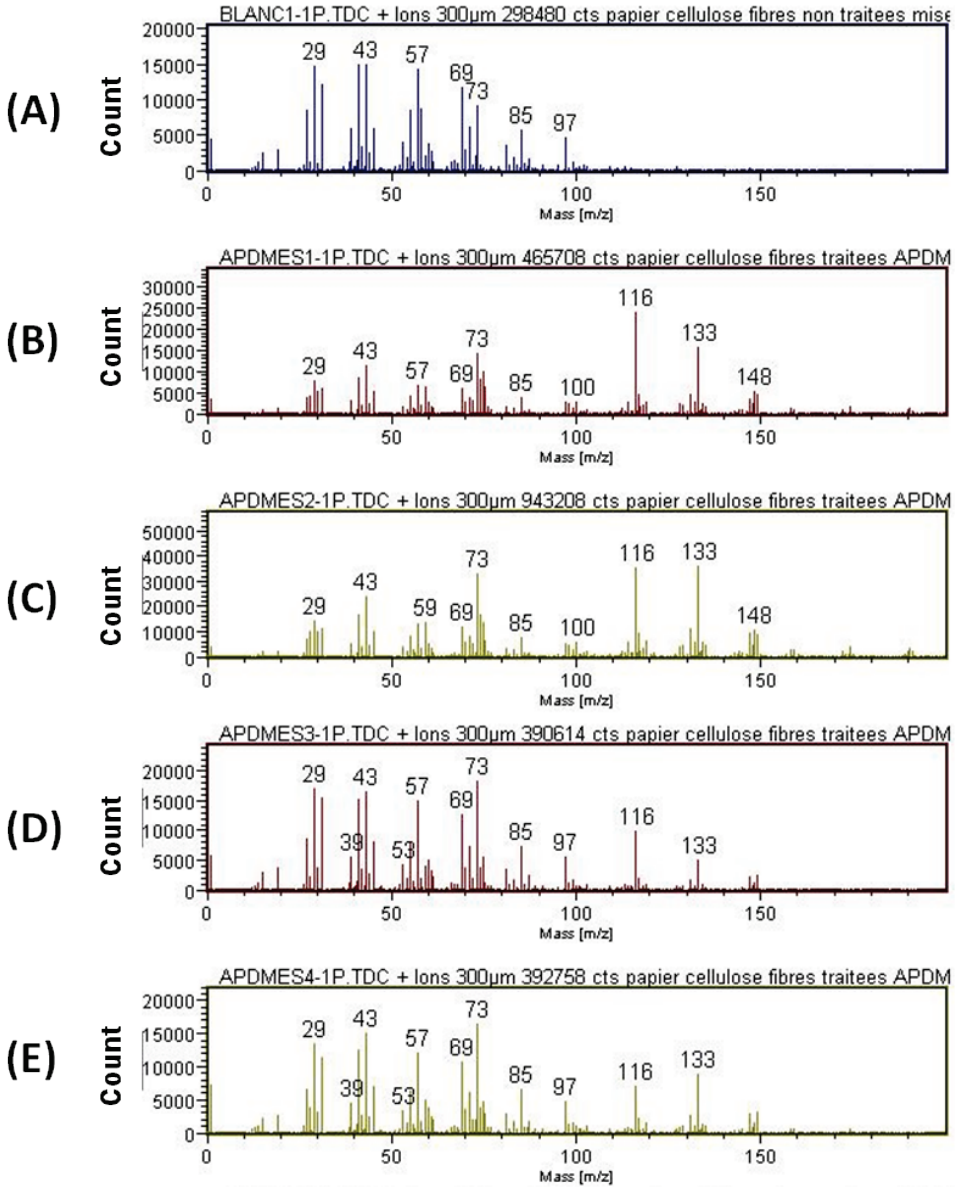

Figure III–19: ToF-SIMS spectra in the positive ion mode (m/z = 0 to 200) of (A) a non-silanized sample; and four APDMES modified samples, where (B) is neither thermally treated nor extracted; (C) is thermally treated but not extracted; (D) is not thermally treated but is extracted; and (E) is both treated and extracted.

At higher m/z, the differences of spectra between the unmodified sample and APDMES-treated ones appear mostly on the positive spectra. Thus, we will focus on the analysis of the positive ions. The set of spectra presented in Figure III–19 shows the positive ions fragments from m/z=0 to 200 for the reference sample and all four APDMES-treated samples.

In this figure, the APDMES-treated samples spectra show enhanced contributions of a new series of peaks, especially at m/z(+) = 116, 133 and 148. At higher m/z, other fragments are detected, with most of them corresponding to small intensity characteristic PDMS signatures.

m/z(+) / Name	Formula	Structure
Hydrolyzed APDMES	$HO\text{-}Si(CH_3)_2\text{-}(CH_2)_3\text{-}NH_2^+$	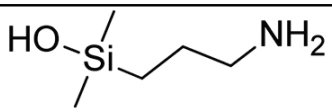
30	$CH_2\text{-}NH_2^+$	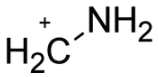
73	$SiC_3H_9^+$	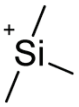
116	$-Si(CH_3)_2\text{-}(CH_2)_3\text{-}NH_2^+$	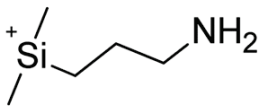
133	$(CH_3)_2Si\text{-}O\text{-}Si(CH_3)_2^+ + H$	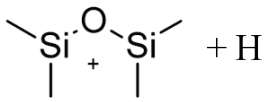
190	$-Si(CH_3)_2\text{-}(CH_2)_3\text{-}NH_2^+ + SiOC_2H_6$	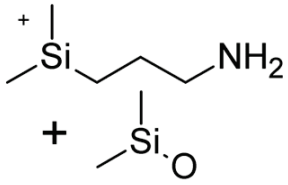

Table III-2: Peak attribution proposed for peaks at m/z(+) = 30, 73, 116, 133 and 190 on APDMES-treated samples analyzed by ToF-SIMS.

In a first attempt, we have chosen the fragment detected at m/z(+) = 116 as a signature ion. The value of m/z detected corresponds to the fragment $-Si(CH_3)_2\text{-}(CH_2)_3\text{-}NH_2^+$, as shown in Table III-2, which corroborates previous findings described in literature [7]. Unfortunately, this fragment is not specific enough to draw clear conclusions regarding the bonding state of the molecule from which it originates. Indeed, this fragment can arise both from the ungrafted adsorbed molecule, from APDMES grafted to the cellulose surface, or from the self-condensed dimer.

Then, we have considered the fragment detected at m/z(+) = 133, which could correspond to the molecular ion $OH\text{-}Si(CH_3)_2\text{-}(CH_2)_3\text{-}NH_2^+$ (see Table III-2 : Hydrolyzed APDMES). However, this cannot be the case since the fragment detected has a m/z close to 133.04, whereas the molecular ion would have a m/z higher than 133.09. With the extreme sensitivity in mass detection of the ToF-SIMS system, such a difference cannot be overlooked. The lower mass of the fragment detected implies that it contains atoms with higher Z numbers. Hence, we propose the attribution of the m/z(+) = 133 peak to the $(CH_3)_2Si\text{-}O\text{-}Si(CH_3)_2^+$ secondary ion as shown in Table III-2. Such a fragment could only be obtained from the APDMES self-condensed dimer.

The spectra after modification also show the presence of other peaks, not referenced in literature, corresponding to secondary ions contributing significantly to the total intensity. A series of peaks are detected at m/z(+) = 73, 74 and 75. The fragment at m/z(+) = 73 corresponds to $SiC_3H_9^+$. Also,

there is a peak at m/z(+) = 148 which follows the same variations as that at 116 after the different treatments. Two other fragments appear at m/z(+) = 174, and 190. Even though the difference in m/z is 16, a more precise mass analysis shows that the fragment at 190 does not correspond to that at 174 with an additional Oxygen atom. Actually, while we do not provide a proposition for the structure detected at m/z(+) = 174, it appears that the fragment at m/z(+) = 190 matches perfectly the mass of that detected at 116 with an additional fragment corresponding to $SiOC_2H_6^+$ (see Table III-2), even though the latter fragment is not detected alone.

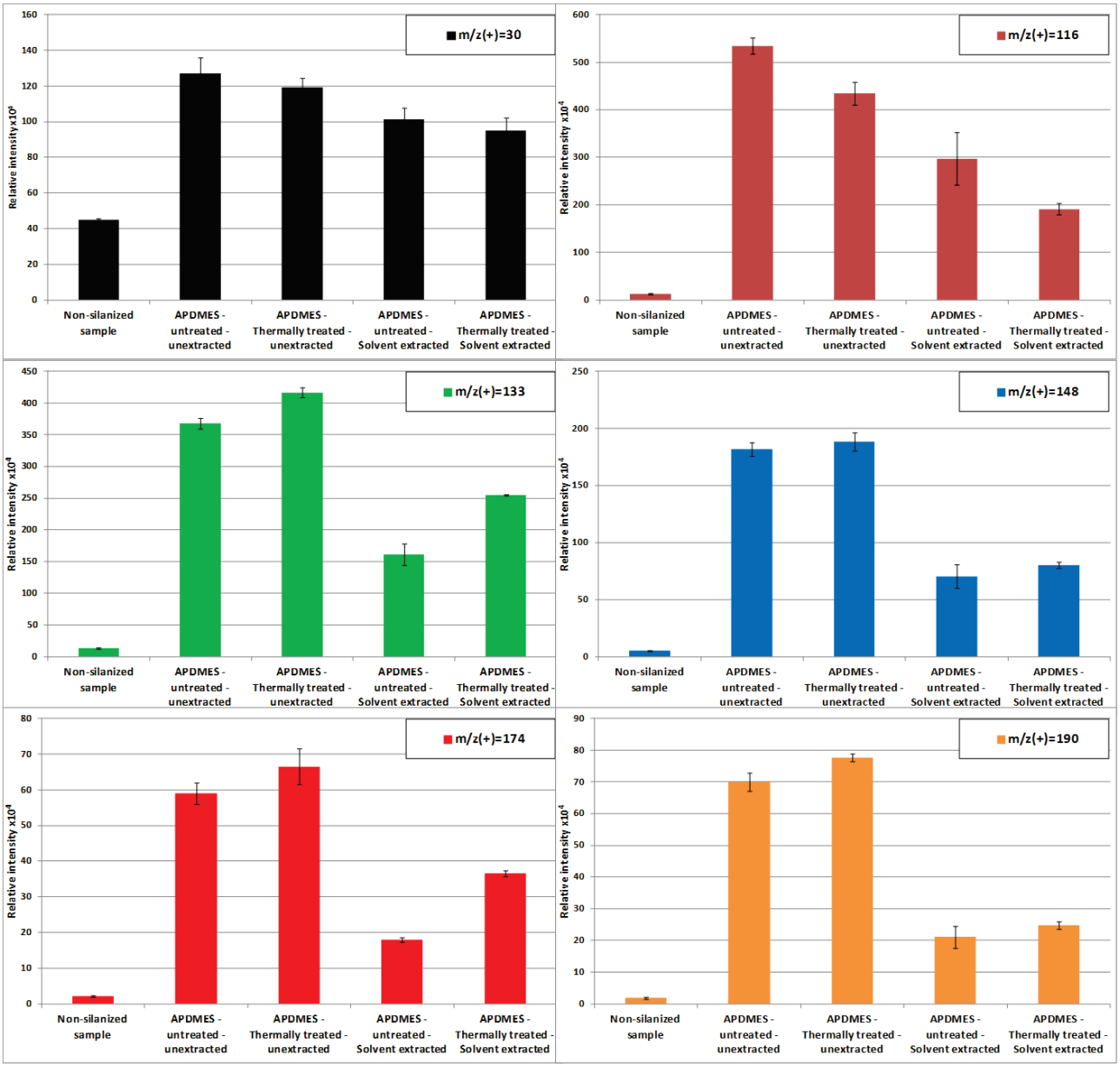

Figure III–20: Variations of the relative intensity of peaks m/z(+) = 30, 116, 133, 148, 174 and 190 on APDMES-treated samples analyzed by ToF-SIMS.

Monitoring the variations of contribution of these fragments to the normalized total intensity (total intensity minus $H^+/^-$ intensity) is interesting, as it appears that different behaviors are observed. As an example, most of the peaks observed are not affected by the thermal treatment (such as m/z(+) = 148 and 190), whereas the importance of the peaks at m/z(+) = 116 (signature peak) and 30 (corresponding to the end of the functional moiety : CH_2-NH_2^+) decrease, and that of the fragments at m/z(+) = 133 and 174 increase. These variations are shown in Figure III–20.

From these data, it is possible to discuss the effect of the thermal treatment on the structures present at the extreme surface of our samples. More specifically, we have observed the presence of two specific secondary ions, at m/z(+) = 116 and 133 respectively, which show very different features. The former signal is not specific to the bonding state of the molecule, whereas the latter arises from self-condensed units. The ratios between the relative intensities of these two fragments for the modified samples are compared in Figure III–21, where it appears clearly that a thermal treatment tends to decrease the 116/133 ratio, whereas the solvent extraction increases it, if the samples are not thermally treated.

It is thus obvious that the thermal treatment, which aims to induce cellulose-silane chemical bonds, also favors the formation of self-condensed dimers, as expected. The extraction protocol allows the removal of an important part of such dimers. However, it appears from the very sensitive ToF-SIMS analysis that a certain amount of dimers is still retained at the surface, which is a new finding.

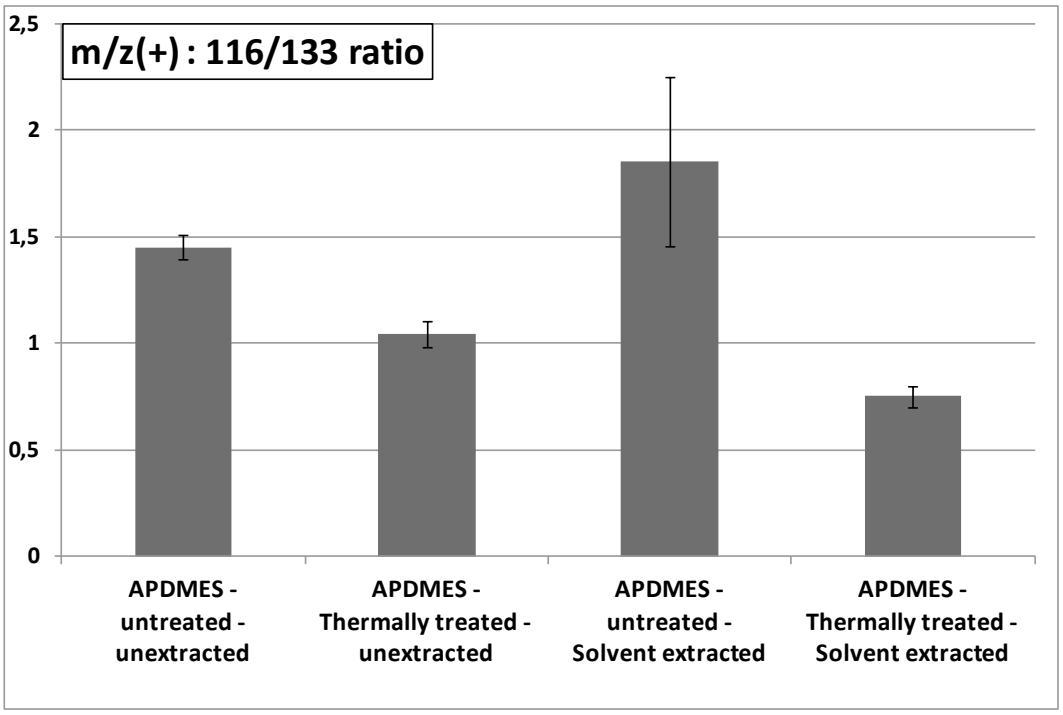

Figure III–21: Variation of the m/z(+) 116/133 ratio for APDMES treated samples.

Since it was not possible to identify secondary ions containing both the silane and cellulose, it is interesting to consider the mode of formation of the secondary ions. It was observed by Dong *et al.* [7] that the ToF-SIMS analysis (positive mode) of aminopropyl terminated PDMS, gave only characteristic fragments at m/z(+) = 116. This fragment includes both the aminopropyl chain and the dimethyl silicon group. The authors did not observe the presence of a fragment at m/z(+) = 58, which would correspond to the aminopropyl functional moiety on its own. Such results were discussed as follow:

"*The terminal group cleavage occurs at the siloxane bond with charge transfer to Si. Silicon is more electropositive than oxygen, so the positive charge would more likely reside on silicon than on oxygen when the Si-O bond is broken. The siloxane bond (799.6 kJ/ mol) is stronger than the silicon-carbon bond (451.5 kJ/ mol), so the Si-C bond should be cleaved more easily. Since silicon is more electropositive than carbon, the positive charge would also reside on silicon when the Si-C bond is broken, forming fragments like [nR +116]+ and [nR + 158]+ rather than [nR + 58]+ and [nR + 100]+. These fragments are observed in the higher mass range*".

These interpretations have a certain interest in the frame of our discussion, since the charge transfer occurring at the silicon atom might play a role on the fragmentation occurring at the surface during ion bombardment in ToF-SIMS experiment.

The ToF-SIMS analysis of APDMES dimers was not reported in literature up-to-date, and thus, the peak observed at m/z(+) = 133 was not described previously. Therefore, we decided to make some propositions regarding its formation: When considering the structure of the dimer, it appears that the electronegative oxygen is at the center of a perfectly symmetric molecule and we can assume that its charge is shared equally between the two neighboring silicon atoms, thus reducing its impact on the cleavage of the Si-O bond, as discussed by Dong [2]. In this eventuality, the formation of fragments with a m/z(+) of 116 would be favored in the case of silane molecules being either ungrafted, or grafted to cellulose. But when APDMES molecules are self-condensed, as fragments at m/z(+) = 133 are formed, comprising the silicon atom, the formation of the fragment at m/z(+) = 116 is hindered since the silicon atom is not available. This means that even if a same quantity of silane is present in the case of a sample containing only hydrolyzed or cellulose-grafted monomers, or in the case of a sample where only dimers are adsorbed, the relative intensity measured at m/z(+) = 116 is expected to be lowered in the second case. However, even though the probability of formation of the fragment is lowered, there is still a significant amount which is formed.

Then, the variations in the relative intensities of these two peaks (m/z(+) = 116 and m/z(+) = 133) can be considered not only in terms of quantity of APDMES present at the surface, but also in terms of its bonding environment. More specifically, since it was shown in our solvent extraction study that our protocol is able to remove ungrafted molecules from the samples (at the scale of sensitivity of EDX), the presence of the fragment at m/z(+) = 116 in large quantities can be interpreted as a sign of the bonding of silane at the cellulose surface.

In overall, the ToF-SIMS study of APDMES-treated samples has allowed to confirm the data obtained by other analytical means, and more particularly those deduced from the XPS study, with a much better accuracy. Also, various secondary ions were identified and their relative intensity variations were discussed. Furthermore, since ToF-SIMS allows to monitor the changes in chemical environment of molecule, such as the changes resulting from its chemical bonding, a mechanism of formation of the secondary ions for the most characteristic peaks was proposed. Based on our observations, even though we were not able to identify a fragment bearing both the silane and cellulose, indirect proofs of the chemical grafting of cellulose by organosilanes were obtained.

III.C.3 Surface characterization of VDMES treated fibers

For VDMES, the same approach was used as for APDMES. Five samples were analyzed in static ToF-SIMS conditions, in both the positive and the negative ion modes. A first observation is that on VDMES modified samples, it was difficult to perform the analysis. More specifically, as measurements were performed on different spots on each sample, it was observed that the surface composition was not homogeneous.

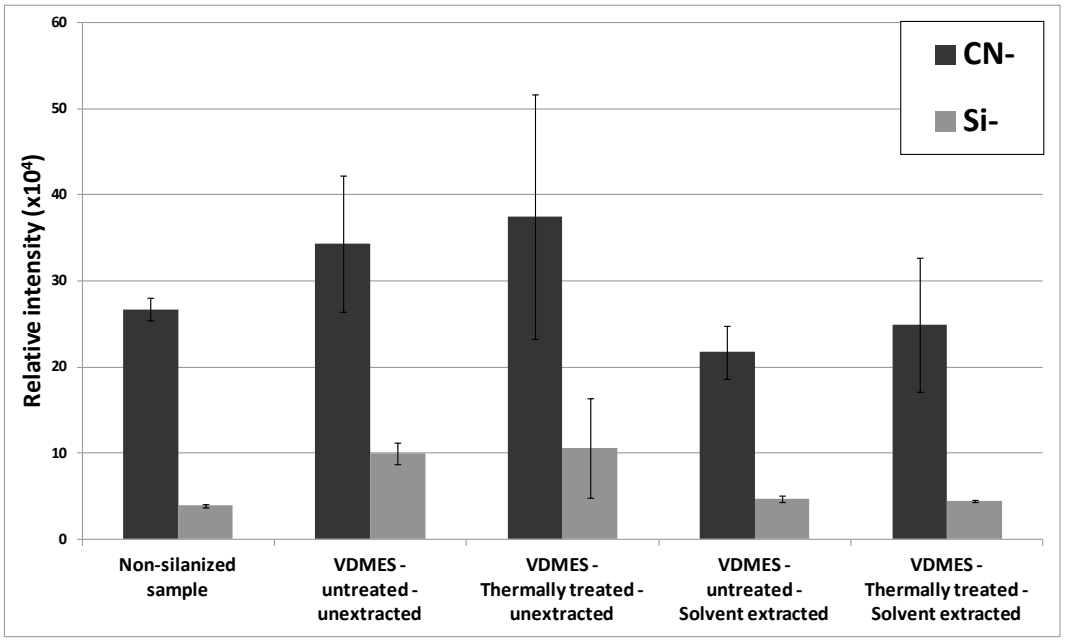

Figure III–22: Relative intensities at m/z(-) = 26 (corresponding to CN^-) and 28 (corresponding to Si^-) for VDMES treated samples.

As for APDMES, all the characteristic peaks of cellulose were observed on the resulting spectra in both modes. Regarding the elementary peaks, it was expected that only Silicon would appear on the spectra, since the structure of VDMES does not bear Nitrogen atoms. Nevertheless, the spectra in the negative mode show the presence of both CN^- and Si^-, as exposed in Figure III–22. Actually, the experimental data show that the two samples which have not undergone any solvent extraction present traces of both Silicon and Nitrogen, even though in much lower quantities than what was observed for APDMES.

These observations are confirmed when controlling the OH^-/CH^- ratio (not shown here), which is lowered for both unextracted samples in comparison to the unmodified cellulose sample. For each of these fragments, after a solvent extraction, the values obtained are equal or very close to those of the unmodified sample. Rather large standard deviations are observed in our measurements, as seen in Figure III–22, which indicates an heterogeneous surface composition onto the VDMES-treated samples. Thus, it is not possible to rationalize the slight differences observed.

When looking at higher m/z region, a few peaks are observed, including at m/z(+) = 116, 133, 148, 174 and 190. These peaks are the same as those observed for APDMES, as confirmed by their precise mass, and are present in rather small quantities. Actually, only one of these secondary ions is expected to be found on MVDES modified samples, namely the ion detected at m/z(+) = 133, since both MVDES and APDMES are able to form a dimer from which this fragment can originate. The outcome of these observations is that MVDES-treated samples have most likely been slightly contaminated with APDMES.

In all cases, after a solvent extraction, either with or without prior thermal treatment, such weakly adsorbed molecules were removed, thus explaining why the spectra corresponding to the extracted samples analyses are very similar to those of the unmodified ones. Since it was shown in our QCM study that MVDES readily adsorbs onto cellulose during the modification process, even though in relatively small quantities, it can be envisaged that prior to the extraction, both silanes are present at the surface. Actually, there could be VDMES grafted, remaining in very small quantities, even after the solvent extraction, which could be detected through the presence of the Silicon elementary peak.

As a conclusion, the surface modifications observed by ToF-SIMS for the VDMES-treated samples are very minute. As the contribution from APDMES traces impacts our analysis, and may cause the large standard deviations observed, it is not possible to draw clear conclusions on this set of samples.

III.C.4 Surface characterization of DAMS treated fibers

DAMS was also analyzed in static ToF-SIMS conditions under both positive and negative ion modes. Again, the characteristic peaks of cellulose were the most important features observed in the spectra for both modes.

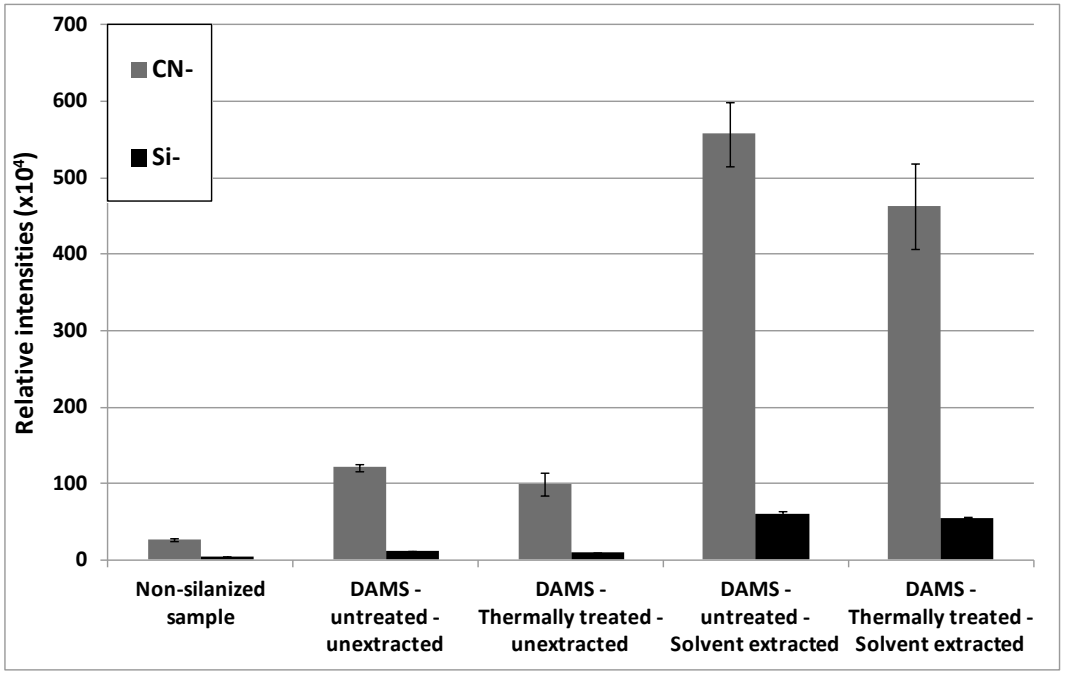

Figure III–23: Relative intensities at m/z(-) = 26 (corresponding to CN^-) and 28 (corresponding to Si^-) for DAMS treated samples.

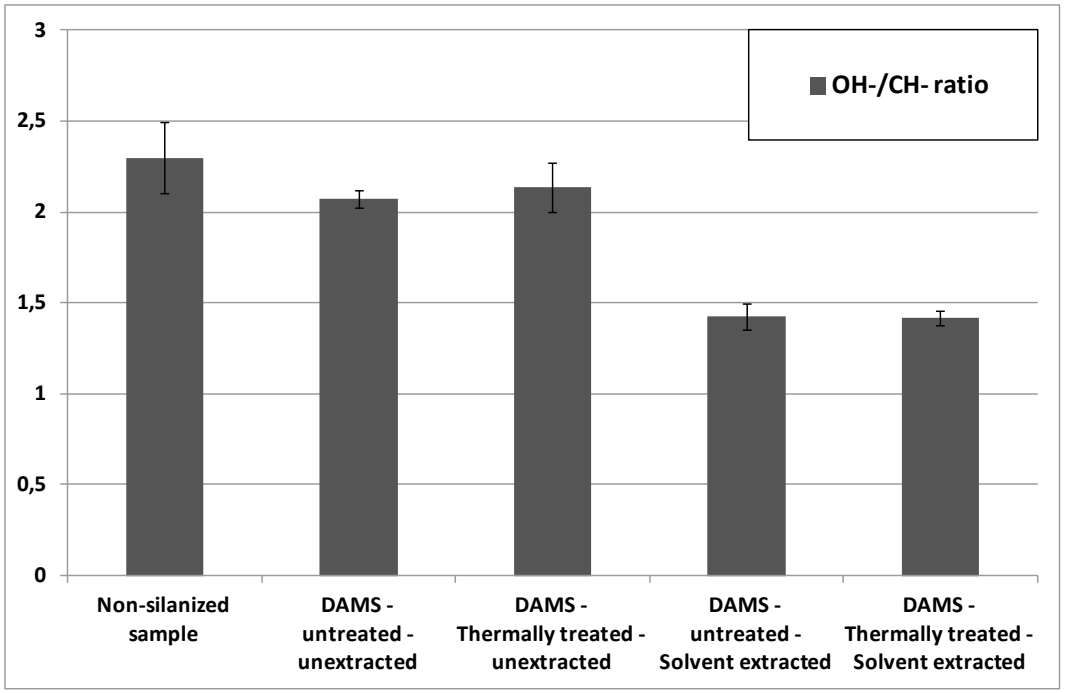

Figure III–24: OH^-/CH^- ratio for VDMES treated samples.

The relative intensities of the Silicon and Nitrogen containing elemental secondary ions are displayed in Figure III–23 where very surprising features are observed. Indeed, for both Silicon and Nitrogen, it seems that the amount detected increases after the solvent extraction, which is unexpected. These observations are further supported by the variation of the OH^-/CH^- ratio, as shown in Figure III–24. This ratio is just slightly diminished after the modification, and it is not further impacted by the thermal treatment; but after the solvent extraction, there is a steep decrease of this ratio. When comparing these results with the O/C ratio obtained by XPS, the data do not match, as it is observed in XPS after the solvent extraction that the O/C ratio is similar to that of the unmodified cellulose. However, the values obtained in XPS regarding the elemental composition of the surface corroborate with the detection of more silicon on the surface after solvent extraction.

In overall, the spectra show that a modification of the surface occurs. Nonetheless, the surprising findings discussed above, regarding the elementary secondary ions, make it impossible to discuss the effect of the thermal treatment on the structures present at the interface. Two hypotheses can be considered at this stage. Either a human error (such as a wrong labeling of the samples) or a problem occurring during the preparation of the samples can be envisaged as a cause. Unfortunately, it was not possible to analyze another set of DAMS modified samples before the completion of this PhD work. Thus this section will be limited to the description of the fragments encountered in the spectra obtained.

First, one can observe a set of peaks at m/z(+) = 116, 133, 148, 174 and 190, corresponding to the peaks previously found on APDMES-modified substrates. Figure III–25 displays that these peaks have a much smaller contribution to the total measured intensity. The peaks at m/z(+) = 116 and 133 are removed by a solvent extraction, thus confirming the idea of a contamination occurring during the sample preparation (most certainly during the drying); whereas the peaks at m/z(+) = 148, 174 and 190 show similar trends to those observed for the atomic secondary ions.

In addition, a set of three peaks more specific to the DAMS-treated samples, and following similar trends, is observed at m/z(+) = 30 (corresponding to $CH_2\text{-}NH_2^+$), 44 (corresponding to $CH_2\text{-}CH_2\text{-}NH_2^+$), and 56 (corresponding to $C_3H_6N^+$). These three peaks are obtained from cleavages occurring at the functional moiety of DAMS. Interestingly, the comparison of the data presented in Figure III–23 (for the elemental fragments CN- and Si- at m/z(-) = 26 and 28 respectively), and those shown in Figure III–26 (for the characteristic DAMS peaks at m/z(+) = 30, 44 and 56), proves that all these peaks are following the same variations after the thermal treatment and/or the solvent extraction. More specifically, the relative intensity of these fragments is increased after a solvent extraction.

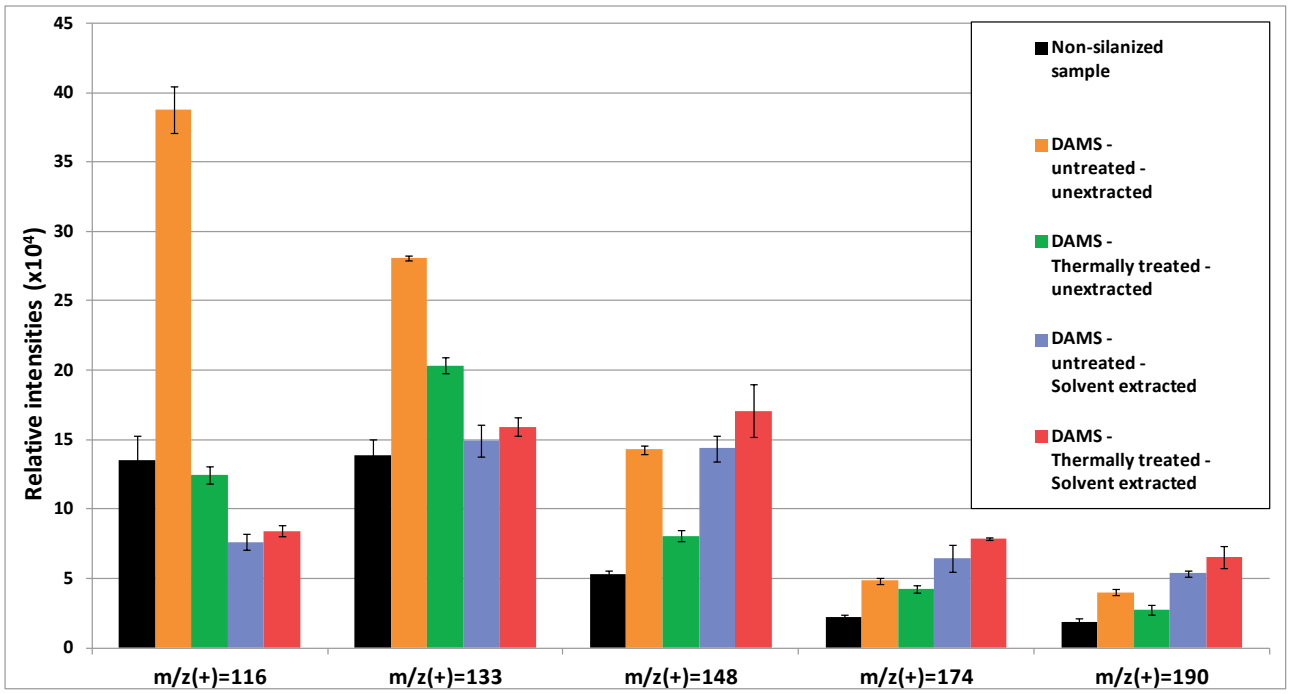

Figure III–25: Relative intensities for potential APDMES-related secondary ions at m/z(+) = 116, 133, 148, 174 and 190 on DAMS treated samples.

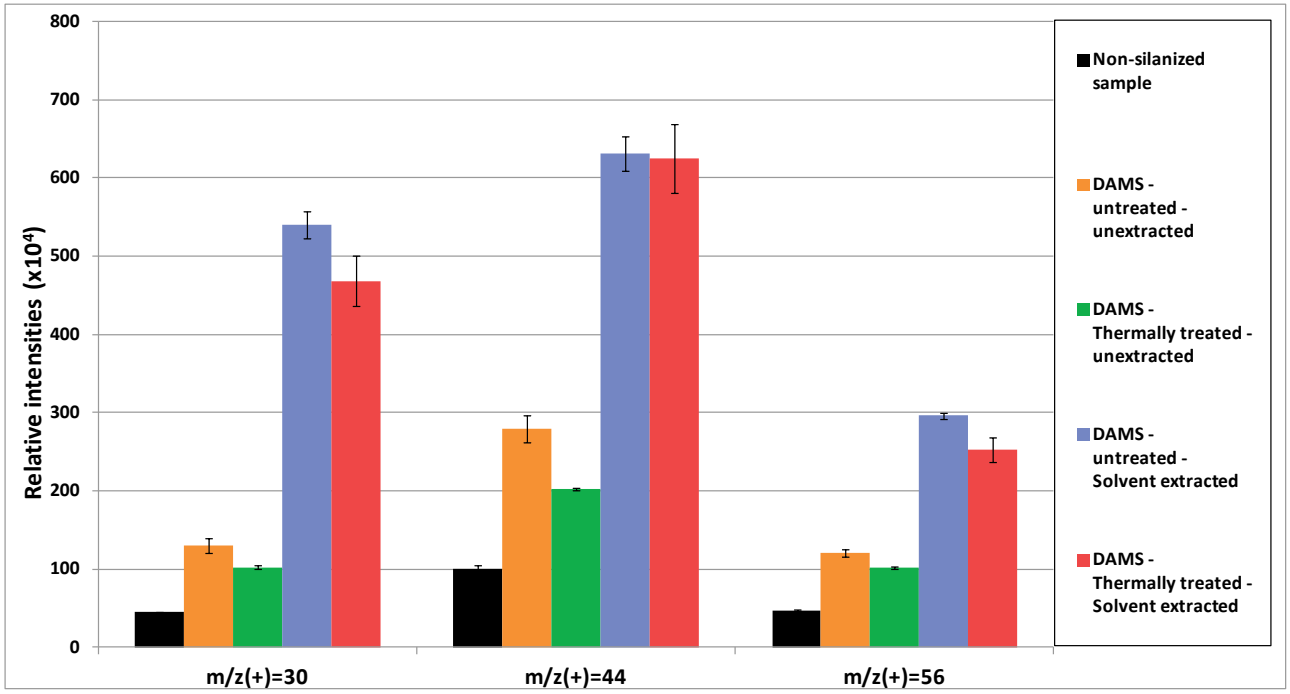

Figure III–26: Relative intensities for characteristic DAMS peaks at m/z(+) = 30, 44 and 56 on DAMS treated samples.

A concluding remark on the study of DAMS modified surfaces by ToF-SIMS is, that despite the uncertainties resulting from unexpected variations of the fragments showing in the spectra, it was possible to confirm the presence of the silane after the treatment. Characteristic peaks were found on every sample, even though the data obtained do not allow discussing the effect of the thermal treatment on the structures present at the interface.

IV. Conclusions and perspectives

In this work, three organosilanes, namely APDMES, VDMES and DAMS, were reacted with cellulose fibers in aqueous suspensions, and the ensuing fibers were used to prepare samples in the form of paper sheets. The prepared samples, as well as those obtained from drop deposits on pristine paper, were used to evaluate the grafting efficiency. It was shown that ungrafted molecules could be removed from the fibers using acetone in combination with an accelerated solvent extractor. Then, the modified paper samples were characterized by SEM-EDX, solid-NMR, XPS and ToF-SIMS, which showed that the process parameters influenced the grafting efficiency. ToF-SIMS allowed identifying precisely the upper molecular fragments at the surface. This technique was so sensitive that it gave rise to identify surface contaminations from an external source or from evaporation-adsorption of silanes. Both XPS and ToF-SIMS showed indirectly that a chemical grafting had indeed occurred between cellulose for at least two of the coupling agents. The surface contamination from another silane did not allow giving clear conclusions on the grafting of VDMES. Nonetheless, this work provides strong evidences about the presence of a chemical bond between cellulose and alkoxysilanes.

This approach should be extended to other mono-alkoxysilane grafting agents, in combination with model cellulose substrate. We have now learned how sensitive is working with ToF-SIMS technique, which gives useful indications about the precautions to be used, when preparing further samples for this technique.

List of references

[1] Technical Association of the Pulp and Paper Industry, *Forming Handsheets for Physical Tests of Pulp*. 2006.

[2] M. Abdelmouleh, S. Boufi, A. Ben Salah, M. N. Belgacem, et A. Gandini, « Interaction of silane coupling agents with cellulose », *Langmuir*, vol. 18, n°. 8, p. 3203-3208, 2002.

[3] M. Castellano, A. Gandini, P. Fabbri, et M. N. Belgacem, « Modification of cellulose fibres with organosilanes: Under what conditions does coupling occur? », *Journal of Colloid and Interface Science*, vol. 273, n°. 2, p. 505-511, 2004.

[4] M. N. Belgacem, G. Czeremuszkin, S. Sapieha, et A. Gandini, « Surface characterization of cellulose fibres by XPS and inverse gas chromatography », *Cellulose*, vol. 2, n°. 3, p. 145-157, 1995.

[5] A. M. Belu, M. C. Davies, J. M. Newton, et N. Patel, « ToF-SIMS characterization and imaging of controlled-release drug delivery systems », *Analytical Chemistry*, vol. 72, n°. 22, p. 5625-5638, 2000.

[6] A. Chilkoti, B. D. Ratner, et D. Briggs, « Static secondary-ion mass spectrometric investigation of the surface structure of organic plasma-deposited films prepared from stable-isotope-labeled precursors. 1. Carbonyl precursors », *Analytical Chemistry*, vol. 63, n°. 15, p. 1612-1620, 1991.

[7] X. Dong, A. Proctor, et D. M. Hercules, « Characterization of Poly(dimethylsiloxane)s by Time-of-Flight Secondary Ion Mass Spectrometry », *Macromolecules*, vol. 30, n°. 1, p. 63-70, 1997.

Chap 4: Evaluation of paper modification by organosilanes

Table of contents

List of figures - 184 -
List of tables - 184 -
I. Paper technology - 185 -
I.A The papermaking process - 185 -
I.B Paper properties - 188 -
I.C Softness - 189 -
I.D Tissue+ - 193 -
I.E Patents on the topic - 196 -
List of references - 198 -
II. Materials and Methods - 201 -
II.A Materials - 201 -
II.B Methods - 202 -
III. Results and Discussion - 205 -
III.A Preliminary study - 205 -
III.B Tissue+ Softwood pulp - 207 -
III.C Tissue+ Eucalyptus pulp - 209 -
III.D Extended study on Eucalyptus pulps - 212 -
III.E Discussion - 216 -
IV. Conclusions and perspectives - 219 -
List of references - 220 -

List of figures

Figure I–1: From trees to paper: Main steps of papermaking - 186 -
Figure I–2: Refining of fibers (Source: [6]) - 187 -
Figure I–3: Creping blade definition diagram (source: [32]) - 191 -
Figure I–4: Possible applications for softener/debonder during tissue manufacturing (source: [36]) - 192 -
Figure II–1: Structure of DAMS. - 201 -
Figure III–1: SEM-EDX analyses for EucaT+ pulps - 212 -
Figure III–2: SEM-EDX analyses for RsxT+ pulps - 212 -
Figure III–3: Possible interactions at the fiber-fiber interface. (Source: [25]) - 218 -

List of tables

Table III 1: Characterization of handsheet papers for RsxTh pulp (32°SR). - 205 -
Table III 2: Morphological analyses for RsxTh pulp. - 206 -
Table III 3: Characterization of handsheet papers for RsxT+ pulps. - 208 -
Table III 4: Morphological analyses for RsxT+ pulps. - 208 -
Table III 5: Characterization of softness handsheet papers for EucaT+ pulps. - 210 -
Table III 6: Morphological analyses for EucaT+ pulps. - 210 -
Table III 7: Characterization of retention handsheet papers for EucaT+ pulps. - 211 -
Table III 8: Characterization of retention handsheet papers for unrefined hyper-washed EucaT+ pulps. - 213 -
Table III 9: Characterization of retention handsheet papers for unrefined EucaBS pulps. - 214 -

The work presented in this part was realized in the frame of a project led by CTP, and aimed at providing papermakers with innovative solutions to overcome the antagonism between softness and mechanical properties. This antagonism is related to the loss of softness, which results mostly from the refining of fibers, a mandatory step to achieve satisfactory mechanical properties.

In this context, it was proposed to use the knowledge acquired from the work described in the previous chapters, and modify cellulose fibers with a chosen organosilane, and then evaluate the resulting samples in term of strength properties and softness.

In order to clarify the context in which this work was carried out, the process of fabrication of paper will be briefly described here, and the main physical properties of paper addressed in this work will be introduced, with a particular focus on softness. Also, the frame of the project as part of which this study was initiated will be further explained, as well as the choices performed for this study.

I. Paper technology

Papermaking techniques have been developed for over 2000 years, and many domains of science were involved in the improvement of this useful material. Today, the research on paper is still a very challenging domain. In order to obtain functional grades of papers at competitive prices, papermakers have to control many steps of the process, both in terms of chemistry and physics. Steps such as: (i) the pulping and bleaching of wood fibers, (ii) the physics of the sheet formation, (iii) the chemistry and physical chemistry involved for properties or process enhancement, and (iv) the steps composing the sheets finishing and converting.

I.A The papermaking process

The market for paper consists of several grades of papers, each having its own properties, corresponding to specific applications. Thus, the challenge for papermakers is to propose a grade of paper with the required qualities for the targeted application, while controlling the cost in an industry where margins are generally rather low [1]. For this purpose, many chemicals are used during the pulping and papermaking processes [1], either as fiber treatments (bleaching, deinking, etc.), as process aids (defoamers, retention aids, drainage aids, etc.), or as functional agents (pigments, wet- and dry-strength enhancers, sizing agents, etc.), which provides the final product its properties. In fact, paper manufacturing involves a large amount of chemistry. The addition of chemicals can occur at different stages, such as during the preparation of the fibers, as part of the process in the wet-end, or as a post-treatment.

The cellulose fibers used for papermaking originate mostly from wood, even though the use of annual crops is regularly investigated [2].

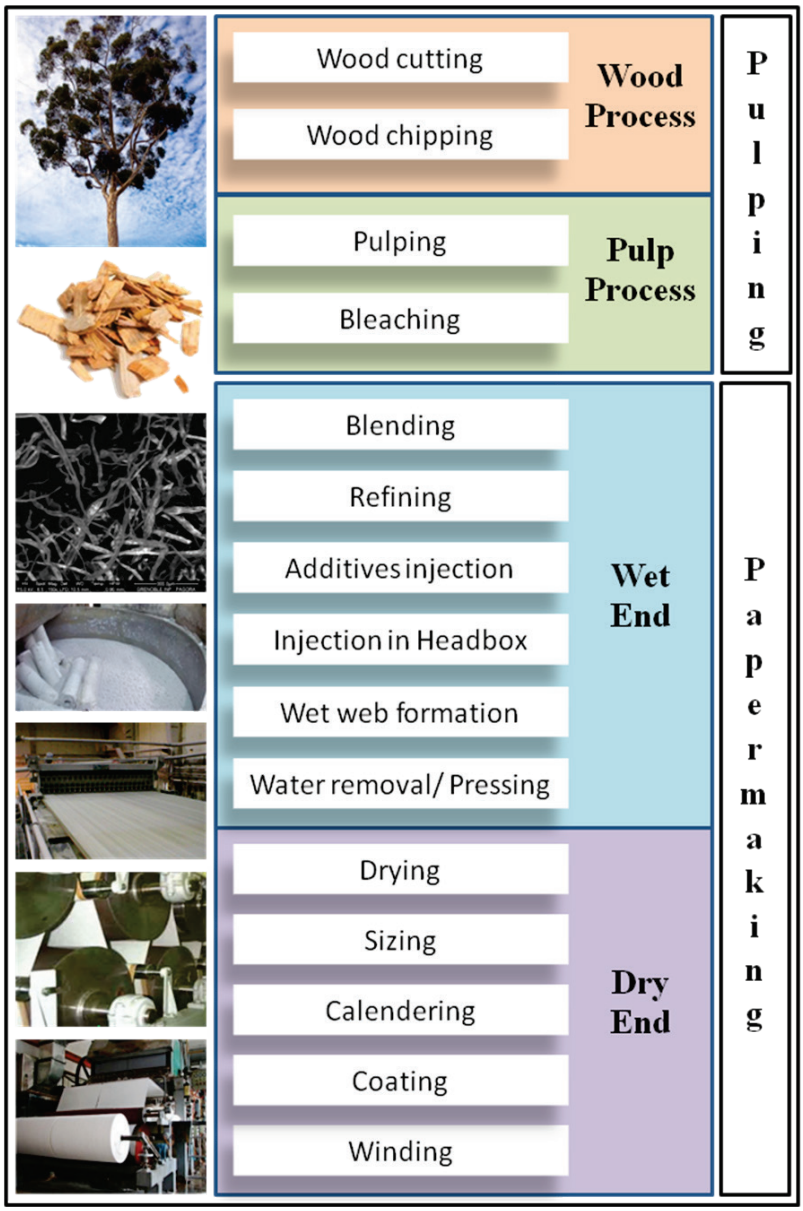

Figure I–1: From trees to paper: Main steps of papermaking

Figure I–1 presents the main steps from the wood transformation until it is converted into paper. First, the wood is cut into chips, which are processed (mechanically or chemically) into a fibrous suspension (pulp) through mechanical processes consisting in separating the fibers from each other by an intensive mechanical action. The process yield is high (close to 90%) and the pulps obtained give papers with low density, high opacity and poor mechanical properties. In chemical pulping, the lignin is dissolved during the cooking step. Consequently, the process yield is rather low (close to 50%), but the pulps give papers with high mechanical properties. After pulping has been performed, bleaching is then carried out for most common paper grades.

In the papermaking process, both virgin or recycled fibers can be used. It is worth noting that, today, more than 50% of the fibers used for papermaking originate from recycling streams.

The papermaking mill can be divided into three main parts: the stock preparation, the paper machine and the finishing operations. It is also usual to consider the paper mill as the association of two parts: the wet end (stock preparation, sheet forming, pressing) and the dry end (drying and finishing). Regarding the stock preparation, and if we focus on the specific case of papers made from virgin chemical pulps, it is common that different types of fibers (ex: hardwood and softwood) are blended together, after a refining operation. Both combined use of various types of fibers and refining confer to the pulp the required properties for the considered paper grade.

The refining operation is an energy-consuming process involving intense mechanical stresses applied to the pulp suspension (see Figure I–2). Such stresses cause the modification of some of the fibers morphological properties, and thus impact the final properties of the paper made from such fibers. More particularly, the shear, compression, and tensile load stresses applied on the fibers are known to have three main effects which are widely discussed in literature [3], [4]: (i) the swelling of the fibers, which arises from water absorption; (ii) the cutting of the fibers which results in a shortening of the average fiber length; and (iii) the fibrillation which increases the specific surface area of the fibers. Both cutting and fibrillation – when fibrils are removed from the wall - are responsible for the increase of the fine elements content in the pulp. Since the intensity of each effect can vary depending on the refining parameters used for a same pulp, refining has to be adapted to the fibers used [3], [5], and the desired properties. It is possible for this purpose to adapt the energy of refining, as well as the type of refiner used.

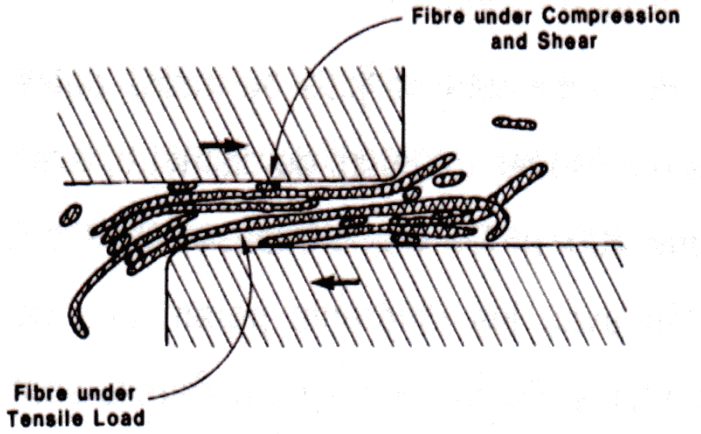

Figure I–2: Refining of fibers (Source: [6])

Refined fibers have a higher flexibility than unrefined ones, and they tend to create more fiber-to-fiber bonds, which allows improvement in mechanical properties and causes the diminution of the bulk. Also, refining modifies the capacity of a pulp suspension to be drained and that of the resulting wet mat to be dried. Quantitatively, the refining can be characterized either by the amount of energy used (for refining a certain amount of fibers), generally given in KWh/t, or by the specific edge load in the refiner, given in $W.s.m^{-1}$. In addition, it is possible to estimate the level of refining of the pulp through the speed of drainage of the diluted fibrous suspension, which can be measured using the Schopper-Riegler test. The result of this drainage test is given in °SR, within a scale varying from 0 to 100°SR. Low SR degrees correspond to no or little refining, whereas higher SR degrees correspond to refined pulps where the fiber morphology has been greatly impacted. As an example, a mild refining of a pine kraft pulp has been reported [7], leading to a Schopper-Riegler index increase from about 13 to 25°SR, and resulting in a diminution of the average fiber length from 2.12 to 2.07mm.

In addition to refining, it is also possible for papermakers to modify the final properties of the paper, or to facilitate the papermaking process by adding chemicals into the pulp suspension in the wet-end part of the paper machine. Most of the wet end additives are added to the fibrous suspension at different points between the blending stage and the headbox. In the same time, the pulp is diluted, at levels as high as 99% or more of water content. This diluted slurry is sent through

the headbox to be evenly distributed on the wire which is moving continuously. During the transfer on the wire, water is removed by different ways, and the paper web is formed. After reaching the end of the wire, the wet web is pressed and conveyed to the drying section where the remaining water is removed. Finally, the paper can go through several finishing steps, such as the sizing, the calendering, or the coating, before being winded into large paper rolls.

The process presented here is actually quite simplified compared to the reality and, as mentioned earlier, does not take into account the increasing use of fibers from recovered papers, which have to be repulped, intensively cleaned and, sometimes, deinked before use [1], [8]. As would be expected, the exploitation of such fibers strongly affects the chemical composition in the pulp and raises several issues. Also, some types of papers, such as tissues, are using different processes due to their specific nature. As an example, in order to maintain the softness and the specific volume of a tissue paper, a steam heated single cylinder (Yankee dryer) is generally used [9] instead of a conventional drying section. The reader interested in these various processes is invited to consult general textbooks on paper production [3], [9-12], or more specific books related to topics such as the history of papermaking [13], or the complexity of the wet-end chemistry [14].

As one can see, papermaking is a very complex industrial process. And more importantly, the conditions used for all the steps listed above, as well as the origin of the fibers, and the chemicals used, are all important parameters in the determination of the properties of the resulting paper.

I.B Paper properties

Various grades of paper can be found, such as newsprint, packaging, printing/writing, coated papers, or tissues, with different paper properties being associated to these grades. A list of important properties is given in Annex 2, and the properties of paper grades in which softness is a relevant issue are better described in section I.C.2 of this chapter.

There are three families of properties under which most physical tests can be classified: (i) the structural properties of the papers, such as the bulk (or specific volume), the thickness, and the basis weight; (ii) the mechanical properties, such as the tensile or tearing strength, which generally result from the structural properties and eventually from the adjunction of additives; and (iii) the optical properties of the finished product, such as the brightness or the opacity, which are particularly important for printing/writing paper grades. Other properties, related to the processability or the recyclability of paper, are also described in literature.

I.C Softness

Softness is the first quality of paper experienced by the user who comes into contact with the material, eventually right after perceiving its optical properties. It is also the first consumer-desired property of tissues [15]. With a global world tissues consumption of over 27 million tons in 2009, and an average annual growth of 3.8% between 1991 and 2009 [16], softness appears to be a key element to control for papermakers. These trends are expected to be sustained thanks to the increasing interests for tissues from emerging markets.

I.C.1 Tissues' softness definition

It is very important to define precisely what softness is, in order to characterize samples with different origins, or treatments. Softness is a very particular quality of a material, owing to the fact that it is a composite property involving different perceptions, including the sight, the sound, and most importantly: the touch [17]. The measurement of softness is associated to "psychophysics", which is the scientific study of the relationship between a stimulus, and the sensation it creates [18-20]. However, since the perception of physical data by the body and their description differ between different cultures, and even between individuals in a same population, defining softness is quite complex.

In the case of tissues, softness is considered to have mainly two components [15], [17]. The first is the "bulk softness", which is related to the flexibility of the tissue: it is the feeling perceived when crumpling a sheet of material in the hand. The second component can be described as the "surface softness", and corresponds to the feeling experienced when smoothly brushing the surface with fingertips.

I.C.2 Softness in papermaking

Many attempts were made to correlate softness evaluations, made by trained panelists, to objective physical properties of papers, more particularly in the frame of the production and characterization of tissue papers. Reviews of such attempts [21], [22] show that even though many different correlations were described, with contradictory observations between studies, a few properties appear to explain a large part of the softness feeling experienced by users. These properties relate to both the fibers and pulp characteristics, and the manufacturing processes. A lot of work has been carried out, and is still currently being performed, in order to provide a better understanding of this property [23], and allow softness improvement. Also, methods for online softness characterization are under investigation, as shown by the recent work from Skedung *et al.* [19], [24-26], which relates the development of new sensors and strategies. The research on softness in tissue applications was largely inspired by the work previously initiated in the textile industry. In

textile applications, softness agents such as silicone releases are used, mainly in order to avoid the increase of fiber-to-fiber interactions during drying.

The current comprehension in tissues is based on the two main components of softness. On one hand, the surface softness was shown to be influenced by properties such as the surface roughness [17], [19], [27], the friction coefficient [27], and the embossing pattern [19] of the finished product. Most likely, such parameters relate to the functioning of the fingertips as sensors and the way of processing data by the human brain. On the other hand, the bulk softness is affected by several parameters. The variations in bulk, and basis weight [27] were found to correlate significantly with softness measurements. As well as the stiffness of the final product [19], the z-direction compressibility [21] or the machine direction-to-cross direction tensile ratio [15]. Some of the properties listed here might impact both the surface and the bulk softness [21].

Most of the paper properties affecting softness relate to the arrangement of the fibers in the material, and to the interactions between these fibers (fiber-to-fiber bonds). As an example, a paper with a low bulk is known to have a higher amount of contacts between fibers, and thus more hydrogen interactions in the system. This means that the system is more constrained, and the fibers have a lower freedom degree between each-other. In the case where the stiffness increases, in the considered range of bulk variation, the perception from the user crumpling the material between his fingers might be negatively impacted.

Since strong relationships exist between the softness and both the fibers origin, and the process and treatments used [28], it is expected that the morphology of the fibers plays a role on softness. The fiber morphology varies between different species, and it is generally acknowledged that fibers with high aspect ratio and longer dimensions are used to bring paper strength. On another hand, *Eucalyptus*, which has rather short fibers, is known to give papers with high softness potential. The effects, on the fiber morphology, of the treatments performed on the pulp are also recognized as a cause for the development or loss of properties. With such considerations in mind, work was previously carried out in CTP [29], [30], on the same pulps as those used in this work. It was shown that it is possible to associate certain morphological analyses with an empirical parameter called: “softness potential” of the pulp. This parameter allows describing properly the softness that will be obtained, after the sheet preparation, from a pulp. The model used is based on five morphological characteristics of the fibers which were found to correlate significantly with softness: the softness increases with the curl index and the percentage of fine elements (% in area), whereas it diminishes when the kink angle, the percentage of broken ends, and the percentage of fine elements (% in length) increase. The model allowed explaining statistically about 80% of the panel tests results. It was also observed that the surface properties (friction coefficient, roughness) of the tested laboratory handsheets and the data obtained from panel tests do not correlate, in opposition to findings on industrial samples.

Refining and the three main effects it has on the fibers (cutting, swelling and fibrillation) have a great effect on the fiber morphology and consequently on the paper properties, including softness. Knowing that refining operations cannot be avoided, since it is the step that allows the paper to have suitable strength properties [6], [9], [28], it is necessary to understand how it affects softness. It is known that refining decreases the bulk of the paper, leading to a denser material, hence affecting its compressibility. Again, this phenomenon is linked to the increase of the fiber-to-fiber bonding, leading to a higher stiffness of the sheet, and thus lower bulk softness.

In order to overcome this effect, and be able to provide materials with suitable strength and increased softness, two approaches are currently used in the industry: the first is a mechanical approach, whereas the second is based on chemical aids.

The mechanical treatment commonly used in the industry, namely creeping, is performed by using a blade to remove the paper from the Yankee dryer, a very common type of drier used for tissues. With a very good control on the blade angle, it is possible to give the paper a specific texture, as shown in Figure I–3.

The force applied by the creping blade onto the surface of the dryer allows breaking bonds and creasing the sheet. The force of the blade also increases the apparent bulk; thus improving the softness of the sheet [31]. This process is particularly difficult to control, and chemical aids are also used during the creping operation (see Figure I–4) in order to control / improve the geometry of the crepe and the release of the paper from the Yankee dryer.

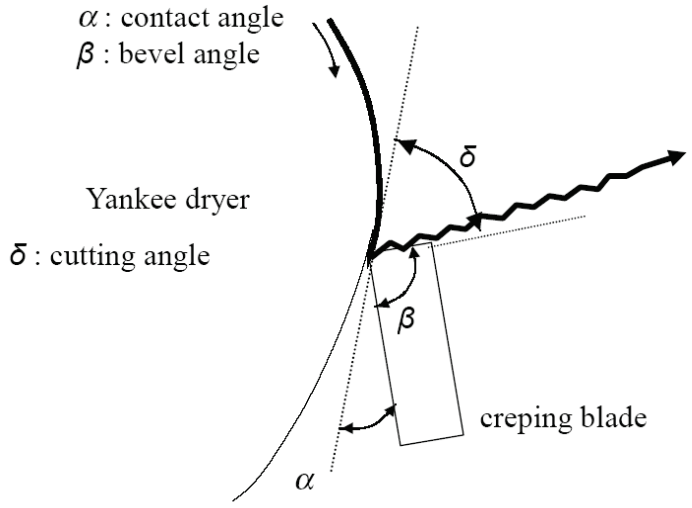

Figure I–3: Creping blade definition diagram (source: [32])

In addition to mechanical processes, chemical aids can be used at the wet-end part of the paper machine, as shown in Figure I–4. These chemicals, generally referred to as debonding agents, are usually cationic (quaternary ammonium) surfactants [33] with fatty chains, and are used as dilute emulsions [34]. The cationic moiety of these agents allows bonding to the weakly anionic surface of cellulose fibers, whereas the fatty chains form a thin lubricant-like film on the fiber surface, preventing excessive inter-fiber bonding [34], [35].

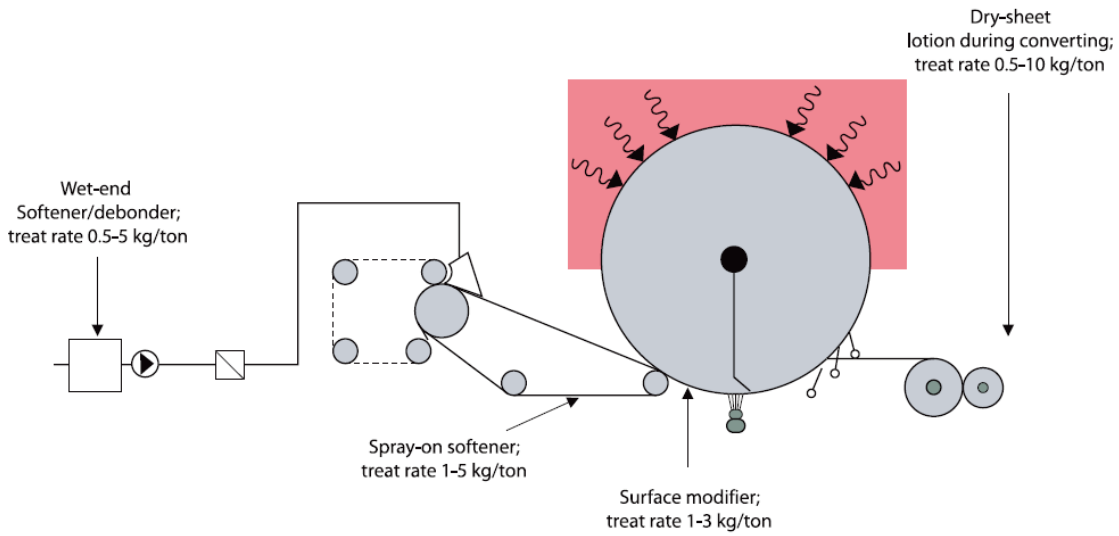

Figure I–4: Possible applications for softener/debonder during tissue manufacturing (source: [36])

In summary, the research started about 70 years ago on tissue softness did not yield yet concluding results explaining the feeling of softness perceived by humans only from objective physical values [21]. The most efficient models up-to-date, based on paper properties, take into account both surface and bulk softness, but are not relevant to laboratory handsheets, owing to the large differences in the methods of preparation [21].

I.C.3 Softness evaluation

Presently, the most recognized protocol for softness evaluation is the use of a so-called "panel tests" [15]. These tests are used to assess the performance of a product, and provide comparative and semi-quantitative results based on the perception from trained panelists. Those panelists often work in the frame of blind tests [19], [25], in order to avoid the bias arising from other properties of the paper such as its color. In such a context, each item is evaluated and compared to a scale of references made up from comparable products.

During such panel-tests, samples conditioned in a controlled environment are tested in different ways, such as brushing the product with fingertips, or crumpling gently the product between fingers [19], [29]. Then, the panelists evaluate the feelings experienced with each sample on a determined scale, based on standards. Other tests, instead of proposing a scaled evaluation, recommend to evaluate if the panelists are able to determine, out of three samples, which one is not similar to the two identical other samples. In addition, the panelist may be invited to classify the softness of the "foreign" sample (more or less softness with respect to that of the two identical ones).

As of today, no other softness evaluation method has been proven to be as accurate as the panel test, despite its prohibitive costs, and the fact that it is a very time-consuming method [15]. Furthermore, softness perception is related to the cultural background of the consumer (as an

example, North American consumers will rate a set of samples in a different order than East Asiatic consumers). Hence, the development of other analytical methods can only be effective when considering a selected market and such methods should be tailored depending on the destination of the end products under scrutiny.

I.D Tissue+

The work presented in this chapter was performed as part of a wider project involving several industrial partners, under the supervision of CTP. This project was based on previous work performed in the company, and was designed to answer specific motivations from papermakers and pulp producers.

I.D.1 Chronology

An extensive work on softness was undertaken by CTP over the previous years, beginning with the "*Softness*" project, which was carried out between 2004 and 2007. Two main axes of research were followed in this project. The first objective was to investigate various commercial virgin pulps refined to exhibit identical mechanical properties, and compare the softness from the resulting papers, in order to establish recommendation on which pulp shall be used for softness applications. The second axe was focused on finding a method allowing continuous online measurement of softness [30].

During the years 2008 and 2009, another project was carried out, namely "*OpTissue*", which was focused more precisely on the study of the pulp potential from recovered fibers, with the specific aim of finding the most suitable sources of recovered paper for softness applications, such as office recovered papers, or newsprints. Also, a part of *OpTissue* was dedicated to providing a comprehension of how each step of the papermaking process impacts the softness of the finished paper [29]. This study confirmed that refining is the step that causes the most important decrease of "softness potential" of the pulp.

Finally, a third project was designed to take place during the period 2009-2011, under the name "*Tissue+*".

I.D.2 Motivations and objectives of Tissue+

In order to help CTP customers to face a very competitive international market, the *Tissue+* project aimed at providing papermakers and pulp producers with innovative solutions for the tissue application, thus helping them to distinguish their own products from those coming from the concurrence. With such a purpose in mind, it is crucial for paper mills to control and develop

different properties. Indeed, such development provides enhanced added value to the product, and also answers an evolution of the demand on the market. Furthermore, such research on the comprehension and the improvement of the paper properties is one of the strategies applied for compensating the increasing costs of raw materials and energy.

While taking advantage of all the data gathered during the previous years, *Tissue+* intended to provide a better comprehension on how the refining process causes the loss of softness potential observed, and to propose original solutions to overcome this phenomenon.

Finally, this project has taken into account the fact that in the past years, new papermaking and pulping technologies, as well as new additives have emerged, which may have rendered previous studies obsolete.

In this context, the main objectives of *Tissue+* were defined as follow:

- Product differentiation increase
- Quality improvement
- New products development
- Lessen customer complaints
- Cost and energy saving: saving potential estimated at ~€200 / T
- CO_2 emissions decrease thanks to thinner papers

I.D.3 Tissue+ work packages

In order to achieve the objectives described above, various ideas were proposed and submitted to the steering committee of the project, which is composed of the industrial partners involved in the project, and CTP experts. The three following axes of research were chosen by the committee as work packages of Tissue+:

- *Enzymatic refining*
- *Grafting / Functionalization*
- *Use of micro-fibrils and nano-particles*

The first work package was focused on the refining of fibers, which was previously investigated in the project *OpTissue*. In the case of *Tissue+*, the investigations were devoted to the impact of enzymes on refining (enzymatic refining), and how the use of such compounds could allow to perform a smoother refining with similar gain of strength properties. Indeed, in order to minimize the negative impact of refining on softness, one of the concepts developed in this work package is to

find a way to provide equivalent mechanical properties while applying a lower refining energy. For this purpose, the use of enzymes, as a pre-treatment prior to refining, could allow to increase the pulp's strength potential at a given refining energy [37], [38], thus limiting the level of refining needed, and the resulting loss of softness. This would help lowering the energy consumption of the process [6], hence giving birth to substantial savings for the producers.

The second work package was focused on the fiber functionalization. It is the objective of the work presented in this chapter. It was envisaged here that cellulose surface modification, by grafting, could allow maintaining a high softness at a level of refining where softness usually drops down, or could allow to enhance mechanical properties without affecting softness, thus limiting the need for refining. More details on this work package, and the motivations of this study, are explained in section I.D.4 of this report.

Finally, the third work package involved the use of cellulose nano- and micro-fibrils as additives. Such materials are still recent and are currently the subject of several studies. Despite being difficult to produce and characterize, they are very promising materials with high reinforcing potential. Such materials could be used to provide higher mechanical properties to pulps with a low level of refining, or they could be used onto the surface of the tissue to impact the surface softness. Noteworthy, such materials, despite their low reactivity inherited from their mostly crystalline structure, have the potential of being modified through surface chemical reactions.

In order to ensure comparative results between the samples in each work package, two types of pulps, one softwood and one hardwood, were selected by the steering committee of *Tissue+*. For each pulp, different conditions of refining were used, and the slurries obtained were shared between the different work packages.

I.D.4 Tissue+ WP2: Cellulose surface modification

The choice of silane coupling agents appeared as a natural solution owing to the versatility of such molecules. For example, the problematic presented here could be addressed by modifying the fibers with a silane which would act similarly to the cationic debonding agents already used in industry, and limit the bonding between fibers, thus modifying the bulk component of softness. A drawback of this method is that the mechanical properties of the paper might be altered as the fiber-to-fiber interactions are lowered. However, the addition of a silane with a functionality which promotes the strength properties in the paper could be envisaged.

Another possibility is the use of a silane aiming at altering the surface softness component. In this context, tri-alkoxysilanes have the advantage of being able to graft onto the fibers, and eventually build small oligomers. Such small silicone chains would have a chemistry similar to some silicone release softeners used in textile applications. Eventually, cellulose modification with such compounds could not only alter the friction coefficient of the material, but also limit the fiber-to-fiber adhesion during drying, hence acting on both components of the tissue softness.

Based on the experience built by our team on silanes and cellulose modification, certain specifications were defined for the choice of a silane molecule. These criteria included : a good water solubility, and a proven reactivity with cellulose. In this context, the choice of an aminosilane imposed itself, and more specifically, the choice was set on DAMS (3-(2-amino-ethylamino)-propyltrimethoxysilane). Indeed, since this molecule had been already thoroughly investigated, by ^{29}Si Nuclear Magnetic Resonance Spectroscopy, and its reactivity toward cellulose had been investigated by various analytical means, it appeared to be the most consistent choice. Furthermore, DAMS being commonly used for diverse applications in large quantities, it is available on the market at interesting bulk prices, in opposition to other research grade molecules.

From a more scientific point of view, various reasons are involved in this choice. In addition to the amine functions providing good solubility, and auto-catalyzed reactivity for reactions involving DAMS in water, the molecule may impact the structure of the tissue in different ways. First, a good silane coverage may inhibit the fiber-to-fiber interactions in the fiber mat, through the diminution of the hydrogen interactions between fibers. Nonetheless, since the silane carries amines, it can also establish hydrogen bonds with cellulose hydroxyls, or with silanes from other fibers, to form physical bonds and thus maintain some strength in the system. But, since the polarity of the amine function is lower than that of hydroxyls born by cellulose (alcohol hydroxyls), the resulting interaction is expected to be weaker than that rising between two cellulose macromolecules. In addition, amine bearing silanes can be positively charged if the amine is protonated, hence providing the chance to create interactions with the weakly negatively charged fibers. Finally, DAMS is able to self-condensate and eventually forms short oligomers bonded to the surface of the fibers, which may act as a lubricant film.

I.E Patents on the topic

While researching for patents relevant to this work, very few documents were found. At the moment of writing, a patent search on the keywords “softness” and “silane”, resulted in 60 answers, most of which are not applicable to the field of papermaking. In fact, only 7 patents were found to relate more or less to this field, with 5 of them having little interest in our case since they only

address the use of organosilicones for textile finishing, or textile softeners. Mostly two documents are highly relevant to this work.

A first patent [39] focused on the use of polysiloxanes bearing quaternary ammonium groups as textile softeners, in a formulation containing glycols, and other compounds, as a fabric softener.

The second patent [40] focused on the use of silicon for softening tissue papers, without reduction in tensile strength. The composition introduced in this document matched some objectives of *Tissue+*, and the formulation also included an amino-alkoxysilane. However the formulation was presented as an emulsion, containing in addition to the silane some silicon fluids, a cationic emulsifier, a nonionic surfactant, a Bronsted base, and water.

Thus, it appears that there is no patent protecting a method for improving the tissue softness by using solutions of silanes in purely aqueous media.

List of references

[1] R. Will, U. Fink, et Y. Ishikawa, *Speciality Paper Chemicals*, SRI Consulting. 2006.

[2] A. L. Hammett, R. L. Youngs, X. Sun, et M. Chandra, « Non-wood fiber as an alternative to wood fiber in China's pulp and paper industry », *Holzforschung*, vol. 55, n°. 2, p. 219-224, 2011.

[3] W. E. Scott, J. C. Abbott, et S. Trosset, *Properties of Paper: An Introduction, Second Edition*, Tappi Press. 1995.

[4] J.-C. Roux, « J6903 - Désintégration et raffinage de la pâte à papier ». Les Techniques de l'Ingénieur, 2008.

[5] Y.-S. Perng, E. I.-C. Wang, Y.-L. Cheng, et Y.-C. Chen, « Effects of fiber morphological characteristics and refiningon handsheet properties », *Taiwan Journal of Forest Science*, vol. 24, n°. 2, p. 127-139, 2009.

[6] M. Lecourt, « Etude de la réduction de la consommation énergétique du raffinage des pâtes chimiques par traitement enzymatique », Université de Provence, Aix-Marseille I, 2010.

[7] D. H. Page, « The beating of chemical pulps - The action and the effects », in *Fundamentals of papermaking*, 1989, p. 1-38.

[8] E. Zeno, « Influence de l'utilisation de la pâte désencrée sur la chimie de la partie humide. », Génie des procédés, Grenoble-INP, 2004.

[9] C. J. Biermann, *Handbook of Pulping and Papermaking, Second Edition*, 2e éd. Academic Press, 1996.

[10] H. Holik, *Handbook of paper and board*. Wiley-VCH, 2006.

[11] S. P.-I. Yhdistys, *Paper and board grades*. Fapet Oy, 2000.

[12] P. Vallette et C. de Choudens, *Le Bois, la pâte, le papier*, 2e éd. Centre technique de l'industrie des papiers, cartons et cellulose, 1989.

[13] P.-M. de Biasi, *Le Papier : Une aventure au quotidien*. Gallimard, 1999.

[14] J. C. Roberts, *Paper chemistry*. Chapman & Hall, New-York, USA: Blackie, 1996.

[15] J. Liu et J. Hsieh, « Characterization of facial tissue softness », *TAPPI Journal*, vol. 3, n°. 4, p. 3-8, avr. 2004.

[16] « RISI, Inc. » [Online]. Available: http://www.risiinfo.com/.

[17] M. B. Lyne, A. Whiteman, et D. C. Donderi, « Multidimensional scaling of tissue quality », *Pulp & paper Canada*, vol. 85, n°. 10, p. 43-50, 1984.

[18] G. A. Gescheider, *Psychophysics: the fundamentals - 3rd ed.*, Erlbaum Associates. New Jersey: Routledge, 1997.

[19] L. Skedung, « Tactile Perception - Role of Physical Properties », 2010.

[20] S. S. Stevens et J. R. Harris, « The scaling of subjective roughness and smoothness. », *Journal of Experimental Psychology*, vol. 64, n°. 5, p. 489-494, 1962.

[21] H. Hollmark et R. S. Ampulski, « Measurement of tissue paper softness: A literature review », *Nordic Pulp and Paper Research Journal*, vol. 19, n°. 3, p. 345-353, 2004.

[22] M. K. Ramasubramanian, « Physical and mechanical properties of towel and tissue », in *Handbook of Physical Testing of Paper*, 2e éd., vol. 1, New York: CRC Press, 2002, p. 690-696.

[23] « PTS - SOftness for TIssue PAper project - SOTIPA ». [Online]. Available: http://www.cornet-sotipa.eu/.

[24] L. Skedung, K. Danerlöv, U. Olofsson, M. Aikala, K. Niemi, J. Kettle et M. W. Rutland, « Finger friction measurements on coated and uncoated printing papers », *Tribology Letters*, vol. 37, n°. 2, p. 389-399, 2009.

[25] L. Skedung, K. Danerlöv, U. Olofsson, C. M. Johannesson, M. Aikala, J. Kettle, M. Arvidsson, B. Berglund et M. W. Rutland, « Tactile perception: Finger friction, surface roughness and perceived coarseness », *Tribology International*, vol. 44, n°. 5, p. 505-512, 2011.

[26] P. M. Hansson, L. Skedung, P. M. Claesson, A. Swerin, J. Schoelkopf, P. A. C. Gane, M. W. Rutland et E. Thormann, « Robust hydrophobic surfaces displaying different surface roughness scales while maintaining the same wettability », *Langmuir*, vol. 27, n°. 13, p. 8153-8159, 2011.

[27] M. Arvidsson, B. Berglund, L. Skedung, M. Aikala, K. Danerlöv, J. Kettle, et M. W. Rutland, « Multidimensional psychophysics : surface feel of printing paper as a function of physical properties ».

[28] J. Gigac et M. Fišerová, « Influence of pulp refining on tissue paper properties », *Tappi Journal*, vol. 7, n°. August, p. 27-32, 2008.

[29] J. Ruiz, V. M. Sacon, F. H. Pescatori Silva, S. Eichhorn, L. Bley, H. Sabel, W. Janssen, G. Eymin Petot-Tourtollet et M. Petit-Conil, « Pulp softness potential : a methodology to assess and compare pulps », *Revue ATIP*, vol. 71, n°. 3, p. 31-45, 2010.

[30] J. Ruiz, V. M. Sacon, F. H. Pescatori Silva, S. Eichhorn, L. Bley, H. Sabel, M. Villette, G. Eymin Petot-Tourtollet et M. Petit-Conil, « Tissue softness potential : an objective on-line industrial value », *Revue ATIP*, vol. 64, n°. 3, p. 10-15, 2010.

[31] L.-sheng Kuo et Y.-lie Cheng, « Effects of creping conditions on the surface softness of tissue paper :Application of sled method », *Tappi Journal*, vol. 83, n°. 12, p. 61, 2000.

[32] J. F. Oliver, « Dry-creping of tissue paper - A review of basic factors », *TAPPI*, vol. 63, n°. 10, p. 91-95, 1980.

[33] P. Fatehi, K. C. Outhouse, H. Xiao, et Y. Ni, « Debonding performance of various cationic surfactants on networks made of bleached Kraft fibers », *Ind. Eng. Chem. Res.*, vol. 49, n°. 22, p. 11402-11407, 2010.

[34] J. S. Conte et G. W. Bender, « Softening and debonding agents », in *Chemical processing aids in papermaking: A practical guide*, TAPPI Press., Kevin J. Hipolit, 1992, p. 166-177.

[35] P. Fatehi, K. Outhouse, et H. Xiao, « Cationic alkoxylated amine surfactant as a debonding agent for papers made of sulfite-bleached fibers », *Ind. Eng. Chem. Res.*, vol. 48, n°. 2, p. 749-754, 2009.

[36] C. Poffenberger, « New additive improves softness with low environmental impact », *Pulp & paper*, vol. 80, n°. 7, p. 40-43, 2006.

[37] M. Lecourt, V. Meyer, J.-C. Sigoillot, et M. Petit-Conil, « Energy reduction of refining by cellulases », *Holzforschung*, vol. 64, n°. 4, p. 441-446, 2010.

[38] M. Lecourt, J.-C. Sigoillot, et M. Petit-Conil, « Cellulase-assisted refining of chemical pulps: Impact of enzymatic charge and refining intensity on energy consumption and pulp quality », *Process Biochemistry*, vol. 45, n°. 8, p. 1274-1278, 2010.

[39] M. Ferenz, S. Herrwerth, et T. Maurer, « Polysiloxanes with quaternary ammonium groups, preparation, and use as textile softeners. », U.S. Patent US20080027202A12008.

[40] R. Arfaoui, G. A. Policello, et I. Procter, « Reactive silicone emulsion composition useful for softening tissue paper and other cellulosics without reduction in tensile strength. », U.S. Patent US20060130990A12006.

II. Materials and Methods

II.A Materials

II.A.1 Silane

The organo-functional silane used here is 3-(2-amino-ethylamino)-propyltrimethoxysilane (DAMS, CAS number: 1-760-24-3). The structure of this silane is given in Figure II–1. Its molar weight is 222.14 g/mol before hydrolysis and the boiling point of the pure product is 264°C. This high purity product (98%) was received from Dow Corning S.A., Seneffe, Belgium (ref: Z-6094).

All fiber modifications were carried out in acidic media, at a pH of 4, which was obtained by adding an appropriate amount of glacial acetic acid to the solution prior to the silane addition. A research grade product from Sigma-Aldrich was used as received.

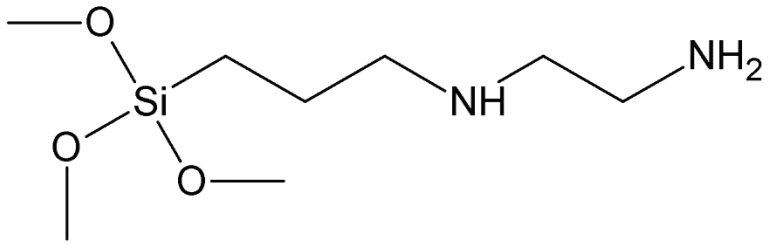

Figure II–1: Structure of DAMS.

II.A.2 Fibers

Various types of fibers were used in this part of the work.

The first type was already introduced in chapter 3 of this work. It is a 100% softwood pulp, refined to 32°SR. This pulp was used in order to assess the modifications on a substrate which had been previously investigated, prior to working on the substrates specifically chosen for *Tissue+*. Samples made from this pulp will be named using the reference "*RsxTh*" all throughout this chapter.

The second and third pulps correspond to specific choices made in the frame of *Tissue+*. The second type of fibers is a commercial pulp, more specifically a 100% softwood bleached kraft pulp, and samples made from it will be labeled using the reference "*RsxT+*".

The third pulp is a commercial bleached *Eucalyptus* kraft pulp from VCP. All samples from this pulp will be labeled using the reference "*EucaT+*".

Finally, an alternative *Eucalyptus* pulp was used, a bleached *Eucalyptus* kraft pulp from Bahia-Sul, whose samples will be labeled "*EucaBS*". This pulp originates from the same geographic area

in Brasil than *EucaT+*, hence presenting similar fiber properties. However, unlike the latter, *EucaBS* was not subjected to an ozone treatment for bleaching.

While the first pulp, R*sxTh*, was only used at one level of refining, which corresponds to its original quality of 32°SR, and *EucaBS* was only used unrefined, both *RsxT+* and *EucaT+* were tested at three different points of refining:

- *RsxT+*: unrefined, and refined with specific edge loads of 1.0 and 1.2 Ws/m,
- *EucaT+*: unrefined, and refined with specific edge loads of 0.2 and 1.0 Ws/m.

The choice of the refining conditions used here was based on previous results obtained during the projects *Softness* and *OpTissue*. Importantly, these different conditions of refining relate to the intensity of the refining performed, and not strictly to a "level" of refining. This means that the conditions used are very different in each case, in terms of load applied onto the fibers and shall not be considered as comparable.

II.B Methods

II.B.1 Pulp modification

The pulp modification was performed using the protocol previously described in chapter 3. All modifications were performed on pulps at 10g/L of fibers, using a concentration of silane equal to 20mmol/L (which corresponds to 44% (w/w) of silane with respect to the dry fiber content). This concentration, which is particularly high in comparison to usual concentrations for additives in papermaking, was used to ensure an excess of product under all conditions, including when the pulp is diluted at the moment of the sheets preparation.

II.B.2 Sheet formation

Two types of handsheets were prepared in this work: retention handsheets and softness handsheets.

In the frame of this study, it was decided to prepare retention handsheets with a basis weight close to 110 g/m². These handsheets are interesting when dealing with chemical additives because the equipment (Retention Handsheet Former) used for their preparation allows forming sheets without diluting excessively the pulp suspension. However, the high fibers concentration favors the flocculation of the pulps, which impacts negatively the strength properties. Retention handsheets were produced following the standard method T205-sp06 (TAPPI standards, [1]). In summary, after the preparation of the fibrous suspension and the modification of the fibers by the silane for 30 minutes, an amount of pulp containing 3 g of dry fibers was introduced in the upper tank of the retention handsheet former, and water was added to reach a concentration of 3g/L. Then, the pulp

was gently stirred for 50s at 800rpm, in order to allow a homogeneous distribution of the fibers into the sheet, without creating high interfacial shear stress on the fiber surface which may remove the adsorbed silanes. The mix was poured onto the wire, and the handsheet was formed after the water was drained. Then, the handsheet was removed from the wire, placed onto a drying plate, with a wire held tight onto its surface in order to minimize dimensional variations, and left to dry at room temperature. Finally, the handsheet was conditioned in a temperature- and humidity-controlled room for at least 48h before further analysis. This procedure was used for both unmodified and silanized samples, and 20 samples were prepared for each condition tested, out of which the 12 samples presenting the most homogeneous fiber distribution were used for the physical tests.

Softness handsheets were prepared on a manual handsheet former. In this procedure, highly diluted suspensions (0.4 g/L) were poured in the upper tank, and stirred manually with a specifically designed stirrer in order to ensure a homogeneous fiber distribution in the tank. Then, the water was drained, thus leading to the formation of the fiber mats which were dried at room temperature, onto drying plates held by drying rings to avoid dimensional variations. All samples were stored under controlled temperature and humidity conditions, similarly to the retention handsheets. For each condition of pulp and refining, 12 samples were prepared, and the 8 samples presenting the most homogeneous fiber distribution were used for physical tests.

II.B.3 Softness measurement

The evaluation of the samples softness was performed by test panels, involving trained panelists from CTP. Two types of tests were carried out for this work.

First, on the samples made from *RsxTh*, triangular tests were performed: panelists were given three non identified samples of softness handsheets, with two samples being exactly similar, and one sample being different (either two blank samples and a silanized sample, or vice-versa). The panelists were asked to identify which was the different sample, and purely qualitatively describe if it is more or less soft than the others. For this purpose, panelists were allowed to both gently crumple the samples, and brush their surface with fingertips.

All other samples were evaluated semi-quantitatively by the panelists, by comparing them with standard samples and giving them a mark ranging between -5 and +5, using both the crumpling and brushing methods. The protocol includes the control of the panelist's accuracy with unlabeled standard samples. The marks given from the different panelists are averaged to give the softness of the sample. The standard deviation measured from CTP panelists shows that difference of less than +/- 0.5 between samples are not significant.

II.B.4 Other physical Properties measurement

All samples were conditioned in a controlled room, under standard conditions of humidity (50 ± 2 %) and temperature (23 ± 1 °C), following the recommendations of ISO 187:1990 [2], at least 48 hours before being tested.

The basis weight of the retention handsheet was measured according to the ISO 536:1995 standard [3], and the thickness and bulk properties were obtained following ISO 534:2005 [4]. The determinations of the tensile properties, tearing resistance and busting strength were made according to ISO 1924-3:2005 [5], ISO 1974:1990 [6], and ISO 2758:2001 [7], respectively.

For softness handsheets, the basis weight was measured following the recommendations of the ISO 12625-6:2005 standard [8]. Also, the thickness and bulk were obtained following ISO 12625-3:2005 [9], and the breaking length and elongation were obtained according to ISO 12625-4:2005 [10]. The burst index and tear index were not measured on softness handsheets.

The differences between the standards for the two types of handsheets can be summarized as follows: (i) for the determination of the basis weight, specific cares have to be taken when cutting the samples, owing to their soft structure, in order to ensure that they have regular areas, and thus provide good measurements; (ii) for the thickness and bulk, the pressure used for the thickness measurement is equal to 100 kPa for retention handsheets, and 2.0 kPa for softness handsheets; (iii) for the breaking length and elongation measurements, the constant rate of elongation used for retention handsheets was 20 mm/min, instead of 50 mm/min for softness handsheets. The test span length for both types of handsheets was 100mm.

II.B.5 Morphological analyses

Morphological analyses were carried out using the MorFi analyzer [11]. This fiber analyzer, based on high resolution optical image analysis, provides various morphological data on a pulp. In the context of our study, we will focus on the most relevant data, i.e. the fiber average length, average weighted length, width, as well as the content in fine elements and the microfibril index. Other parameters described as important in literature or in previous work from CTP, namely the broken ends percentage, the curl index and the kink index, were found to remain roughly constant in our study. Hence these results are not discussed here.

All pulps were analyzed twice, and when significant differences were observed, measurements were reproduced. The results given hereafter were obtained by averaging results from two analyses.

II.B.6 SEM-EDX

SEM-EDX analyses were performed using the protocol and equipment described in chapter 3.

III. Results and Discussion

The work presented in this chapter focuses solely on the results of the second work package of *Tissue+*. A preliminary study was performed using a softwood pulp, before working on the pulps retained for the project. In addition, in order to answer certain questions arising from the main study, complementary experiments were carried out and their results are discussed hereafter.

III.A Preliminary study

In order to verify the interest of using DAMS to modify cellulose in the frame of *Tissue+*, a preliminary study was carried out with the softwood pulp used in the previous chapter (pulp refined at 32°SR). The objective was to assess if a modification performed in the conditions previously described would allow improving either the softness, or the breaking length of the handsheets, or both, at a given refining level. As stated earlier, two types of handsheets were prepared, and tested. The data corresponding to the physical properties and the softness evaluation for both types are presented in Table III-1, whereas the morphological characteristics of the pulps are shown in Table III-2.

***RsxTh* (32°SR)**			***Physical tests***							***Panel tests***
			Basis weight (g/m^2)	**Thickness (µm)**	**Bulk (cm^3/g)**	**Breaking length (m)**	**Elongation (%)**	**Burst index: I_E ($kPa/(m^2.g)$)**	**Tear index: I_D ($mN/(m^2.g)$)**	**Softness (mean)**
Softness Handsheets	*Blank*	*x*	**23**	**136**	**5,87**	**1327**	**6,34**	-	-	**No distinctive difference between the blank and modified samples**
		σ(x)	0,7	5	0,25	69	1,15			
		σ%(x)	3,0	3,7	4,3	5,2	18,1			
	Silanized	*x*	**21**	**118**	**5,49**	**1879**	**6,68**	-	-	
		σ(x)	0,7	3	0,36	123	0,76			
		σ%(x)	3,3	2,2	6,6	6,6	11,4			
Retention Handsheets	*Blank*	*x*	**110**	**309**	**2,74**	**2129**	**1,74**	**1,87**	**3,72**	-
		σ(x)	1,3	20	0,17	263	0,42	0,28	0,42	
		σ%(x)	1,2	6,5	6,2	12,4	24,1	15,0	11,3	
	Silanized	*x*	**118**	**359**	**2,99**	**2576**	**2,43**	**2,03**	**4,01**	-
		σ(x)	2,4	14	0,10	280	0,39	0,17	0,62	
		σ%(x)	2,0	4,0	3,2	10,9	16,0	8,4	15,5	

Table III-1: Characterization of handsheet papers for *RsxTh* pulp (32°SR).

When comparing the trends between the two types of handsheet regarding their physical properties, important differences are observed. More specifically, the bulk of the softness handsheets is twice as high as that of the retention handsheets, whereas, as expected, their breaking length is significantly lower. Also, the elongation of the softness samples is extremely high. These features are difficult to explain taking into account that drying conditions and shrinkage are well controlled. However, important data to consider are the basis weight of the sheet as well as the formation conditions. Indeed, softness handsheets have basis weights close to $20g/m^2$, whereas retention handsheets are closer to $110g/m^2$, and basis weight is known to affect drastically paper properties [12]. In addition, it shall be observed that the modes of preparation of the handsheets differ, not only during the production of the handsheet, with a different concentration of the pulp

used in the tank of the handsheet former, but also during the drying. In fact, the softness handsheets were held by drying rings (drying under constrains), thus ensuring that no shrinkage occurred during drying. Such rings were not available at the size of the retention handsheets, which were maintained in a felted dryer, and left to dry at room temperature. As a result, it appears that it is not possible to compare the results obtained with the different types of sheets, both on this pulp and on the other ones, as described in the next sections.

Regarding the softness samples, the basis weights of the two series, i.e. the unmodified and silanized samples, are very similar. The variation in bulk is barely significant in sight of the standard deviation measured. In terms of breaking length, there is a clear increase (of over 40%) observed after the silane treatment, whereas the variation of elongation is not significant. Finally, the softness which has been solely evaluated by a triangular qualitative panel test has been shown to remain roughly constant between treated and untreated samples.

For the retention sheets, the silanized samples bulk is slightly higher than that of unmodified ones, but the difference is too small. Oppositely, the breaking length of the silanized samples is significantly higher than that of the references, with more than 20% of property enhancement in this case. Finally, the elongation, the burst index and the tear index are all improved by the modification, but the improvements cannot be qualified as clearly significant due to the high standard deviations on these measurements. Such standard deviations on the retention handsheets suggest that the fiber distribution in the sheets is bad, probably because of the type of handsheet former used. However, this former is more convenient to study the retention of chemicals such as silanes on the fibers as stated previously. The low quality of the fiber distribution gives birth to areas with lower fiber contents which are points of failure during the mechanical tests. The experimental drying method used on these handsheets may have allowed certain shrinkage of the sheets to occur during drying, yielding more failure points.

		Morphological analyses					
		Average length (µm)	**Average weighted length (µm)**	**Width (µm)**	**Fine elements (% total length)**	**Microfibril index**	**Average weighted length / width ratio**
Blank	*x*	**944**	**1495**	**30**	**30,5**	**0,84**	**50**
	σ(x)	4,2	31,0	0,2	0,06	0,01	
	σ%(x)	0,4	2,1	0,7	0,2	0,8	
Silanized	*x*	**950**	**1507**	**29,2**	**30,5**	**0,85**	**52**
	σ(x)	14,0	29,0	0,3	0,66	0,01	
	σ%(x)	1,5	1,9	1,0	2,2	1,5	

Table III-2: Morphological analyses for *RsxTh* pulp.

As expected, the morphological properties of the fibers are not impacted by the silane addition, as shown in Table III-2. The length of the fibers may seem short for a softwood; however, the rather

important level of refining of this pulp, as witnessed by the Shopper-Riegler index of 32°, is likely to be responsible for this feature since refining causes cutting and fibrillation of the fibers. This short length of the fibers is responsible for the low aspect ratio of this pulp, in comparison to raw softwood pulps which have generally a ratio above 60-65.

Thus, it appears that the silane treatment of the *RsxTh* pulp successfully caused an increase in terms of breaking length, without impacting significantly the other properties of the paper, and more importantly its softness. The property enhancement is higher on softness sheets than on retention sheets, with 40% and 20% respectively, but this phenomenon is regularly observed, since the density of the material is lower. The silane treatment with DAMS therefore seems to be a potential solution to the *Tissue+* problematic. Therefore, it was decided to continue our investigations on *RsxT+* and *EucaT+* pulps.

III.B Tissue+ Softwood pulp

Based on the results obtained with our preliminary study, samples were prepared with the *RsxT+* pulp, at three different refining conditions. This pulp was used unrefined, thus presenting a Shopper-Riegler value of 13.5°, and refined at specific edge loads of 1.0 and 1.2 Ws/m, thus producing pulps with Shopper-Riegler values of 17° and 23° respectively.

With this pulp, it was not possible to obtain softness handsheets, at any level of refining, after the addition of the silane. Hence, no softness evaluation could be performed. Indeed, from visual observations, it was observed that the pristine pulp had a tendency to flocculate. Moreover, the flocculation level was significantly increased after the addition of silane. Also, in the considered range of the Shopper-Riegler degree, the flocculation increased with the intensity of refining applied, and even a continuous stirring could not allow keeping a sufficiently homogeneous fiber distribution to produce the handsheets, owing to the very low thickness of the softness handsheets.

Despite this flocculation phenomenon, it was possible to produce retention handsheets with unrefined fibers and those refined at an intensity of 1.0 Ws/m, thanks to the higher basis weight used. However, the pulp refined at 1.2 Ws/m could not be used here either. Nonetheless, since the pulps were strongly flocculated, the handsheets produced presented a rather poor formation. This impacted strongly the mechanical properties measured, first through the existence of weak zones which favor a diminution of the values obtained, and secondly through the important values of standard deviation, as shown in the results exposed in Table III-3.

Retention Handsheets			*Physical tests*						
			Basis weight (g/m²)	Thickness (µm)	Bulk (cm^3/g)	Breaking length (m)	Elongation (%)	Burst index: I_E (kPa/(m².g))	Tear index: I_D (mN/(m².g))
RsxT+ Unrefined (13,5°SR)	*Blank*	*x*	**108**	**402**	**3,74**	**1032**	**1,18**	**0,9**	**2,02**
		σ(x)	2,2	5	0,08	145	0,18	0,12	0,19
		σ%(x)	2,0	1,3	2,1	14,1	15,3	13,3	9,4
	Silanized	*x*	**109**	**405**	**3,73**	**1304**	**1,4**	**1,27**	**2,4**
		σ(x)	2,7	15	0,1	153	0,19	0,11	0,31
		σ%(x)	2,5	3,8	2,7	11,7	13,6	8,7	12,9
RsxT+ 1,0 Ws/m (17°SR)	*Blank*	*x*	**108**	**384**	**3,6**	**1268**	**1,32**	**1,12**	**2,18**
		σ(x)	3,1	19	0,17	180	0,21	0,15	0,25
		σ%(x)	2,9	4,9	4,7	14,2	15,9	13,4	11,5
	Silanized	*x*	**113**	**403**	**3,57**	**1577**	**1,58**	**1,52**	**2,68**
		σ(x)	2,3	15	0,18	129	0,22	0,13	0,39
		σ%(x)	2,0	3,8	5,0	8,2	13,9	8,6	14,6
RsxT+ 1,2 Ws/m (23°SR)	*Blank*	*x*	**Flocculation**						
		σ(x)							
		σ%(x)							
	Silanized	*x*							
		σ(x)							
		σ%(x)							

Table III-3: Characterization of handsheet papers for *RsxT*+ pulps.

Similarly to the *RsxTh* pulp, the data presented in Table III-3 show that the addition of DAMS in *RsxT*+ pulps does not impact significantly the bulk of the material. However, for both the unrefined pulp and that refined at 1.0 Ws/m, properties enhancements are observed, despite the rather important standard deviations. More specifically, the breaking length increased by 26 and 24%, the burst index by 41 and 36%, and the tear index by 19 and 23%, for the unrefined and the refined pulp respectively. Finally, the elongation seems to be increased, as well, by 19 and 20%, respectively. Nevertheless, the significance of these results is questioned in sight of the standard deviation observed.

			Morphological analyses					
			Average length (µm)	Average weighted length (µm)	Width (µm)	Fine elements (% total length)	Microfibril index	Average weighted length / width ratio
RsxT+ Unrefined (13,5°SR)	*Blank*	*x*	**1361**	**2129**	**28,6**	**16,5**	**0,34**	**74**
		σ(x)	14,9	19,8	0,0	0,95	0,03	
		σ%(x)	1,1	0,9	0,0	5,8	7,3	
	Silanized	*x*	**1346**	**2125**	**28,2**	**16,3**	**0,34**	**75**
		σ(x)	11,6	16,8	0,1	0,06	0,01	
		σ%(x)	0,9	0,8	0,4	0,4	2,6	
RsxT+ 1,0 Ws/m (17°SR)	*Blank*	*x*	**1307**	**2089**	**29,1**	**19,59**	**0,45**	**72**
		σ(x)	4,2	19,8	0,1	0,31	0,02	
		σ%(x)	0,3	0,9	0,2	1,6	5,1	
	Silanized	*x*	**1301**	**2081**	**28,7**	**18,94**	**0,45**	**73**
		σ(x)	8,9	16,6	0,2	0,36	0,02	
		σ%(x)	0,7	0,8	0,6	1,9	4,2	
RsxT+ 1,2 Ws/m (23°SR)	*Blank*	*x*	**1278**	**2049**	**29,3**	**20,74**	**0,50**	**70**
		σ(x)	8,5	7,1	0,1	1,01	0,00	
		σ%(x)	0,7	0,3	0,5	4,9	0,8	
	Silanized	*x*	**Flocculation**					-
		σ(x)						
		σ%(x)						

Table III-4: Morphological analyses for *RsxT*+ pulps.

As seen in the morphological analyses (Table III-4), the silane treatment does not impact the fiber characteristics, whereas it can be seen that modifying the intensity of refining causes a decrease of fiber length (-4 and -6 % at 1.0 and 1.2 Ws/m, respectively), as discussed in the previous section. It also causes a very slight increase in width due to the swelling of the fibers. Also, as expected, the microfibril index increases with the refining intensity, as well as the fine element contents. Noteworthy, the decrease in fiber length causes the aspect ratio to decrease too. Even though, the ratio presented on this pulp are much higher than those obtained on the *RsxTh* pulp. Such high aspect ratios contribute to the high levels of flocculation in suspensions made from these fibers.

III.C Tissue+ Eucalyptus pulp

For the *EucaT+* pulp, it was possible to produce both softness and retention sheets, and no visible flocculation was observed during the sheet production. This pulp was used unrefined, with a Schopper-Riegler degree of 16°SR, and refined at specific edge loads of 0.2 and 1.0 Ws/m, at 20 and 29°SR, respectively.

III.C.1 Softness handsheets

The results of the physical analyses carried out on softness handsheets are presented in Table III-5, and the morphological properties are shown in Table III-6.

A first observation, regarding the samples production, is that it was not possible to remove the silanized softness handsheets from the wire for the *EucaT+* pulp refined at 1.0Ws/m. Thus, the properties from this series cannot be compared to others, and no softness evaluation was performed. Two possible explanations for this observation are proposed: (i) at a higher level of refining, and hence on a pulp having a higher specific area, a greater quantity of silane adsorbs, and the action of the silane promotes the flocculation, leading to failure points in the wet mat; (ii) the action of the silane favors the water retention, and the amount of water in the wet mat after its formation does not allow to produce enough wet-strength to allow the removal of the mat from the wire. It was possible to produce the other samples; however they were also very difficult to remove from the wire. These features find an explanation in the morphological analyses presented in Table III-5, where it appears that the fibers have undergone an important cutting (-6.3 % for the average length) at a refining load of 1.0 Ws/m. This cutting strongly affects the capacity of the fibers to form a web with sufficient strength to be pulled off from the wire while it is still wet.

Softness Handsheets			Physical tests					Panel tests
			Basis weight (g/m²)	Thickness (µm)	Bulk (cm^3/g)	Breaking length (m)	Elongation (%)	Softness (mean)
EucaT+ Unrefined (16°SR)	*Blank*	*x*	**22**	**110**	**5,05**	**895**	**2,04**	**3,8**
		σ(x)	0,6	4	0,3	85	0,23	
		σ%(x)	2,5	4,0	5,9	9,5	11,3	
	Silanized	*x*	**22**	**105**	**4,73**	**875**	**1,95**	**3,8**
		σ(x)	0,7	6	0,31	72	0,3	
		σ%(x)	3,0	5,2	6,6	8,2	15,4	
EucaT+ 0,2 Ws/m (20°SR)	*Blank*	*x*	**21**	**95**	**4,53**	**2031**	**4,12**	**1**
		σ(x)	0,1	3	0,15	109	0,36	
		σ%(x)	0,3	3,3	3,3	5,4	8,7	
	Silanized	*x*	**22**	**93**	**4,29**	**1936**	**3,7**	**0,5**
		σ(x)	0,2	3	0,15	162	0,45	
		σ%(x)	0,9	3,7	3,5	8,4	12,2	
EucaT+ 1,0 Ws/m (29°SR)	*Blank*	*x*	**22**	**96**	**4,44**	**1453**	**2,88**	**-**
		σ(x)	0,4	4	0,1	87	0,29	
		σ%(x)	2,0	4,2	2,3	6,0	10,1	
	Silanized	*x*	Impossible to withdraw wet sheets from wire					**-**
		σ(x)						
		σ%(x)						

Table III-5: Characterization of softness handsheet papers for *EucaT*+ pulps.

The results presented in Table III-6 show that, at a stronger refining load, the cutting effect on the fibers is much more drastic, whereas the width, the percentage in fine elements and the microfibril index are barely affected by the increase in edge load. This shows that on *Eucalyptus* pulps, important refining intensities (1.0 $Ws.m^{-1}$) tend to damage the pulps, instead of enhancing their properties. Such features, already described in literature [13], explain the more important gain in breaking length observed at the first refining specific edge load (+127%), in comparison with the second one (+62 %). In addition, the elongation varies following the same trend as the breaking length and, finally, the softness, which is given only for the first two points of refining, decreases significantly as the refining increases, as discussed before.

			Morphological analyses					
			Average length (µm)	Average weighted length (µm)	Width (µm)	Fine elements (% total length)	Microfibril index	Average weighted length / width ratio
EucaT+ Unrefined (16°SR)	*Blank*	*x*	**700**	**810**	**16,2**	**24,6**	**0,54**	**50**
		σ(x)	2,1	9,9	0,2	0,34	0,00	
		σ%(x)	0,3	1,2	0,9	1,4	0,7	
	Silanized	*x*	**708**	**832**	**16,8**	**23,9**	**0,61**	**50**
		σ(x)	6,4	9,2	0,4	0,55	0,01	
		σ%(x)	0,9	1,1	2,4	2,3	1,8	
EucaT+ 0,2 Ws/m (20°SR)	*Blank*	*x*	**693**	**812**	**16,4**	**25,3**	**0,62**	**50**
		σ(x)	0,7	0,7	0,0	0,54	0,03	
		σ%(x)	0,1	0,1	0,0	2,1	4,5	
	Silanized	*x*	**697**	**815**	**16,9**	**24,8**	**0,63**	**48**
		σ(x)	1,4	8,1	0,1	0,34	0,01	
		σ%(x)	0,2	1,0	0,8	1,4	1,8	
EucaT+ 1,0 Ws/m (29°SR)	*Blank*	*x*	**656**	**777**	**16,7**	**26,3**	**0,63**	**47**
		σ(x)	1,4	1,4	0,1	0,58	0,01	
		σ%(x)	0,21	0,18	0,42	2,21	2,21	
	Silanized	*x*	**649**	**781**	**17**	**26,2**	**0,64**	**46**
		σ(x)	2,6	2,3	0,1	0,37	0,02	
		σ%(x)	0,4	0,3	0,5	1,4	2,8	

Table III-6: Morphological analyses for *EucaT*+ pulps.

When considering the impact of the silane addition, it appears that the only significant effect observed is the loss of bulk (about 5~7 % of loss). Unlike what was observed on softwood pulps, the breaking length is not impacted by the treatment. Besides, as shown by the panel test results, the softness of the papers produced from such pulps remains constant. In addition, the results exposed in Table III-6 confirm that on this pulp too, the silane treatment does not impact the fiber morphology. Finally, the fiber aspect ratios of all the pulps studied here are in the range of 45-50, that is much lower than the values observed on softwood pulps.

III.C.2 Retention handsheets

The analyses carried out on retention handsheets, whose results are shown in Table III-7, present similar trends than those carried out on softness sheets. The silane modification does not impact the mechanical properties of the paper, and if any minor variations were to occur, the important standard deviations would not allow discriminating them.

The morphological properties of the pulps used for the preparation of these handsheets were already discussed earlier, based on the data presented in Table III-6.

In conclusion, it appears that the silane added to the pulp does not affect the properties of the *Eucalyptus* pulps for both types of sheets. Thus, in order to understand the lack of results on these pulps as compared to the two softwood pulps studied above, a complementary study was initiated, and the results from these investigations are presented in the next section, III.D.

Retention Handsheets			***Physical tests***						
			Basis weight (g/m^2)	**Thickness (µm)**	**Bulk (cm^3/g)**	**Breaking length (m)**	**Elongation (%)**	**Burst index: I_E ($kPa/(m^2.g)$)**	**Tear index: I_D ($mN/(m^2.g)$)**
EucaT+ Unrefined (16°SR)	*Blank*	*x*	**110**	**366**	**3,33**	**955**	**1,28**	**0,5**	**1,58**
		σ(x)	1,1	18	0,17	90	0,24	0,05	0,21
		σ%(x)	1,0	4,9	5,1	9,4	18,8	10,0	13,3
	Silanized	*x*	**111**	**369**	**3,32**	**963**	**1,14**	**0,45**	**1,59**
		σ(x)	0,9	15	0,11	76	0,17	0,07	0,23
		σ%(x)	0,8	4,1	3,3	7,9	14,9	15,6	14,5
EucaT+ 0,2 Ws/m (20°SR)	*Blank*	*x*	**102**	**317**	**3,11**	**1702**	**1,13**	**0,74**	**2,92**
		σ(x)	0,8	17	0,15	174	0,18	0,1	0,33
		σ%(x)	0,8	5,4	4,8	10,2	15,9	13,5	11,3
	Silanized	*x*	**100**	**323**	**3,22**	**1681**	**1,83**	**0,94**	**3**
		σ(x)	0,7	11	0,11	189	0,35	0,08	0,41
		σ%(x)	0,7	3,4	3,4	11,2	19,1	8,5	13,7
EucaT+ 1,0 Ws/m (29°SR)	*Blank*	*x*	**110**	**362**	**3,24**	**1297**	**1,01**	**0,5**	**1,92**
		σ(x)	0,7	16	0,1	125	0,11	0,07	0,17
		σ%(x)	0,7	4,4	3,1	9,6	10,9	14,0	8,9
	Silanized	*x*	**113**	**348**	**3,11**	**1338**	**1,09**	**0,57**	**2,03**
		σ(x)	1,0	12	0,11	82	0,11	0,05	0,24
		σ%(x)	0,8	3,5	3,5	6,1	10,1	8,8	11,8

Table III-7: Characterization of retention handsheet papers for *EucaT*+ pulps.

III.D Extended study on Eucalyptus pulps

The modification of *Eucalyptus* fibers (*EucaT*+) did not show any significant effect on their mechanical properties, in comparison with softwood pulps. First, the success of the silane retention was questioned, since all our work in the previous parts was performed on softwood pulps. Hence, it was decided to verify if the silane had effectively adsorbed and condensed onto the fibers from hardwood origins. Also, the composition of the pulp in terms of fine elements was considered, since from the comparison of Table III-4 and Table III-6 it appears that the content of fine elements and the microfibril index are significantly more important in *EucaT*+ than in *RsxT*+. Finally, the effect of specific treatments undergone by the fibers prior to their use in the project was addressed. More specifically, the *Eucalyptus* pulp *EucaT*+ is bleached using an ozone treatment, which is known to impact the chemical composition of the cellulose fibers. Thus, it was decided to carry out tests on *Eucalyptus* fibers originating from the same geographic area, but bleached with an ozone-free treatment. In this case, ozone sequences were replaced by chlorine dioxide.

III.D.1 Assessment of the silane modification

In order to assess the success of the silane treatment in an efficient way, it was decided to use SEM-EDX analyses to verify the presence of silicon, as a signature of the silane, on both untreated and treated samples from unrefined *RsxT*+ and *EucaT*+. The comparison of the EDX spectra of both pulps is shown in Figure III–1 and Figure III–2, respectively. It appears that both pulps present significant levels of silicon after the silane treatment, sheet formation and drying, whereas the pristine pulps are silicon-free.

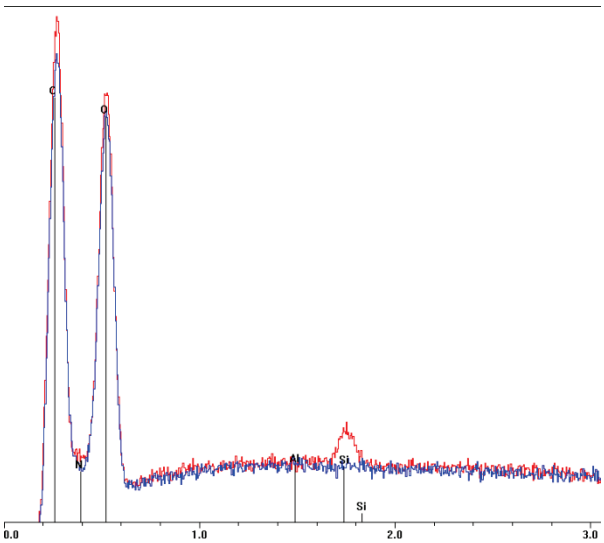

Figure III–1: SEM-EDX analyses for *EucaT*+ pulps (unmodified in blue and silanized in red)

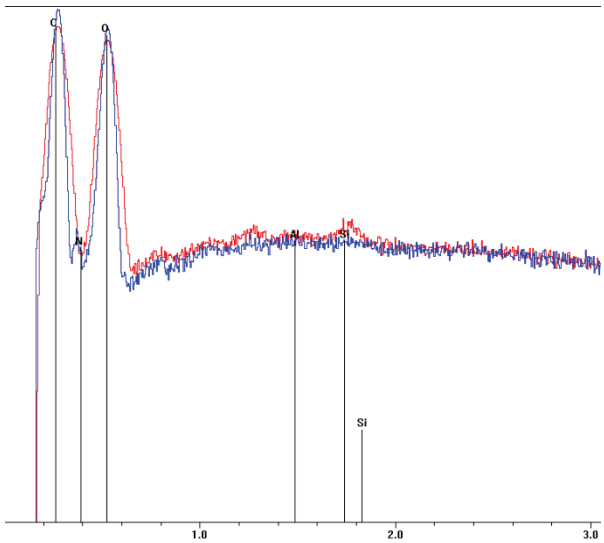

Figure III–2: SEM-EDX analyses for *RsxT*+ pulps (unmodified in blue and silanized in red)

In fact, there is qualitatively more silicon detected in *EucaT*+ pulps than in *RsxT*+, since the silicon peak is clearly visible without magnification on the former, whereas on the latter, it was necessary to use an exponential magnification to enhance the peaks of heavier atoms, thus making clearer the contrast between treated and untreated samples.

III.D.2 Role of fine elements

It is known that the fine elements have high specific area, which makes them able to adsorb higher amount of additives from the solution. As stated before, the amount of fine elements and the microfibril index are slightly higher in *Eucalyptus* pulps to compare with *RsxT*+. So, it was decided to produce handsheets, before and after silane modification, using a fine-free pulp. Hence, unrefined *EucaT*+ pulp was hyper-washed, meaning that is it was thoroughly rinsed on a sieve (with a mesh size of 200µm in our case), in order to remove fine elements.

The prepared pulp was used to produce both softness and retentions sheets. The results, presented in Table III-8, show that the hyper-washing greatly affected the strength properties of the pristine pulp, which are divided by more than two due to the absence of the fine elements. Furthermore, one can see that the silane treatment does not impact the characteristics measured here, hence showing that the fines have a negligible role on the lack of effect of the silane treatment on *Eucalyptus* pulps.

EucaT+ Unrefined (Hyper Washed)			*Physical tests*							*Panel tests*
			Basis weight (g/m^2)	Thickness (µm)	Bulk (cm^3/g)	Breaking length (m)	Elongation (%)	Burst index: I_E ($kPa/(m^2.g)$)	Tear index: I_D ($mN/(m^2.g)$)	Softness (mean)
Softness Handsheets	*Blank*	*x*	**22**	**117**	**5,39**	**396**	**0,77**	-	-	**5,1**
		σ(x)	0,8	5	0,4	49	0,07			
		σ%(x)	3,5	4,5	7,4	12,4	9,1			
	Silanized	*x*	**21**	**108**	**5,2**	**406**	**0,74**	-	-	**4,8**
		σ(x)	1,0	5	0,33	52	0,13			
		σ%(x)	4,8	5,0	6,3	12,8	17,6			
Retention Handsheets	*Blank*	*x*	**114**	**474**	**4,14**	**383**	-	**0,12**	**1,2**	-
		σ(x)	2,0	12	0,04	42		0,02	0,12	
		σ%(x)	1,8	2,5	1,0	11,0		16,7	10,0	
	Silanized	*x*	**109**	**426**	**3,97**	**393**	-	**0,11**	**1,19**	-
		σ(x)	4,0	15	0,13	50		0,02	0,1	
		σ%(x)	3,7	3,5	3,3	12,7		18,2	8,4	

Table III-8: Characterization of retention handsheet papers for unrefined hyper-washed *EucaT*+ pulps.

III.D.3 Impact of pulp bleaching

As mentioned before, the *Eucalyptus* fibers provided for this project were subjected to an ozone bleaching treatment. Such treatment is known to cause an oxidation of the fibers, increasing their negative charge. This may affect the nature of the silane-fiber interactions in the conditions used in this work, the selected silane being cationized under acidic conditions. In order to verify this

hypothesis, samples were prepared from another *Eucalyptus* pulp, which was not ozone-treated, the Bahia-Sul pulp. This pulp originates from the same location as the VCP pulp, hence ensuring similar conditions of growth and similar fiber morphological properties.

Softness and retention handsheets were prepared from unrefined pulp to produce unmodified and silanized samples. These samples were evaluated in terms of their physical properties. The results of these tests, presented in Table III-9, are quite interesting since it appears that a slight decrease of bulk is observed after the silane modification. More importantly, there are slight improvements of the breaking length for both softness sheets, with an increase of up to 13%. Despite the high value of standard deviation associated with these data, slight enhancements in terms of elongation, and burst and tear indexes are observed. In addition, it is confirmed that the softness is not modified by the treatment, also for *EucaBS*.

EucaBS Unrefined			***Physical tests***							***Panel tests***
			Basis weight (g/m²)	**Thickness (µm)**	**Bulk (cm^3/g)**	**Breaking length (m)**	**Elongation (%)**	**Burst index: I_E (kPa/(m².g))**	**Tear index: I_D (mN/(m².g))**	**Softness (mean)**
Softness Handsheets	*Blank*	*x*	**20**	**97**	**4,93**	**873**	**1,15**	-	-	**2,7**
		σ(x)	1,0	6	0,43	38	0,17			
		σ%(x)	5,2	5,7	8,7	4,4	14,8			
	Silanized	*x*	**22**	**105**	**4,83**	**906**	**1,32**	-	-	**2,5**
		σ(x)	0,4	6	0,31	135	0,27			
		σ%(x)	1,7	5,7	6,4	14,9	20,5			
Retention Handsheets	*Blank*	*x*	**112**	**440**	**3,95**	**553**	-	**0,17**	**2,03**	-
		σ(x)	1,3	19	0,15	58		0,02	0,13	
		σ%(x)	1,2	4,3	3,8	10,5		11,8	6,4	
	Silanized	*x*	**105**	**401**	**3,81**	**625**	-	**0,21**	**2,36**	-
		σ(x)	5,7	18	0,32	67		0,04	0,33	
		σ%(x)	5,4	4,5	8,4	10,7		19,0	14,0	

Table III-9: Characterization of retention handsheet papers for unrefined *EucaBS* pulps.

These results show that the fiber chemistry could be involved in the phenomenon described above, but it is also quite clear that the positive effects of the silane treatment on this pulp are very limited, in comparison to what was observed on softwood pulps.

III.D.4 Effect of aspect ratio and flocculation

It is also necessary to consider the aspect ratio of the fibers, and how it impacts the flocculation, since this phenomena was found to be more pronounced for softwood pulps.

The softwood pulps have aspect ratios in the range of 70, at the exception of the *RsxTh* pulp. According to data available in literature [14], typical softwood fibers have lengths ranging between 1.8 and 2.5 mm, and widths in the range of 25 to 50 µm. The pulps used in this work have average

weighted lengths measured at ~1.5 and ~2.1 mm for *RsxTh* and *RsxT*+, respectively, and both have a width close to 30 µm. The low value of fiber length for *RsxTh* pulps explains the low value of their aspect ratio (in the range of 50), despite a similar width to that of *RsxT*+ (~30µm). Most likely, this pulps aspect ratio results from the stronger cutting effect undergone by these refined fibers, as shown by the higher Schopper-Riegler values measured in comparison with *RsxT*+ pulps (32° for *RsxTh*, 13.5 to 23° for *RsxT*+). The silane modification induces positive enhancements of desired properties on all these pulps, without softness loss. However, flocculation phenomena made it impossible to produce part of the samples. It was unexpected that such strong flocculation phenomena would occur when preparing the modified sheets, since the pulps were expected to gain a stronger positive charge after the amine-bearing silane addition in acidic medium. However, it shall be reminded that prior to the formation, the pulp is diluted, and thus the pH of the slurry is increased, which will tend to diminish the charge from the adsorbed silanes amine groups on the fiber surfaces. This could, eventually, lead to a cancellation of the natural negative charge of the fibers, without cationization. With the diminution in charge, the repulsion between fibers diminishes, which favors the flocculation, as observed in our experiments.

Hardwood fibers have typical fiber lengths ranging from 0.7 to 1.1 mm, and widths between 10 and 35 µm [14]. The *EucaT*+ *Eucalyptus* fibers used here have an average weighted length of ~0.8 mm and a width close to 16 µm. All the *Eucalyptus* pulps used in our study had an aspect ratio in the range of 45-50. On these pulps, little or no effects were observed on the paper properties, after the silane treatment.

In papermaking, the aspect ratio of fibers is known to give an indication on their tendency to flocculate [12]. Higher is the aspect ratio, more pronounced is the flocculation. It appears that the aspect ratio of the fiber is not related to the efficiency of the silane modification. However it has a role on the flocculation of the pulp, and impacts the capacity to produce laboratory paper sheets, as well as the standard deviations measured. Despite increasing the flocculation of the pulps, the silane addition gives positive results on pulps which usually have tendencies to flocculate (softwood), while having no measurable impact on the *Eucalyptus* pulp used in this work. Hence, the role of the silane, coupled with that of the aspect ratio of the fibers under scrutiny, is likely to be related to the flocculation phenomenon. In the case where the silane coupling agent acts in the pulp like an anti-flocculent (which is in opposition with our visual observations after the silane addition), and enhance the sheet formation, the systems where the higher aspect ratios are observed would be more impacted, since they tend to flocculate more. However, this explanation would not provide an understanding on the reasons why the modification of the *RsxTh* pulp yielded good results whereas that of hardwoods with similar aspect ratio did not.

III.E Discussion

In light of all the elements developed above, it is possible to develop a better understanding of the effects of the addition of DAMS in a cellulose pulp, to try to describe how the properties of the paper are affected, and propose the mechanism associated with this treatment.

The following points summarize the observations made above:

- The addition of DAMS in the *RsxTh* pulp resulted in better mechanical properties of paper, both for retention and softness handsheets.
- These results were confirmed on *RsxT*+. However, the flocculation phenomena observed on this pulp, did not allow producing softness handsheets. Moreover, the addition of the silane coupling agent increased the tendency of the pulp to flocculate.
- On *EucaT*+, the silane addition did not cause any significant effect, in terms of physical properties of the paper. This treatment impacted, negatively, the removal of the sample from the wire after the wet web formation.
- The silane modification was successfully carried out on *EucaT*+, as assessed by SEM-EDX analyses, and the high amount of fine elements in the pulp did not cause the lack of improvements.
- *Eucalyptus* fibers with a less oxidized surface were slightly impacted by the presence of DAMS in the pulp, in term of strength enhancement. However, the positive effect of the treatment remained rather weak.
- In all cases, the silane addition did not significantly impact the softness of the paper produced from the modified pulps, as shown by the test panels' results.

Based on these observations, it is possible to discuss the potential mechanisms of action of DAMS on a cellulose pulp.

In addition to the argument developed when studying the Bahia-Sul *Eucalyptus* pulp, and in regard to the chemistry of the fibers after ozone treatment, it is possible to consider the difference of chemistry between softwood and *Eucalyptus* fibers. In fact, wood fibers contain other natural polymers than cellulose, like hemicelluloses, whose nature and amount vary between species. Importantly, *Eucalyptus* fibers contain more xylan than softwoods, which in turn are richer in glucomannan. The xylan content, in weight percent compared to the dry weight of the wood, has been reported to be about 18~20% and 5~8%, for *Eucalyptus* and softwoods respectively; whereas the content of glucomannan of the same species has been reported at 1~4% and 15~19%, respectively [15], [16].

In native wood, most of the carboxyl groups contributing to the fiber surface charges originate from uronic acid residues, bound to xylan in hardwoods such as *Eucalyptus*, or arabino-xylan in softwoods [17]. It is worth to note, that xylans are more charged (presence of carboxylic moieties) than softwood hemicelluloses [18]. This charge density is further increased when the fibers have been subjected to oxidizing treatments such as ozone bleaching. The surface charge density of fibers is known to contribute in developing tensile strength of low-density paper structure [19]. In this context, the use of xylans obtained from the cooking of selected wood species, as a paper strength additive, has been investigated [20], [21].

This higher negative charge borne by hardwoods is expected to play a role on the interactions of such fibers with our selected silane, which in the acidic conditions bears a positively charged protonated amine groups. At the acidic pH of 4 under which the modifications are carried out, prior to the dilution and sheet formation, the amount of carboxyl anions is rather low. This is due to the acidic character of the solution, with the pH being very close to the pKa of carboxyl functions (pKa~4.5). However, even though their amount might be rather low, these groups are expected to contribute to the adsorption of the silane onto the surface, in addition to the interactions between cellulose hydroxyls and silanols. Together with the high specific surface of this pulp, the charge density correlates well with the higher amount of silane retained on *Eucalyptus*, as shown by SEM-EDX analyses. This higher amount shall provide the fibers with a more important positive charge, owing to the cationic character of the silane. Our experimental results show that there is no or little effect of the silane treatment on the paper properties of materials obtained from hardwoods fibers, despite the higher amount of silane retained. This indicates that the action of the silane does not seem to be directly related to the surface modification of the fibers.

In order to explain the observed behaviors, we propose to discuss the role of natural polymers, other than cellulose, found in papermaking fibers. The role of xylan in the surface charge of hardwoods was already discussed above, and the parameters impacting this system are discussed in the literature [22]. Similarly, xyloglucan was reported to improve the tensile index values of paper, and improve the sheet formation [23], [24]. Such an increase in tensile strength is attributed to an increase of relative bonded areas between the fibers.

Even though the cooking of the wood chips ~~is~~ is known to dissolve a significant part of the hemicelluloses present in the wood, these dissolved hemicelluloses may partially re-adsorb on the fibers surface. It has been proposed that such polymeric molecules play an important role in the phenomena occurring at fiber-fiber bonds [25], [26]. Such phenomena mostly involve three major mechanisms [26]: (i) mechanical interlocking due to surface roughness; (ii) molecular interdiffusion of surface molecules; and (iii) chemical interactions/attractions of surface molecules. Currently it is accepted, that the fiber surface resembles to a polyelectrolyte gel [27], where the fibrils favor interlocking between fibers, and the swollen/hydrated area promotes contact between fibers, thus

favoring the interdiffusion, and the creation of an important number of bonded areas during drying. The most important sources of interactions at the fiber-fiber interface are reviewed in Figure III–3.

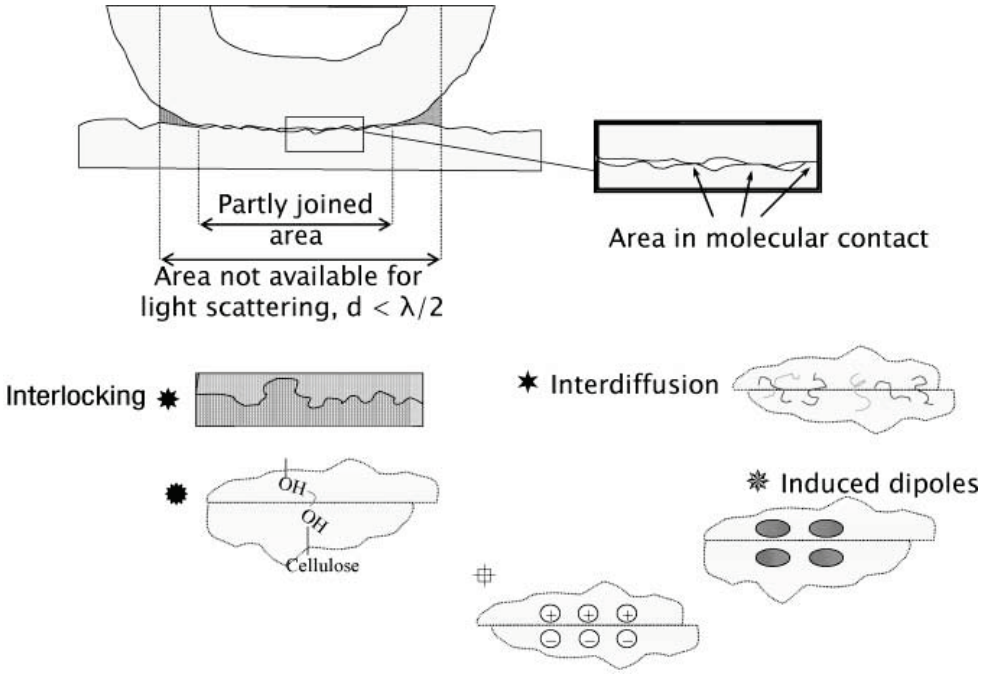

Figure III–3: Possible interactions at the fiber-fiber interface. (Source: [25])

In the conditions used for the pulp modifications, a rather large amount of silane is adsorbed at the fiber surfaces. Furthermore, the change in pH occurring at the dilution step, prior to the sheet formation, is likely to favor the self-condensation of the aminosilane used here. This aminosilane presents a high hydrophilic character which might favor the retention of water molecules. Overall, it is possible that the silane treatment applied to the fibers gives birth to an OH-rich interphase at the fibers surface, which would be highly hydrated and favor the retention of water during drying, thus acting like a dry strength additive. Such a network would favor the area in molecular contact between fibers, and act in the same way as xylan does. The formation of such a gel-like structure at the local scale of the surface might bring significant improvements in the case of fibers whose composition is poor in xylan, such as softwood fibers. However, in the case of xylan-rich materials, such as *Eucalyptus* fibers, this effect is already provided by the fraction of xylan present on the surface, and thus the silane treatment seems to be ineffective in terms of strength improvements.

Of course, the proposed mechanism must be considered as hypothetic and has to be confirmed or invalidated by other experiments. A deeper investigation would be necessary to confirm or invalidate this hypothesis, but we considered that it is slightly beyond the scope of this work.

IV. Conclusions and perspectives

The work described in this chapter, carried out in the frame of the *Tissue+* project, describes a study on the potential use of organosilanes in papermaking applications. The effects of adding an aminosilane in different pulps have been studied, and the data obtained have been thoroughly discussed. This discussion has led to the proposition of a mechanism for the interactions between the selected silane and the fibers.

The method developed here has been shown to be successful for modifying certain pulps. However, it was not so successful in treating *Eucalyptus* fibers. Unfortunately, this type of fiber is widely used in tissue applications, which are the target of the project presented here. Thus, the interest of the cellulose modification by DAMS for textile applications is very poor. In addition, the conditions used here are not fully representative of industrial conditions, since the silane agent was used in quantities much more important than usually done in industry. The sheet formation in a laboratory handsheet maker is far from being similar to that in a full scale paper machine. As a consequence, it would be very difficult to foresee the improvements given to an industrial tissue production from the treatment proposed here. Only pilot tests may allow ascertaining our results in real industrial conditions.

Nonetheless, other organosilanes with different functionalities could be useful for the addressed problematic. In any case, the data presented in this study are valuable, as they provide a better understanding on the interaction between silanes and cellulose.

List of references

[1] Technical Association of the Pulp and Paper Industry, *Forming Handsheets for Physical Tests of Pulp*. 2006.

[2] ISO - International Organization for Standardization, *Paper, board and pulps - Standard atmosphere for conditioning and testing and procedure for monitoring the atmosphere and conditioning of samples*. ISO - International Organization for Standardization, 1990.

[3] ISO - International Organization for Standardization, *Paper and board - Determination of grammage*. ISO - International Organization for Standardization, 1995.

[4] ISO - International Organization for Standardization, *Paper and board - Determination of thickness, density and specific volume*. ISO - International Organization for Standardization, 2005.

[5] ISO - International Organization for Standardization, *Paper and board - Determination of tensile properties -- Part 3: Constant rate of elongation method (100 mm/min)*. ISO - International Organization for Standardization, 2005.

[6] ISO - International Organization for Standardization, *Paper - Determination of tearing resistance (Elmendorf method)*. ISO - International Organization for Standardization, 1990.

[7] ISO - International Organization for Standardization, *Paper - Determination of bursting strength*. ISO - International Organization for Standardization, 2001.

[8] ISO - International Organization for Standardization, *Tissue paper and tissue products - Part 6: Determination of grammage*. ISO - International Organization for Standardization, 2005.

[9] ISO - International Organization for Standardization, *Tissue paper and tissue products - Part 3: Determination of thickness, bulking thickness and apparent bulk density*. ISO - International Organization for Standardization, 2005.

[10] ISO - International Organization for Standardization, *Tissue paper and tissue products - Part 4: Determination of tensile strength, stretch at break and tensile energy absorption*. ISO - International Organization for Standardization, 2005.

[11] R. Passas, C. Voillot, G. Tarrajat, G. Caucal, B. Khelifi, et G. E. Tourtollet, « MorFi as a novel technology for morphological analysis of fibres. », *Récents Progrés en Génie des Procédés*, vol. 15, n°. 259-264, 2001.

[12] W. E. Scott, J. C. Abbott, et S. Trosset, *Properties of Paper: An Introduction, Second Edition*, Tappi Press. 1995.

[13] V. Manfredi, « Optimizing eucalyptus pulp refining », *Journal of Tianjin University of science and technology*, vol. 19, n°. 1, p. 41-50, 2004.

[14] Y.-S. Perng, E. I.-C. Wang, Y.-L. Cheng, et Y.-C. Chen, « Effects of fiber morphological characteristics and refiningon handsheet properties », *Taiwan Journal of Forest Science*, vol. 24, n°. 2, p. 127-139, 2009.

[15] O. Sevastyanova, « On the importance of oxidizable structures in bleached kraft pulps », KTH, 2005.

[16] M. Margarido, « Etude sur la modélisation mathématique de la cuisson Kraft des espèces pures et mélanges de bois pour la production de pâte à papier », Thèse de doctorat, Institut national polytechnique (Grenoble), 2009.

[17] Y. V. Sood, R. Tyagi, S. Tyagi, P. C. Pande, et R. Tondon, « Surface charge of different paper making raw materials and its influence on paper properties », *Journal of Scientific and Industrial Research*, vol. 69, n°. 4, p. 300-304, 2010.

[18] B. C. Saha, « Hemicellulose bioconversion », *Journal of Industrial Microbiology & Biotechnology*, vol. 30, n°. 5, p. 279-291, 2003.

[19] Laine et P. Stenius, « Effect of charge on the fibre and paper properties of bleached industrial kraft pulps », *Paperi ja PuuPaper and Timber*, vol. 79, n°. 4, p. 257-266, 1997.

[20] P. Fardim et N. Durán, « Retention of cellulose, xylan and lignin in kraft pulping of eucalyptus studied by multivariate data analysis: influences on physicochemical and mechanical properties of pulp », *Journal of the Brazilian Chemical Society*, vol. 15, n°. 4, p. 514-522, 2004.

[21] P. Fardim et N. Durán, « Effects of kraft pulping on the interfacial properties of Eucalyptus pulp fibres », *Journal of the Brazilian Chemical Society*, vol. 16, n°. 5, p. 915-921, 2005.

[22] Z. Li et E. Brännvall, « Characterisation of dissolved spruce xylan in kraft cooking », *Nordic Pulp and Paper Research Journal*, vol. 26, n°. 4, p. 1-7, 2011.

[23] M. Christiernin, G. Henriksson, M. Lindström, H. Brumer, T. T. Teeri, T. Lindström et J. Laine, « The effects of xyloglucan on the properties of paper made from bleached kraft pulp », in *Nordic Pulp & Paper Research Journal*, vol. 18:2, s. 182-187, Nordic Pulp & Paper Research Journal, 2003.

[24] H. Yan, T. Lindström, et M. Christiernin, « Some ways to decrease fibre suspension flocculationand improve sheet formation », *Nordic Pulp and Paper Research Journal*, vol. 21, n°. 1, p. 36-43, 2006.

[25] T. Lindström, L. Wagberg, et T. Larsson, « On the nature in joint strength of paper - A review of dry and wet strength resins used in paper manufacturing », in *Advances in paper science and technology*, Cambridge, U.K., 2005, vol. 1, p. 457-562.

[26] M. Eriksson, « The influence of molecular adhesion on paper strength », KTH, 2006.

[27] R. Pelton, « A model of the external surface of wood pulp fibers », *Nordic Pulp and Paper Research Journal*, vol. 8, n°. 1, p. 113-119, 1993.

General conclusions and Perspectives

General conclusions

Within the context of bio-renewable resources valorization, this thesis work has been dedicated to the modification of cellulosic fibers with organosilane grafting agents. More particularly, in order to fit within the papermaking process, we have focused our research on performing the modifications in purely aqueous media. Very little work was available when this project was initiated. The two main axes of this research were the characterization of silane molecules reactions in aqueous media, and the understanding of the interactions between such molecules and the fibrous substrates. The final part of this work was devoted to the application of such an approach in a concrete case of papermaking problematic.

The characterization of the reactions of various alkoxysilanes in aqueous media with several concentrations, pH and temperature was performed, using *in-situ* ^{29}Si NMR spectroscopy. It was demonstrated that the use of purely aqueous media can provide solutions with increased reactivity or shelf life in comparison with classical alcohol/water reaction medium. This result is of a particular importance, since it goes against generally accepted ideas. The effect of pH on the silane solution was confirmed as the most important parameter for the control of the reactions kinetics. Even though it appeared that, under certain conditions, insoluble structures were formed, for all the investigated compounds we found the conditions allowing the preparation of solutions containing reactive species ranging from 75 to 100%.

In the second part of this work, we provided an extensive description of the silane-cellulose interaction. Starting with the heterogeneous modification in the liquid phase, the adsorption of the chosen compounds onto model cellulosic surfaces was observed *in-situ*, using an innovative

technique, the QCM (quartz crystal microbalance). It allowed the description of the kinetics of adsorption of three different silanes onto cellulose, and the evaluation of the amount of silane retained over time. It was shown unambiguously that hydrolyzed silanes adsorb onto cellulose fibers, within a few minutes of contact time between purely aqueous silane solution and the surface. The impact of the concentration, the temperature and the pH, on the kinetics was also evaluated and discussed.

Then, the characterization of the silane-cellulose interface was studied combining the use of SEM-EDX, solid-NMR, XPS, and ToF-SIMS. The data obtained in this part confirm that organosilanes are capable of forming chemical bonds with cellulose. The thermal treatment of the modified samples was shown to enhance the retention of molecules at the surface, but was not mandatory to the creation of such strong bonds. Indeed, even a simple drying at room temperature was sufficient to allow the creation of strong bonds in detectable quantities.

Finally, the potential use of organosilanes in papermaking applications was evaluated. An aminosilane was used, aiming at answering the antagonism between the development of strength properties and the softness of paper. The method for cellulose modification developed in this work was proven to be successful for modifying certain pulps, but did not bring significant paper properties enhancements in the case of *Eucalyptus* fibers. As this type of fiber is widely used in tissue applications, for which the softness is a key issue, the interest of the cellulose modification by the selected silanes appeared to be very poor. A mechanism describing the interactions between the selected silane and the fibers in the pulp was proposed.

In conclusion, this work has brought forth several original findings. The ^{29}Si NMR data for silane in a pure water solvent were acquired. Then, a better understanding of cellulose modification by organosilanes in aqueous media was achieved. Many process variables were considered, such as the concentration in silane, the temperature, the pH of the solution, or the origin of the substrate. In addition, various process steps were studied, and the sheet formation protocol was optimized. Also, the modified paper samples were studied at different scales from the bulk to the top atomic surface in terms of chemical characterization, and were also evaluated with specific paper testing techniques. Beyond the selection of suitable analytical means, the strategy adopted in our study, based on the use of mono-alkoxysilanes, has allowed to confirm previous findings regarding the nature of the silane-cellulose interaction. Furthermore, the structures present at the interface after the silane treatment were characterized with a precision higher than any work published up-to-date.

Perspectives

This work provides an extensive review of the behaviors occurring in aqueous solutions of organosilanes with various functional moieties. However, the silane selection used here is very limited in regard of all the structures commercially available. Only two functionalities could be evaluated in this work, namely amino- and vinyl-, for the modification of cellulose, and only an aminosilane was tested in an actual papermaking problematic. Nonetheless, other organosilanes with different functionalities or structures could be tested to solve some papermaking issues. Even though certain molecules available on the market have a low solubility in water, it can be envisaged to use emulsion techniques to adsorb such agents on the surface, where they could react through a proper control of the reaction conditions.

Another important point to consider here is that this work was focused on a specific papermaking problematic. The agents used here could allow to answer different problematic with more success.

Most importantly, the data presented in this report provide a better understanding on the interaction between silanes and cellulose, which could constitute a starting point for future work on silane modification of other natural polysaccharides. More specifically, the modification of other bio-renewable products, such as starch or hemi-celluloses, could be envisaged. With such modifications being carried out in solution, it would be possible to increase substantially the amount of silane retained, and create new functional bio-based compounds. Eventually, such compounds could find applications in the papermaking industry, to enhance the strength properties, or the sizing of the paper.

Annex 1: Hydrolysis-condensation kinetics of 3-(2-amino-ethylamino)propyl-trimethoxysilane

The following article, based on the results presented in the first chapter of this dissertation, has been published in an international peer-reviewed journal.

Materials Science and Engineering C 32 (2012) 487–493

Contents lists available at SciVerse ScienceDirect

Materials Science and Engineering C

journal homepage: www.elsevier.com/locate/msec

Hydrolysis-condensation kinetics of 3-(2-amino-ethylamino)propyl-trimethoxysilane

Olivier Paquet [a], Marie-Christine Brochier Salon [b], Elisa Zeno [a], Mohamed Naceur Belgacem [b,*]

[a] Centre Technique du Papier, Domaine Universitaire, B.P. 251, 38044 Grenoble CEDEX 9, France
[b] Laboratoire de Génie des Procédés Papetiers (UMR 5518 CNRS-CTP-INPG), Grenoble INP-Pagora, 461 Rue de la papeterie, F-38402 St Martin d'Hères, France

ARTICLE INFO

Article history:
Received 8 July 2011
Received in revised form 3 October 2011
Accepted 29 November 2011
Available online 7 December 2011

Keywords:
Organosilanes
3-(2-amino-ethylamino)propyl-trimethoxysilane
^{29}Si NMR spectroscopy
Hydrolysis
Condensation

ABSTRACT

The kinetics of the hydrolysis and self-condensation reactions of 3-(2-amino-ethylamino)propyl-trimethoxysilane (DAMS) were investigated by *in situ* ^{29}Si NMR spectroscopy using pure water and an alcoholic (80:20 w/w ethanol/water) solvent mixture as reaction media. In both media, the reactivity of the silane was strongly influenced by the pH of the medium during the initial stage of the reaction. The silanols produced by hydrolysis in water were much more stable than those produced in the alcoholic solvent mixture, the latter of which were susceptible to self-condensation, yielding siloxane bridges. The active silanol reactivity (SR), which is a simple parameter that reflects the silanol content in the solution as a function of the reaction time, was proposed for evaluating the reactivity of a solution of DAMS. SR was maintained at a good level (high silanol group concentration) when pure water was used as the reaction medium. The pH of the reaction appears to be the predominant parameter for determining the SR during the first 2 h, regardless of the reaction solvent.

1. Introduction

Organofunctional silanes are commonly used as surface modifiers in various industrial applications and have been particularly used in glass-based materials [1,2]. More recently, these alkoxysilanes have been successfully used for the surface modification of natural fibers, which bear surface hydroxyl groups [3–6]. Grafting of alkoxysilanes onto such hydroxyl-bearing surfaces often occurs via intermediate silanols, formed by the hydrolysis of silanes with water or atmospheric moisture. The silanols, once formed, either can be adsorbed onto the substrate, or may undergo self-condensation to yield polysiloxane structures. Grafting efficiency is maximized by promoting the hydrolysis reaction while limiting the self-condensation process, given that the latter phenomenon decreases the reactivity of the silane solution [1].

The conventional surface modification process is carried out in a mixture of organic solvent and water. The relative ratio of the solvents has a direct effect on the reaction yields (hydrolysis vs. self-condensation); in particular, the solvent composition affects the relative abundance of various species and the reactivity of the solution [7,8]. Many other parameters also influence the reactions between the alkoxysilanes and water [7], such as the temperature [9], pH [10], and concentration of the silane [11,12].

In most cases, both industrial applications and literature studies deal only with the preparation of 1% or 2% w/w silane solutions in mixed alcohol–water solvents [13,14]. The molar ratio of water added to the medium is generally rather low relative to the number of hydrolysable groups, with a maximum of 20% w/w water. Organic solvents are used to improve the miscibility between water and the silane as necessary [1].

NMR spectroscopy (especially, ^{29}Si NMR) has been reported to be a powerful tool for investigating the kinetics of the reactions occurring with organosilanes (both hydrolysis and self-condensation) [9,13,15-21]. Most current studies have been conducted at a concentration of 10% w/w to facilitate the detection of low concentration species and for fast reaction kinetics. This analytical technique is the only one that allows the direct *in situ* observation of the evolution of the ratios of the different silane-born structures in the medium, including transient species. For this purpose, a commonly used nomenclature refers to silane structures as being of the M, D, T, or Q types depending on the number of Si–O– bridges formed by the silicon atom studied; these notations correspond to 1, 2, 3, or 4 Si–O– bridges, respectively. Glaser and Wilkes [22] introduced a slightly different notation by adding the index "i" to the existing notation, where i is the number of siloxane (Si–O–Si) linkages attached to the silicon atom of interest. Therefore, when considering 3-(2-amino-ethylamino)propyl-trimethoxysilane (DAMS) belonging to the T family structure group, i is equal to 0 in the case of uncondensed silanes and silanols. Herein, the notations T^0_H and T^0_R are used to denote the silane and silanol units, respectively. For dimers or end chain units, i takes the value 1 (T^1). T^2 indicates parts of a linear chain, whereas T^3 is associated to totally condensed species belonging to a tri-dimensional network. The structures of the DAMS molecules corresponding to each of these notations are presented in Fig. 1. T^0_H and T^1 are considered as the most

* Corresponding author. Tel.: +33 476826962; fax: +33 476826933.
E-mail address: Naceur.Belgacem@pagora.grenoble-inp.fr (M.N. Belgacem).

0928-4931/$ – see front matter © 2011 Elsevier B.V. All rights reserved.
doi:10.1016/j.msec.2011.11.022

Reference under Glaser and Wilkes' [22] notation	Chemical structure
T^0_R 3-(2-amino-ethylamino)propyl-trimethoxysilane	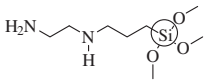
T^0_H 3-(2-amino-ethylamino)propyl-silanetriol	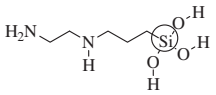
T^1	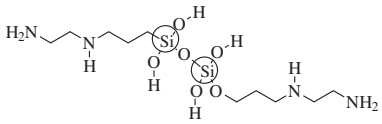
T^2	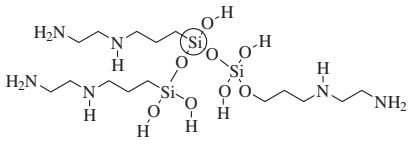
T^3	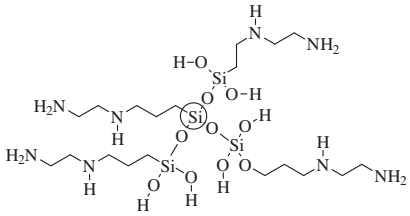

Fig. 1. Structure of DAMS and its hydrolysis and self-condensation products. The silicon atom of interest is encircled.

interesting species for reactions with OH-rich substrates because hydroxyl moieties remain available in these structures for linking with such surfaces. Compounds possessing T^2 groups are also theoretically reactive with OH-bearing surfaces; however, steric hindrance may impede such a reaction. Finally, the T^3 species, which are totally condensed, are unsuitable for surface grafting.

In situ ^{29}Si NMR spectroscopy has been particularly applied to the study of the behavior of γ-amino-propyl-triethoxy-silane (APES) and γ-diethylene-triamino-propyl-trimethoxy-silane (TAS), in water/alcohol solutions [23]. The high reactivity of aminosilanes makes them particularly interesting since it has been demonstrated that the presence of the amine functionality in these molecules produces a catalytic effect on the hydrolysis reaction in the presence of water. Moreover, aminosilanes exhibit excellent solubility in water, which could allow for the possibility of working in a purely aqueous medium; this in turn could offer important environmental advantages. This is particularly important within the context of the modification of natural fibers.

Based on the aforementioned considerations, our aim is to investigate the possibility of using aminosilanes for the modification of cellulose using pure water as a medium. Herein, the kinetics of the hydrolysis and self-condensation reactions of the aminosilane molecule, 3-(2-amino-ethylamino)propyl-trimethoxysilane (DAMS, structure below), in pure water were compared with the kinetics in an 80/20 w/w ethanol/water mixture. The effect of pH was evaluated in both media. The reactions were monitored by *in situ* ^{29}Si NMR spectroscopy for a period of 48 h.

To the best of our knowledge, there is currently only one report on amino-bearing silane in pure water; however, that study focused on blending [15]. The *in situ* observation of the hydrolysis and condensation structures formed by DAMS has been reported in one study; however, in that study, observations were made in an alcoholic medium only [16].

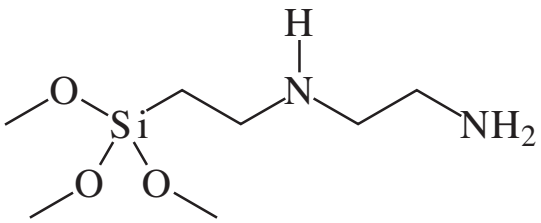

DAMS

2. Experimental

2.1. Materials

Reactions were carried out in two different media: (i) pure deuterium oxide was used as a model for a purely aqueous medium and (ii) a solution of deuterium oxide and ethanol-d_6 (20:80 w/w) was used as an aqueous alcoholic solvent. In both media, experiments were performed under two different pH conditions: (i) at an unmodified pH of 10.5 and (ii) at a pH of 4 after the addition of an adequate volume of glacial acetic acid. The choice of pH values was motivated by our previous studies involving other silane coupling agents, which showed that the self-condensation reaction was accelerated in basic pH, whereas acidic pH stabilizes the formation of silanol-bearing derivatives.

High-purity-grade (99.96 at.% D) deuterium oxide (D_2O) and deuterated ethanol (CD_3-CD_2-OD, ethanol-d_6 99.5 at.% D, anhydrous) were purchased from Sigma–Aldrich and used as received. Glacial acetic acid was obtained as a research grade product from Sigma–Aldrich, used as received. 3-(2-Amino-ethylamino)propyl-trimethoxysilane (DAMS, CAS number: 1760-24-3) was received from Dow Corning and used as received. DAMS was a high-purity product (Z-6094) with over 98% of active molecules.

2.2. NMR kinetics setup

DAMS (10% w/w, 0.35 mL, 1.6 mmol) was weighed directly into clean tubes containing an appropriate amount of pure deuterium oxide (90% w/w, 2.9 mL, 161.6 mmol) or a mixture of deuterium oxide (18% w/w, 0.59 mL, 32.3 mmol) and ethanol-d_6 (72% w/w, 2.9 mL, 49.8 mmol). For the experiments in acidic conditions, an appropriate amount of glacial acetic acid (0.16 mmol, 0.16 mL) was added prior to the addition of DAMS. The initial reaction time was fixed after the addition of DAMS to the tube. Kinetic monitoring was carried out directly in the NMR tubes by following "*in-situ*" the evolution of the relevant NMR signals. All experiments were performed by using ^{29}Si NMR spectroscopy to monitor the modification of the chemical environment of the central silicon atom of the silane molecule.

The validity of the method was assessed by using ^{1}H and ^{13}C NMR spectra to investigate the release of methanol during the hydrolysis reaction. All of the spectra were acquired on Varian UNITY 400 and MERCURY 400 spectrometers. For ^{29}Si, a 10 mm BB probe operating at 79.455 MHz was used to optimize the signal/noise ratio, thus minimizing the acquisition times and allowing for monitoring of the kinetics of the relatively fast reaction. All chemical shifts were measured with respect to a coaxial insert tube containing tetramethylsilane (TMS) solution as an external reference.

The delays and pulses used allowed for quantitative measurements (T_1 measurements were previously performed by the inversion-recovery method). The spectral width was 12 kHz and the relaxation delay 100 s, with proton decoupling applied only during the acquisition period in order to avoid negative NOE. The number of scans was increased with kinetic reaction time.

Peaks assignments of DAMS and the various structures resulting from the interaction of DAMS with water are as follows for ^{29}Si NMR: $T^0_H = -40.2$ ppm, $T^0_R = -43.2$ ppm, $T^1 = -48$ to -50 ppm, $T^2 = -56$ to -62 ppm, and $T^3 = -62$ to -74 ppm. The intensity of each peak (surface area) was calculated and used to construct the kinetic curves.

In order to simplify the evaluation of the reactivity of the DAMS solution over time, the active silanol reactivity (SR) of the solution, which is a simple parameter that reflects the silanol content in the solution as a function of the reaction time, is proposed as a measurement parameter. This parameter is abbreviated SR herein and is adapted from an empirical expression (Eq. (1)) proposed by Beari et al. [24]:

T^0_R and T^3 structures do not contribute to SR because they do not bear any silanol groups.

$$SR = \frac{\left(3 * \%T^0_H\right) + \left(2 * \%T^1\right) + \left(1 * \%T^2\right)}{3} \quad (1)$$

Due to the very fast kinetics of the hydrolysis reaction, it is assumed here that the hydrolysis is complete for all molecules and that there are no partially hydrolyzed silanols in solution.

3. Results and discussion

Before starting the data collection, the validity of the ^{29}Si NMR method was confirmed by using a complementary ^{1}H and ^{13}C NMR study to follow the kinetics in a mixed ethanol/water solvent medium under unmodified pH conditions, as previously published for several silane coupling agents [23]. The results of these experiments are not presented here, but the kinetics curves constructed on the basis of the spectra associated to the three nuclei were in good agreement.

3.1. Kinetics studies in 80/20 w/w alcohol/water solvent system

The behavior of a 10% w/w solution of DAMS in an 80/20 w/w alcohol/water mixture under unmodified pH conditions was evaluated from the spectra presented in Fig. 2a and the kinetics of formation and/or consumption of the different species present in the reaction medium, derived from these spectra, are given in Fig. 3a. Under these conditions, the hydrolysis seems to be highly efficient, as evidenced by the total consumption of alkoxy moieties before the first acquisition is performed after a reaction time of 10 min (T^0_H moieties

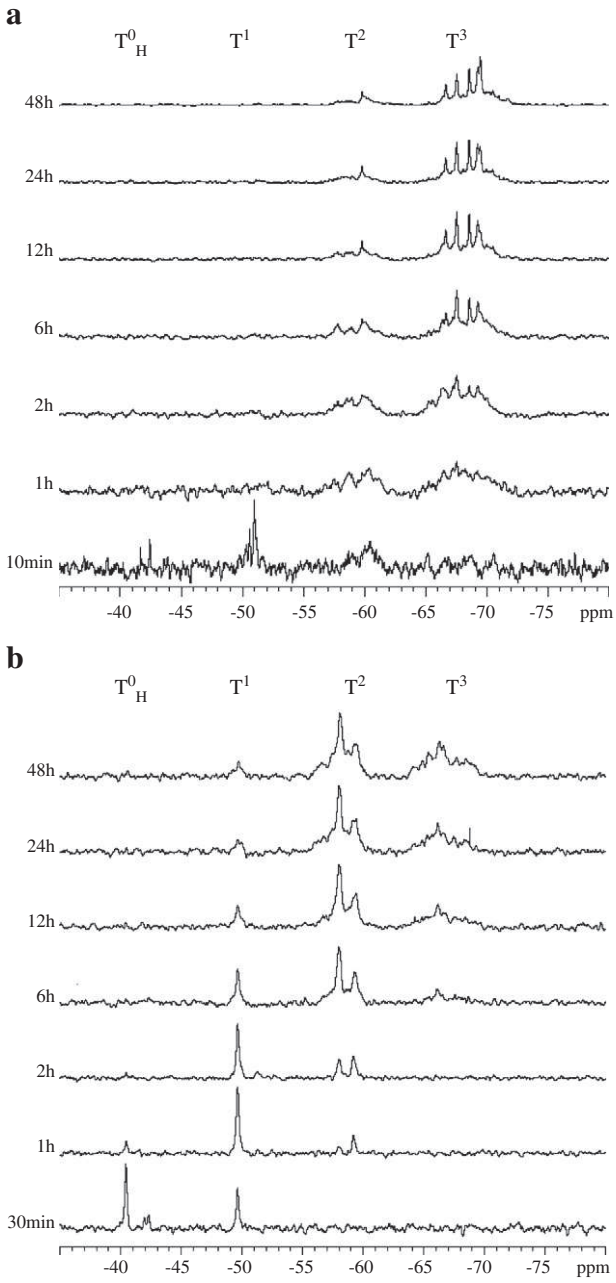

Fig. 2. ^{29}Si NMR spectra of the hydrolysis and self-condensation reaction products of DAMS (solvent: mixed ethanol/water solutions (80/20 w/w); concentration: 10% w/w; temperature: 25 °C; (a) unmodified pH; (b) acidic medium).

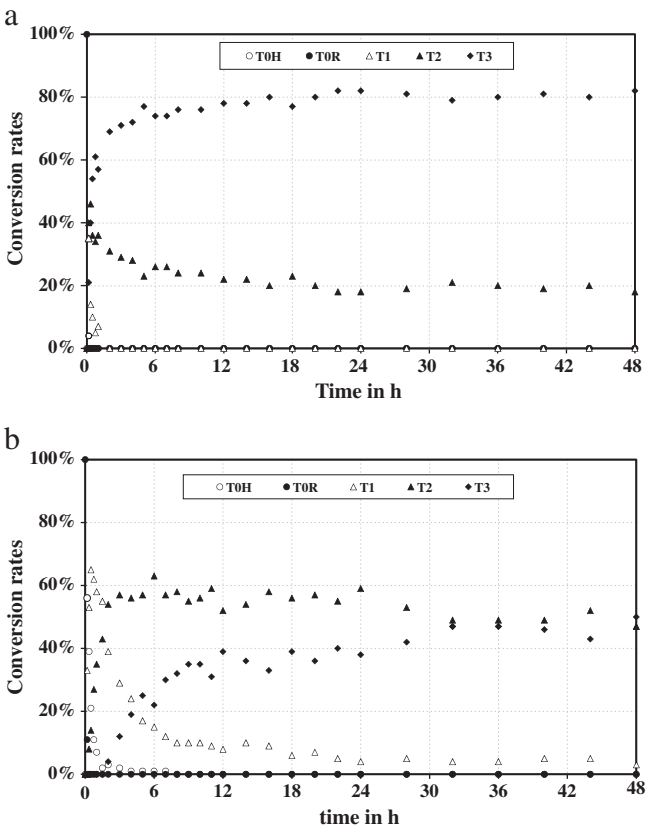

Fig. 3. Kinetics plot of hydrolysis and self-condensation reactions of DAMS as deduced from ^{29}Si NMR spectra presented in Fig. 2 under (a) unmodified pH and (b) acidic conditions.

were not detected). At the moment of data acquisition, the concentration of T^1 species had already passed its maximum value and had started to decline, indicating that more condensed structures were formed. In fact, the condensation of T^1 species into T^2 and T^3 structures was already detected at the relatively short time of t = 10 min. The concentration of T^3 species increased regularly to reach an equilibrium value of 80% after 20 h of reaction time. The relatively fast reactivity of DAMS was anticipated based on the amino functional groups within its structure, the presence of which is known to catalyze the reaction of this silane toward water or moisture, as reported for γ-amino-propyl-trialkoxy-silanes [16].

At t = 2 h, all of the T^1 structures had reacted and the concentration of more condensed structures started to become important as evidenced by the broadening of the peaks in the NMR spectra. In fact, after 2 h only T^2 and T^3 condensed structures were detected in the reaction medium. Equilibrium was achieved after 20 h because the condensation phenomenon might be significantly slowed due to the lack of accessibility to some of the hydroxyl groups in the network.

The reaction of a 10% w/w solution of DAMS in 80/20 w/w alcohol/water mixture under acidic conditions was subsequently investigated; the NMR spectra are presented in Fig. 2b and the derived kinetic data are presented in Fig. 3b. Under these conditions, the hydrolysis of DAMS was complete at t = 20 min. The T^0_H hydrolyzed structure presents a maximum at 10 min, with a concentration of 56%. T^1 reaches a concentration of 65% at 30 min before beginning to decline. T^2 and T^3 species appeared rapidly at 1 h and 2 h, respectively. The concentration of the latter increased regularly to reach values of 40% and 50% at 24 and 48 h, respectively.

Examination of the concentration of the structures bearing silanol groups that are potentially interesting for cellulose grafting, namely T^0_H and T^1, reveals that the former was still detected, but only at trace level, after 90 min of reaction time. After 8 h, there was no evidence of T^0_H species, whereas the concentration of T^1 species had diminished to reach a ratio equal to or lower than 10% and declined slowly but consistently after 8 h. Experiments carried out over 48 h show that equilibrium is not attained and that the reactions progress slowly toward a higher degree of condensation.

The kinetics under acidic pH conditions are in agreement with the literature data, which indicate that the protective role of acidic pH stabilizes hydrolyzed silanes against condensation. The presence of acetic acid appreciably limited the T^0_H consumption kinetics. Indeed, T^0_H species were present during the first 8 h under acidic conditions, whereas these species totally disappeared after less than 30 min in the unmodified pH system.

3.2. Kinetics studies in pure water

The hydrolysis and self-condensation kinetics of DAMS in pure water under the two pH values were evaluated.

Without pH modification, DAMS hydrolysis began immediately on initiation of the reaction and was followed by self-condensation. The spectra of the solution obtained at various reaction times are presented in Fig. 4a, and the derived kinetics plots are presented in Fig. 5a. For that experiment, no data could be obtained between 24 and 44 h due to a technical problem during the acquisition. However, the data for the last few hours of the 48-h kinetic run were acquired. Initial silanes remained detectable up to 15 min, whereas totally condensed T^3 species were already detectable at the first measurement. Such features explain the small quantity of detected T^0_H species. The very fast nature of the condensation results in few hydrolyzed species being available in the solution. Nevertheless, equilibrium between the various moieties appears to be reached after 1 h. Pristine silanes are totally hydrolyzed during the first 30 min whereas hydrolyzed uncondensed species reached a maximum content (around 12%) after 15 min and their concentration was subsequently stabilized between 5 and 7%. T^1 condensed species were present over the entire duration of the experiment; reaching an equilibrium value close to 13% after 1 h, whereas T^2 species reached a maximum concentration of 50% after 15 min of reaction. The quantity of T^2 species declined to 40% after 1 h. During the first hour of the reaction, the content of totally condensed species, T^3, increased to reach a value of around 41%. After 1 h of reaction time, T^2 and T^3 species constituted the most abundant class in the reaction mixture, accounting for 80% of the total species with equal quantities of 40% for each of them.

Purely aqueous medium was found to suppress the self-condensation reaction of the T^0_H structures. In fact, these species are not totally consumed even after 48 h of reaction, in contrast with the events in alcoholic medium where these structures were totally consumed before the first acquisition (10 min after solution preparation) at the same pH.

The NMR spectra corresponding to the hydrolysis kinetics in pure water and under acidic conditions are presented in Fig. 4b. The kinetic curves constructed from these spectra are shown in Fig. 5b. The rate of the hydrolysis step was found to be very fast, almost instantaneous. Thus, after 20 min, hydrolyzed silane species (T^0_H) constitute almost 50% of the solution and T^1 moieties represent another 40%, the rest of the solution being composed of T^2 structures. The amount of T^0_H species diminished rather rapidly and reached a value of 8% after 3 h, whereas the content of T^2 structures increased slowly from 14% to 50% between 20 min and 3 h of reaction time. The appearance of totally condensed T^3 structures did not occur until the second hour of reaction with a maximum quantity that did not exceed 25%. After 9 h, equilibrium between the concentrations of the reactive species was achieved. Thus, the amounts of T^0_H, T^1, T^2, and T^3 in the reaction mixture were ca. 8%, 20%, 52%, and 20%, respectively.

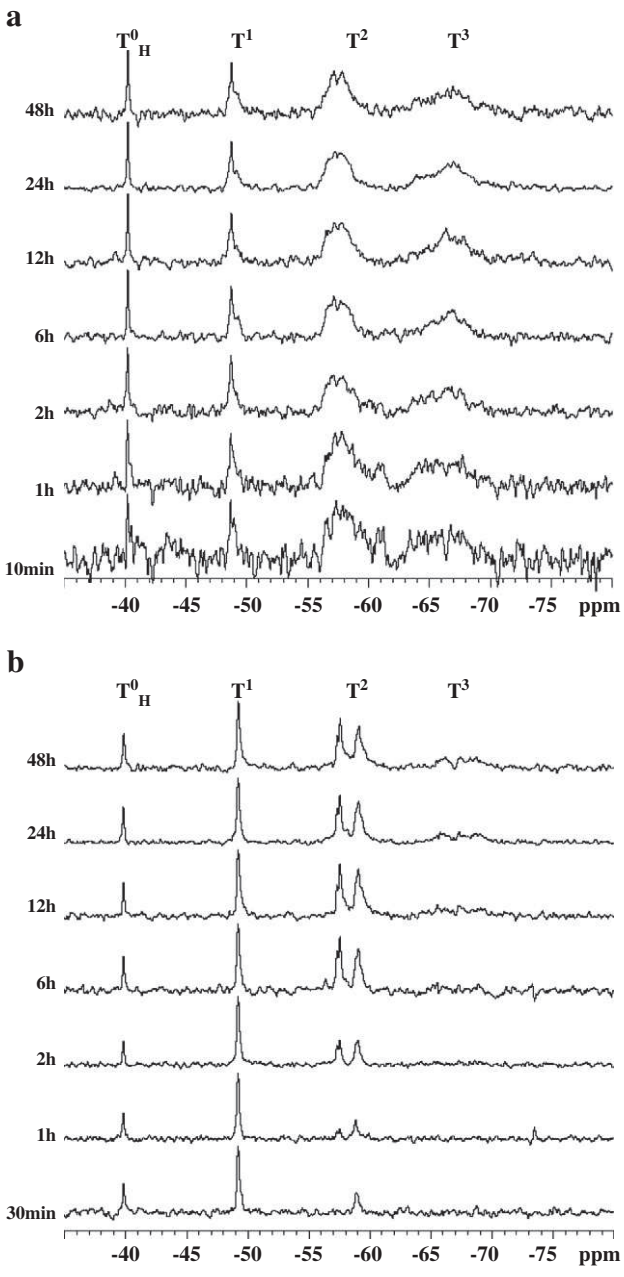

Fig. 4. ^{29}Si NMR spectra of the hydrolysis and self-condensation reaction products of DAMS (solvent: pure water; concentration: 10% w/w; temperature: 25 °C; (a) unmodified pH; (b) acidic medium).

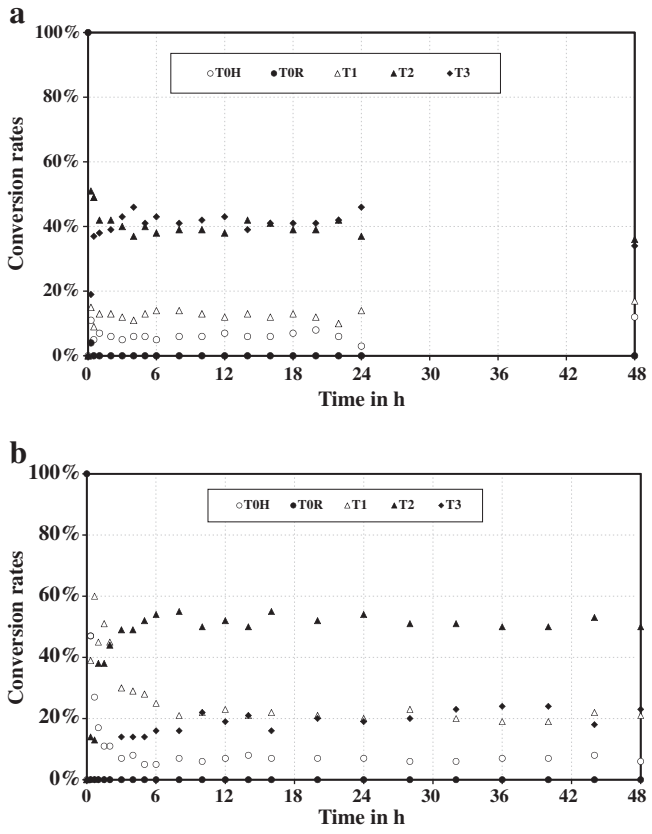

Fig. 5. Kinetics plot of hydrolysis and self-condensation reactions of DAMS as deduced from ^{29}Si NMR spectra presented in Fig. 4 under (a) unmodified pH and (b) acidic conditions.

For both experiments carried out in purely aqueous medium, complete disappearance of the uncondensed structures was not achieved for the duration of the analysis (48 h), which is contrary to the common idea that the use of alcoholic solvents with a limited amount of moisture or water is optimal for control of the self-condensation reactions of silanes. Indeed, the data presented here suggest that in the case of an organofunctional silane-bearing amine groups, the use of a purely aqueous medium leads to better control of the condensation reactions and produces a reactive mixture in which the equilibrium between the various reactive structures is set, and in which T^0_H species remain viable over long periods of time.

A detailed analysis of the ratio of T^0_H species at 24 and 48 h under unmodified pH in pure deuterium oxide shows a surprising increase from 3 to 12%. This unexpected trend could be explained by the occurrence of a reversible condensation reaction in the aqueous medium. However, it should be recalled that silanol self-condensation is generally believed to be irreversible in organic solvent media. Consequently, further investigations of the reversibility of the reaction in pure water would be necessary to confirm this hypothesis.

Another possible explanation could be the formation of insoluble compounds in the reaction medium, which tend to segregate from the medium thus becoming undetectable by the NMR spectrometer. In this case, the absolute ratio of T^0_H would be over-estimated. Such a phenomenon has been previously reported in a paper comparing the behaviors of a monoaminosilane, γ-amino-propyl-triethoxy-silane (APES), and a triaminosilane, γ-diethylene-triamino-propyl-trimethoxy-silane (TAS) [23]. It was observed in that paper that the reaction of the triaminosilane with water in an 80/20 w/w alcohol/water mixture yielded insoluble condensed structures, whereas the reaction products of the monoaminosilane remained soluble in the same medium. Whereas this explanation is plausible, this phenomenon is not observed in the present study under the acidic conditions in purely aqueous medium. The protective effect of the acid against the formation of larger structures may have prevented the occurrence of precipitation.

3.3. Pure water vs. alcoholic medium

With respect to the concentration of T^1 species under the varying reaction conditions, it was observed that in alcoholic media these structures were totally consumed or only existed in trace amounts after a few hours. However, for both unmodified and acidic pH conditions employed in aqueous media, these structures were present in contents close to 15 and 20%, respectively, after 48 h. Because T^3 structures are not suitable for grafting (given that the OH

Table 1
Concentration of the different DAMS derived species, as determined by ^{29}Si NMR (DAMS concentration: 10% w/w with respect to the solvent; T = 25 °C).

		T^0_R	T^0_H			
Medium	pH	t-0%	t-max (%)	t–0%	% at 24 h	% at 48 h
CD_3-CD_2-OD/D_2O	Unmodified	20 min	Not detected	t = 10 min	0	0
80/20 w/w %	Acidic	20 min	10 mn (56%)	t = 8 h	0	0
100% D_2O	Unmodified	30 min	15 mn (11%)	Not reached	3	12
	Acidic	20 min	20 mn (47%)	Not reached	7	6
		T^1				
		t-init (%)	t-max (%)	t–0%	% at 24 h	% at 48 h
CD_3-CD_2-OD/D_2O	Unmodified	10 min (35%)	10 mn (35%)	t = 2 h	0	0
80/20 w/w %	Acidic	10 min (33%)	30 mn (65%)	Not reached	4	3
100% D_2O	Unmodified	15 min (15%)	15 mn (15%)	Not reached	14	17
	Acidic	20 min (39%)	40 mn (60%)	Not reached	20	21
		T^2				
		t-init (%)	t-max (%)	% at 24 h	% at 48 h	
CD_3-CD_2-OD/D_2O	Unmodified	10 min (40%)	20 mn (46%)	18	18	
80/20 w/w %	Acidic	20 min (8%)	6 h (63%)	59	47	
100% D_2O	Unmodified	15 min (51%)	15 mn (51%)	37	36	
	Acidic	20 min (14%)	8 h (55%)	54	50	
		T^3				
		t-init (%)	t-max (%)	% at 24 h	% at 48 h	
CD_3-CD_2-OD/D_2O	Unmodified	10 min (20%)	20 h (86%)	82	82	
80/20 w/w %	Acidic	2 h (4%)	48 h (50%)	38	50	
100% D_2O	Unmodified	15 min (19%)	24 h (46%)	46	34	
	Acidic	3 h (14%)	36 h (24%)	19	23	

functionality is no longer present), the data show unambiguously that the purely aqueous reaction medium is much more favorable for the production of a reactive solution having available hydroxyls groups over a long period of time.

Table 1 summarizes the data relating to the time of appearance, the time of total consumption, the time of highest ratio and the ratios at t = 24 h and t = 48 h of the species in solution for the various media used herein.

3.4. Silane reactivity parameter

The SR values were calculated according to Eq. (1). Due to its very simple character, this model does not take into account the accessibility of the hydroxyl groups and excludes any steric hindrance considerations, even though it is commonly understood that lowered accessibility of some moieties arises upon the formation of larger structures due to steric effects. For example, in a highly condensed molecule comprising mixed T^2 and T^3 species, the remaining hydroxyls of some T^2 structures may be entrapped in the tri-dimensional network and hence become unavailable for adsorption and grafting onto the substrate under study. As a consequence, it can be assumed that the reactivity stated herein is slightly over-estimated for reaction times at which an important condensation has occurred.

The SR values were plotted as a function of time for the four reactions described herein, as presented in Fig. 6. Two significant trends were observed:

(i) Fig. 6a shows that over longer periods, reactive silanols are maintained at a good level for the purely aqueous solutions, in contrast with the SR in mixed alcoholic solvents, indicating that the condensation reactions were limited in the purely aqueous solutions, thus yielding a reactive mixture with appreciable potential reactivity.

(ii) However, as shown in Fig. 6b, during the first couple of hours of the reaction, the pH of the reaction seems to be the predominant parameter determining the SR, independent of the medium used. Indeed, for both of the experiments performed under acidic conditions the SR reached a maximum of almost 80% vs. less than 40% for unmodified pH conditions. However, a less steep decline of SR over time is observed for the reaction carried

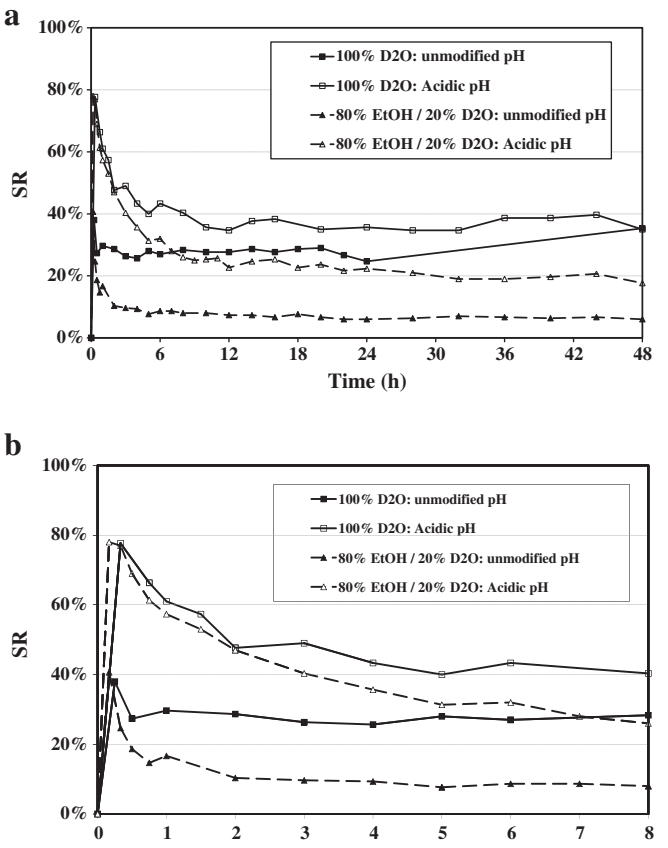

Fig. 6. Active silanol reactivity (SR) parameter as a function of time for different reaction time intervals: (a) 0–48 h and (b) 0–8 h.

out in purely aqueous medium compared with that conducted in a mixed alcoholic solvent.

4. Conclusions

The kinetics of hydrolysis and self-condensation of 3-(2-amino-ethylamino)propyl-trimethoxysilane (DAMS) in water and in an ethanol/water mixture were compared. The reactions were studied under unmodified and acidic pH conditions by means of ^{29}Si NMR spectroscopy for a period of 48 h. It was shown for the first time that equilibrium between hydrolyzed and condensed species is achieved in a purely aqueous medium, in contrast to the events in aqueous organic solvent media where hydrolyzed species (silanols) disappear over time. The relative ratio of silanols in water is influenced by the pH, which is in agreement with the protective role of acidic media against self-condensation. The reactivity of purely aqueous DAMS solutions, as indicated by the SR parameter, is much higher than that of aqueous alcoholic solutions regardless of the pH and the solution age.

These findings are particularly interesting in view of using DAMS for the modification of natural fibers under environmentally friendly conditions. In fact, the possibility of efficient surface modification by applying silanes in water opens new perspectives, which are currently under study in our laboratory.

Acknowledgement

Dow Corning S.A. is gratefully acknowledged for supplying the silane coupling agent used in this work.

References

[1] E.P. Plueddemann, Silane Coupling Agents, Springer, 1991.
[2] K.L. Mittal, Silanes and Other Coupling Agents, VSP, 2000.
[3] M.C. Brochier-Salon, G. Gerbaud, M. Abdelmouleh, C. Bruzzese, S. Boufi, M.N. Belgacem, Magn. Reson. Chem. 45 (2007) 473–483.
[4] M. Castellano, A. Gandini, P. Fabbri, M.N. Belgacem, J. Colloid Interface Sci. 273 (2004) 505–511.
[5] M. Abdelmouleh, S. Boufi, A. ben Salah, M.N. Belgacem, A. Gandini, Langmuir 18 (2002) 3203–3208.
[6] M.A. Tshabalala, P. Kingshott, M.R. VanLandingham, D. Plackett, J. Appl. Polym. Sci. 88 (2003) 2828–2841.
[7] M. Abel, R. Allington, R. Digby, N. Porritt, S. Shaw, J. Watts, Int. J. Adhes. Adhes. 26 (2006) 2–15.
[8] F. Osterholtz, E. Pohl, J. Adhes. Sci. Technol. 6 (1992) 127–149.
[9] T. Ogasawara, A. Yoshino, H. Okabayashi, C.J. O'Connor, Colloids Surf. A 180 (2001) 317–322.
[10] R. Bel-Hassen, S. Boufi, M.C. Brochier-Salon, M. Abdelmouleh, M.N. Belgacem, J. Appl. Polym. Sci. 108 (2008) 1958–1968.
[11] N. Kim, D.H. Shin, Y.T. Lee, J. Membr. Sci. 300 (2007) 224–231.
[12] S. Savard, L. Blanchard, J. Léonard, R.E. Prud'homme, Polym. Compos. 5 (1984) 242–249.
[13] S. Torry, A. Campbell, A. Cunliffe, D. Tod, Int. J. Adhes. Adhes. 26 (2006) 40–49.
[14] C.M. Bertelsen, F.J. Boerio, Prog. Org. Coat. 41 (2001) 239–246.
[15] C. Heitz, G. Laurent, R. Briard, E. Barthel, J. Colloid Interface Sci. 298 (2006) 192–201.
[16] M.C. Brochier-Salon, M. Bardet, M.N. Belgacem, Silicon Chem. 3 (2008) 335–350.
[17] C. Corminbœuf, T. Heine, J. Weber, Chem. Phys. Lett. 357 (2002) 1–7.
[18] R.J. Hook, J. Non-Cryst. Solids 195 (1996) 1–15.
[19] M.C. Brochier-Salon, P. Bayle, M. Abdelmouleh, S. Boufi, M.N. Belgacem, Colloids Surf. A 312 (2008) 83–91.
[20] S.E. Rankin, A.V. McCormick, Magn. Reson. Chem. 37 (1999) S27–S37.
[21] H. Jiang, Z. Zheng, J. Xiong, X. Wang, J. Non-Cryst. Solids 353 (2007) 4178–4185.
[22] R.H. Glaser, G.L. Wilkes, Polym. Bull. 19 (1988) 51–57.
[23] M.C. Brochier-Salon, M. Abdelmouleh, S. Boufi, M.N. Belgacem, A. Gandini, J. Colloid Interface Sci. 289 (2005) 249–261.
[24] F. Beari, M. Brand, P. Jenkner, R. Lehnert, H.J. Metternich, J. Monkiewicz, H.W. Siesler, J. Organomet. Chem. 625 (2001) 208–216.

Annex 2: A selection of important paper properties

I. Physical Properties

The physical properties of a paper depends on the fibers used for its fabrication, the mechanical treatments undergone by the fibers, the chemicals added during the process, and the process parameters, including the concentration of the pulp used, the configuration of the paper machine, etc.

- Basis Weight (or Grammage): The Basis Weight of a paper is the weight per unit area (g/m^2). In order to reduce production costs, papermakers aim at getting all desired properties with a minimum possible basis weight.
- Bulk: The Bulk indicates the relation between the thickness of the sheet and its basis weight (cm^3/g). It is the inverse of the density. For a given paper, decrease in bulk, often resulting from a more intense refining of the pulp suspension, makes the sheet smoother, less opaque, with higher tensile, burst or internal bond strength. Reducing the bulk often leads to a decrease of the stiffness and the tearing strength, at least after a critical value of the bulk. High bulk is desirable in absorbent papers while lower bulk is preferred for printing papers.
- Formation: Formation is an indicator of how uniformly the fibers and fillers are distributed in the sheet. A poorly formed sheet will have more weak spots, which will affect its strength properties.
- Friction: This property is measured as a coefficient of friction, which is the ratio of the frictional force, to a force acting perpendicular to the sheet surfaces.

II. Optical Properties

Optical properties are very important for certain grade of papers such as printing/writing, whereas they are often neglected for packaging, or newsprints grades. They are impacted by the type of pulp used and the refining operation but can be enhanced by subsequent addition of mineral fillers and pigments in the fibrous suspension.

- Brightness and Whiteness: Brightness is defined as the percentage of reflectance of blue light (wavelength=457nm). Whiteness refers to how much a paper diffusely reflects light of all wavelengths throughout the visible spectrum.
- Gloss: Gloss is the specular reflection of light. It is a particularly important finish for magazines, advertisements and other specialty markets.
- Opacity: Opacity is the measure of how much light is kept away from passing through a sheet.

III. Strength Properties

Strength properties are essential for several applications, such as packaging or printing.

- Bursting Strength: Bursting strength tells how much pressure a paper can tolerate before rupture (kPa). It is often expressed as the Burst Index (kPa/(g/m²)), which is the bursting strength divided by the basis weight.
- Internal bond strength (Ply Bond or Scott Bond): It is a measure of the ability of a paper or paperboard to resist splitting when a tensile load is applied through the paper thickness, i.e. in the Z direction of the sheet. It is generally expressed in J/m².
- Elongation (Stretch): Stretch is the amount of distortion which paper undergoes under tensile stress, often expressed as a percentage of elongation.
- Tearing Resistance: Tearing resistance/strengths is the ability of the paper to withstand tearing force (mN).
- Tensile Strength: This is the tensile force required to produce a rupture in a strip of paper (kN/m). Good tensile strength is indicative of suitable fiber strength, fiber bonding and fiber length.
- Wet Strength: Some grades of paper such as tea bag paper, coffee filter paper etc. come in contact with water while being used. Hence, they have to be strong enough to withstand tear, rupture or falling apart when saturated with water. To impart wet strength, papers are chemically treated.

List of abbreviations

°C : Celsius degrees
°SR : Schopper-Riegler index
AFM : Atomic Force Microscopy
APDMES : AminoPropylDiMethylEthoxysilane
APS : AminoPropyltriethoxySilane
ASE : Accelerated Solvent Extractor
ATR-FTIR : Attenuated Total Reflectance - Fourier-Transform InfraRed spectroscopy
Conc. : Concentration
CTP : Centre Technique du Papier (Pulp and paper technical and research center)
D : Dissipation
DAMS : 2-(3-aminopropyl)-ethyltrimethoxysilane
DMDMS : DiMethylDiMethoxySilane
EDX : Energy Dispersive X-ray spectroscopy
EtOH : Ethanol
EucaBS : *Eucalyptus* fibers from Bahia-Sul
EucaT+ : *Eucalyptus* fibers used specifically for project *Tissue+*
FTIR : Fourier-Transform InfraRed spectroscopy
MTMS : MethylTriMethoxySilane
MVDES : MethylVinylDiEthoxySilane
MVDMS : MethylVinylDiMethoxySilane
NMR : Nuclear Magnetic Resonance spectroscopy
PDMS : Poly-DiMethylSiloxane
QCM : Quartz Crystal Microbalance
QCM-D : Quartz Crystal Microbalance with Dissipation monitoring
RsxT+ : Softwood fibers used specifically for project *Tissue+*
RsxTh : Softwood fibers used all throughout this thesis work
SEM : Scanning Electron Microscopy
SEM-EDX : Scanning Electron Microscopy with Energy Dispersive X-ray spectroscopy
SIMS : Secondary Ions Mass Spectroscopy
SR : Silanol Reactivity parameter
T° : Temperature
TEA : TriEthylAmine
TMMS : TriMethylMethoxySilane
ToF-SIMS : Time of Flight – Secondary Ions Mass Spectroscopy
UHV : Ultra High Vacuum
VDMES : VinylDiMethylEthoxySilane
XPS : X-ray Photoelectron Spectroscopy (aka. ESCA : Electron Spectroscopy for Chemical Analysis)

Résumé:

Ce manuscrit de thèse traite de la modification de fibres de cellulose, en solutions purement aqueuses, par les organosilanes. Les réactions en phase aqueuse de silanes portants différents groupements chimiques réactifs ont été évaluées *in-situ* par spectrométrie par résonance magnétique nucléaire et l'influence de divers paramètres (pH, concentration, température) a été étudiée. Les aminosilanes se sont montrés particulièrement adaptés à l'utilisation en conditions correspondant à celles couramment utilisées dans le procédé papetier. En outre, l'adsorption des agents chimiques les plus prometteurs sur des surfaces modèles de cellulose a été testée par la technique de microbalance à quartz, en fonction des mêmes paramètres. Cette étude a montré qu'une bonne couverture de la surface est atteinte avec des cinétiques de quelques minutes, et est suivie d'une légère adsorption continue dans le temps. La nature des interactions entre divers silanes et la cellulose a été testée, et a révélé que le greffage, réalisé avec succès dans ce travail, relève d'interactions fortes. Enfin, deux types de fibres (résineux et feuillus) ont été utilisés afin de mesurer le potentiel d'utilisation des organosilanes pour répondre à une problématique industrielle impliquant les propriétés mécaniques du papier et sa douceur. Des résultats mitigés ont été obtenus, bien que le succès du procédé de greffage ait été avéré pour les différentes fibres.

Mots clés : cellulose, papier, silanes, organosilanes, hydrolyse, condensation, fonctionnalisation, greffage, RMN ^{29}Si, microbalance à quartz, XPS, ToF-SIMS, propriétés mécaniques, douceur.

Abstract:

This dissertation describes the chemical modification of cellulosic fibers by organosilanes. The reactions of silanes bearing various functional groups were carried out in pure aqueous solution and followed *in-situ* by nuclear magnetic resonance spectrometry. The effect of pH, concentration, and temperature on the reaction kinetics was studied. Aminosilanes could be processed in conditions similar to those commonly used in the papermaking. Furthermore, the adsorption of the most promising grafting agents on model cellulose surfaces was investigated by mean of a quartz crystal microbalance, and the effect of the same parameters was evaluated. This study showed that a good surface coverage is attained rapidly, i.e., within only a few minutes. Then, a slower but continuous adsorption was observed over time. The nature of the interactions between various silanes and cellulose was tested. It was shown that the grafting was successfully performed, thus giving rise to the formation of strong interactions between the adsorbate and the adsorbent. Finally, two types of fibers (softwood and hardwood) were used in order to evaluate the effect of organosilanes on mechanical properties and the softness of paper. The results obtained showed quite modest effects, even though the success of the grafting was assessed on both types of fibers.

Keywords : cellulose, paper, silanes, organosilanes, hydrolysis, condensation, functionalization, grafting, ^{29}Si NMR, quartz crystal microbalance, XPS, ToF-SIMS, mechanical properties, softness.